Decoupling of Information Propagation from Energy Propagation

by

Robert H. Jonsson

A thesis
presented to the University of Waterloo
in fulfillment of the
thesis requirement for the degree of
Doctor of Philosophy
in
Applied Mathematics

Waterloo, Ontario, Canada, 2016

© Robert H. Jonsson 2016

Author's Declaration

This thesis consists of material all of which I authored or co-authored: see Statement of Contributions included in the thesis. This is a true copy of the thesis, including any required final revisions, as accepted by my examiners.

I understand that my thesis may be made electronically available to the public.

Statement of Contributions

Most of the results of this thesis were previously published in the single-authored publication [38], and two co-authored publications [39, 40].

In the research that led to the two co-authored publications I was responsible of all calculations, I made significant discoveries leading to the main results of the publications, and wrote the first drafts for the publications which were then co-edited with my collaborators.

Some sections and chapters of this thesis consist of adapted and extended parts of the co-authored publication [39], and the single-authored publication [38]. These are marked clearly by comments at the beginning of the respective sections or chapters.

On the co-authored publication [39] are based: Section 3.2, Appendix A, and Chapter 4.

On the single-authored publication [38] are based: Section 2.3.2, Section 2.4, Chapter 7, and Section 6.1.

Where figures have been reproduced from the three mentioned publications, the sources are cited in the captions.

Abstract

Information and energy are concepts central to our understanding of nature. Their relevance, in physics, ranges from fundamental physics, e.g., in black hole physics, all the way to future quantum computing technology. This thesis investigates how information and energy propagate in quantum fields. The main result is that in massless fields the propagation of information can decouple from the propagation of energy partially and, under special circumstances, even completely.

It has been known that in general curved spacetimes, and also in odd-dimensional Minkowski space, signals can propagate slower than light even in a massless field. Here it is shown that the energy-to-information ratio of these classical timelike signals can approach zero. The extreme case is marked by two-dimensional Minkowski space. In this case, timelike signals reach arbitrarily far into the future lightcone, without diluting, and they carry no energy at all. Instead, the energy cost associated with the detection of energyless signals has to be provided by the receiver, much as in a collect call.

Technically, sender and receiver are modelled as basic first-quantized systems coupling locally to the relativistic quantum field, i.e., as Unruh-DeWitt particle detectors. This gives rise to a standard quantum channel from the sender to the receiver. Thus, the tools of quantum information can be applied to investigate the combined impact of relativistic and quantum effects on the propagation of information.

In the perturbative regime, signals analogous to phase modulation are shown to overcome signals analogous to amplitude modulation: It is shown that the sender has to prepare superpositions of eigenstates, to achieve signalling effects at leading order. Signals from pure energy eigenstates are subdominant, and only appear in next-to-leading order. The classical channel capacities resulting from optimal signalling states are calculated.

Analyzing the energy injected into the field by the sender, it is shown that signals reach further in spacetime than the energy radiated by the sender, both for timelike, as well as for lightlike signals. Instead, the energy budget is balanced by the energy that the receiver has to provide when decoupling the detector from the field. This switching cost is particularly sensitive to timelike signals.

Timelike signals are also demonstrated to occur between harmonic oscillators coupling to the field inside a cavity. This model could be instrumental for future research, because it can be treated non-perturbatively using Gaussian methods.

Such numerical calculations only take into account a finite number of field modes. It is shown that relativistic properties of the field can still be resolved reliably, because the number of necessary modes scales with the desired accuracy, namely following a power law.

Acknowledgements

I thank Achim Kempf for his outstanding and inspirational mentorship, and support as PhD supervisor. I thank Eduardo Martín-Martínez for his friendship, mentorship and collaboration. I thank Katja Ried for the great collaboration over the past years.

I thank Patrick Hayden, Thomas Jennewein and Ray McLenaghan for serving as examiners of this thesis, for valuable comments and discussions. I thank Robert König, Ralph Schützhold, and Jorma Louko for helpful and insightful discussions that contributed to this thesis. I thank Joseph Emerson and Florian Girelli for serving on my advisory committee.

I thank Jason Yufang Hao, William Donnelly, Mikhail Panine, Aidan Chatwin-Davies, Eric Webster, Daniel Hümmer, Jason Pye, David Layden, and Guillaume Verdon-Akzam, Nayeli Rodríguez Briones, and also Rastko Anicic, Yangang Chen, Aida Ahmadzadegan, Eric Brown, and Wilson Brenna for all the great times in, around and outside of the Kempf Lab.

I thank Dainy, Gunes, Joanna, Michael, Rubin, Sascha, and all my wonderful housemates for their friendship.

I thank Alma Kunert for reminding me of the importance of a complete bibliography.

And last but not least, I thank the Canadian and German tax payers, for funding my studies, mainly through the institutions of the Ontario Trillium Scholarship, and the German National Academic Foundation.

Dedicated to the memory of Anna Wohl and Gunborg Jonsson.

Table of Contents

List of Figures

Chapter 1

Introduction

Motivation - Relativistic Quantum Communication

What would happen if we were to take the physics of an ordinary, everyday wireless phone call and push it to the very frontiers of our understanding of physics? What if we describe the signalling devices as quantum systems, that move along relativistic trajectories through a curved spacetime, and communicate via quantum fields?

This question, which motivates the present thesis, brings together three fundamental branches of theoretical physics: general relativity, quantum theory and information theory. It combines them in a regime yet to be fully explored. A regime where several fascinating results point toward deep connections between the three theories, while it is still unknown if and how they might emerge from a common, more fundamental theory of nature that is yet to be discovered.

General relativity and quantum field theory, the foundations of our current understanding of nature, continue to resist their unification. Their partial combination in the study of quantum field theory in curved background spacetimes, however, already led to the most stunning predictions, such as the Hawking radiation of black holes, particle creation in expanding universes, cosmic inflation or, even in flat spacetime, the Unruh effect.

At the heart of these phenomena lies the observation that particles are an observer-dependent concept, much as time is in general relativity. For example, in the Unruh effect a uniformly accelerated observer perceives as a thermal state, what an inertial observer in Minkowski space perceives as the vacuum state of the field. The quantum fluctuations of the field, which look like vacuum noise to an inertial observer, conspire to look like the

fluctuations of a thermally excited state with respect to the accelerated observer's choice of field basis states.

Information theoretical questions have uncovered further fascinating links between quantum theory and gravity. Well known and active research topics of this kind include the entropy of black holes, the black hole information paradox, the Bekenstein bound, the vacuum entanglement of quantum fields, black hole thermodynamics, and the holographic principle.

In this general context, studying communication via quantum fields in curved spacetimes contributes a new perspective exploring the impact of spacetime curvature and relativistic effects on quantum fields. Spacetime curvature impacts quantum communication between relativistic observers via the quantum field in at least two different ways: Firstly, the sender, the receiver, and the propagating signal experience general relativistic effects, such as time dilation and gravitational red-shifts, depending on their motion and location. Secondly, spacetime curvature modulates the quantum fluctuations of the field. These constitute an omnipresent source of noise in the communication channel between devices communicating via the field, against which the signal has to compete.

Approaching this interplay of general relativistic and quantum phenomena from the point of view of information transmission will allow us to measure and quantify arising effects in terms of information theoretic quantities such as communication channel capacities.

Context - Relativistic Quantum Information

This thesis falls into the research field of relativistic quantum information. This field emerged over recent years, inspired by the development of quantum information. (See [55], and other articles of this special issue.) Relativistic quantum information investigates the impact of relativity on quantum information processes, and approaches question from quantum field theory in curved spacetimes with tools from quantum information. The interest in these questions is often twofold: On the one hand, it searches to uncover fundamental principles of the interplay between gravity and quantum theory. On the other hand, it explores relativistic quantum fields as a potential resource for quantum information tasks.

When modelling the interaction of relativistic observers with a quantum field, one needs to take into account that there is no global notion of particles. One way to achieve this is to model the observers themselves by basic first quantized quantum systems that couple to the field along a given observer's worldline [23, 81]. Such particle detector models have proven

to be an important tool in the study of quantum field theory in curved spacetimes, and can in fact be used to demonstrate all the well-known effects mentioned above [29, 30, 81].

In the context of relativistic quantum information, particle detectors have been used to study questions such as whether the relativistic motion of a qubit that is coupled to a field can be used to perform quantum gates on the qubit [57]. Or, it has been shown that entanglement can be swapped from the vacuum correlations of the field onto a pair of detectors, even when they are spacelike separated [69]. This entanglement extraction can, in principle, distinguish the geometry of different cosmological spacetimes [79, 60, 72] and it could be used as a resource for quantum information processing [58, 71]. In quantum energy teleportation protocols the vacuum entanglement of the field is used to teleport energy between two parties interacting locally with the field through particle detectors [34, 35, 36, 83].

In this thesis, the focus lies on signalling between detectors, i.e., the ability to transmit information through the influence of one detector on the other, that is mediated by the quantum field. Besides other results, we make particularly interesting observations on the relation between information transport and energy transport in massless quantum fields.

Result - Decoupling of Information Transmission and Energy Transmission

The central observation of this thesis is that a signal that carries information through a massless field does not necessarily carry energy from the sender to the receiver. This decoupling of a flow of information from the flow of energy in the field arises, because information can be imprinted into the amplitude of the field without directly contributing to the field's energy density, to which only the field's derivatives contribute.

Studying signalling between Unruh-DeWitt particle detectors provides an information-theoretical framework in which the interesting consequences of this phenomenon can be explored. In a communication setting, the effects of the sender on the receiver can be encapsulated in the map from the sender's initial state to the receiver's final state. Such maps between density matrices are known as quantum channels in quantum information theory, and a range of methods has been developed to analyze their properties.

This framework for signalling between detectors via relativistic fields was introduced in [19, 20, 21]. Building up in these works this thesis completes the perturbative analysis of the channel. In particular, it identifies the optimal input states that the sender needs to use in order to maximize the signalling strength in leading order of perturbation theory.

Intuitively, one might expect that energy eigenstates maximize the impact of the sender on the quantum field and evoke the strongest signals. However, for interactions in the perturbative regime, these are the sender's worst possible choice. Instead, the sender needs to use equal weighted superpositions of energy eigenstates, in order to obtain optimal signalling strength. The maximum achievable leading order signalling strength is found to be given by a relatively simple, Fourier-type integral over the field commutator. This integral is also shown to determine the leading order behaviour of the resulting Shannon capacitiy of the channel.

Therefore, to leading order, signalling effects between detectors correspond to the classical behaviour of the field, because the commutator is given by the field's classical Green functions and independent of the quantum state of the field. Accordingly, the Green function's support in spacetime determines where in spacetimes signals can propagate.

It has long been known that signals in massless fields do generally not propagate strictly at the speed of light, but a part of the signal typically propagates slower than the speed of light. This might appear counterintuitive, since massless fields in 3+1D Minkowski spacetime are one of the few exceptions to which the so called Huygens principle applies, i.e., the Green functions have lightlike support only. However, in general curved spacetimes, and also in odd-dimensional Minkowski spacetime, the Green functions of the field have support inside the lightcone as well. This means that signals can partially propagate slower than light, even in a massless field.

These timelike signals highlight the decoupling of information transmission and energy transmission. They can carry both information and energy into the sender's future lightcone. However, their energy density decays faster than their signalling strength such that their energy-to-information ratio approaches zero. Instead, timelike signals between Unruh-DeWitt detectors modulate the energy that is required from the receiver to couple and decouple his detector and the field. This means that the information content of timelike signals between detectors is partially encoded in the energy costs associated with the signal's detection.

The most extreme case of this phenomenon occurs in 1+1D Minkowski space. In this case, timelike signals reach arbitrarily far into the future lightcone of the sender, without diluting. In contrast, the field's energy density propagates strictly at the speed of light. Thus, a receiver in the future lightcone can obtain information without obtaining any energy from the receiver. Instead, any energy cost associated with the detection of the signal has to be provided by the receiver when switching their detector on and off.

This findings highlight that the information carried by a signal, and the energy injected into the field at the signal's emission can travel different paths in spacetime. The impli-

cations of this aspect for the general interplay of spacetime geometry, information and energy, e.g., in the context of black hole physics, or known results on the energy costs of information processing, are yet to be explored.

Synopsis and Conventions

The thesis is organized as follows:

Chapter 2 reviews the quantization of a Klein-Gordon field in Minkowski spacetime. The field commutator which is central to the propagation of signals in the field is calculated for Minkowski space of different dimensions, and in a one-dimensional Dirichlet cavity. The propagation of field operators and field energy density in 1+1D Minkowski spacetime is discussed in detail. This chapter shows that timelike signals in massless field lead to a decoupling of information propagation and energy propagation.

Chapter 3 studies the structure and classical capacity of the channel between two two-level Unruh-DeWitt particle detectors using time-dependent perturbation theory. We briefly review the Unruh-DeWitt particle detector model. Then we discuss how to calculate the channel from a perturbative treatment of the detector-field interaction. For the calculation of optimal signalling states and channel capacities the channel is represented in the Bloch sphere picture. The central result is that a relatively simple Fourier-type integral over the field commutator yields the strength of signalling effects to leading order in perturbation theory.

Chapter 4 discusses the questions how many modes of the field, e.g., in a numerical calculation, need to be taken into account in order to be able to accurately model the relativistic features of the quantum field. By studying the size of signalling effects it is shown that the number of modes necessary scales with a power law in the desired accuracy.

Chapter 5 discusses the characteristics of the leading order signalling effects for timelike and lightlike separated detectors. The signalling strength between detectors in lightlike contact is optimized when the detector are resonant with each other, in which case can grow arbitrarily large for long interaction times. This is in contrast to signalling between timelike separated detectors where resonance between the detectors is irrelevant. The signalling strength between inertial and uniformly accelerated detectors is calculated. The effect of the relativistic motion enters into the corresponding integrals through the appearance of the relativistic Doppler shift.

Chapter 6 studies, using perturbation theory, the energy density injected into the field by a detector coupling to the vacuum of the field. It discusses in detail the energy necessary

to couple and decouple a detector and the field, and the energy exchange occurring under the interaction. An analysis of how these processes are affected by signalling between detectors shows that timelike signals modulate the energy required by the receiver to switch their detector.

Chapter 7 studies timelike signals between harmonic oscillators coupling to the field inside a one-dimensional Dirichlet cavity. This setup is of interest, because it allows us to study timelike signals while treating the time evolution non-perturbatively.

We close with a discussion of the results and directions for future research.

In signalling scenarios the sender will often be referred to as Alice, and the receiver as Bob. These terms are used interchangeably throughout the thesis. We use natural units $c = \hbar = k_B = 1$, and $(+, -, ..., -)$ as signature of the Minkowski spacetime metric.

Chapter 2

Quantum Field Theory: Field and Commutator

The decoupling of information transmission and energy transmission arises in massless fields because the amplitude of the field does not contribute to the field's energy directly, but only its derivatives do. Thus, when a sender encodes a signal into the field's amplitude, the absolute value of the amplitude does not contribute to the field's energy *per se*, but only the part of the signal does where the amplitude changes in time or in space.

This can lead to a decoupling of a flow of information from the flow of energy in the field, in particular, in spacetimes where Huygens principle does not apply [22]. The Huygens principle, i.e., propagation strictly at the speed of light, is a familiar property of massless fields in 3+1D Minkowski spacetime. Less familiar, maybe, is the fact that Huygens principle is an exception rather than the norm. It only applies to very special geometries as, e.g., 3+1D Minkowski spacetime, higher *odd*+1D Minkowski spacetimes, and certain special cases of curved spacetimes. In general, signals in massless fields do not propagate strictly at the speed of light, but part of the signal propagates slower.

By this phenomenon, senders can affect the amplitude of the field inside their future lightcone. Such timelike signals may also carry some energy into the future lightcone. However, the energy does not reach as far into the lightcone as the imprint into the field's amplitude does. This is because the energy density, since it only depends on the derivatives of the field, decays faster than the field's amplitude. In the extreme case of 1+1D Minkowski spacetime, timelike signals even propagate arbitrary far into the future lightcone, without diluting, while carrying no energy at all.

We begin this chapter with a brief review of the massless Klein-Gordon field and the

Huygens principle, and of the quantization of the Klein-Gordon field. We go on to calculate the field's Wightmann function, whose imaginary part is the commutator of the field, which we will find to be a central quantity in the study of signalling scenarios. Also this calculation is exemplary for momentum space integrations that appear in perturbative calculations later in the thesis. Finally, in Section 2.4, we demonstrate how the decoupling of an information flow from the energy flow in 1+1D Minkowski spacetime follows from expressing the field in terms of its left- and right-moving observables.

2.1 The Klein-Gordon field and Huygens principle

In this thesis, we will consider a real, massless Klein-Gordon field in flat $(n+1)$-dimensional Minkowski space. In this case the Klein-Gordon equation reads

$$\Box\phi = 0 \tag{2.1}$$

where $\Box = \frac{\partial^2}{\partial t^2} - \frac{\partial^2}{\partial {x_1}^2} - ... - \frac{\partial^2}{\partial {x_n}^2}$ denotes the d'Alembertian. The field $\phi(t, \vec{x})$ is a function of the spacetime coordinates $(t, \vec{x}) = (t, x_1, ..., x_n)$. For example, in 1+1 dimensions the massless Klein-Gordon equation is therefore

$$\left(\partial_t^2 - \partial_x^2\right)\phi(t, x) = 0, \tag{2.2}$$

which is the wave equation describing the transverse displacement of an elastic string. The 1+1 dimensional case will play a central role in this thesis, because here information can completely decouple from the transmission of energy as Section 2.4 will show. Ultimately, this is possible because the amplitude of the field does not occur in the Lagrangian density of the massless Klein-Gordon field

$$\mathcal{L} = \frac{1}{2}\eta^{\mu\nu}\partial_\mu\phi\partial_\nu\phi \tag{2.3}$$

where $\eta^{\mu\nu} = \text{diag}(+, -, ..., -)$ denotes the Minkowski metric. When the field amplitude ϕ, or rather its amplitude square ϕ^2, contributes to the field's Lagrangian through

$$\mathcal{L} = \frac{1}{2}\left(\eta^{\mu\nu}\partial_\mu\phi\partial_\nu\phi - m^2\phi^2\right) \tag{2.4}$$

then the field is called massive. A massive Klein-Gordon field obeys the equation

$$\left(\Box + m^2\right)\phi = 0. \tag{2.5}$$

In classical field theory Green functions are used to solve the field equations with a prescribed source term

$$\Box\phi(x) = \mu(x). \tag{2.6}$$

They are solutions to the field equation with a Dirac δ-distribution as a source term on the right-hand side

$$\Box G(x, x') = \delta(x - x'), \tag{2.7}$$

such when integrated against the prescribed source $\mu(x)$ they provide a solution to (2.6), since

$$\Box_x \int \mathrm{d}x'\, G(x, x')\mu(x') = \mu(x). \tag{2.8}$$

The solution to (2.7) is not unique and different choices of Green functions are possible. Two particularly important Green functions are the retarded Green function $G_{ret}(x, x')$, which is non-vanishing only when x lies in the future of x', and the advanced Green function $G_{adv}(x, x')$, which is non-vanishing only when x lies in the past of x'. The retarded Green function can thus be thought of as propagating the effect of a disturbance of the field into the future, whereas the advanced Green function propagates it backwards in time. An instructive review and calculation of the Green functions of a scalar Klein-Gordon field in flat, and in curved spacetime is found in [68].

The support of the Green functions thus encode how signals can propagate in the field. Causality, i.e., that no signal can propagate faster than the speed of light, is encoded in the fact that the Green functions vanish at spacelike separations. In 3+1D Minkowski spacetime the support of the Green functions is, in fact, restricted to strictly lightlike separations, i.e., to the boundary of the lightcone. This means that all signals propagate strictly at the speed of light. If this is the case on a given spacetime, then it is said to obey the *Huygens principle*.

The Huygens principle can equivalently be formulated in terms of the Cauchy problem. This is the problem of how the solution to the field equation in the future of some spacelike n-dimensional surface S depends on the prescribed values for the field and its normal derivative on S. If the solution to $\phi(x)$ at some point x in the future of S only depends on an arbitrarily small neighbourhood of the intersection of S with the null lightcone emanating from x, then the spacetime is said to satisfy the Huygens principle [22].

While one might think that it would be a natural property of a massless field that all signals propagate strictly at the speed of light, this is actually only holds in very special cases [22, 62, 63]. Even in flat spacetimes of $n+1$ dimensions it only holds for odd $n \geq 3$, but is violated in all other cases. We will see this explicitly in the calculations of the Wightmann function in Section 2.3 below.

2.2 Quantization of a Scalar Klein-Gordon Field

The ultimate goal of this research is to investigate the interplay of quantum effects with relativistic effects and, in particular, spacetime curvature. Therefore we give the following review of field quantization in the diction of quantum field theory in curved spacetimes [8, 28, 84]. It serves to introduce notation, and as reference for following chapters. Within the scope of this thesis we only consider scenarios in flat Minkowski spacetime and in Dirichlet cavities. Therefore, a background familiarity with quantum field theory as taught, e.g., in courses on particle physics is sufficient for the lecture of this thesis. As we will see, passing from flat spacetime to curved spacetimes would, generally speaking, only affect the results of this thesis in as far as the commutator of the field is affected.

This section is similar to the review of quantization in [8]. Note, however, that there the the spacetime dimension denoted by n includes the time dimension, whereas we are going to denote by n the spatial dimensions only, i.e., n in [8] corresponds to $n+1$ here.

In quantum field theory, the field and its derivatives at each spacetime point are operators. In the Heisenberg picture, these operators obey the Klein-Gordon equation and are therefore interdependent. A complete set of observables is given just by the collection of all field operators ϕ and their canonically conjugate

$$\pi = \frac{\partial \mathcal{L}}{\partial \left(\partial_t \phi\right)} = \partial_t \phi \tag{2.9}$$

across a Cauchy hypersurface of the spacetime, such as a slice of constant time in Minkowski space [84]. All other field operators can be expressed in terms of such a set of complete observables. This is analogous to how initial data of the classical field and its momentum on a Cauchy hypersurface determines the value of the field everywhere else in spacetime.

Furthermore, the so called *equal time commutation relations* are imposed on the field operators and their conjugate.

$$[\phi(t,\vec{x}),\phi(t,\vec{y})] = 0 \qquad [\pi(t,\vec{x}),\pi(t,\vec{y})] = 0 \qquad [\phi(t,\vec{x}),\pi(t,\vec{y})] = \mathrm{i}\delta(\vec{x}-\vec{y}) \tag{2.10}$$

To find a representation of these, the field operator can be expanded in terms of plane wave solutions to the Klein-Gordon equation, to which we will refer to as field modes,

$$\phi(t,\vec{x}) = \int \mathrm{d}^n\vec{k}\,\frac{1}{\sqrt{(2\pi)^n 2\omega_{\vec{k}}}}\left(\mathrm{e}^{-\mathrm{i}(\omega t-\vec{k}\cdot\vec{x})}a_{\vec{k}} + \mathrm{e}^{\mathrm{i}(\omega t-\vec{k}\cdot\vec{x})}a^\dagger_{\vec{k}}\right), \tag{2.11}$$

where $\omega_{\vec{k}} = \sqrt{|\vec{k}|^2+m^2}$. The operators $a_{\vec{k}}$ (and $a^\dagger_{\vec{k}}$) are called annihilation (and creation) operators since the equal time commutation relations for the field operators are equivalent to the commutation relations

$$\left[a_{\vec{k}}, a_{\vec{l}}\right] = 0, \qquad \left[a^\dagger_{\vec{k}}, a^\dagger_{\vec{l}}\right] = 0, \qquad \left[a_{\vec{k}}, a^\dagger_{\vec{l}}\right] = \delta^{(n)}(\vec{k}-\vec{l}). \tag{2.12}$$

These are used for the standard Fock representation of the fields Hilbert space with the vacuum state $|0\rangle$ such that

$$a_{\vec{k}}\,|0\rangle = 0. \tag{2.13}$$

The single particle states are created by acting on the vacuum with the corresponding creation operator

$$a^\dagger_{\vec{k}}\,|0\rangle = \left|1_{\vec{k}}\right\rangle \tag{2.14}$$

which we also will denote as $\left|\vec{k}\right\rangle = \left|1_{\vec{k}}\right\rangle$. The multi-particle states are correspondingly defined as

$$\left|n^{(1)}_{\vec{k_1}}, n^{(2)}_{\vec{k_2}}, ..., n^{(s)}_{\vec{k_s}}\right\rangle = \frac{1}{\sqrt{n^{(1)}!n^{(2)}!...n^{(s)}!}}\left(a^\dagger_{\vec{k_1}}\right)^{n^{(1)}}\left(a^\dagger_{\vec{k_2}}\right)^{n^{(2)}}...\left(a^\dagger_{\vec{k_s}}\right)^{n^{(s)}}|0\rangle \tag{2.15}$$

which in particular also yields

$$a_{\vec{k}}\left|n_{\vec{k}}\right\rangle = \sqrt{n}\left|(n-1)_{\vec{k}}\right\rangle. \tag{2.16}$$

When we expand the field operator $\phi(t,\vec{x}) = \int \mathrm{d}^n\vec{k}\,u_{\vec{k}}(t,\vec{x})\,a_{\vec{k}} + u^*_{\vec{k}}(t,\vec{x})\,a^\dagger_{\vec{k}}$ in terms of the field modes

$$u_{\vec{k}}(t,\vec{x}) = \frac{1}{\sqrt{(2\pi)^n 2\omega}}\mathrm{e}^{-\mathrm{i}(\omega t-\vec{k}\cdot\vec{x})}, \tag{2.17}$$

the modes are chosen to be orthonormalized

$$\left(u_{\vec{k}}, u_{\vec{l}}\right) = \delta^{(n)}\left(\vec{k}-\vec{l}\right) \tag{2.18}$$

with respect to the Klein-Gordon scalar product

$$(\phi_1, \phi_2) = -\mathrm{i} \int \mathrm{d}^n \vec{x} \; (\phi_1(t, \vec{x}) \partial_t \phi_2^*(t, \vec{x}) - \phi_2^*(t, \vec{x}) \partial_t \phi_1(t, \vec{x})) \tag{2.19}$$

for any fixed time coordinate t. This orthonormalization yields the equivalence of the equal time commutation relations and the commutation relations for the annihilation and creation operators.

When the spacetime is spatially compact the plane wave solutions form a discrete set instead of a continuous set, since the spectrum of the d'Alembertian is discrete. Hence the field operator is expanded in terms of a sum

$$\phi(t, \vec{x}) = \sum_{\vec{j}} u_{\vec{j}}(t, \vec{x}) a_{\vec{j}} + u_{\vec{j}}^*(t, \vec{x}) a_{\vec{j}}^\dagger \tag{2.20}$$

where the modes now obey the orthonormalization condition

$$\left(u_{\vec{i}}, u_{\vec{j}}\right) = \delta_{\vec{i}\vec{j}} \tag{2.21}$$

with a Kronecker symbol ($\delta_{\vec{i}\vec{j}} = \delta_{i_1 j_1} \delta_{i_2 j_2} ... \delta_{i_n j_n}$) instead of the Dirac δ-distribution on the right hand side.

One example of a spatially compact and flat spacetime is an $(n+1)$-dimensional torus with length L. The torus is obtained from Minkowski space by identifying points that differ by L in any spatial coordinate, i.e., $(t, x_1, ..., x_i + L, ..., x_n) \sim (t, x_1, ..., x_i, ..., x_n)$. The plane wave solutions on the torus are

$$u_{\vec{j}}(t, \vec{x}) = \frac{1}{\sqrt{L^n 2\omega_{\vec{j}}}} \mathrm{e}^{-\mathrm{i}\left(\omega_{\vec{j}} t - \vec{k_j} \cdot \vec{x}\right)} \tag{2.22}$$

with $\vec{j} \in \mathbb{Z}^n$, $\vec{k_j} = \frac{2\pi}{L} \vec{j}$ and $\omega_{\vec{j}} = \sqrt{\vec{k_j}^{\,2} + m^2}$. And the field operator is then expanded as

$$\phi(t, \vec{x}) = \sum_{\vec{j}} \frac{1}{\sqrt{L^n 2\omega_{\vec{j}}}} \left(\mathrm{e}^{-\mathrm{i}\left(\omega_{\vec{j}} t - \vec{k_j} \cdot \vec{x}\right)} a_{\vec{j}} + \mathrm{e}^{\mathrm{i}\left(\omega_{\vec{j}} t - \vec{k_j} \cdot \vec{x}\right)} a_{\vec{j}}^\dagger \right) \tag{2.23}$$

In general, to translate expressions from Minkowski space with its continuous spectrum into their counterpart on the torus with its discrete spectrum, and vice versa, one can apply the following replacements [8, 9]

$$\int \mathrm{d}^n \vec{k} \to \Delta V \sum_{\vec{j}}, \quad \delta^{(n)}\left(\vec{k} - \vec{l}\right) \to \frac{\delta_{\vec{i}\vec{j}}}{\Delta V}, \quad u_{\vec{k}}(t, \vec{x}) \to \frac{u_{\vec{j}}(t, \vec{x})}{\sqrt{\Delta V}}, \quad a_{\vec{k}} \to \frac{a_{\vec{j}}}{\sqrt{\Delta V}} \tag{2.24}$$

with $\Delta V = \left(\frac{2\pi}{L}\right)^n$. For example, this yields the commutation relations for the creation and annihilation operators

$$\left[a_{\vec{k}}, a^\dagger_{\vec{l}}\right] = \delta^{(n)}(\vec{k} - \vec{l}) \rightarrow \left[a_{\vec{i}}, a^\dagger_{\vec{j}}\right] = \delta_{\vec{i}\vec{j}}. \tag{2.25}$$

If the field is massless the so called zero mode of the field requires a treatment different from the one applied so far: Above, each mode of the field modes is treated as a separate quantum harmonic oscillator of frequency $\omega_{\vec{j}}$. However, when the field is massless we have $\omega_{\vec{j}} = \left|\vec{k_j}\right|$. So for the zero mode we would obtain $\omega_{\vec{0}} = 0$ which of course does not correspond to a harmonic oscillator. Instead the zero mode needs to be treated in analogy to a free, non-relativistic particle on the real line [59].

Later we will use a different case of a spatially compact space, which we refer to as a $(n+1)$-dimensional Dirichlet cavity. Here the space is restricted to the n-dimensional (hyper)cube of side length L, i.e, $\vec{x} \in [0, L]^n$, and so called Dirichlet boundary conditions are imposed on the field: This means that the field operators have to vanish on the hypercube's boundary. The mode functions for the field in a Dirichlet cavity are

$$u_{\vec{j}}(t, \vec{x}) = \frac{1}{\sqrt{L^n \omega_{\vec{j}}}} \sin\left(x_1 \frac{j_1 \pi}{L}\right) \sin\left(x_2 \frac{j_2 \pi}{L}\right) ... \sin\left(x_n \frac{j_n \pi}{L}\right) \mathrm{e}^{-\mathrm{i}\omega_{\vec{j}} t} \tag{2.26}$$

with $\omega_{\vec{j}} = \sqrt{\vec{k_j}^2 + m^2}$ as usual, however the wave vector in the Dirichlet cavity is given by

$$\vec{k_j} = \frac{\pi}{L}\vec{j} \tag{2.27}$$

where the entries of $\vec{j} = (j_1, j_2, ..., j_n)$ are all positive integers, i.e., $j_i \geq 1$.

2.3 Wightmann Function and Field Commutator

The commutator of the field is the central object when studying the propagation of signals in a quantum field. Because the commutator encodes the dependence of the field operator at one point on other field operators at earlier times. First of all, this means that sending information from one point to another in spacetime via a quantum field is possible only if the field commutator between those two points does not vanish [26, 19]. And, as we will see in Chapter 3, the size of the commutator determines the signalling strength between observers interacting locally with the field to leading order in perturbation theory.

The commutator arises as the imaginary part of the Wightmann function of the field. In the following, we review this relation, and calculate the Wightmann function and the commutator in Minkowski spacetime of arbitrary dimension, and in one-dimensional Dirichlet cavities.

A detailed treatment of the commutator's relation to the different Green functions of the Klein-Gordon field, their representations in terms of contour integrals, and their relation to the different two-point function of the quantum field is found in Chapter 4 of [28] and Chapter 2.7 of [8].

The commutator of the field operators at two different points in spacetime is proportional to the identity operator

$$[\phi(t,\vec{x}),\phi(t',\vec{x}')] \propto \mathrm{i}\,\mathbb{I}. \tag{2.28}$$

This is a direct consequence of the commutator of creation and annihilation operators being proportional to the identity operator, which we observe when use the expansion of the field of (2.11) above. (This also applies to the commutators $[\phi,\pi']$ and $[\pi,\pi']$.)

In fact, the commutator of the field is determined just by the classical wave equation: It is a homogeneous solution of the wave equation, and is given as

$$[\phi(t,\vec{x}),\phi(t',\vec{x}')] = \mathrm{i}\,(G_{adv}(t,\vec{x},t,\vec{x}') - G_{ret}(t,\vec{x},t,\vec{x}'))\,\mathbb{I} \tag{2.29}$$

in terms of the advanced and the retarded Green functions of the classical wave equation $(\Box + m^2)\,\phi = 0$. Therefore the spacetime points between which one can transmit signals via the quantum field, are the same as for the classical field. It is known from the analysis of the classical wave equation as a partial differential equation that the advanced and retarded Green functions vanish for spacelike separations between $(t,\vec{x})$ and $(t',\vec{x}')$, but are supported only inside the lightcone.

To evaluate the commutator in the context of quantum field theory, we can use that it equals the imaginary part of the Wightmann function $\langle 0|\,\phi(t,\vec{x})\phi(t',\vec{x}')\,|0\rangle$.

$$\begin{aligned}[\phi(t,\vec{x}),\phi(t',\vec{x}')] &= \langle 0|\,[\phi(t,\vec{x}),\phi(t',\vec{x}')]\,|0\rangle = \langle 0|\,\phi(t,\vec{x})\phi(t',\vec{x}')\,|0\rangle - \langle 0|\,\phi(t',\vec{x}')\phi(t,\vec{x})\,|0\rangle \\ &= 2\mathrm{i}\Im\left(\langle 0|\,\phi(t,\vec{x})\phi(t',\vec{x}')\,|0\rangle\right)\end{aligned} \tag{2.30}$$

The Wightmann function, in turn, can be evaluated using the field operator's expansion in terms of mode operators. Here $|0\rangle$ denotes the vacuum state of the field.

Since the commutator is proportional to the identity its expectation value is the same for any state of the field. The anti-commutator of the field, $\{\phi(t,\vec{x}),\phi(t',\vec{x}')\}$, is a non-trivial operator of the field, and its expectation value is sensitive to the field state. Thus

one can think of the quantum properties of the vacuum state as being encoded in the real part of the Wightmann function.

$$\langle 0|\,\{\phi(t,\vec{x}),\phi(t',\vec{x}')\}\,|0\rangle = 2\Re\,\langle 0|\,\phi(t,\vec{x})\phi(t',\vec{x}')\,|0\rangle \tag{2.31}$$

Such quantum properties are the quantum fluctuations of the field, and the entanglement contained in them, even between spacelike separated regions of spacetime.

Accordingly, the imaginary part and the real part of the Wightmann function also differ in their support in spacetime. The imaginary part, yielding the commutator, is restricted to the lightcone. This is, at essence, what guarantees causality in relativistic quantum fields. However, the real part of the Wightmann function also has support outside of the lightcone at spacelike separations. The calculation of the Wightmann function reveals an interesting dependency of the real part and imaginary part, and thus the commutator, on the spacetime dimension.

2.3.1 The Wightmann Function in Minkowski space

In terms of the field modes $u_{\vec{k}}$ the Wightmann function is given by

$$\langle 0|\,\phi(t,\vec{x})\phi(t',\vec{x}')\,|0\rangle = \int \mathrm{d}^n\vec{k}\,u_{\vec{k}}(t,\vec{x})u^*_{\vec{k}}(t',\vec{x}') \tag{2.32}$$

as follows directly from the expansion of the field operator and the commutation relations for the mode operators $a_{\vec{k}}$ and $a^\dagger_{\vec{k}'}$. Which for the plane wave modes of $(n{+}1)$-dimensional Minkowski space yields

$$\langle 0|\,\phi(t,\vec{x})\phi(t',\vec{x}')\,|0\rangle = \int \mathrm{d}^n\vec{k}\,\frac{1}{(2\pi)^n 2\omega_{\vec{k}}}\mathrm{e}^{-\mathrm{i}(\omega\Delta t-\vec{k}\cdot\Delta\vec{x})} \tag{2.33}$$

where we introduced $\Delta t = t - t'$ and $\Delta\vec{x} = \vec{x} - \vec{x}'$.

This integral expression does not represent a function on the Minkowski spacetime $\mathbb{R}^{n+1}$ (or rather on $\mathbb{R}^{n+1}\times\mathbb{R}^{n+1}$). It is, in fact, divergent for lightlike separations, i.e., when $\Delta t^2 - \Delta\vec{x}^2 = 0$. Instead the integral represents a distribution which acts on test functions on Minkowski spacetime. Which means that in order to get a well-defined finite result the expression should be integrated against two test functions in Minkowski spacetime, before the momentum integration is carried out.

A representation for such distributions in which the distribution's support is readily analyzed is the so called iϵ-prescription. It is obtained by multiplying into the integrand

a factor of $\mathrm{e}^{-\epsilon\omega}$ with $\epsilon > 0$. With this factor the momentum integration can be performed directly, which results in a finite complex function. To evaluate the distribution for a particular pair of test functions, this complex function is integrated against the test functions first, and the limit of $\epsilon \to 0$ is taken at the end.

We will now derive the iϵ-representation for the Wightmann function of a massless field. The calculation for a massive field is analogous and can be found in [80] (Note that whereas we use n to denote only the spatial dimensions of $(n+1)$-dimensional Minkowski time, in [80], the symbol n is used to denote all spacetime dimensions, including time.)

For a massless field we have $\omega = \left|\vec{k}\right|$. We denote this by $k = \left|\vec{k}\right|$ and also introduce $\Delta x = |\Delta\vec{x}| \geq 0$. The Wightmann function then reads

$$\begin{aligned}
\langle 0|\,\phi(t,\vec{x})\phi(t',\vec{x}')\,|0\rangle &= \int \mathrm{d}^n\vec{k}\,\frac{1}{(2\pi)^n 2k}\mathrm{e}^{-\mathrm{i}(k\Delta t-\vec{k}\cdot\Delta\vec{x})}\mathrm{e}^{-k\epsilon} \\
&= \int_0^\infty \mathrm{d}k\,k^{n-1}\int_0^\pi \mathrm{d}\varphi_1\,\sin^{n-2}\varphi_1\frac{\mathrm{e}^{-\mathrm{i}k(\Delta t-\Delta x\cos\varphi_1)}\mathrm{e}^{-k\epsilon}}{(2\pi)^n 2k} \\
&\qquad \times \underbrace{\int_0^\pi \mathrm{d}\varphi_2\,\sin^{n-3}\varphi_2 \ldots \int_0^\pi \mathrm{d}\varphi_{n-2}\,\sin\varphi_{n-2}}_{=\sqrt{\pi}^{n-3}\left(\Gamma\left(\frac{n-1}{2}\right)\right)^{-1}}\underbrace{\int_0^{2\pi}\mathrm{d}\varphi_{n-1}}_{=2\pi} \\
&= \frac{1}{\pi^{\frac{n+1}{2}}2^n\Gamma\left(\frac{n-1}{2}\right)}\int_0^\infty \mathrm{d}k\,k^{n-2}\int_0^\pi \mathrm{d}\varphi_1\,\sin^{n-2}\varphi_1\mathrm{e}^{-\mathrm{i}k(\Delta t-\Delta x\cos\varphi_1)}\mathrm{e}^{-k\epsilon} \\
&= \frac{1}{\pi^{\frac{n+1}{2}}2^n\Gamma\left(\frac{n-1}{2}\right)}\int_0^\infty \mathrm{d}k\,k^{n-2}\int_{-1}^1 \mathrm{d}u\,\left(1-u^2\right)^{\frac{n-3}{2}}\mathrm{e}^{-\mathrm{i}k(\Delta t-\Delta x u)}\mathrm{e}^{-k\epsilon} \\
&= \frac{\Gamma\left(\frac{n-1}{2}\right)}{4\pi^{\frac{n+1}{2}}}\left(\epsilon+\mathrm{i}\Delta t\right)^{1-n}\left(1+\frac{\Delta x^2}{\left(\epsilon+\mathrm{i}\Delta t\right)^2}\right)^{\frac{1-n}{2}} \\
&= \frac{\Gamma\left(\frac{n-1}{2}\right)}{4\pi^{\frac{n+1}{2}}}\frac{1}{\left(\left(\epsilon+\mathrm{i}\Delta t\right)^2+\Delta x^2\right)^{\frac{n-1}{2}}} \\
&= \frac{\Gamma\left(\frac{n-1}{2}\right)}{4\pi^{\frac{n+1}{2}}}\frac{1}{\left(2\mathrm{i}\epsilon\Delta t-\Delta t^2+\Delta x^2\right)^{\frac{n-1}{2}}}.
\end{aligned} \tag{2.34}$$

Here, in the spherical integration, we assumed that $n \geq 3$, however the result holds for

$n \geq 2$ as well. (Whereas $n = 1$ will be discussed below in equation (2.43).) In the last step ϵ^2 was dropped in the denominator since it is subdominant to $2\mathrm{i}\epsilon\Delta t$ and hence does not affect the behaviour of the distribution.

For even spacetime dimensions we can use the Sokhotskii formulae to express the Wighmann function in terms of the Dirac δ-distribution. We have [12]

$$\frac{1}{(x \pm \mathrm{i}\epsilon)^k} = \mathcal{P}\frac{1}{x^k} \pm \mathrm{i}\pi\frac{(-1)^k}{(k-1)!}\delta^{(k-1)}(x) \text{ for } k = 1, 2, 3, ... \tag{2.35}$$

where $\mathcal{P}$ denotes the Cauchy principal value and $\delta^{(k)}(x)$ is the k-th order distributional derivative of the Dirac δ-distribution $\delta(x) = \delta^{(0)}(x)$, i.e.,

$$\int_{-\infty}^{\infty} \mathrm{d}x\, f(x)\delta^{(k)}(x) = (-1)^k f^{(k)}(0), \tag{2.36}$$

as explained in detail in chapter 2.2.B of [12]. Applying this to even spacetime dimensions, i.e., for $n = 3, 5, 7, ...$, we can rewrite the Wightmann function as

$$\begin{aligned}
&\langle 0|\, \phi(t + \Delta t, \vec{x} + \Delta\vec{x})\phi(t, \vec{x})\, |0\rangle \\
&= \frac{\Gamma\left(\frac{n-1}{2}\right)}{4\pi^{\frac{n+1}{2}}} \frac{1}{\left(2\mathrm{i}\epsilon\Delta t - \Delta t^2 + \Delta x^2\right)^{\frac{n-1}{2}}} \\
&= \frac{\Gamma\left(\frac{n-1}{2}\right)}{4\pi^{\frac{n+1}{2}}} \left(\mathcal{P}\frac{1}{\left(-\Delta t^2 + \Delta x^2\right)^{\frac{n-1}{2}}} + \mathrm{sgn}(\Delta t)\mathrm{i}\pi\frac{(-1)^{\frac{n-1}{2}}}{\left(\frac{n-3}{2}\right)!}\delta^{\left(\frac{n-3}{2}\right)}\left(-\Delta t^2 + \Delta x^2\right) \right).
\end{aligned} \tag{2.37}$$

Being twice the imaginary part of the Wightmann function, the commutator in these dimensions is

$$[\phi(t + \Delta t, \vec{x} + \Delta\vec{x}), \phi(t, \vec{x})] = \mathrm{i}\frac{(-1)^{\frac{n-1}{2}}\,\mathrm{sgn}(\Delta t)}{2\pi^{\frac{n-1}{2}}}\delta^{\left(\frac{n-3}{2}\right)}\left(-\Delta t^2 + \Delta x^2\right). \tag{2.38}$$

Thus the commutator of the field in even spacetime dimensions, $n + 1 \geq 4$, has (singular) support only on the boundary of the lightcone and vanishes between points that are not null separated. This means that signals propagate only at the speed of light in these dimensions, and the Huygens principle is satisfied. The case that we will consider as a frequent example in later chapters is 3+1D Minkowski space. Here we have

$$[\phi(t + \Delta t, \vec{x} + \Delta\vec{x}), \phi(t, \vec{x})] = -\mathrm{i}\frac{\mathrm{sgn}(\Delta t)}{2\pi}\delta\left((-\Delta t + \Delta x)(\Delta t + \Delta x)\right)$$

$$= \frac{\mathrm{i}}{4\pi\Delta x}\left(\delta(\Delta t+\Delta x)-\delta(-\Delta t+\Delta x)\right). \tag{2.39}$$

In odd spacetime dimensions ($n = 2, 4, 6, ...$) the Wightmann function

$$\langle 0|\,\phi(t+\Delta t,\vec{x}+\Delta\vec{x})\phi(t,\vec{x})\,|0\rangle = \frac{\Gamma\left(\frac{n-1}{2}\right)}{4\pi^{\frac{n+1}{2}}}\frac{1}{\left(\sqrt{2\mathrm{i}\epsilon\Delta t-\Delta t^2+\Delta x^2}\right)^{n-1}} \tag{2.40}$$

is singular on the lightcone as well. Away from the lightcone it is purely imaginary for timelike separations and purely real for spacelike separations

$$\langle 0|\,\phi(t+\Delta t,\vec{x}+\Delta\vec{x})\phi(t,\vec{x})\,|0\rangle = \frac{\Gamma\left(\frac{n-1}{2}\right)}{4\pi^{\frac{n+1}{2}}}\begin{cases}\frac{1}{\left(\sqrt{-\Delta t^2+\Delta x^2}\right)^{n-1}}, & \text{if } \Delta x^2>\Delta t^2\\ \frac{-\mathrm{i}\,\mathrm{sgn}(\Delta t)}{\left(\sqrt{\Delta t^2-\Delta x^2}\right)^{n-1}}, & \text{if } \Delta t^2>\Delta x^2\end{cases}. \tag{2.41}$$

In particular this means that the commutator of the field has support even inside the lightcone for timelike separations. This means that the field amplitude at any given point in spacetime is dependent not only on the boundary of its past lightcone but also on the lightcone's interior. Vice versa, this means that signals can propagate even slower than light in the massless field, and the Huygens principle is not satisfied.

Among the odd-dimensional Minkowski spacetimes, we will in particular consider scenarios in 2+1D Minkowski spacetime. Here the field commutator evaluates to

$$[\phi(t+\Delta t,\vec{x}+\Delta\vec{x}),\phi(t,\vec{x})] = \frac{1}{4\pi^2}\frac{-\mathrm{i}\,\mathrm{sgn}(\Delta t)}{\sqrt{\Delta t^2-\Delta x^2}}\Theta(\Delta t^2-\Delta x^2). \tag{2.42}$$

The most extreme example of timelike support of the commutator we find in 1+1D Minkowski space. However, one difficulty here is that the Wightmann function of a massless field in 1+1 dimensions cannot be treated the same way as above since it is infrared divergent for $k \to 0$. However, this divergence only affects the real part of the Wightmann function. The imaginary part is still finite and given by

$$[\phi(t,x),\phi(t',x')] = \frac{\mathrm{i}}{2}\,\mathrm{sgn}\,(t'-t)\,\theta\left((t-t')^2-(x-x')^2\right). \tag{2.43}$$

This can be calculated readily from the expansion of the field operator in 1+1 dimensions, as done in the appendix of [56], or from the Wightmann function of the massive Klein-Gordon field in the zero mass limit, as done in [80].

The commutator being constant in the entire future lightcone means that signals imprinted in the amplitude of the field reach arbitrarily far into the future ligthcone, without diluting at all. We will consider the case of 1+1D Minkowski space in detail in Section 2.4. In the following we first evaluate the Wightmann function inside a Dirichlet cavity, which shows that the commutator of the field there corresponds closely to the commutator in free 1+1D Minkowski space that we just calculated.

2.3.2 Wightmann Function in one-dimensional Dirichlet cavity

Note: This section consists of adapted and expanded passages from [38].

Inside a (1+1)-dimensional cavity with vanishing Dirichlet boundary conditions the field operator can be expanded as

$$\phi(t,x) = \sum_{j=1}^{\infty} \frac{1}{\sqrt{j\pi}} \sin(j\pi x/L) \left(a_j \mathrm{e}^{-\mathrm{i}\frac{j\pi}{L}t} + a_j^\dagger \mathrm{e}^{\mathrm{i}\frac{j\pi}{L}t} \right). \tag{2.44}$$

The length of the cavity imposes an infrared cutoff on the field. This avoids the infrared divergence that appeared in the Wightmann function in free (1+1)-dimensional Minkowski space. The field operator expansion yields an analytically summable expression for the Wightmann function of the field, which is

$$\begin{aligned} \langle 0| \phi(t,x)\phi(t',x') |0\rangle &= \sum_{j=1}^{\infty} \frac{1}{j\pi} \sin(j\pi x/L) \sin(j\pi x'/L) \mathrm{e}^{\mathrm{i}j\pi(t'-t)/L} \\ &= \frac{1}{4\pi} \left(\ln\left(1 - \mathrm{e}^{-\mathrm{i}\pi\frac{t-t'-x-x'}{L}}\right) - \ln\left(1 - \mathrm{e}^{-\mathrm{i}\pi\frac{t-t'-x+x'}{L}}\right) \right. \\ &\qquad \left. - \ln\left(1 - \mathrm{e}^{-\mathrm{i}\pi\frac{t-t'+x-x'}{L}}\right) + \ln\left(1 - \mathrm{e}^{-\mathrm{i}\pi\frac{t-t'+x+x'}{L}}\right) \right). \end{aligned} \tag{2.45}$$

The imaginary part of the Wightmann function, which yields the commutator, has a particularly simple structure

$$\begin{aligned} [\phi(t,x), \phi(t',x')] &= -\sum_{j=1}^{\infty} \frac{2\mathrm{i}}{\pi j} \sin(j\pi x/L) \sin(j\pi x'/L) \sin\left(j\pi(t-t')/L\right) \\ &= \frac{\mathrm{i}}{2} \left(\left\lfloor \frac{t-t'+x-x'}{2L} \right\rfloor + \left\lfloor \frac{t-t'-x+x'}{2L} \right\rfloor \right. \\ &\qquad \left. - \left\lfloor \frac{t-t'+x+x'}{2L} \right\rfloor - \left\lfloor \frac{t-t'-x-x'}{2L} \right\rfloor \right) \end{aligned} \tag{2.46}$$

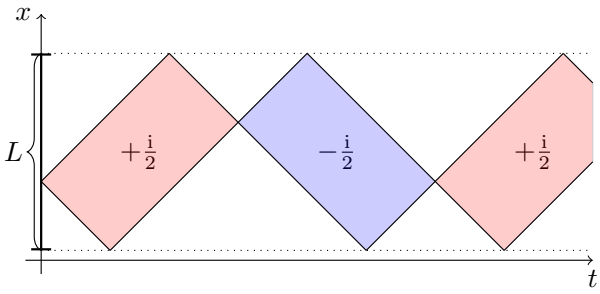

Figure 2.1: [38] Sketch of $[\phi(t=0,x_1),\ \phi(t,x)]$, the commutator of a massless Klein-Gordon field in a one-dimensional cavity of length L with Dirichlet boundary conditions. In the red areas it takes the value $+\frac{\mathrm{i}}{2}$ and in the blue areas it takes the value $-\frac{\mathrm{i}}{2}$.

where $\lfloor x \rfloor = \mathrm{floor}(x)$ denotes the floor function.

As seen in Figure 2.1 the commutator inside the cavity resembles very much the commutator in free (1+1)-dimensional Minkowski space with the only difference that the lightcone structure is reflected off the cavity walls. When (t,x) and (t',x') are close, the commutator is identical to the commutator in (1+1)-dimensional Minkowski space: It vanishes at spacelike separations, and it takes the value $+\frac{\mathrm{i}}{2}$ when (t,x') lies in the future lightcone of (t,x). For large separations, the lightcone structure is reflected by the cavity walls, such that the commutator is periodic in $t'-t$ with periodicity $2L$.

In particular, this shows that timelike signalling is possible inside Dirichlet cavities as well. The phenomenon of timelike signalling in massless fields is therefore not dependent on the zero mode of the field, because the zero mode is not present in the Dirichlet cavity.

The real part of the Wightmann function, yiedling the anti-commutator of the field, inside the cavity is

$$\begin{aligned}
&\langle 0|\left(\phi(t,x)\phi(t',x')+\phi(t',x')\phi(t,x)\right)|0\rangle \\
&= \frac{1}{4\pi}\left(\ln\left(1-\cos\left(\pi\frac{t-t'-x-x'}{L}\right)\right)-\ln\left(1-\cos\left(\pi\frac{t-t'-x+x'}{L}\right)\right)\right. \\
&\qquad \left.-\ln\left(1-\cos\left(\pi\frac{t-t'+x-x'}{L}\right)\right)+\ln\left(1-\cos\left(\pi\frac{t-t'+x+x'}{L}\right)\right)\right). \qquad (2.47)
\end{aligned}$$

It shows that the vacuum correlations of the field, through the real part of the Wightmann function, contain information about the total length of the cavity: For example, the equal-time correlations between the field operators at two points in the cavity do not only depend on the distance between the two points but also on their distance to the cavity walls. This

is because the vacuum state of the field is not translationally invariant due to the Dirichlet boundary conditions.

2.4 Massless field in 1+1D Minkowski space

Note: This section consists of adapted and expanded passages from [38].

In 1+1D Minkowski spacetime the decoupling of information propagation from energy propagation can readily be observed from the structure of the field operators themselves. This is because there are two particularly simple solutions for the field and its conjugate momentum which elucidate the propagation of signals and energy within the field. The first one, the d'Alembert solution, expresses the field operator and its conjugate at any point in spacetime in terms of the operators on any spatial slice of constant time. The second one expresses the field and its conjugate in terms of left- and right-moving parts of the field operator and its conjugate.

These solutions explain why energy injected into the field by a sender propagates away at the speed of light, whereas the sender can change the field's amplitude in the entire future lightcone.

The reason is that the field's energy density operator at a given spacetime point can be expressed in terms of field operators located on the boundary of the point's past lightcone. However, the decomposition of the field amplitude at a given point involves operators acting on the field inside the point's entire past lightcone. Hence the field amplitude at a given point contains information from its entire past lightcone.

Therefore, a receiver that misses all the lightrays emanating from the sender, cannot collect any of the energy that the sender injected into the field. However, the receiver can still obtain information from the sender that is imprinted into the field's amplitude.

In (1+1)-dimensional Minkowski space the massless Klein-Gordon equation simplifies to the well-known wave equation

$$\left(\frac{\partial^2}{\partial t^2} - \frac{\partial^2}{\partial x^2}\right)\phi(t,x) = 0. \tag{2.48}$$

The expansion of the field operator in terms of plane wave field modes reads

$$\phi(t,x) = \int_{-\infty}^{\infty} \mathrm{d}k \, \frac{1}{\sqrt{4\pi|k|}} \left(\mathrm{e}^{-\mathrm{i}(|k|t-kx)} a_k + \mathrm{e}^{\mathrm{i}(|k|t-kx)} a_k^\dagger\right). \tag{2.49}$$

Here we used that n-dimensional momentum integral expression are translated into 1+1D Minkowski space, by replacing $\int \mathrm{d}^n\vec{k} \to \int_{-\infty}^{\infty} \mathrm{d}k$ and $|\vec{k}| = k \to |k|$.

Because the collection of all field operators $\phi(x,t)$ and their canonical conjugate momentum $\pi(t,x) = \partial_t\phi(t,x)$ located on a Cauchy hypersurface forms a complete set of observables [84], any observable acting on the field can be expressed in terms of field operators $\phi(t,x)|_{t=t^*}$ and $\pi(t,x)|_{t=t^*}$ located only on an arbitrarily chosen slice of constant time $t = t^*$. In particular we have the so called d'Alembert solution which work both for classical fields as well as for the quantum field operators [34]:

$$\phi(t,x) = \frac{1}{2}\left(\phi(0,x+t) + \phi(0,x-t) + \int_{x-t}^{x+t} \mathrm{d}y\, \pi(0,y)\right) \tag{2.50}$$

$$\pi(t,x) = \frac{1}{2}\left(\pi(0,x+t) + \pi(0,x-t) + \partial_x\phi(0,x+t) - \partial_x\phi(0,x-t)\right). \tag{2.51}$$

Note that these formulae are time translation invariant, and thus for $s < t$

$$\phi(t,x) = \frac{1}{2}\left(\phi(s,x+t-s) + \phi(s,x-t+s) + \int_{x-t+s}^{x+t-s} \mathrm{d}y\, \pi(s,y)\right) \tag{2.52}$$

and correspondingly for $\pi(t,x)$. We see right from this formula, that the field amplitude operator $\phi(t,x)$ is equal to a composition of field operators on earlier time slices covering every point in the past lightcone. Therefore the field amplitude at a particular spacetime point depends on the field's history inside the point's entire past lightcone. It can thus be used to receive signals from a timelike separated sender. In contrast, the conjugate $\pi(t,x)$ is composed of operators located only on the boundary of the lightcone.

The energy density of the field, i.e. the T_{00}-component of the energy-momentum tensor, reads [8]

$$T_{00}(t,x) = \frac{1}{2}\left((\partial_t\phi(t,x))^2 + (\partial_x\phi(t,x))^2\right) = \frac{1}{2}\left((\pi(t,x)^2 + (\partial_x\phi(t,x))^2\right). \tag{2.53}$$

From equation (2.50) above we have

$$\partial_x\phi(t,x) = \frac{1}{2}\left(\partial_x\phi(0,x+t) + \partial_x\phi(0,x-t) + \pi(0,x+t) - \pi(0,x-t)\right), \tag{2.54}$$

together with (2.51) this gives

$$T_{00}(t,x) = \frac{1}{4}\left((\pi(0,x+t) + \partial_x\phi(0,x+t))^2 + (\pi(0,x-t) - \partial_x\phi(0,x-t))^2\right). \tag{2.55}$$

The energy density of the field at any point in spacetime can thus be written in terms of field operators located only on the boundary of the point's lightcone. Thus the energy density measured in the field at one point in spacetime could only have been detected by earlier measurements on the boundary of the point's lightcone. Conversely, any energy density injected into the field at some location will only be observable along the boundary of the future lightcone of the point. This means that no energy can be carried by the field between timelike separated points in (1+1)-dimensional Minkowski space.

An alternative explanation for the decoupling of the flow of information from the flow of energy can be given by separating the field into a left-moving and a right-moving sector. The two terms on the right hand side of equation (2.55), which sum up to give the energy density, then have a direct interpretation in terms of the energy flux from the left- and right-moving sectors of the field.

To see this, we split the field operator into a left- and a right moving part

$$\phi(t,x) = \phi_+(t,x) + \phi_-(t,x) \tag{2.56}$$

with

$$\begin{aligned}
\phi_-(t,x) &= \int_0^\infty \mathrm{d}k\, \frac{1}{\sqrt{4\pi|k|}}\left(\mathrm{e}^{-\mathrm{i}(|k|t+kx)}a_k + \mathrm{e}^{\mathrm{i}(|k|t+kx)}a_k^\dagger\right) \\
&= \int_0^\infty \mathrm{d}k\, \frac{1}{\sqrt{4\pi k}}\left(\mathrm{e}^{-\mathrm{i}k(t-x)}a_{+k} + \mathrm{e}^{\mathrm{i}k(t-x)}a_{+k}^\dagger\right) \\
\phi_+(t,x) &= \int_{-\infty}^0 \mathrm{d}k\, \frac{1}{\sqrt{4\pi|k|}}\left(\mathrm{e}^{-\mathrm{i}(|k|t+kx)}a_k + \mathrm{e}^{\mathrm{i}(|k|t+kx)}a_k^\dagger\right) \\
&= \int_0^\infty \mathrm{d}k\, \frac{1}{\sqrt{4\pi k}}\left(\mathrm{e}^{-\mathrm{i}k(t+x)}a_{-k} + \mathrm{e}^{\mathrm{i}k(t+x)}a_{-k}^\dagger\right)
\end{aligned} \tag{2.57}$$

The conjugate momentum is correspondingly split into

$$\pi(t,x) = \pi_+(t,x) + \pi_-(t,x) \tag{2.58}$$

with

$$\pi_\pm(t,x) = \partial_t \phi_\pm(t,x). \tag{2.59}$$

These operators depend only on the so called lightcone coordinates $x_\pm = t \pm x$. E.g., $\phi_-(t,x) = \phi_-(u,y)$ if and only if $t - x = u - y$, and ϕ_- are therefore called the right moving field operators.

With these definitions follows

$$\partial_x \phi_\pm(t,x) = \pm \partial_t \phi_\pm(t,x) = \pm \pi_\pm(t,x). \tag{2.60}$$

So $\pi(t,x) \pm \partial_x \phi(t,x) = 2\pi_\pm(t,x)$, and

$$T_{00}(t,x) = (\pi_+(t,x))^2 + (\pi_-(t,x))^2 . \tag{2.61}$$

Which shows that the energy density of a massless Klein-Gordon field is the sum of the left and right moving energy flux.

Expressing the field operator in terms of left- and right-movers at first makes it less evident how signals can propagate slower than the speed of light. After all, the field operator at any point is given as the sum of its left and right moving part both of which are propagating strictly at the speed of light. The resolution is that the left and right moving field operators are not localised operators, but the commutator between different left moving (or different right moving) field operators is not zero.

When calculating the commutators of the left- and right-moving operators we directly see that operators acting on different sectors of the field always commute. For operators acting on the same sector we find

$$[\phi_\pm(t,x), \phi_\pm(u,y)] = \frac{\mathrm{i}}{2\pi} \int_0^\infty \mathrm{d}k \, \frac{\sin\left(k\left((u-t) \pm (y-x)\right)\right)}{k} = \frac{\mathrm{i}}{4} \mathrm{sgn}((u-t) \pm (y-x)) \tag{2.62}$$

$$[\phi_\pm(t,x), \pi_\pm(u,y)] = \frac{\mathrm{i}}{2\pi} \int_0^\infty \mathrm{d}k \, \cos\left(k\left((u-t) \pm (y-x)\right)\right) = \frac{\mathrm{i}}{2} \delta((u-t) \pm (y-x)) \tag{2.63}$$

$$[\pi_\pm(t,x), \pi_\pm(u,y)] = \frac{\mathrm{i}}{2\pi} \int_0^\infty \mathrm{d}k \, \sin\left(k\left((u-t) \pm (y-x)\right)\right) = -\frac{\mathrm{i}}{2} \delta'((u-t) \pm (y-x)) \tag{2.64}$$

where $\delta'(x)$ denotes the derivative of the Dirac δ-distribution.

At first sight, the appearance of the commutator $[\pi_\pm(t,x),\pi_\pm(u,y)] = -\frac{\mathrm{i}}{2}\delta'((u-t)\pm(y-x))$ might seem contradictory, since it has its singular support where $u=t$ and $x=y$. Would this imply that the operator $\pi_\pm(t,x)$ does not commute with itself? Here it is necessary to remember that the field operators actually are operator valued distributions. In order to obtain an operator these distributions need to be smeared out by a test function, say $\int_{-\infty}^{\infty}\mathrm{d}x\, f(x)\pi_\pm(0,x)$. The operator we now obtained does commute with itself, as it should.

$$\begin{aligned}
&\left[\int_{-\infty}^{\infty}\mathrm{d}x\, f(x)\pi_\pm(0,x),\int_{-\infty}^{\infty}\mathrm{d}y\, f(y)\pi_\pm(0,y)\right]\\
&=\int_{-\infty}^{\infty}\mathrm{d}x\int_{-\infty}^{\infty}\mathrm{d}y\, f(x)f(y)\frac{-\mathrm{i}}{2}\delta'(\pm(y-x))\\
&=\frac{-\mathrm{i}}{4}\int_{-\infty}^{\infty}\mathrm{d}v\int_{-\infty}^{\infty}\mathrm{d}w\, f((v+w)/2)f((v-w)/2)\delta'(\pm w)\\
&=\frac{\pm\mathrm{i}}{4}\int_{-\infty}^{\infty}\mathrm{d}v\,\frac{\mathrm{d}}{\mathrm{d}w}\, f((v+w)/2)f((v-w)/2)|_{w=0}\\
&=\frac{\pm\mathrm{i}}{8}\int_{-\infty}^{\infty}\mathrm{d}v\,\left(f'(v/2)f(v/2)-f(v/2)f'(v/2)\right)=0
\end{aligned}\tag{2.65}$$

Where we used the coordinate change $v=x+y, w=y-x$, such that $x=\frac{1}{2}(v-w), y=\frac{1}{2}(v+w)$ and $\mathrm{d}x\,\mathrm{d}y=\frac{1}{2}\mathrm{d}v\,\mathrm{d}w$.

The commutation relations above imply that in models which allow observers to directly couple to the $\phi_\pm(t,x)$ operators, signaling would be possible between arbitrary points in spacetime. This problem does not occur for observers that only couple to the canonically conjugate operators. In fact, even if just one of two parties couples only to the operators $\pi_\pm(t,x)$ signaling is possible only between lightlike separated points in spacetime due to the singular support on the lightcone's boundary of commutators involving $\pi_\pm(t,x)$.

2.5 Conclusion - Timelike Propagation and Huygens Principle

Two-dimensional, i.e., 1+1D Minkowski spacetime marks the most distinct case of a timelike support of the commutator. Typically, the commutator decays with increasing distance inside the future lightcone. This is also what we observed above for odd-dimensional Minkowski spacetimes, such as 2+1D Minkowski spacetime.

In most spacetimes, in particular also four-dimensional ones, the Huygens principle does not hold. In fact, it has proven to be a challenging and rich problem to identify the classes of spacetimes where Huygens principle does apply [22, 62, 63]. The calculation of the commutator of a quantum field, or the Greens function of a classical field, with timelike support can be very involved and is not always possible in a closed form. For the physically very interesting case of expanding FLRW universes solutions are known [17, 68], and, in works following up on the results presented in this thesis, timelike signalling has been studied in these and other cosmological scenarios [10, 11]. The Greens function in black hole spacetimes is more complicated, and can be expressed in terms of expansions [18, 87] that can be evaluated numerically.

For the purpose of this thesis, we will study signalling in 2+1D Minkowski space as the prototype example of a timelike supported, but decaying commutator of the field. In spacetimes where the commutator of the field is non-constant inside the future lightcone also the fields energy density can propagate slower than the speed of light. To see this, consider the commutator between the field and its conjugate momentum. Since the conjugate momentum is given by the time derivative of the field, we have

$$\begin{aligned}[\phi(t,\vec{x}),\pi(u,\vec{y})] &= [\phi(t,\vec{x}),\partial_u\phi(u,\vec{y})] = \partial_u\left[\phi(t,\vec{x}),\phi(u,\vec{y})\right] \\ &\propto \partial_u \frac{1}{\sqrt{(t-u)^2-|\vec{x}-\vec{y}|^2}} = \frac{(u-t)}{\left((t-u)^2-|\vec{x}-\vec{y}|^2\right)^{3/2}}. \end{aligned} \tag{2.66}$$

which shows that acting on the field through the field operator in one point affects the field's derivative, and thus the field's energy density, inside the future lightcone. Hence, timelike signals arising from decaying commutators are accompanied by some flow of energy. However, this flow of energy decays at a higher order in the spacetime distance.

This leads to an asymptotic decoupling of information transmission from energy transmission, in the sense that the ratio of propagating signalling strength to propagating field energy density diverges. As such this is only a qualitative observation at this point. We will be able to quantify this consideration in the next chapter, by the introduction of a

concrete model of signalling device by which sender and receiver couple locally to the field along their worldlines.

This approach yields a more operational approach to signal and energy propagation in quantum fields. And, it incorporates naturally the impact of the quantum fluctuations of the field, encoded in the real part of the Wightmann function. These constitute a source of noise against which the signal may have to compete.

Chapter 3

The quantum channel between Unruh-DeWitt detectors

To study the propagation of information, and quantum information from one point in spacetime to another, we need a description of sender and receiver that are localized in spacetime. This, however, is difficult within the formalism of relativistic quantum field theory, because of the lack of a position operator.

To circumvent this problem, we draw inspiration from the interaction between atoms and quantum fields. There, the atom's internal states can be described as a quantum-mechanical system with its own Hilbert space, that is coupled to the field through the field operator at some fixed (non-quantized) position. The idea we follow here, is to build a prototype model of wireless quantum communication analogously [19, 21, 20]. To this end, we equip sender and receiver with simplified model atoms (two-level system or harmonic oscillators) as quantum signalling devices, which can couple to the field along the sender's and observer's worldlines.

Sender and receiver have direct control only, i.e., can manipulate and perform measurements, only on their own signalling device. In particular, they need to use the signalling device to act on the quantum field, or to probe it. The sender has to encode their message in the initial state of their signalling device before coupling it to the field. Analogously, the receiver has to recover the message only from the final state of their own detector after coupling it to the field. Thus, the field only serves as a medium for the signal from the sender to the receiver.

All influence that the sender, Alice, has on the receiver, Bob, is encapsulated in the map from Alice's initial state to Bob's final state. Such maps between the input and

output states of physical processes are known as quantum channels in the field of quantum information. There they are of great interest, since they capture a system's ability to process information encoded in quantum systems. Accordingly, a great range of methods has been developed for the study of their information theoretical channel capacities [64, 86]. These results can be directly applied to our framework, to explore the information capacities allowed for by quantum fields.

This approach is very general, and can be applied and compared to results for signal propagation in other quantum systems as well. Let us therefore briefly review how the quantum channel arises mathematically, before specifying a particular type of signalling device.

The total Hilbert space $\mathcal{H}$ of the system is given by the tensor product of the sender's, the field's and the receiver's Hilbert spaces.

$$\mathcal{H} = \mathcal{H}_{\mathcal{A}} \otimes \mathcal{H}_{\mathcal{F}} \otimes \mathcal{H}_{\mathcal{B}} \tag{3.1}$$

Before any interaction between the devices and the field take place, we assume that the devices and the field are in a product state:

$$\rho_0 = \rho_{\mathcal{A},0} \otimes \rho_{\mathcal{F},0} \otimes \rho_{\mathcal{B},0}. \tag{3.2}$$

The time evolution of the system under the couplings between the signalling devices and the field is given by some unitary operator U, that depends on the details of the interaction. The final state of the total system, after the interactions have taken place, is thus

$$\rho = U\rho_0 U^\dagger \tag{3.3}$$

which, in general, will be a non-separable state. Since the receiver only has access to the state of his own signalling device, we take the partial trace over the sender's Hilbert space and the field's Hilbert space to obtain the, generally mixed, final state of the receiver.

$$\rho_{\mathcal{B}} = \mathrm{Tr}_{\mathcal{A},\mathcal{F}}\, \rho = \mathrm{Tr}_{\mathcal{A},\mathcal{F}}\, U\rho_0 U^\dagger. \tag{3.4}$$

The quantum channel map from the sender's initial state to the receiver's final state is therefore given by

$$\xi : \rho_{\mathcal{A},0} \mapsto \rho_{\mathcal{B}} = \mathrm{Tr}_{\mathcal{A},\mathcal{F}}\, U\rho_0 U^\dagger. \tag{3.5}$$

To model the signalling devices we will use the Unruh-DeWitt particle detector model, which is a widely used tool in the study of quantum field theory in curved spacetimes, and

relativistic quantum information. This framework was first considered in [19, 21, 20]. We begin by a general review of the framework, and of the Unruh-DeWitt particle detector model in the first two sections. Then we discuss the general structure of the channel and how it results from a perturbative treatment of the system's time evolution. Here we generalize earlier results from [19] and, in particular, identify superpositions of energy eigenstates as the sender's optimal choice of signalling states. We go on to derive the Bloch picture representation of the channel. Upon this we base the subsequent calculation of the channel's classical capacity.

The key observation of this chapter is that the commutator of the field operator is the object that decides between which points in spacetime signalling is possible: It was shown in [19] that in order to send signals from one point in spacetime to another point via the quantum field, it is necessary that the commutator does not vanish. Here we observe, that this is also sufficent: We find that a relatively simple, Fourier-type integral over the commutator of the field yields the leading order behaviour of the signalling strength and the channel capacity between two Unruh-DeWitt detectors.

3.1 Unruh-DeWitt particle detectors

In general spacetimes different observers may perceive the particle content of a given quantum field state differently. In fact, the concept of particles, as an excitation of a particular field mode, is an observer-dependent concept, much like time is. This is because just as observers may use different coordinates to parametrize spacetime, they may also use different sets of modes to expand the field operator.

This means that what is the vacuum state of the field with respect to one observer, can be an excited state with respect to another observer. An example of this, known as the Unruh effect, is that in Minkowski spacetime the vacuum state of a quantum field according to intertial observers in Minkowski space is a thermally excited state from the point of view of a uniformly accelerated observer [81].

The question how many particles are present in a given quantum field state is therefore not a well defined question to ask since the answer is not unique. Instead, we can only ask how many particles a particular observer will detect in a given field state. This question can be approached in a natural and operational way using model particle detectors. These model the interaction of a localized observer with the quantum field along a given worldline.

The detector model used most widely is attributed to Unruh [81] and DeWitt [23]. It can be thought of as a simple model for the interaction of an atom with a background

quantum field. In its simplest form the *Unruh-DeWitt particle detector* consists of just a two-level system. Typically, the detector is assumed to start out in his ground state before it is coupled to the field. Through the interaction with the field, the detector can be excited, i.e., its state can acquire some overlap with the excited state. The detector is said to have detected a particle, when a measurement performed on the detector finds the detector in its excited state.

The model treats the atom's internal degrees of freedom as a quantum-mechanical system, and also the coupling to the field along the detector's worldline is described fully unitary. However, the atom's worldline, i.e., its position in spacetime, is not quantized but corresponds to the fixed classical worldline of a given observer.

The interaction Hamiltonian which couples the detector and the field is proportional to the product of the detector's so called monopole operator and the field operator at the detector's location. Hence in the Schrödinger picture it is proportional to

$$H_{\text{int}} \propto m \otimes \phi(\vec{x}) = (|e\rangle\langle g| + |g\rangle\langle e|) \otimes \phi(\vec{x}). \tag{3.6}$$

where $\{|g\rangle, |e\rangle\}$ is the energy eigenbasis of the detector, the monopole operator is $m = |e\rangle\langle g| + |g\rangle\langle e|$, and $\phi(\vec{x})$ is the field operator of a scalar Klein-Gordon field.

We will use the Dirac interaction picture. In this picture the operators evolve according to their free Hamiltonians, and the state of the combined detector-field system evolves only under the action of the interaction Hamiltonian. The free Hamiltonian of the detector two-level system is $H_d = \Omega\,|e\rangle\langle e|$. Accordingly, in the Heisenberg picture, the monopole operator reads

$$m(\tau) = \mathrm{e}^{\mathrm{i}H_d\tau}\,(|e\rangle\langle g| + |g\rangle\langle e|)\,\mathrm{e}^{-\mathrm{i}H_d\tau} = \mathrm{e}^{\mathrm{i}\Omega\tau}\,|e\rangle\langle g| + \mathrm{e}^{-\mathrm{i}\Omega\tau}\,|g\rangle\langle e| \tag{3.7}$$

where τ is the proper time of the detector along its relativistic wordline. With the Heisenberg picture field operator $\phi(t, \vec{x})$ the interaction Hamiltonian for the Dirac interaction picture then is

$$H_{\text{int}}(\tau) \propto \left(\mathrm{e}^{\mathrm{i}\Omega\tau}\,|e\rangle\langle g| + \mathrm{e}^{-\mathrm{i}\Omega\tau}\,|g\rangle\langle e|\right) \otimes \phi\left(t(\tau), \vec{x}(\tau)\right). \tag{3.8}$$

In order to obtain the full Unruh-DeWitt interaction Hamiltonian in the form which we will be using only two more factors are needed in front of this term: The coupling constant λ and a switching function $\eta(\tau)$. Together with these the full interaction Hamiltonian reads

$$H_{\text{int}}(\tau) = \lambda\,\eta(\tau)\left(\mathrm{e}^{\mathrm{i}\Omega\tau}\,|e\rangle\langle g| + \mathrm{e}^{-\mathrm{i}\Omega\tau}\,|g\rangle\langle e|\right) \otimes \phi\left(t(\tau), \vec{x}(\tau)\right). \tag{3.9}$$

The switching function is used to switch the coupling of detector and the field on and off. It is a real valued function taking values between 0 and 1

$$\eta(\tau) \in [0,1]. \tag{3.10}$$

In general, the switching function needs to be a smooth and compactly supported function in order to guarantee well-defined behaviour of the model, and to avoid divergent results when coupling a single detector to the field [33, 54, 74]. However, as far as the leading order effects arising from signalling between two detectors are concerned, we will be able to even use sharp switching functions, which we define as

$$\chi_{[0,T]}(\tau) = \begin{cases} 1 \text{ if } \tau \in [0,T] \\ 0 \text{ else} \end{cases} . \tag{3.11}$$

These functions model a sharp, instantaneous switching of the detector, with the switch-on happening at proper time $\tau = 0$ and the switch-off at proper time $\tau = T$.

Even when using smooth and compactly supported switching functions certain divergences can occur. (In particular, if we allow for arbitrary initial states of the detector, as we discuss on Page 43.) These are due to the field operator $\phi(t, \vec{x})$ being an operator valued distribution which needs to be integrated against a test function. To avoid all of these divergences one can smear out the detector in space. (See [53], and references therein.) To this end the spatial profile of the detector is modelled by a profile function $f(\tau, \vec{x})$, such that the smeared out interaction Hamiltonian reads

$$H_{\text{int}}(\tau) = \lambda\, \eta(\tau) \left(\mathrm{e}^{\mathrm{i}\Omega\tau} \, |e\rangle\langle g| + \mathrm{e}^{-\mathrm{i}\Omega\tau} \, |g\rangle\langle e| \right) \otimes \int \mathrm{d}^n\vec{x}\, f(\tau, \vec{x})\, \phi\left(t(\tau), \vec{x}\right). \tag{3.12}$$

Non-smeared detectors, i.e., pointlike detectors, then correspond to having a Dirac-delta like profile function $f(\vec{x}) = \delta(\vec{x})$.

Dimensionality of the coupling constant

The coupling constant λ is typically used as the perturbative parameter in perturbative treatments of the time evolution. When doing so, we need to keep in mind that, dependent on the spacetime dimension, λ may not be a dimensionless parameter.

This is, because in an $(n+1)$-dimensional spacetime the Klein-Gordon field has mass dimension

$$[\phi] = \frac{n-1}{2} \tag{3.13}$$

where $[\Omega] = 1$. This can be read of from the field's Lagrangian density $\mathcal{L} = \frac{1}{2}\eta^{\mu\nu}\partial_\mu\phi\partial_\nu\phi$ in (2.3), or from the constant time commutation relation $[\phi(t,\vec{x}), \pi(t,\vec{y})] = \delta(\vec{x}-\vec{y})$. The interaction Hamiltonian needs to be of mass dimension $[H_{\text{int}}] = 1$. Therefore, the dimension of the coupling constant is

$$[\lambda] = \frac{3-n}{2}. \tag{3.14}$$

The coupling constant is dimensionless only in 3+1 dimensions. However, in 1+1 dimensions, for example, it has the dimension of mass (or energy). This means, that when we consider the perturbative expansion, e.g., of the detector excitation probability

$$P \sim \lambda^2 P_2 + \mathcal{O}(\lambda^2), \tag{3.15}$$

then the term P_2 has dimensions which exactly cancel the dimension of λ, such that the contribution to the probability is dimensionless.

When λ has a dimension, it needs to be compared to the physical parameters of the problem in order to make sure that it is perturbatively small. Interestingly, the quantities to which λ should be compared to, seem to be suggested directly by the form of the terms in the perturbative expansion.

We will observe this in Chapter 3 for the perturbative expansion of signalling effects between two detectors. For example, in 1+1D Minkowski space, where λ has the dimension of energy, the terms are inverse proportional to the detector energy gap for resting detectors. This suggests $\lambda/\Omega << 1$ as the perturbative parameter. Furthermore, when the detector is accelerated, the contributions are inverse proportional to the acceleration of accelerated observers, suggesting λ/a as perturbative parameter. In the case when the energy gap of the detector vanishes $\Omega = 0$, they are proportional to the total interaction time instead, suggesting λT as the perturbative parameter.

Detectors in motion

It is also important to note that the interaction Hamiltonian as defined above generates time translations with respect to the detector proper time τ. If instead a different time parameter, e.g., coordinate time t, is used in calculations then the interaction Hamiltonian needs to be corrected by a factor of $\frac{\mathrm{d}\tau}{\mathrm{d}t}$ such that, for example, the interaction Hamiltonian for a pointlike detector with respect to coordinate time t reads

$$H_{\text{int}}(t) = \lambda\, \eta(\tau(t)) \frac{\mathrm{d}\tau(t)}{\mathrm{d}t} \left(\mathrm{e}^{\mathrm{i}\Omega\tau(t)} \left|e\right\rangle\!\left\langle g\right| + \mathrm{e}^{-\mathrm{i}\Omega\tau(t)} \left|g\right\rangle\!\left\langle e\right| \right) \otimes \phi\left(t, \vec{x}(t)\right). \tag{3.16}$$

This is particularly important for the study of signalling between relativistically moving detectors that we are aiming for. In general, the proper times of sender and receiver will differ. In this case, we use some global time coordinate to calculate the joint time evolution of interacting detectors and the field. A detailed discussion of this aspect can also be found in [15].

The detection of a particle by an Unruh-DeWitt particle detector is modelled by an excitation of the detector, as mentioned before. Even a detector that is initialized in its ground state has, in general, a non-vanishing probability to be found in its excited state after interacting with the field. The probability for a particular observer to measure a particle in a given field state is, therefore, modelled as the probability for a detector to get excited when coupling to the field along the observer's worldline. Indeed, this approach can be applied to famous phenomena of quantum field theory in curved spacetime such as the Unruh effect [81], Hawking radiation [30], or the creation of particles in expanding universes [29].

Hence, the leading order transition probability has been the subject of an extensive body of literature, which include, but is by no means limited to [33, 54, 78, 80], and the references therein. In the context of this thesis, it is also interesting to note that the thermal response of a detector experiencing the Unruh effect changes from a Planck to a Fermi-Dirac behaviour for Minkowski spacetime of different dimension, depending on whether the Huygens principle holds [66].

In the next section, the leading order excitation probability appears as one of the different coefficients appearing in the quantum channel between two Unruh-DeWitt detectors. There, it belongs to the contributions to Bob's final state which are independent of the signal from Alice, i.e., which constitute the noise present in the channel.

3.2 Perturbative analysis of the channel

Note: This section consists mainly of adapted and expanded parts of [39].

In the context of signalling between two detectors, we do not only need to calculate the transition probability between two particular states of a single detector, but we need the full final state of the receiver resulting from arbitrary input states of the sender and of the receiver. Therefore, it is most convenient to describe the time evolution of the detectors in terms of their density matrix.

As discussed in the introduction to this chapter, we equip both the sender, also referred to as Alice ($\mathcal{A}$), and the receiver, also referred to as Bob ($\mathcal{B}$), with pointlike Unruh-DeWitt

detectors. The total Hilbert space of the system is therefore composed as the tensor product space

$$\mathcal{H} = \mathcal{H}_{\mathcal{A}} \otimes \mathcal{H}_{\mathcal{F}} \otimes \mathcal{H}_{\mathcal{B}} \tag{3.17}$$

of Alice's Hilbert space $\mathcal{H}_{\mathcal{A}} = \mathbb{C}^2$, Bob's Hilbert space $\mathcal{H}_{\mathcal{B}} = \mathbb{C}^2$ and the Hilbert space of the quantum field $\mathcal{H}_{\mathcal{F}}$. We put the field's space as the middle factor for later notational convenience.

As mentioned before, we work in the Dirac interaction picture. This means that the time evolution under the free field Hamiltonian and the free detector Hamiltonians is absorbed into the operators such that only the interaction Hamiltonian acts on the states. For the two detectors, and with respect to coordinate time t, it reads

$$\begin{aligned} H_{\text{int}}(t) = {} & \lambda_{\mathcal{A}}\, \chi_{\mathcal{A}}(t) \left(\mathrm{e}^{\mathrm{i}\Omega_{\mathcal{A}}\tau_{\mathcal{A}}(t)} \left|e_{\mathcal{A}}\right\rangle\!\left\langle g_{\mathcal{A}}\right| + \mathrm{e}^{-\mathrm{i}\Omega_{\mathcal{A}}\tau_{\mathcal{A}}(t)} \left|g_{\mathcal{A}}\right\rangle\!\left\langle e_{\mathcal{A}}\right| \right) \otimes \phi\left(t, \vec{x}_{\mathcal{A}}(t)\right) \otimes \mathbb{I}_{\mathcal{B}} \\ & + \lambda_{\mathcal{B}}\, \chi_{\mathcal{B}}(t)\, \mathbb{I}_{\mathcal{A}} \otimes \phi\left(t, \vec{x}_{\mathcal{B}}(t)\right) \otimes \left(\mathrm{e}^{\mathrm{i}\Omega_{\mathcal{B}}\tau_{\mathcal{B}}(t)} \left|e_{\mathcal{B}}\right\rangle\!\left\langle g_{\mathcal{B}}\right| + \mathrm{e}^{-\mathrm{i}\Omega_{\mathcal{B}}\tau_{\mathcal{B}}(t)} \left|g_{\mathcal{B}}\right\rangle\!\left\langle e_{\mathcal{B}}\right| \right) \end{aligned} \tag{3.18}$$

where we absorbed the switching function and derivative of the proper times into the functions $\chi_{\mathcal{D}}(t) = \eta_{\mathcal{D}}(\tau_{\mathcal{D}}(t)) \frac{\mathrm{d}\tau_{\mathcal{D}}(t)}{\mathrm{d}t}$.

The communication between Alice and Bob is modelled as follows: Initially, the switching functions are chosen to vanish. So the detectors are not coupled to the field and Alice and Bob can prepare them for the interaction. To encode her message, Alice is free to prepare her detector in any state she chooses, which we denote by its density matrix $\rho_{\mathcal{A},0}$. And Bob prepares his detector in some fixed initial state $\rho_{\mathcal{B},0}$.

We assume the field to start out in the vacuum, and the initial state of the system to be a product state

$$\rho_0 = \rho_{\mathcal{A},0} \otimes \left|0\right\rangle\!\left\langle 0\right| \otimes \rho_{\mathcal{B},0}. \tag{3.19}$$

However, all results of this chapter also hold for other initial states of the field with the property that their odd n-point functions ($n = 1, 3, 5, ...$) vanish, e.g., for multi-particle Fock states or thermal states.

Then the detectors are coupled to the field. For simplicity, we assume that all interactions take place within the coordinate time interval $t \in (0, T)$. In this interval the initial state evolves unitarily under the action of H_{int} into a final state ρ_T. The final state will, in general, be an entangled state of the detectors and the field.

As discussed in the introduction to this chapter, the resulting quantum channel map from Alice's initial density matrix to Bob's final density matrix is then given by

$$\xi : \rho_{\mathcal{A},0} \mapsto \rho_{\mathcal{B},T} = \mathrm{Tr}_{\mathcal{A},\mathcal{F}}\left(\rho_T\right). \tag{3.20}$$

To obtain Bob's final state, the partial trace is taken over Alice's and the field's Hilbert space.

3.2.1 Perturbative time evolution

To obtain the time evolution operator under the interaction Hamiltonian from a time $t = 0$ to a time $t = T$, we use the Dyson series of standard time-dependent perturbation theory

$$U(T,0) = \mathbb{I} \underbrace{-\mathrm{i}\int_0^T \mathrm{d}t_1\, H_{\mathrm{int}}(t_1)}_{U^{(1)}} \underbrace{-\int_0^T \mathrm{d}t_1 \int_0^{t_1} \mathrm{d}t_2\, H_{\mathrm{int}}(t_1)H_{\mathrm{int}}(t_2)}_{U^{(2)}} + \dots \tag{3.21}$$

which expands the formal solution for $U(0,T)$ in powers of the coupling constant such that $U^{(k)} \sim \mathcal{O}(\lambda^k)$. From the expansion of the time evolution operator, we also obtain an expansion of the final density matrix ρ_T. Denoting the initial density matrix of the field-detectors system by ρ_0 as above, we get that after a time T,

$$\rho_T = [\mathbb{I} + U^{(1)} + U^{(2)} + \mathcal{O}(\lambda^3)]\rho_0[\mathbb{I} + U^{(1)} + U^{(2)} + \mathcal{O}(\lambda^3)]^\dagger. \tag{3.22}$$

This is, $\rho_T = \rho_0 + \rho_T^{(1)} + \rho_T^{(2)} + \mathcal{O}(\lambda^3)$, where

$$\rho_T^{(1)} = U^{(1)}\rho_0 + \rho_0 U^{(1)^\dagger} \sim \mathcal{O}(\lambda) \tag{3.23}$$

$$\rho_T^{(2)} = U^{(1)}\rho_0 U^{(1)^\dagger} + U^{(2)}\rho_0 + \rho_0 U^{(2)^\dagger} \sim \mathcal{O}(\lambda^2) \tag{3.24}$$

$$\dots$$

$$\rho_T^{(n)} = \sum_{k=0}^{n} U^{(n-k)}\, \rho_0\, U^{(k)^\dagger} \sim \mathcal{O}(\lambda^n) \tag{3.25}$$

and $U^{(0)} = \mathbb{I}$ is understood. The symbol $\mathcal{O}(\lambda^n)$ stands for the combined powers of the two coupling constants, i.e., $\mathcal{O}(\lambda_{\mathcal{A}}^i \lambda_{\mathcal{B}}^j) \sim \mathcal{O}(\lambda^{i+j})$.

In [19], the expansion of the final density matrix was formulated in terms of commutators between H_{int} and ρ_0. Here we choose to use the Dyson expansion of $U(t)$ instead, because it facilitates the intuitive interpretation of the different perturbative processes and leads to an integral structure that is advantageous for numerical evaluation.

Note that all the perturbative corrections from (3.25) to the final density matrix ρ_T are traceless:

$$\mathrm{Tr}\, \rho_T^{(n)} = 0. \tag{3.26}$$

Therefore, independent of up to which order $\mathcal{O}(\lambda^n)$ in the coupling constant the corrections are taken into account, the trace of the final state is always preserved,

$$\operatorname{Tr} \rho_T = 1. \tag{3.27}$$

It is not necessay to introduce any normalization constant in front of ρ_T at any order in perturbation theory, if all terms up to this order are consistently taken into account. To see this, let us verify that the derivative of the left hand side of (3.26) with respect to the switching time T vanishes:

$$\frac{\partial}{\partial T} \operatorname{Tr} \rho_T^{(n)} = 0, \ \forall\, T \geq 0. \tag{3.28}$$

As all the $\rho_T^{(n)}$ are identically zero for $T = 0$, their trace also vanishes for $T = 0$. Hence, if (3.28) is true then $\operatorname{Tr} \rho_T^{(n)}$ vanishes for all T. To evaluate (3.28) we differentiate (3.25):

$$\begin{aligned} \frac{\partial}{\partial T} \operatorname{Tr} \rho_T^{(n)} = \operatorname{Tr} \Bigg[& \left(-\mathrm{i}\, H_{\mathrm{int}}(T) U^{(n-1)}\right) \rho_0 + \sum_{k=1}^{n-1} \left(-\mathrm{i}\, H_{\mathrm{int}}(T) U^{(n-k-1)}\right) \rho_0\, U^{(k)\dagger} \\ & + \sum_{k=1}^{n-1} U^{(n-k)}\, \rho_0 \left(\mathrm{i}\, U^{(k-1)\dagger} H_{\mathrm{int}}(T)\right) + \rho_0 \left(\mathrm{i}\, U^{(n-1)\dagger} H_{\mathrm{int}}(T)\right) \Bigg] \end{aligned} \tag{3.29}$$

where we used $\frac{\partial}{\partial T} U^{(n)} = -\mathrm{i}\, H_{\mathrm{int}}(T) U^{(n-1)}$, which follows from (3.21). Using the cyclic property of the trace, we can rewrite (3.29) so as to have $H_{\mathrm{int}}(T)$ stand first in every term of the sum. Then we see that the terms form pairs that exactly cancel each other, so (3.29) vanishes. This shows that $\operatorname{Tr} \rho_T^{(n)}$ is indepent of T and vanishes for all T.

Independently of this observation, the Dyson expansion is not unitary order by order, but instead it is unitary up to the power of the perturbative parameter of the first ignored term in the perturbative expansion.

To obtain Bob's output density matrix $\rho_{\mathcal{B},T}$ as defined in (3.20), we trace out the field and Alice's detector from ρ_T. All $\rho_T^{(n)}$, with n odd, do not contain diagonal matrix elements in the field components, hence they drop out when the partial trace over the field is taken. This is because the field starts out in the vaccuum state, hence the partial trace over the field can be expressed as a vaccuum n-point function of the field. These n-point functions are identically zero for odd numbers of field operators. So the contributions to $\rho_{\mathcal{B},T}$ are all of even power in the coupling constant.

$$\rho_{\mathcal{B},T} = \rho_{\mathcal{B},0} + \operatorname{Tr}_{A,\mathcal{F}} \rho_T^{(2)} + \operatorname{Tr}_{\mathcal{A},\mathcal{F}} \rho_T^{(4)} + \mathcal{O}(\lambda^6) \tag{3.30}$$

3.2.2 Structure of the channel

In order to compare different signalling scenarios quantitatively, all the perturbative contributions derived in the previous section have to be evaluated up to the desired order (typically leading, or next-to-leading order) in the coupling constant. However, important qualitative features of the channel from Alice to Bob can already be derived from the form of the interaction Hamiltonian and the Dyson series expansion of the time evolution operator. They determine which elements of Bob's final density matrix are linearly dependent on which elements of Alice's initial density matrix. Moreover, they also determine at which order in perturbation theory these contributions first arise.

This analysis of the channel's general structure was done in [19] under the assumption that Bob initializes his detector in its groundstate, $\rho_{\mathcal{B},0} = |g_{\mathcal{B}}\rangle\langle g_{\mathcal{B}}|$. We will first review and discuss these results, and then generalize the analysis to arbitrary initial states of Bob.

Ground state as initial state for Bob

The dependence of Bob's output density matrix on the elements of Alice's input density matrix is captured by the quantum channel ξ from (3.20).

$$\xi\left[\rho_{\mathcal{A},0}\right] = \rho_{\mathcal{B},T} \tag{3.31}$$

Denoting Alice's initial density matrix as

$$\rho_{\mathcal{A},0} = \theta\,|e\rangle\langle e| + \gamma\,|e\rangle\langle g| + \gamma^*\,|g\rangle\langle e| + \beta\,|g\rangle\langle g| = \begin{pmatrix} \theta & \gamma \\ \gamma^* & \beta \end{pmatrix}, \tag{3.32}$$

it's general structure is given by [19]

$$\rho_{\mathcal{B},T} = \xi\left[\begin{pmatrix} \theta & \gamma \\ \gamma^* & \beta \end{pmatrix}\right] = \begin{pmatrix} P & 0 \\ 0 & 1-P \end{pmatrix} + \begin{pmatrix} \theta A + \beta B & \gamma C + \gamma^* D^* \\ \gamma^* C^* + \gamma D & -\theta A - \beta B \end{pmatrix}. \tag{3.33}$$

The term P accounts for the noise observed by Bob and is independent of the presence of Alice's detector. Indeed, it is not affected by the elements of the density matrix of Alice in (3.33). The terms that account for the influence of Alice's detector on Bob's detector are those labeled A, B, C and D. A, B and P are real, while C and D are complex. They depend on the parameters of the detectors, their wordline, the field and the switching function. Their lowest order contributions are:

$$P = \lambda_{\mathcal{B}}^2\,P_2 + \lambda_{\mathcal{B}}^4\,P_4 + \mathcal{O}(\lambda_{\mathcal{B}}^6) \tag{3.34}$$

$$A = \lambda_{\mathcal{A}}^2 \lambda_{\mathcal{B}}^2 \, A_4 + \mathcal{O}(\lambda^6) \tag{3.35}$$
$$B = \lambda_{\mathcal{A}}^2 \lambda_{\mathcal{B}}^2 \, B_4 + \mathcal{O}(\lambda^6) \tag{3.36}$$
$$C = \lambda_{\mathcal{A}} \lambda_{\mathcal{B}} \, C_2 + \mathcal{O}(\lambda^4) \tag{3.37}$$
$$D = \lambda_{\mathcal{A}} \lambda_{\mathcal{B}} \, D_2 + \mathcal{O}(\lambda^4) \tag{3.38}$$

Here again the symbol $\mathcal{O}(\lambda^n)$ stands for the combined powers of the two coupling constants. The expressions for C_2, D_2, A_4, B_4, P_2 and P_4 are rather complex and are given in Appendix A where some interesting points about their mathematical form are also discussed.

We can understand both the general structure of the channel and the form of the individual terms by discussing how they originate from the perturbative expansion of the system's final state. Every term $U^{(k)}$ in the expansion of the time evolution operator in (3.21) can be expanded into 2^k summands, by using that the interaction Hamiltonian (3.18) is the sum $H_{\text{int}} = H_{\text{int},\mathcal{A}} + H_{\text{int},\mathcal{B}}$ of the interaction Hamiltonian for each of the detectors. Accordingly, each $\rho_T^{(k)}$ can be written as a sum of terms sorted by their orders in the coupling constants $\lambda_{\mathcal{A}}$ and $\lambda_{\mathcal{B}}$. In this fashion, the lowest order contribution to $\rho_{B,T}$, which reads

$$\rho_{\mathcal{B},T}^{(2)} = \text{Tr}_{\mathcal{A},\mathcal{F}} \, \rho_T^{(2)} = \text{Tr}_{\mathcal{A},\mathcal{F}} \left[U^{(1)} \rho_0 U^{(1)\dagger} + U^{(2)} \rho_0 + \rho_0 U^{(2)\dagger} \right], \tag{3.39}$$

contains terms of order $\mathcal{O}(\lambda_{\mathcal{A}}^2)$, $\mathcal{O}(\lambda_{\mathcal{B}}^2)$ and $\mathcal{O}(\lambda_{\mathcal{A}}\lambda_{\mathcal{B}})$.

The terms of order $\mathcal{O}(\lambda_{\mathcal{A}}^2)$ do not contribute to $\rho_{B,T}$ because they cancel out when the partial trace over detector $\mathcal{A}$ is taken. This holds true for all terms that do not contain any power of $\lambda_{\mathcal{B}}$, hence no terms of order $\mathcal{O}(\lambda_{\mathcal{A}}^n)$ contribute to $\rho_{B,T}$.

The terms of order $\mathcal{O}(\lambda_{\mathcal{B}}^2)$ contribute to either the upper or to the lower diagonal element of $\rho_{B,T}$. The contribution of this kind originating from $U^{(1)} \rho_0 U^{(1)\dagger}$ is proportional to $|e_{\mathcal{B}}\rangle\langle e_{\mathcal{B}}|$, while the $\mathcal{O}(\lambda_{\mathcal{B}}^2)$ contribution from $U^{(2)}\rho_0 + \rho_0 U^{(2)\dagger}$ leads to terms that are proportional to $|g_{\mathcal{B}}\rangle\langle g_{\mathcal{B}}|$. Although they come with different structures of nested integrals, the coefficients of these matrix elements are equal up to an overall sign. They both constitute P_2, the lowest order contribution to P.

It is important to remark that, as mentioned above, P is nothing but the excitation probability of the single detector in the vacuum state of the quantum field. This quantum noise term is independent of the presence of the second detector and it contains only terms of order $\mathcal{O}(\lambda_{\mathcal{B}}^n)$. Any terms that describe an interaction between the two detectors have to contain powers of both coupling constants, i.e., they are $\mathcal{O}(\lambda_{\mathcal{A}}^i \lambda_{\mathcal{B}}^j)$.

The terms of order $\mathcal{O}(\lambda_{\mathcal{A}}^i \lambda_{\mathcal{B}}^j)$, with i and j odd, always appear multiplied by γ or γ^* (off-diagonal elements of A's initial state) and $|e_{\mathcal{B}}\rangle\langle g_{\mathcal{B}}|$ or $|g_{\mathcal{B}}\rangle\langle e_{\mathcal{B}}|$ (off-diagonal elements

of B's final state), so they contribute to the factors C or D, which couple the off-diagonal elements of $\rho_{\mathcal{A},0}$ and $\rho_{B,T}$ as in the general structure of the quantum channel (3.20).

This means that the terms of order $\mathcal{O}(\lambda_{\mathcal{A}}\lambda_{\mathcal{B}})$ from (3.39) are the lowest order terms that account for any signalling from A to B if the initial state of Alice's detector is such that $\gamma \neq 0$.

As all the terms contributing to $\rho_{B,T}$ are of even (combined) powers in the coupling constant, the only other class of terms contributing to the channel are of order $\mathcal{O}(\lambda_{\mathcal{A}}^i\lambda_{\mathcal{B}}^j)$, with both i and j even. These terms couple the diagonal terms of both density matrices and hence contribute to the factors A and B in (3.20). The lowest order terms in this class are of order $\mathcal{O}(\lambda_{\mathcal{A}}^2\lambda_{\mathcal{B}}^2)$ as indicated in (3.35) and (3.36).

Arbitrary initial states of Bob

After the previous analysis, we now analyze the general structure of the quantum channel, analogously, for arbitrary initial states of Bob's detector. To allow arbitrary initial states for both detectors, we denote the two detectors' initial density matrices by

$$\rho_{\mathcal{A},0} = \begin{pmatrix} \theta & \gamma \\ \gamma^* & \beta \end{pmatrix}, \quad \rho_{\mathcal{B},0} = \begin{pmatrix} \varphi & \delta \\ \delta^* & \kappa \end{pmatrix}. \tag{3.40}$$

With the same kind of argument as above, that explained the structure of the channel (3.33) in the simplified scenario, and using the tracelessness and hermiticity of the density matrix, we can deduce that the final state of Bob's detector for general initial states of both detectors is of the form:

$$\begin{aligned}
\rho_{\mathcal{B},T} &= \mathrm{Tr}_{\mathcal{A},\mathcal{F}}[\rho_T] = \mathrm{Tr}_{\mathcal{A},\mathcal{F}}\left[U(T,0)\,\rho_T\,U(T,0)^\dagger\right] \\
&= \begin{pmatrix} \varphi & \delta \\ \delta^* & \kappa \end{pmatrix} + \begin{pmatrix} \kappa P + \varphi Q & \delta R + \delta^* S^* \\ \delta^* R^* + \delta S & -\kappa P - \varphi Q \end{pmatrix} \\
&\quad + \gamma \begin{pmatrix} \delta I + \delta^* J & \kappa C + \varphi G \\ \kappa D + \varphi H & -\delta I - \delta^* J \end{pmatrix} + \gamma^* \begin{pmatrix} \delta J^* + \delta^* I^* & \kappa D^* + \varphi H^* \\ \kappa C^* + \varphi G^* & -\delta J^* - \delta^* I^* \end{pmatrix} \\
&\quad + \theta \begin{pmatrix} \kappa A + \varphi E & \delta K + \delta^* L^* \\ \delta L + \delta^* K^* & -\kappa A - \varphi E \end{pmatrix} + \beta \begin{pmatrix} \kappa B + \varphi F & \delta M + \delta^* N^* \\ \delta N + \delta^* M^* & -\kappa B - \varphi F \end{pmatrix}
\end{aligned} \tag{3.41}$$

Here $A, B, E, F, P, Q \in \mathbb{R}$ are real, whereas all other Latin letters stand for complex constants, that depend on the parameters, the geometry and the switching functions of the set-up. The constants A, B, C, D, P are the ones which were already introduced in (3.33).

The constants multiplying γ and γ^*, the off-diagonal elements of $\rho_{\mathcal{A},0}$, are all of order $\mathcal{O}(\lambda^2)$. As discussed for C and D earlier, all their perturbation expansions are of the form

$$X = \lambda_{\mathcal{A}}\lambda_{\mathcal{B}}X_2 + \mathcal{O}(\lambda^4), \text{ for } X = C, D, G, H, I, J, \tag{3.42}$$

whereas the terms that multiply the diagonal elements θ and β of $\rho_{\mathcal{A},0}$ are of order $\mathcal{O}(\lambda^4)$,

$$Y = \lambda_{\mathcal{A}}^2\lambda_{\mathcal{B}}^2Y_4 + \mathcal{O}(\lambda^6), \text{ for } Y = A, B, E, F, K, L, M, N. \tag{3.43}$$

The noise terms, which arise from the interaction of Bob's detector with the field alone, and which are independent of Alice's presence

$$Z = \lambda_{\mathcal{B}}^2Z_2 + \mathcal{O}(\lambda_{\mathcal{B}}^4), \text{ for } Z = P, Q, R, S \tag{3.44}$$

also contribute at leading order $\mathcal{O}(\lambda_{\mathcal{B}}^2)$ in perturbation theory.

In Appendix A.2 we calculate the leading order terms in the perturbative expansion of Bob's final state $\rho_{\mathcal{B},T}$ in (3.41), i.e., all the $\mathcal{O}(\lambda^2)$ contributions to the X and Z coefficients. Interestingly, all second order contributions to the signalling X coefficients (3.42) are given by one of two different integral expressions (see (A.20)):

$$G_2 = -C_2 \quad H_2 = -D_2 \quad I_2 = D_2 \quad J_2 = C_2 \tag{3.45}$$

Such that the leading order contribution in the perturbative expansion of Bob's final state in (3.41) simplifies to

$$\begin{aligned}\rho_{\mathcal{B},T} = &\begin{pmatrix}\varphi & \delta\\ \delta^* & \kappa\end{pmatrix} + \lambda_{\mathcal{B}}^2\begin{pmatrix}\kappa P_2 + \varphi Q_2 & \delta R_2 + \delta^* S_2^*\\ \delta^* R_2^* + \delta S_2 & -\kappa P_2 - \varphi Q_2\end{pmatrix}\\ &+ \lambda_{\mathcal{A}}\lambda_{\mathcal{B}}\left[\gamma\begin{pmatrix}\delta D_2 + \delta^* C_2 & (\kappa-\varphi)C_2\\ (\kappa-\varphi)D_2 & -\delta D_2 - \delta^* C_2\end{pmatrix} + \text{H.c.}\right]\\ &+ \mathcal{O}(\lambda^4)\end{aligned} \tag{3.46}$$

with leading order signalling contributions

$$C_2 = \int_0^T \mathrm{d}t_1 \int_0^{t_1} \mathrm{d}t_2\ \chi_{\mathcal{A}}(t_2)\chi_{\mathcal{B}}(t_1)\mathrm{e}^{\mathrm{i}(\Omega_{\mathcal{B}}\tau_{\mathcal{B}}(t_1)-\Omega_{\mathcal{A}}\tau_{\mathcal{A}}(t_2))}\left[\phi(x_{\mathcal{A}}(t_2)), \phi(x_{\mathcal{B}}(t_1))\right] \tag{3.47}$$

$$D_2 = \int_0^T \mathrm{d}t_1 \int_0^{t_1} \mathrm{d}t_2\ \chi_{\mathcal{A}}(t_2)\chi_{\mathcal{B}}(t_1)\mathrm{e}^{-\mathrm{i}(\Omega_{\mathcal{B}}\tau_{\mathcal{B}}(t_1)+\Omega_{\mathcal{A}}\tau_{\mathcal{A}}(t_2))}\left[\phi(x_{\mathcal{B}}(t_1)), \phi(x_{\mathcal{A}}(t_2))\right] \tag{3.48}$$

and leading order noise contributions

$$P_2 = \int_0^T \mathrm{d}t_1 \int_0^T \mathrm{d}t_2 \; \chi_{\mathcal{B}}(t_1)\chi_{\mathcal{B}}(t_2)\mathrm{e}^{\mathrm{i}\Omega_{\mathcal{B}}(\tau_{\mathcal{B}}(t_1)-\tau_{\mathcal{B}}(t_2))} \langle \phi(x_{\mathcal{B}}(t_2))\phi(x_{\mathcal{B}}(t_1))\rangle \tag{3.49}$$

$$Q_2 = -\int_0^T \mathrm{d}t_1 \int_0^T \mathrm{d}t_2 \; \chi_{\mathcal{B}}(t_1)\chi_{\mathcal{B}}(t_2)\mathrm{e}^{-\mathrm{i}\Omega_{\mathcal{B}}(\tau_{\mathcal{B}}(t_1)-\tau_{\mathcal{B}}(t_2))} \langle \phi(x_{\mathcal{B}}(t_2))\phi(x_{\mathcal{B}}(t_1))\rangle \tag{3.50}$$

$$\begin{aligned} R_2 = -\int_0^T \mathrm{d}t_1 \int_0^{t_1} \mathrm{d}t_2 \; & \chi_{\mathcal{B}}(t_1)\chi_{\mathcal{B}}(t_2)\mathrm{e}^{\mathrm{i}\Omega_{\mathcal{B}}(\tau_{\mathcal{B}}(t_1)-\tau_{\mathcal{B}}(t_2))} \\ & \times \left(\langle \phi(x_{\mathcal{B}}(t_1))\phi(x_{\mathcal{B}}(t_2))\rangle + \langle \phi(x_{\mathcal{B}}(t_2))\phi(x_{\mathcal{B}}(t_1))\rangle\right) \end{aligned} \tag{3.51}$$

$$S_2 = \int_0^T \mathrm{d}t_1 \int_0^T \mathrm{d}t_2 \; \chi_{\mathcal{B}}(t_1)\chi_{\mathcal{B}}(t_2)\mathrm{e}^{-\mathrm{i}\Omega_{\mathcal{B}}(\tau_{\mathcal{B}}(t_1)+\tau_{\mathcal{B}}(t_2))} \langle \phi(x_{\mathcal{B}}(t_2))\phi(x_{\mathcal{B}}(t_1))\rangle \,. \tag{3.52}$$

Note that P_2 constitutes the leading order contribution for a single detector to get excited from the ground to its initial state by coupling to the vacuum state of the field. This is the term which, as mentioned in the previous section, has been extensively studied in the literature in the context of effects as the Unruh effect, Hawking radiation and the like.

Before we go on to discuss the implications and physical interpretation of the channel structure in the next section, it is interesting to note a couple of points on these leading order contributions to the channel coefficients.

First we note, that the leading order signalling contributions only involve the commutator of field operators which, as discussed in Section 2.3 corresponds to a homogenous solution of the classical field equations. In particular, the commutator is independent of the fields quantum state. Therefore, to leading order in perturbation theory, the signal is not affected, or not sensitive, to the quantum properties of the field. In contrast, all leading order noise contributions involve the full Wightmann function of the field, or in the case of R_2 just its real part. (The imaginary part is equal to the commutator, as discussed in Section 2.3.) This means that only the noise contributions to the channel are sensitive to the properties of the field's quantum state at leading order in perturbation theory.

A second, more technical remark concerns the convergence of the integrals above. The field operators are, strictly speaking, operator valued distributions rather than operators on their own. Consequently, the Wightmann functions are distributions in spacetime rather than functions on spacetime. Therefore, to guarantee convergence of integrals that involve

the Wightmann function as above, the field operators should be integrated against test functions, i.e., smeared detectors should be used. However, for pointlike detectors the Wightmann function pulls back to yield a distribution on $\mathbb{R}\times\mathbb{R}$ corresponding to the cross-product of the detector's proper time with itself. (For further reference, see [74, 42, 43].) Accordingly, integrals such as P_2, Q_2 and S_2 give well-defined finite results as long as smooth, compactly supported or rapidly decaying test functions are used for the switching functions $\chi(t)$.

This argument does not apply to terms with a nested integral structure such as R_2. Due to its nested integral structure, the integration region has a sharp boundary along the $t_1 = t_2$ line in the integration plane, even when the switching function itself is smooth on $\mathbb{R}$. Therefore, as far as terms with nested integrals such as R_2 are concerned, the detector needs to be smeared out by a spatial profile in order to guarantee convergence. This aspect appears not to have been addressed in the literature before and should therefore be interesting to study further.

3.2.3 Superposition states are optimal signalling states

When studying any quantum communication setting, it is important to find out which states Alice, the sender, should use to encode her message in order to make optimal use of the channel at hand. For the channel we are investigating here, we will be able to answer this question by analyzing its action in the Bloch sphere picture in the subsequent section. The key insight into this question, however, already follows from the perturbative expansion of the channel coefficients that we discussed in the previous section. It was first discussed in [39].

On first view, it might appear natural to assume that Alice should initialize her detector in the excited state in order to achieve as strong an effect as possible on Bob's state. However, the discussion in the previous section shows that, actually, this is Alice's worst possible choice, for settings within the regime of perturbation theory.

This is because the contributions to Bob's final density matrix that depend on the diagonal elements of Alice's initial density matrix θ and β are all multiplied by the Y-type channel coefficients of equation (3.43) which only contribute at order $\mathcal{O}(\lambda_{\mathcal{A}}^2\lambda_{\mathcal{B}}^2)$. As such they are dominated by the noise contributions by two powers in the coupling constant, since the Z-type noise terms in (3.44) are of order $\mathcal{O}(\lambda_{\mathcal{B}}^2)$. For example, if Bob initializes his detector in the ground state $\rho_{\mathcal{B}} = |g_{\mathcal{B}}\rangle\langle g_{\mathcal{B}}|$ and Alice uses her energy eigenstates as

signalling states, then Bob's final state is given by

$$\xi\left(|e_{\mathcal{A}}\rangle\langle e_{\mathcal{A}}|\right) = \begin{pmatrix} P+A & 0 \\ 0 & 1-P-A \end{pmatrix} \quad \text{or} \quad \xi\left(|g_{\mathcal{A}}\rangle\langle g_{\mathcal{A}}|\right) = \begin{pmatrix} P+B & 0 \\ 0 & 1-P-B \end{pmatrix}. \tag{3.53}$$

Here the signalling contributions A and B are of order $\mathcal{O}(\lambda^4)$ whereas the noise term is P is of order $\mathcal{O}(\lambda^2)$.

In order to have a signal that competes with the noise contributions of leading order in perturbation theory, Alice needs to make use of the X-type channel coefficients in (3.42) which are of order $\mathcal{O}(\lambda_{\mathcal{A}}\lambda_{\mathcal{B}})$. These are the coefficients that, in Bob's final density matrix (3.41), multiply the off-diagonal elements of Alice's initial density matrix. This is only possible, if Alice initializes her detector in a coherent superposition of the energy eigenstates. They are the only signalling contributions that enter Bob's final state at leading order $\mathcal{O}(\lambda^2)$ of perturbation theory, as we saw in (3.46).

For example, Alice can achieve this by using states like $|\pm\rangle = \frac{1}{\sqrt{2}}\left(|g\rangle \pm |e\rangle\right)$ as signalling states. When Bob starts out in the ground state then his final state reads

$$\xi\left(|\pm\rangle\langle\pm|\right) = \begin{pmatrix} P+\frac{1}{2}(A+B) & \pm\frac{1}{2}(C+D^*) \\ \pm\frac{1}{2}(C^*+D) & 1-P-\frac{1}{2}(A+B) \end{pmatrix}. \tag{3.54}$$

Here the off-diagonal elements receive leading order signalling contributions at order $\mathcal{O}(\lambda^2)$ which do not even compete directly with the noise term as they contribute to different density matrix elements. The outcome of a measurement on Bob's detector with respect to basis of $|\pm\rangle$-states will not be affected by the diagonal elements of the density matrix above, but only by its off-diagonal elements. Therefore, only the signalling contributions but not the noise contributions will affect the expectation value of such a measurement.

From the analysis of the previous section, we see that Alice needs to prepare coherent superpositions of energy eigenstates in order to influence Bob's final state at leading order in perturbation theory. The analysis of the channel in the Bloch sphere picture will show that, in fact, equal weighted superpositions of energy eigenstates are Alice's optimal choice of signalling states.

There is one technical, and one more intuitive explanation to this phenomenon: Technically, the reason for the suppression of signals from energy eigenstates is that they have a vanishing expectation value of the interaction Hamiltonian. Therefore, they have a weaker impact on the quantum field than equal-weighted superpositions of energy eigenstates. This is because the latter, under the free time evolution of the detector, oscillate into eigenstates of the monopole operator in the interaction Hamiltonian. More intuitively this

can be understood by viewing the energy eigenstates of the detector as the stationary states of a model atom. These states however, by definition, do not emit much radiation. The radiating states of an atom are not part of its energy eigenstate basis, but are superpositions of energy eigenstates. Hence, in this picture, the superposition states of the detector could be viewed as radiating states, which explains why they have a stronger immediate impact on the field.

The initial state of Bob is not of as fundamental importance as the initial state of Alice, because in general his final state is always affected by some signalling contributions at order $\mathcal{O}(\lambda^2)$. However, it is interesting to see that one observation from the above example generalizes: The contributions to the off-diagonal elements of $\rho_{\mathcal{B},T}$ are proportional to the diagonal elements φ, κ of the initial state $\rho_{\mathcal{B},0}$ of Bob and vice versa. This suggests that to detect the signals sent from Alice, the final measurement on the state of Bob should be done in a basis which is unbiased (in the sense of mutually unbiased bases) with respect to the basis to which Bob's initial state belongs.

It is interesting to note that the leading order signalling contributions cannot be explained in terms of the exchange of real (on-shell) particle excitations of the field. Such processes, i.e., processes where there is a non-zero probability to detect the field in a one-particle state after the coupling of the sender to the field are of order $\mathcal{O}(\lambda_{\mathcal{A}}^2\lambda_{\mathcal{B}}^2)$. (In terms of Feynman diagrams they would involve one vertex at the sender's detector and one vertex at the receiver's detector, resulting in an amplitude of $\mathcal{O}(\lambda_{\mathcal{A}}\lambda_{\mathcal{B}})$ and hence a probability of $\mathcal{O}(\lambda_{\mathcal{A}}^2\lambda_{\mathcal{B}}^2)$.) Hence they are next-to-leading order only.

The discussion of this section, of course, is valid only for the perturbative regime. Beyond the perturbative regime, for long interaction durations between the detectors and the field, e.g., the role of particle exchange processes may be more important. To address this aspect, non-perturbative methods would have to be applied.

However, within the perturbative regime, by definition, the leading order dominates over next-to-leading order terms. We now understand that, in this regime, superposition of energy eigenstates are the optimal choice of signalling states for Alice.

3.3 Bloch sphere picture of channel

The Bloch sphere picture gives a geometric interpretation of a qubit's state space, and of the action of qubit quantum channels. For the channel between two two-level Unruh-DeWitt detectors it is particularly useful in order to understand which signalling states are Alice's optimal choice.

We begin with a brief review of the Bloch sphere picture and the representations of qubit channels, i.e., quantum channels mapping qubit states to qubit states, in the Bloch sphere picture. Then we derive the Bloch sphere representation for the channel studied above for a couple of different initial states of Bob's detector.

Introductions to the Bloch sphere picture are part of most textbooks on quantum information, such as [64, 86]. An introduction to the Bloch sphere representation of qubit channels is found in [67], and the references therein.

3.3.1 The Bloch sphere

Because a qubit density matrix ρ is a hermitean matrix with unit trace, it can be written in terms of the Pauli matrices

$$\sigma_X = \begin{pmatrix} 0 & 1 \\ 1 & 0 \end{pmatrix}, \quad \sigma_Y = \begin{pmatrix} 0 & -\mathrm{i} \\ \mathrm{i} & 0 \end{pmatrix}, \quad \sigma_Z = \begin{pmatrix} 1 & 0 \\ 0 & -1 \end{pmatrix}, \tag{3.55}$$

as

$$\begin{aligned} \rho &= \frac{1}{2}(\mathbb{I} + \vec{\rho}\cdot\vec{\sigma}) = \frac{1}{2}(\mathbb{I} + \rho_X\sigma_X + \rho_Y\sigma_Y + \rho_Z\sigma_Z) \\ &= \frac{1}{2}\begin{pmatrix} 1+\rho_Z & \rho_X - \mathrm{i}\rho_Y \\ \rho_X + \mathrm{i}\rho_Y & 1-\rho_Z \end{pmatrix}, \end{aligned} \tag{3.56}$$

and represented by a real, three-component vector $\vec{\rho} = (\rho_X, \rho_Y, \rho_Z)$. The coefficients of the vector are exactly the expectation value of the state for a measurement of the observables of the corresponding Pauli matrices.

$$\rho_X = \mathrm{Tr}\,(\rho\,\sigma_X) = \langle X\rangle \quad \rho_Y = \mathrm{Tr}\,(\rho\,\sigma_Y) = \langle Y\rangle \quad \rho_Z = \mathrm{Tr}\,(\rho\,\sigma_Z) = \langle Z\rangle\,. \tag{3.57}$$

This uses that $\mathrm{Tr}\,\sigma_I\sigma_J = 2\delta_{IJ}$, which holds including for the identity matrix $\sigma_0 = \mathbb{I}$.

In the Bloch sphere picture the state space of a qubit is represented as the unit ball in $\mathbb{R}^3$. Pure states are represented by points on the unit sphere, whereas mixed states correspond to points lying within the unit ball. The coordinates of the point representing a particular qubit states are exactly given by the three-vector $\vec{\rho} = (\rho_X, \rho_Y, \rho_Z)$.

The connection is easy to see for a pure qubit state. Any given pure qubit state $|\psi\rangle$ can be expressed with respect to the basis $\{|+Z\rangle, |-Z\rangle\}$ in terms of two angle parameters $\theta \in [0, \pi]$ and $\phi \in [0, 2\pi]$, as

$$|\psi\rangle = \cos\frac{\theta}{2}\,|+Z\rangle + \mathrm{e}^{\mathrm{i}\phi}\sin\frac{\theta}{2}\,|-Z\rangle\,. \tag{3.58}$$

These angles can be viewed as the spherical coordinates of the point representing the state $|\psi\rangle$ on the unit sphere in $\mathbb{R}^3$, which in this context is referred to as the Bloch sphere. In terms of these angles, the state's expectation values for the measurements of the Pauli matrices are

$$\langle X\rangle = \cos\phi \quad \langle Y\rangle = \sin\phi \quad \langle Z\rangle = \cos^2\frac{\theta}{2} - \sin^2\frac{\theta}{2} = \cos\theta. \tag{3.59}$$

These are exactly the cartesian coordinates of a point on the Bloch sphere with polar coordinates (θ, ϕ), which motivates the identification of the vector coefficients in $\vec{\rho} = (\rho_X, \rho_Y, \rho_Z)$ with the cartesian coordinates of the state in the Bloch sphere. The state $|\psi\rangle$ can also be rewritten in terms of its Pauli matrix expectation values as

$$|\psi\rangle = \sqrt{\frac{1+\langle Z\rangle}{2}}\,|+Z\rangle + \sqrt{\frac{1-\langle Z\rangle}{2}}\,(\langle X\rangle + \mathrm{i}\,\langle Y\rangle)\,|-Z\rangle\,. \tag{3.60}$$

The density matrix of mixed states is characterised by their square not having unit trace. In the case of a mixed qubit state we have

$$\frac{1}{2} \leq \mathrm{Tr}\left(\rho^2\right) < 1 \tag{3.61}$$

In terms of the three vector representation this means that the norm of the vector $\vec{\rho}$ is $|\vec{\rho}| < 1$, because the norm of a state's Bloch vector is determined by the trace of the squared density matrix.

$$\mathrm{Tr}\,\rho^2 = \frac{1}{4}\,\mathrm{Tr}\begin{pmatrix}(1+\rho_Z) & (\rho_X - \mathrm{i}\rho_Y)\\ (\rho_X + \mathrm{i}\rho_Y) & (1-\rho_Z)\end{pmatrix}^2 = \frac{1}{2}(1+\rho_Z^2+\rho_Y^2+\rho_X^2) = \frac{1}{2} + \frac{1}{2}\,|\vec{\rho}|^2 \tag{3.62}$$

In the following we will use the convention that identifies the excited state $|e\rangle$ of a two-level qubit detector with the $|+Z\rangle$ state.

3.3.2 Calculating the Bloch sphere picture of a channel

In the Bloch picture, any given qubit channel $\xi : \rho_i \mapsto \rho_o$ can be represented by an affine map acting on $\mathbb{R}^3$ as

$$\begin{aligned}&\mathbb{R}^3 \to \mathbb{R}^3\\ &\vec{\rho_i} \mapsto \vec{\rho_o} = \Lambda\vec{\rho_i} + \vec{v},\end{aligned} \tag{3.63}$$

where Λ is a real 3x3-matrix and $\vec{v}$ is a constant, real 3-vector [47, 7]. In order to determine Λ and $\vec{v}$ it is therefore sufficient to know the action of the channel on one eigenstates of each Pauli matrix, and the completely mixed state, since the Pauli eigenstates correspond to a basis of $\mathbb{R}^3$ in the Bloch sphere picture

$$|+X\rangle \equiv (1,0,0) \quad |+Y\rangle \equiv (0,1,0) \quad |+Z\rangle \equiv (0,0,1) \tag{3.64}$$

and the completely mixed state corresponds to the null vector $\vec{0} \in \mathbb{R}^3$. Therefore the image of the completely mixed state determines $\vec{v}$, and consequently the image of the three Pauli eigenstates can be used to derive Λ. These calculations are possible by a straightforward application of the identifications between qubit density matrices and the Bloch sphere that we discussed in the previous section.

For evaluation using a computer algebra system, we have found the following ansatz very convenient and efficient. Instead of evaluating the channel for the states corresponding to the four vectors $(1,0,0), (0,1,0), (0,0,1), (0,0,0)$, we evaluate the channel for the density matrices corresponding to the Bloch vectors $(t,0,0)$, $(0,t,0)$ and $(0,0,t)$ for some real variable t.

$$\rho_{X,t} = \xi\left(\frac{1}{2}(\mathbb{I} + t\,\sigma_X)\right) \quad \rho_{Y,t} = \xi\left(\frac{1}{2}(\mathbb{I} + t\,\sigma_Y)\right) \quad \rho_{Z,t} = \xi\left(\frac{1}{2}(\mathbb{I} + t\,\sigma_Z)\right). \tag{3.65}$$

By grouping the Bloch vectors that correspond to these density matrices into the columns of a 3x3 matrix, we obtain

$$(\vec{\rho_{X,t}}, \vec{\rho_{Y,t}}, \vec{\rho_{Z,t}}) = t\,\Lambda + (\vec{v}, \vec{v}, \vec{v})\,. \tag{3.66}$$

From this matrix both Λ and $\vec{v}$ can be easily obtained as the coefficients with respect to zeroth and first order in t by a computer algebra system.

3.3.3 Single Detector

We can also use the Bloch sphere picture to analyze how a single detector is affected by the interaction with a field, because the map from a single detector's initial state to its final state is a quantum channel map as well. Therefore, the impact of the interaction with the field, and its correlations along the worldline of the detector, can be represented in the Bloch sphere picture.

The Bloch sphere picture gives an intuitive description of the change of a detector's state under the interaction with the field. This is in particular helpful to address scenarios as in

[57], which show that quantum gates could be performed on two-level detectors through relativistic motion in adequately prepared quantum fields in one-dimensional cavities.

The general form of a single detector's state after coupling to the field was already contained in the general form of the sender's final state that was discussed in equation (3.41). If the sender is not coupled to the field then this states exactly corresponds to the situation where the sender is alone and only coupling to the vacuum state of the field. Hence the final density matrix of a single detector coupling to the field has the form

$$\rho_{\mathcal{B},T} = \begin{pmatrix} \varphi & \delta \\ \delta^* & \kappa \end{pmatrix} + \begin{pmatrix} \kappa P + \varphi Q & \delta R + \delta^* S^* \\ \delta^* R^* + \delta S & -\kappa P - \varphi Q \end{pmatrix}, \tag{3.67}$$

where we used the same notation as in (3.41), i.e., the detector's initial state is given by

$$\rho_{\mathcal{B},0} = \begin{pmatrix} \varphi & \delta \\ \delta^* & \kappa \end{pmatrix} \tag{3.68}$$

and the coefficients P, Q, R, S are the same as introduced before in Section 3.2.2.

As mentioned before, the coefficient P denotes the probability for a detector that started out in the ground state to be found in the excited state after the interaction with the field. It has therefore been the subject of extensive study in the literature. It is easily seen that Q analogously denotes the deexcitation probability of an initially excited detector. The Bloch sphere picture of the channel will yield a similarly intuitive interpretation of the remaining R and S coefficients.

Applying the method described in the previous section to the channel $\rho_{\mathcal{B},0} \mapsto \rho_{\mathcal{B},T}$, and identifying $|e_{\mathcal{A}}\rangle = |+Z\rangle$ and $|g_{\mathcal{A}}\rangle = |-Z\rangle$, we obtain

$$\begin{aligned} \vec{\rho_{\mathcal{B},T}} &= \begin{pmatrix} 1 + \Re(R) + \Re(S) & \Im(R) + \Im(S) & 0 \\ -\Im(R) + \Im(S) & 1 + \Re(R) - \Re(S) & 0 \\ 0 & 0 & 1 - P + Q \end{pmatrix} \vec{\rho_{\mathcal{B},0}} + \begin{pmatrix} 0 \\ 0 \\ P + Q \end{pmatrix} \\ &= \vec{\rho_0} + \begin{pmatrix} \Re(R) + \Re(S) & \Im(R) + \Im(S) & 0 \\ -\Im(R) + \Im(S) & \Re(R) - \Re(S) & 0 \\ 0 & 0 & Q - P \end{pmatrix} \vec{\rho_0} + \begin{pmatrix} 0 \\ 0 \\ P + Q \end{pmatrix}. \end{aligned} \tag{3.69}$$

The action of the matrix can be understood in terms of its singular value decomposition. For this we first write $R = |R|e^{i\phi_R}$ and $S = |S|e^{i\phi_S}$, such that $\Re(R) = \cos\phi_R|R|$ and $\Im(R) = \sin\phi_R|R|$, and analogously for S. In this notation the singular value decomposition [64] expresses the matrix as the product

$$\begin{pmatrix} \Re(R) + \Re(S) & \Im(R) + \Im(S) & 0 \\ -\Im(R) + \Im(S) & \Re(R) - \Re(S) & 0 \\ 0 & 0 & Q - P \end{pmatrix} = \mathbf{UOMO^t} \tag{3.70}$$

with the rotation matrices

$$\mathbf{U} = \begin{pmatrix} \cos\phi_R & \sin\phi_R & 0 \\ -\sin\phi_R & \cos\phi_R & 0 \\ 0 & 0 & 1 \end{pmatrix} \quad \mathbf{O} = \begin{pmatrix} \cos\frac{\phi_R+\phi_S}{2} & -\sin\frac{\phi_R+\phi_S}{2} & 0 \\ \sin\frac{\phi_R+\phi_S}{2} & \cos\frac{\phi_R+\phi_S}{2} & 0 \\ 0 & 0 & 1 \end{pmatrix} \tag{3.71}$$

and the diagonal matrix

$$\mathbf{M} = \begin{pmatrix} |R|+|S| & 0 & 0 \\ 0 & |R|-|S| & 0 \\ 0 & 0 & Q-P \end{pmatrix}. \tag{3.72}$$

We can view the action of this matrix as the composition of rotations about the Z-axis and a multiplication by the diagonal matrix $\mathbf{M}$.

Altogether, the effect of the interaction with the field on a single detectors state can be described as follows in the Bloch sphere picture: Mostly, the final state remains close to the initial state, since the initial state $\rho_{\mathcal{B},0}$ occurs on the right-hand side of (3.69) above. However, a correction vector is added to the original state vector. The correction along the Z-axis consists of a shift, whose size is determined by the coefficients P and Q, and the detector's initial expectation value of $\langle Z\rangle$. The correction in the X-Y-plane of the Bloch sphere is obtained by a series of rotations, determined by the complex arguments of the R and S coefficients, and a stretching, determined by the absolute values of the R and S coefficients

It is interesting to note, that if the initial state of the detector is pure, the correction vector that is added to the initial state vector has to be inward pointing, so as to connect the initial state to a valid physical final state within the Bloch sphere. This indicates that the final state after the interaction typically will be a mixed state, which is to be expected since the interaction will generally entangle the detector with the field.

3.3.4 Bloch picture of the channel between two detectors

We now derive the Bloch sphere representation of the channel between two two-level Unruh-DeWitt detectors. Expressing it as a map of the form

$$\vec{\rho}_{\mathcal{A},0} \mapsto \vec{\rho}_{\mathcal{B},T} = \Lambda\vec{\rho}_{\mathcal{A},0} + \vec{v} \tag{3.73}$$

will give a geometric picture of how Alice's initial state Bloch vector needs to be contracted and shifted in order to obtain Bob's final state. We will do this analysis for three different types of initial states of Bob: For Bob starting out in the completely mixed state, for Bob starting out in an energy eigenstate, and for Bob starting out in an equal weighted superposition of energy eigenstates.

Receiever initialized in the completely mixed state

It arguably could be easier to initialize a two-level system in the completely mixed state rather than in a pure initial state. Therefore, it is interesting to ask if the completely mixed state is a viable choice for Bob's initial state.

If Bob starts out in the completely mixed state, then it follows from equation (3.41) that the channel takes the form

$$\rho_{\vec{B},T} = \frac{1}{2}\begin{pmatrix} \Re\left(C+D+G+H\right) & \Im\left(C+D+G+H\right) & 0 \\ \Im\left(D+H-C-G\right) & \Re\left(C+G-D-H\right) & 0 \\ 0 & 0 & A+E-B-F \end{pmatrix}\rho_{\vec{A},0} + \begin{pmatrix} 0 \\ 0 \\ P+Q+\frac{1}{2}(A+E+B+F) \end{pmatrix} \tag{3.74}$$

in the Bloch picture. The channel matrix bears some similarity with the case where Bob is initialized in an energy eigenstate, which we investigate below. However, we notice that the leading order signalling contribution to this channel vanish, since as discussed in equation (3.45), we have $G_2 = -C_2$ and $H_2 = -D_2$.

Therefore, if Bob is initialized in the completely mixed state, any signal from Alice only affects Bob's final state at order $\mathcal{O}(\lambda^4)$, which is sub-dominant to the vacuum noise of order $\mathcal{O}(\lambda^2)$ as discussed before. This suggests that Bob needs to initialize his detector in a pure state in order to be sensitive to Alice's signal at leading order in perturbation theory.

Receiver initialized in energy eigenstate

The scenario where Bob initializes his detector in the ground state, is the one that was considered first in the literature in [19], and also Chapter 4 is focussed on this setting. We first encountered this channel in equation (3.33). Applying the methods discussed above, we find that its Bloch picture representation is

$$\rho_{\vec{B},T} = \begin{pmatrix} \Re\left(C\right)+\Re\left(D\right) & \Im\left(C\right)+\Im\left(D\right) & 0 \\ -\Im\left(C\right)+\Im\left(D\right) & \Re\left(C\right)-\Re\left(D\right) & 0 \\ 0 & 0 & A-B \end{pmatrix}\rho_{\vec{A},0} + \begin{pmatrix} 0 \\ 0 \\ 2\,P+A+B-1 \end{pmatrix}. \tag{3.75}$$

where the coefficients P, A, B, C, D are the ones defined earlier for the density matrix picture. As expected, we see that Bob's detector remains close to its initial state, the

ground state represented by the Bloch vector $(0, 0, -1)$, up to corrections determined by the channel coefficients P, A, B, C, D.

The matrix that appears above has the same structure as the matrix that we already analyzed for the single detector channel. Accordingly, it has a similar singular value composition. Writing $C = |C|e^{i\phi_C}$ and $D = |D|e^{i\phi_D}$ we obtain

$$\begin{pmatrix} \Re(C) + \Re(D) & \Im(C) + \Im(D) & 0 \\ -\Im(C) + \Im(D) & \Re(C) - \Re(D) & 0 \\ 0 & 0 & A - B \end{pmatrix} = \mathbf{UOMO^{tr}} \tag{3.76}$$

with

$$\mathbf{U} = \begin{pmatrix} \cos\phi_C & \sin\phi_C & 0 \\ -\sin\phi_C & \cos\phi_C & 0 \\ 0 & 0 & 1 \end{pmatrix} \quad \mathbf{O} = \begin{pmatrix} \cos\frac{\phi_C+\phi_D}{2} & -\sin\frac{\phi_C+\phi_D}{2} & 0 \\ \sin\frac{\phi_C+\phi_D}{2} & \cos\frac{\phi_C+\phi_D}{2} & 0 \\ 0 & 0 & 1 \end{pmatrix} \tag{3.77}$$

and the diagonal matrix

$$\mathbf{M} = \begin{pmatrix} |C| + |D| & 0 & 0 \\ 0 & |C| - |D| & 0 \\ 0 & 0 & A - B \end{pmatrix}. \tag{3.78}$$

It is also possible to choose the diagonal matrix positive, by instead using

$$\begin{aligned} \mathbf{M}' &= \begin{pmatrix} |C| + |D| & 0 & 0 \\ 0 & ||C| - |D|| & 0 \\ 0 & 0 & |A - B| \end{pmatrix} \\ \mathbf{U}' &= \begin{cases} \begin{pmatrix} \cos\phi_C & \sin\phi_C & 0 \\ -\sin\phi_C & \cos\phi_C & 0 \\ 0 & 0 & \mathrm{sgn}(A-B) \end{pmatrix} & \text{if } |C| \geq |D| \\ \begin{pmatrix} \cos\phi_D & \sin\phi_D & 0 \\ -\sin\phi_D & \cos\phi_D & 0 \\ 0 & 0 & \mathrm{sgn}(A-B) \end{pmatrix} & \text{if } |C| < |D| \end{cases} \end{aligned} \tag{3.79}$$

whereas $\mathbf{O}$ remains unchanged.

The geometrical Bloch sphere picture of the channel's action is now clear, and a sketch of it is given in Figure 3.1: The Bloch sphere of all possible initial states that the sender

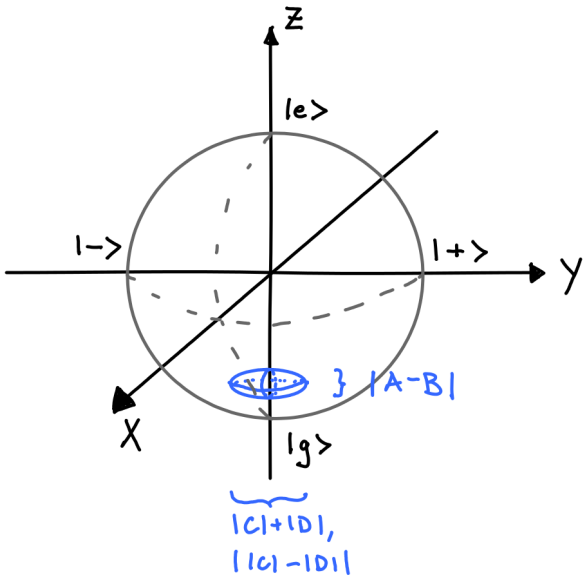

Figure 3.1: Sketch of the set of final receiver states, if the receiver is initialized in its ground state $|g_{\mathcal{B}}\rangle$. The Bloch sphere of the sender's possible initial states is contracted to an ellipsoid close to the receiver's ground state. The ellipsoid's diameter in the $X-Y$-plane is determined by the absolute values of the C and D channel coefficients. The ellipsoid's diameter along the Z-axis is determined by the A and B coefficients.

can choose from is contracted to an ellipsoid which lies close to the receiver's initial ground state. The centre of this ellipsoid always lies on the Z-axis.

The key observation is that the ellipsoid's diameters along the X-axis and the Y-axis are determined by the C and D coefficients, whereas the diameter along the Z-axis is determined by the A and B coefficients. As discussed earlier, the C and D coefficients are in the class of signalling contributions that are of leading order in perturbation theory, whereas the A and B coefficients only enter subdominantly in next-to-leading order. Therefore, in general, the diameter of the ellipsoid in the X-Y-plane is of order $\mathcal{O}(\lambda^2)$ whereas it is only of order $\mathcal{O}(\lambda^4)$ along the Z-axis.

Due to the block structure of the channel matrix, the Z-component of the final state of the receiver depends only on the Z-component of the initial state of the sender, and the final X-component and Y-component depend only on the initial X-component and Y-component of the sender. Whereas the relation of the Z-components is just linear, the action of the channel in the X-Y-plane consists of a sequence of rotations and a contraction:

First, Alice's initial state vector is rotated around the Z-axis by the angle $\Delta\phi = -\frac{\phi_C+\phi_D}{2}$. Then the diagonal matrix $\mathbf{D}$ is applied which contracts the state vector. If Alice's initial state is aligned optimally, then it is contracted by the factor $|C|+|D|$, in the worst case it is contracted by the factor $|C|-|D|$. Afterwards the state vector is rotated further around the Z-axis, this time by the angle $\Delta\phi = -\frac{\phi_C-\phi_D}{2}$.

What does this imply for Alice's choice of signalling states? In the Bloch sphere picture the distance between two state Bloch vectors gives their trace distance

$$D(\rho_1,\rho_2) = \frac{1}{2}\operatorname{Tr}(\rho_1-\rho_2) = \frac{1}{2}|\vec{\rho}_1-\vec{\rho}_2| \tag{3.80}$$

which is a measure for the distinguishability of two states. It corresponds to the probability of correctly identifying one state out of a pair of states in a single measurement [64]. One would intuitively expect that Alice has to choose her signalling states such that the corresponding final states of Bob's detector have maximal distance from each other in the Bloch sphere picture. In the subsequent section we will see, that this intuition is correct for single, and sequential uses of the channel. For multiple, parallel uses Section 3.4.3 shows that still a pair of input states maximizes the Holevo capacity of the channel. However, this are not strictly orthogonal to each other and, thus, the corresponding output states do not maximize the trace distance.

In order to send a signal to Bob that leaves his state in one of two possible state that Bob has the highest probability of telling apart successfully, Alice needs to choose her initial state such that Bob's final state lies on either end of the ellipsoid's longest semi-principal axis. From the geometric interpretation of the channel that we discussed above, we know that this semi-principal axis lies in $X-Y$-plane and has a length of $2(|C|+|D|) \sim 2\lambda_{\mathcal{A}}\lambda_{\mathcal{B}}(|C_2|+|D_2|)+\mathcal{O}(\lambda^4)$. Alice can achieve this by using the initial states with Bloch vectors

$$\vec{\psi_\pm} = \pm\left(\cos\left(\frac{\phi_C+\phi_D}{2}\right), \sin\left(\frac{\phi_C+\phi_D}{2}\right), 0\right) \tag{3.81}$$

which correspond to the two pure orthogonal input ket states

$$|\psi_\pm\rangle = \frac{1}{\sqrt{2}}\left(|e_{\mathcal{A}}\rangle + \mathrm{e}^{\mathrm{i}\frac{\phi_C+\phi_D}{2}}|g_{\mathcal{A}}\rangle\right). \tag{3.82}$$

These lead to the optimal possible trace distance between Bob's corresponding final states which is

$$\frac{1}{2}\operatorname{Tr}\left(\xi(|\psi_+\rangle\langle\psi_+|)-\xi(|\psi_-\rangle\langle\psi_-|)\right) = |C_2|+|D_2|+\mathcal{O}(\lambda^4). \tag{3.83}$$

The behaviour of the channel if Bob initializes his detector in the excited state $\vec{\rho_{B,0}} = (0,0,1) \equiv |e_B\rangle\langle e_B|$ instead of the ground state, is completely analogous. When Bob starts in the excitedet state, the Bloch representation of the channel takes the form

$$\vec{\rho}_{\mathcal{B},T} = \begin{pmatrix} \Re(H) + \Re(G) & \Im(G) + \Im(H) & 0 \\ -\Im(G) + \Im(H) & -\Re(H) + \Re(G) & 0 \\ 0 & 0 & E - F \end{pmatrix} \vec{\rho_{A,0}} + \begin{pmatrix} 0 \\ 0 \\ 1 + 2\,Q + E + F \end{pmatrix}. \tag{3.84}$$

Since $G_2 = -C_2$ and $H_2 = -D_2$, the leading order signalling contributions are the same up to an overall sign. Therefore the results from above, for the ground state as Bob's initial state, carry over to the scenario with the excited state as Bob's initial state.

Using the Bloch picture representation we are able to confirm our earlier result, that Alice's optimal signalling state are superposition of energy eigenstates, that lie in the equator of the Bloch sphere. In the Bloch picture we are also able to readily identify the signalling states that maximize the trace distance between Bob's corresponding final detector states.

Here, in the scenario where Bob initializes his detector in an energy eigenstate, he will have to tune the measurement of his final state to the complex arguments of the complex channel coefficients C_2 and D_2, in order to distinguish the two output states lying on the opposite poles of the ellipsoid of possible output states.

Receiver initialized in equal weighted superposition of energy eigenstates

The optimization of Bob's final measurement can be traded against an optimization of Bob's initial state, as we will see now. This is possible, when Bob initializes his detector in an equal weighted superposition of energy eigenstates, where the precise relative phase of the superposition state as to be optimized according to the complex values of the channel coefficients. Then, Bob can simply perform a final measurement in the energy eigenbasis in order to optimally use the leading order signalling contributions from Alice's signal.

We assume that Bob initializes his detector in a pure state on the equator of his Bloch sphere, i.e., we have

$$\vec{\rho_{B,0}} = \begin{pmatrix} \cos(r) \\ \sin(r) \\ 0 \end{pmatrix} \tag{3.85}$$

for some real parameter r. Under this assumption, the channel takes the following form

$$\begin{aligned}\rho_{\vec{B},T} = &\frac{1}{2}\begin{pmatrix} \Re\left(C+D+G+H\right) & \Im\left(C+D+G+H\right) & 0 \\ \Im(-C+D-G+H) & \Im(C-D+G-H) & 0 \\ 0 & 0 & A-B+E-F \end{pmatrix}\rho_{\vec{A},0} \\ &+\cos(r)\begin{pmatrix} 0 & 0 & \frac{1}{2}\Re\left(K+L-M-N\right) \\ 0 & 0 & \frac{1}{2}\Im(-K+L+M-N) \\ \Re(I+J) & \Im(I+J) & 0 \end{pmatrix}\rho_{\vec{A},0} \\ &+\sin(r)\begin{pmatrix} 0 & 0 & \frac{1}{2}\Im(K+L-M-N) \\ 0 & 0 & \frac{1}{2}\Re(K-L-M+N) \\ \Im(I-J) & \Re(-I+J) & 0 \end{pmatrix}\rho_{\vec{A},0} \\ &+\frac{1}{2}\begin{pmatrix} \cos(r)(2+2\Re(R+S)+\Re(K+L+M+N) \\ \cos(r)(2\Im(-R+S)+\Im(-K+L-M+N)) \\ 0 \end{pmatrix} \\ &+\frac{1}{2}\begin{pmatrix} \sin(r)(2\Im(R+S)+\Im(K+L+M+N)) \\ \sin(r)(2+2\Re(R-S)+\Re(K-L+M-N)) \\ 0 \end{pmatrix} \\ &+\frac{1}{2}\begin{pmatrix} 0 \\ 0 \\ 2(P+Q)+A+B+E+F \end{pmatrix}. \end{aligned} \tag{3.86}$$

The leading order, $\mathcal{O}(\lambda^2)$ contributions to the channel have a very simple form. Using again that $C_2 = -G_2$ and $D_2 = -H_2$ we have

$$\begin{aligned}&\rho_{\vec{B},T} = \\ &\lambda_{\mathcal{A}}\lambda_{\mathcal{B}}\begin{pmatrix} 0 & 0 & 0 \\ 0 & 0 & 0 \\ \cos(r)\Re(I_2+J_2)+\sin(r)\Im(I_2-J_2) & \cos(r)\Im(I_2+J_2)+\sin(r)\Re(-I_2+J_2) & 0 \end{pmatrix}\rho_{\vec{A},0} \\ &+\lambda_{\mathcal{B}}^2\begin{pmatrix} \cos(r)(1+\Re(R_2+S_2)+\sin(r)\Im(R_2+S_2) \\ \cos(r)\Im(-R_2+S_2)+\sin(r)(1+\Re(R_2-S_2)) \\ P_2+Q_2 \end{pmatrix}+\mathcal{O}(\lambda^4). \end{aligned} \tag{3.87}$$

So the optimal choice of signalling states for Alice, that to leading order in perturbation theory maximize the trace distance between Bob's corresponding final states , lie on the equator of Alice's Bloch sphere again, i.e., are equal-weighted superpositions of energy eigenstates, as we expected.

Bob can detect the signal by measuring his detector in the energy eigenbasis. Assuming that Alice's input state is $\rho_{A,0}^{\vec{}} = (\cos(s), \sin(s), 0)$ we have

$$\begin{aligned}\langle Z_B \rangle = \lambda_{\mathcal{A}}\lambda_{\mathcal{B}} \cos(s) \left(\cos(r)\Re(I_2 + J_2) + \sin(r)\Im(I_2 - J_2)\right) \\ + \lambda_{\mathcal{A}}\lambda_{\mathcal{B}} \sin(s) \left(\cos(r)\Im(I_2 + J_2) + \sin(r)\Re(-I_2 + J_2)\right) + x l_{\mathcal{B}}(P_2 + Q_2) + \mathcal{O}(\lambda^4)\end{aligned} \tag{3.88}$$

for the Z-component of Bob's final state.

Through the choice of Bob's initial state Alice's influence on this expectation value can be maximized. For this Bob needs to choose his initial state with $r = r_m := \frac{1}{2}(\arg(I_2) - \arg(J_2))$, and Alice uses initial states $\rho_{A,0} = \pm(\cos(s_m), \sin(s_m), 0)$ with

$$\tan s_m = \frac{\cos r_m \Im(I_2 + J_2) - \sin r_m \Re(I_2 - J_2)}{\cos(r_m)\Re(I_2 + J_2) + \sin r_m \Im(I_2 - J_2)}. \tag{3.89}$$

Then the expectation values are

$$\langle Z_B \rangle = \lambda_{\mathcal{B}}^2(P_2 + Q_2) \pm \lambda_{\mathcal{A}}\lambda_{\mathcal{B}} \left(|I_2| + |J_2|\right) + \mathcal{O}(\lambda^4), \tag{3.90}$$

which yields a trace distance of $\lambda_{\mathcal{A}}\lambda_{\mathcal{B}}(|I_2| + |J_2|) + \mathcal{O}(\lambda^4)$, which is identical to the maximal trace distance in the previous scenario of $\lambda_{\mathcal{A}}\lambda_{\mathcal{B}}(|C_2| + |D_2|) + \mathcal{O}(\lambda^4)$, because $C_2 = J_2$ and $D_2 = I_2$.

This already suggests $|C_2| + |D_2|$ as an estimate for the channel capacity of signalling between two Unruh-DeWitt detectors. We will find this confirmed by the discussion of different communication tasks, and channel capacities in the following section.

3.4 Classical channel capacity

In the previous section we saw that the maximum influence Alice can take on Bob's final state, as measured by the trace distance between output states, to leading order is $\sim \lambda^2(|C_2| + |D_2|)$, i.e., determined by the integrals that where defined in equations (3.47) and (3.48). If Alice wants to use this influence in order to transmit information to Bob, her signal has to compete with the local vacuum noise, that Bob's detector is experiencing, and which also is of leading order $\mathcal{O}(\lambda^2)$. Of course, the noise will never render the channel capacity equal to zero, since, as for all communication channels, any non-zero signal-to-noise ratio guarantees a non-vanishing classical Shannon channel capacity. However, the

question is how far the classical capacity will be reduced, as the noise here is comparable to the signal strength.

We will discuss this questions from three different point of views: We are going to analyze a scenario where Alice has to transmit one classical bit to Bob, in a single use of the channel. Here, we find that the noise actually has no impact on the probability of Bob correctly deducting Alice's bit from the measurement on his detector. Allowing for repeated uses of this protocol, which constitutes a so called binary asymmetric channel, we calculate the resulting Shannon channel capacity. Finally, using a result by Berry [6], we derive a perturbative expansion of the Holevo capacity of the quantum channel, for the scenario where Bob initializes his detector in the ground state.

In all these analyses, the resulting capacities depend on the quantity $|C_2| + |D_2|$, which motivates the use of this quantity as an estimate of the channel capacity between two Unruh-DeWitt detectors.

3.4.1 Transmission of one bit from Alice to Bob

A very basic way to assess a qubit channel's capability to transmit classical information is to try to transmit one bit from Alice to Bob by a single use of the channel. What is the success probability of Bob correctly inferring the bit Alice was sending him? As we will see now, this probability is determined by the trace distance between Bob's final states that we discussed above.

For the analysis of this information task we assume that Alice and Bob can agree and optimize their communication protocol beforehand. They both know where and when they will couple to the field and can optimize Alice's pair of input states, in which she encodes '0' and '1' respectively, as well as they can optimize Bob's initial state and final measurement.

Then, Alice is given a randomly selected bit, she chooses her initial state accordingly and couples her detector to the field. Bob initialized his detector in the previously chosen input state, couples his detector to the field in order to detect Alice's signal, and after decoupling his detector performs a (projective) measurement on his detector. Since we are working with two-level detectors, this measurement has two possible outcomes. In case of the first outcome Bob will guess that Alice was sending him a '0', in the case of the other outcome he will guess '1'.

Bob's probability of guessing correctly increases above $\frac{1}{2}$ exactly by the trace distance between the two states. Therefore, using the results from the previous section, Alice and Bob can maximize the probability of Bob guessing the original bit correctly by Alice

choosing her signalling states for '0' and '1' such that trace distance between the resulting final states of Bob is as large as possible.

Bob has to choose his measurement as the projection onto a pure qubit state whose Bloch vector is parallel to the semi-axis along which the two possible output states of his detector are aligned. For example, if Bob initializes his detector in an equal weighted superposition of energy eigenstates, as discussed at the end of the previous section, then his final states lie on the Z-axis of the Bloch sphere, so that Bob will make a measurement with respect to one of the energy eigenstates of his detector. This is the scenario that was considered in [40].

Of course, the measurement outcome after which Bob will guess '1' is the one that is more likely when Alice did encode '1'. We denote the probability that Bob will measure and guess '1' when Alice encoded '1' by p. The probability that Bob measures and guesses '1' despite Alice actually encoding '0' we denote as q. The diagram Figure 3.2 shows that Bob's probability of guessing the bit correctly is

$$P_{\text{bit}} = \frac{1}{2} + \frac{1}{2}(p - q). \tag{3.91}$$

However, $\frac{1}{2}(p - q)$ is exactly the trace distance between the two possible final states of Bob's detector. The results in the previous section showed that this trace distance can be maximized such that the success probability for the transmission of one bit in a single use of the channel grows as

$$P_{\text{bit}} = \frac{1}{2} + \lambda_{\mathcal{A}}\lambda_{\mathcal{B}}\left(|C_2| + |D_2|\right) + \mathcal{O}(\lambda^4). \tag{3.92}$$

As anticipated, the quantity $|C_2| + |D_2|$ gives the leading order improvement in Bob's probability to guess Alice's bit correctly.

This transmission of one bit in a single use of the channel was first discussed in [40], however there, in equation (5), the optimization over Alice's and Bob's initial states was not performed yet. Also, in [40], Alice was assumed to encode '1' by coupling her detector to the field whereas to encode '0' she would not couple to the field at all. Using two orthogonal input states, as above, doubles the gain in success probability since it doubles the trace distance between Bob's possible final states. (Also we note that in [40] in the caption of Figure 2, and the corresponding passage in the text, the success probability should read $\frac{1}{2} + \frac{1}{2}|S(t)|$ instead of $\frac{1}{2} + |S(t)|$.)

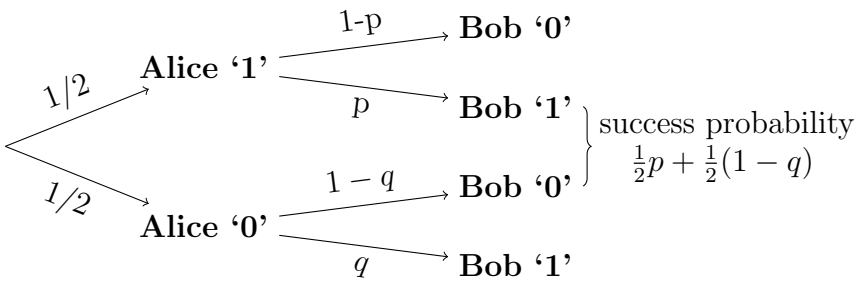

Figure 3.2: [40] The success probability for the correct transmission of one bit in a single use of a binary asymmetric channel is $\frac{1}{2}p + \frac{1}{2}(1-q) = \frac{1}{2} + \frac{1}{2}(p-q)$, assuming $p - q \geq 0$.

3.4.2 Capacity as a classical binary asymmetric channel

The protocol developed in the previous channel for the transmission of one bit constitutes what is known as a classical binary asymmetric channel [77]. These are channels where the sender can choose between two possible inputs which modulate the probability of the receiver's outcome, just as sketched in Figure 3.2. The classical Shannon channel capacity of theses channels is known to be [77]

$$C(p,q) = \frac{-qh(p) + ph(q)}{q-p} + \log_2\left(1 + 2^{\frac{h(p)-h(q)}{q-p}}\right) \tag{3.93}$$

with the binary entropy function [77, 64]

$$h(x) = -x\log_2(x) - (1-x)\log_2(1-x), \tag{3.94}$$

where the classical capacity measures the number of bits that can reliably transmitted per channel use in the limit of large numbers of channel uses [64, 76, 86].

To adopt this formula to the signalling between Unruh-DeWitt detectors, we assume the following perturbative expansions for p and q

$$\begin{aligned} p &\sim P_0 + \lambda^2(P_2 + S_2) + \lambda^4(P_4 + S_4) + \mathcal{O}(\lambda^6) \\ q &\sim P_0 + \lambda^2(P_2 - S_2) + \lambda^4(P_4 - S_4) + \mathcal{O}(\lambda^6) \end{aligned} \tag{3.95}$$

which yields

$$C \sim \lambda^4 \frac{1}{2\ln 2} \frac{S_2^2}{P_0(1-P_0)} + \mathcal{O}(\lambda^6). \tag{3.96}$$

In our case $P_0 + \lambda^2 P_2 + ...$ corresponds to the noise contributions, that are independent of Alice's presence, to the probability for Bob to find a measurement outcome corresponding to '1'. This means P_0 is the probability for Bob to detect '1' in his original initial state. This probability will typically be $\frac{1}{2}$, because Bob's final measurement typically has to be performed with respect to a basis that is unbiased to his initial state, as we observed in our earlier discussion. The coefficient S_2 is simply $S_2 = |C_2| + |D_2|$. Hence, setting $\lambda = \lambda_{\mathcal{A}} = \lambda_{\mathcal{B}}$, altogether we obtain

$$C \sim \lambda^4 \frac{2}{\ln 2} \left(|C_2| + |D_2|\right)^2 + \mathcal{O}(\lambda^6). \tag{3.97}$$

This expression is only a lower estimate for the asymptotic behaviour of the classical capacity of the channel between two Unruh-DeWitt detectors, because we are restricting Alice and Bob to use the channel as a classical channel in each round of use, and do not allow Bob to perform joint measurements on the output. However, from this result we can already tell that the channel's classical capacity is robust against the noise in the channel, at least as far as the asymptotic behaviour in the coupling constant is concerned.

3.4.3 Holevo capacity

We close this section by deriving an expression for the full Holevo capacity for the quantum channel between two Unruh-DeWitt detectors assuming that the receiver initializes his detector in its ground state. For this we use results by Berry [6].

The Holevo capacity of a channel, is the number of classical bits that can reliably transmitted per use of the quantum channel in the limit of large numbers of channel uses, if the sender is restricted to encode separable states over the different channel uses, whereas the receiver is allowed to perform joint measurements on all obtained outputs [64, 86, 6]. It is given by

$$C(\xi) = \sup_{\{p_i, \rho_i\}} S\left(\xi\left(\bar{\rho}\right)\right) - \sum_i p_i S(\xi(\rho_i)) \tag{3.98}$$

with the von Neumann entropy $S(\rho) = -\operatorname{Tr} \rho \log_2 \rho$. The optimization is taken over ensembles of signalling states where the individual signalling states ρ_i appear with relative frequency p_i, which implies $\sum_i p_i = 1$. We denote by $\bar{\rho} = \sum_i p_i \rho_i$ the average input state of the ensemble.

The Holevo capacity can also be computed by the following min-max formula [75, 6]

$$C(\xi) = \min_{\bar{\rho}} \max_{\rho_0} D\left(\xi(\rho_0) || \xi(\bar{\rho})\right) \tag{3.99}$$

where the maximum is taken over all input states of the receiver, the minimum is taken over all average states of ensembles of input states, and

$$D(\rho_1||\rho_2) = \mathrm{Tr}\,(\rho_1 \log_2 \rho_1 - \rho_1 \log_2 \rho_2) \tag{3.100}$$

denotes the relative entropy.

As discussed in [75, 6], and the references therein, it is generally known that for noisy channels ensembles of pure signalling states are optimal. Also the number of states in an optimal ensemble of a state acting on a Hilbert space of dimension d does not exceed d^2. For qubit channels, there are known examples that have optimal signalling ensembles consisting of four states. Interestingly, even if the qubit channel only requires optimal ensembles of two states, these states aren't necessarily orthogonal if the channel is non-unital, i.e., if it maps (some) pure input states to mixed output states.

In [6], Berry discusses and characterizes a class of qubit channels for which the optimal signalling ensembles contain only two states. These channels are assumed to have a Bloch sphere represenation of the general form

$$\vec{\rho} \mapsto \begin{pmatrix} m_1 & 0 & 0 \\ 0 & m_2 & 0 \\ 0 & 0 & m_3 \end{pmatrix} \vec{\rho} + \begin{pmatrix} 0 \\ 0 \\ t \end{pmatrix} \tag{3.101}$$

for real-valued constants m_1, m_2, m_3, t. This does not seem to match the Bloch representation of the channel when Bob initializes his detector in the ground state which we found in (3.75), because the channel matrix there was not diagonal. However, from the singular value decomposition of the channel matrix, we see that the channel ξ can be written as

$$\xi = \Gamma_{\mathbf{UO}} \circ \xi' \circ \Gamma_{\mathbf{O}^{\mathbf{tr}}}, \tag{3.102}$$

where $\Gamma_{\mathbf{UO}}$ and $\Gamma_{\mathbf{O}^{\mathbf{tr}}}$ are the unitary channels induced by the matrices $\mathbf{O}$ and $\mathbf{U}$ in equation (3.77). These will not change the capacity of the channel, and therefore the capacity of ξ is identical to the capacity of ξ' which is of the desired from above, with $m_1 = |C| + |D|$, $m_2 = |C| - |D|$, $m_3 = A - B$ and $t = 2P + A + B - 1$.

Defining $m_m = \max(|m_1|, |m_2|)$ Berry shows that if $m_m > |m_3|$ and

$$\frac{t^2 m_3^2}{m_m^2 - m_3^2} - 1 + m_m^2 + t^2 \leq 0 \tag{3.103}$$

then there is an optimal ensemble consisting of two states. These states, in the Bloch sphere picture, lie equidistant from the Z-axis, on a line perpendicular to and intersecting the Z-axis (Theorem 2 of [6]). This criterion holds in our case, since $|C|+|D| \sim \lambda^2(|C_2|+|D_2|) >$

$A - B \sim \lambda^4(A_4 - B_4)$, and

$$\frac{t^2 m_3^2}{m_m^2 - m_3^2} - 1 + m_m^2 + t^2 \sim -4\lambda^2 P_2 + \mathcal{O}(\lambda^4) \tag{3.104}$$

and P_2 is always positive. Because in our case $m_1 = |C| + |D| > |C| - |D| = m_2$ these two optimal states also lie in the X-Z-plane of the Bloch sphere. Berry gives a determination equation for the angle θ that the Bloch vectors of the optimal states enclose with the Z-axis. For our case it yields a perturbative expansion of

$$\theta \sim \frac{\pi}{2} - \frac{\lambda^2}{4} \frac{(A_4 - B_4)\ln(\lambda^2 P_2)}{P_2} + \mathcal{O}(\lambda^3). \tag{3.105}$$

This means that to zeroth order the optimal pair of signalling input states for Alice lie on opposite poles of the Bloch equator and are hence orthogonal states. The leading order perturbative correction moves the location typically below the Bloch equator, such that the states are not strictly orthogonal to each other anymore.

However, a perturbative expansion of the resulting channel capacity shows, that this correction to the optimal angle is irrelevant to the leading order behaviour of the channel's Holevo capacity. Thus the leading order contribution to the Holevo capacity is also achieved by the pair of orthogonal input states.

The Holevo capacity of the channel ξ expands as

$$C \sim -\lambda^4 \ln(\lambda^2 P_2) \frac{\left(|C_2| + |D_2|\right)^2}{4 \ln 2} + \mathcal{O}(\lambda^6). \tag{3.106}$$

Due to the logarithm of the leading order noise contribution, $\ln(\lambda^2 P_2)$, the leading order behaviour of the Holevo capacity is of higher order than the $\mathcal{O}(\lambda^4)$ behaviour that we derived for the use as a binary asymmetric channel. The smaller the noise is, the closer to pure states are the final states of Bob, since the centre of the ellipsoid of output states moves closer to the boundary of the Bloch sphere. This results in an advantage if Bob uses joint measurements on multiple output states, which is a strategy captured by the Holevo capacity. As before we see that the quantity $|C_2| + |D_2|$ features as the signalling contribution that determines the channel's capability to transmit classical information to leading order.

If $\lambda^2 P_2 \to 0$ could be made arbitrarily small, then it seems as if the leading order contribution to the Holevo capacity C could be made arbitrarily large, which appears to be unphysical. However, we note that to achieve very small values of P_2 typically smooth

switching functions have to be used, and the detector has to be coupled to the field for a long time. As we will see in Chapter 5, this generally leads to a decrease of the size of $|C_2|$ and $|D_2|$ which overall could lead to a decrease of the leading order contribution to C.

The Holevo capacity that results from restricting Alice's possible input states to her energy eigenstates, i.e., only optimizing over p_i but dropping the optimization over ρ_i, is discussed in [19]. For this pair of input states a closed form expression for the capacity was found in terms of the coefficients P, A and B.

3.5 Conclusion

The main result of this chapter is the estimate for the leading order signalling strength between two two-level detectors, which is given by

$$|C_2| + |D_2| \tag{3.107}$$

with C_2 and D_2 as defined in (3.47) and (3.48). We can use this term as a measure for the signalling strength, because we have shown that it sets the leading order contribution to the successful transmission of a single bit, to the channel capacity of the associated binary asymmetric channel, and to the Holevo capacity for the transmission of classical information through the quantum channel.

We see that Alice, in order to achieve leading order signalling effects, needs to initialize her detector in superpositions of energy eigenstates. Signals from energy eigenstates only occur at next-to-leading order in perturbation theory.

Bob can detect leading order signalling effects even when he starts out in an energy eigenstate. However, he will have to optimize the basis for his final measurement according to the physical parameters of the interaction in order to optimally detect the signal. This measurement basis will then consist of equal-weighted superpositions of the energy eigenstates. Alternatively, Bob can use a final measurement in the energy eigenbasis, if he optimizes his initial state so as to be optimally sensitive under the given physical parameters of the coupling.

Chapter 5 looks at the leading order signalling strength of both lightlike and timelike signals, between detectors at rest and also detectors in relativistic motion. However, first, in Chapter 4, we use the quantum channel framework to explore what finite number of modes is required to accurately reproduce the relativistic properties of a quantum field, e.g, in numerical calculations.

Chapter 4

Relativistic Accuracy with Finite Numbers of Modes

Note: This chapter largely consists of adapted and extended parts of [39].

The original motivation for the study of the quantum channel between Unruh-DeWitt detectors is to develop an information-theoretic framework for the study of information propagation in relativistic quantum field theories. In this chapter, however, we apply the framework to a slightly different question that could be phrased as: which models of quantum fields in cavities are relativistic *enough*?

When modelling quantum fields in optical, or microwave cavities typically only finitely many modes of the field are taken into account. On one hand, this is a practical necessity in any numerical computation. On the other hand, it is also physically founded since the frequency range of real cavities is always limited. Most importantly, the few-modes or even single-mode models are justified by their successful description of many experimental implementations of light-matter interactions. A well-known example of this is the Jaynes-Cummings model. It can be derived from the Unruh-DeWitt interaction hamiltonian through single-mode, and rotating-wave approximations.

Generally speaking, the finite-mode number approximations are valid in what one could call the Galilean regime. This would be the regime, where it is irrelevant that the propagation velocity of signals is bounded, and interaction times are long with respect to the propagation time of the signal. In this regime, it is of less importance that models which take into account only a finite number of modes do violate relativistic causality by allowing for faster-than-light signalling [5]. For example, if localized detectors were able to couple to just a single mode of the field, this could be used for faster-than-light signalling, because

interacting with a single mode is a highly non-local operation. The mode fills the entire space and, therefore, any change to the state of the mode could immediately be detected by any other detector having access to the single mode at a different point in space.

As discussed earlier, the causality of quantum field theory is encoded in the lightcone structure of the commutator, which strictly vanishes at spacelike separations. It follows from this sharply defined support of the commutator, that an infinite number of modes is necessary to obtain a strictly causal description of the quantum field: A finite number of modes can only resolve the sharp light cone structure of the commutator up to some limited accuracy, and will exhibit the Gibbs overshoot phenomenon at the light cone boundary. (See also [88].)

In this chapter we investigate how many field modes are necessary to suppress non-causal effects below some desired level of accuracy, in order to obtain a description of matter-light interactions that is valid beyond the non-relativistic regime.

In parts our approach is inspired by the so-called Fermi problem first posed by Fermi in [27]. This is the question how fast one atom in some excited state can cause another atom, prepared in its ground state at some distance, to get excited by the transmission of excitations via the quantum vacuum of the electric field. How would causality, and a finite propagation speed of the excitations be guaranteed given that the Wightman function of the field is non-vanishing at spacelike separations? This question is addressed in an extended body of literature, including several rediscoveries of the question and its solution. A brief but very interesting review of the problem's history is given in [24].

In essence, the resolution to the Fermi problem is to carefully consider which measurements a localized observer can perform, having access only to the second atom. Effects on the outcome probabilities for such measurements propagate at most at the speed of light. In contrast, faster-than-light signalling effects tend to be artefacts of non-local, joint measurements on the state of both atoms and the field.

The quantum channel between Unruh-DeWitt detectors provides a quantum-information theoretic framework for the Fermi problem [19]. It was shown that the channel respects causality to all orders of perturbation theory, because the commutator of the field vanishes at spacelike separations. Of particular interest in this context are also the works on the Fermi problem in circuit QED [70] and in discrete systems [88].

When only a finite number of the field modes inside a cavity are taken into account, i.e., when a ultraviolet (UV) cutoff is imposed on the field, then faster-than-light error terms arise in the Fermi problem. We take the size of these error terms as an estimate for the accuracy with which the relativistic properties of the field can be represented by a given

number of field modes. We find that the size of the errors decay for larger total numbers of modes following a power-law decay.

4.1 The quantum channel inside a cavity

In the following we study the quantum channel between two detectors inside a cavity in different communication settings. For the purpose of this chapter, we restrict ourselves to the case where the receiver detector is initialized in its ground state. Therefore the channel is of the general form (3.33), where only the coefficients P, A, B, C, D occur.

Here we are interested in how the magnitude of the imposed UV-cutoff, i.e., the number of field modes that are taken into account, affects the accuracy with which causality is respected by the model. In other words, we will study the magnitude of faster-than-light error terms, that arise from the leading order contributions to the coefficients P, A, B, C, D, as a function of the UV-cutoff.

As a first setting, we will consider what we will call the Fermi problem scenario, i.e., we study signalling from detector $\mathcal{A}$ to detector $\mathcal{B}$ under the condition that the initial state of the first detector is either the ground or the excited state. Although it appears to be a very natural choice to use the energy eigenstates for signalling, we know from the previous section that these signalling terms are suppressed by two orders in the coupling constant: here, the effect on Bob's detector is only of order $\mathcal{O}(\lambda^4)$, whereas the effect is of order $\mathcal{O}(\lambda^2)$ for any other set of pure input states.

To illustrate this, we will consider a second scenario where detector $\mathcal{A}$ initially is prepared in either the state

$$|+\rangle = \frac{1}{\sqrt{2}}\left(|g\rangle + |e\rangle\right) \tag{4.1}$$

or

$$|-\rangle = \frac{1}{\sqrt{2}}\left(|g\rangle - |e\rangle\right). \tag{4.2}$$

In what follows we consider a massless Klein-Gordon field inside a one-dimensional Dirichlet cavity as discussed in Section 2.3.2. Also we choose both detectors to be resonant with a field mode, so $\Omega_{\mathcal{A}} = \Omega_{\mathcal{B}} = \omega_n$ for some given resonance mode number n.

The detectors are switched on and off sharply at $t = 0$ and $t = T$ respectively, i.e., the switching function is defined to be $\chi(t) = 1$ for $t \in (0, T)$ and vanish at all other times. Under these conditions the perturbative terms of the leading order contributions to the

channel coefficients P, A, B, C, D in (3.34), (3.35), (3.36), (3.37), (3.38) are analytically integrable (although very involved to obtain). Even though different switching protocols could be considered, to have detector $\mathcal{B}$ switched in parallel with the first detector is the most conservative setting in order to detect any error terms that would propagate signals from $\mathcal{A}$ to $\mathcal{B}$ outside the lightcone.

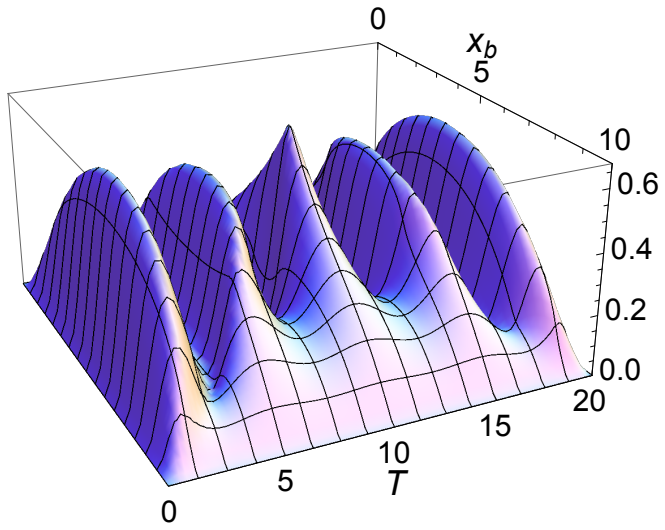

Figure 4.1: [39] Leading order contribution P_2 to the single detector excitation probability (3.34) for a detector at x_b in a cavity of length $L = 10$. The detector is resonant to the fourth field mode ($n = 4$). The contribution P_2 is periodic with a periodicity of $T_{\text{per}} = 2L$. The number of valleys in every period is equal to n. For the calculation a cutoff of $N_C = 100$ modes was used. (All plotted quantities are dimensionless.)

Before we study the influence of detector $\mathcal{A}$ on the final state of $\mathcal{B}$ we review the contribution to $\rho_{\mathcal{B},T}$ in (3.33) which is independent of the presence of detector $\mathcal{A}$. This is the term P in (3.34) which captures the probability of the single detector $\mathcal{B}$ to get excited on its own due to the switching, i.e., which captures its vacuum noise.

Figure 4.1 shows the lowest order contribution P_2 to the single detector excitation probability which is mostly induced from the vacuum due to the sudden switching. It is non-negative and periodic with a periodicity of $T_{\text{per}} = 2L$, which is twice the cavity crossing time. When the detector is tuned resonant to a field mode with an even mode number n (as in the figure), the term P_2 peaks at the light-crossing time of the cavity for a detector positioned at the middle of the cavity. If n is odd P_2 vanishes here. The number of valleys

per period along the T-axis is equal to the resonance mode number n. The contribution of the non-resonant modes makes the probability non-zero in these valleys.

In Figure 4.2, one example of the second order contribution P_4 is plotted. P_4 captivates the probability of a single detector to get excited and deexcited again during the interaction interval. Hence it gives a non-positive correction to the single detector excitation probability.

All other contributions to $\rho_{\mathcal{B},T}$ depend on the initial state of Alice's detector.

As we know from the channel's general structure, in the Fermi problem the contribution of $\mathcal{A}$ to the state of $\mathcal{B}$ appears only in the diagonal elements of Bob's density matrix. Hence, as discussed earlier, in the Fermi problem the signalling terms which are of order $\mathcal{O}(\lambda^4)$ compete directly with the single detector excitation probability $P \sim \mathcal{O}(\lambda^2)$ This might, on the one hand, mask effects of causality violations in the excitation probability of Bob and, on the other hand, hinder the ability of Alice to signal Bob.

Therefore, as a second example, we will consider a slightly altered version of the Fermi problem where Bob performs his measurement in the $\{|+\rangle, |-\rangle\}$ basis such that Bob can detect the $\mathcal{O}(\lambda^2)$ effect of Alice's input without any influence of P on the measurement outcomes.

4.2 Signalling in the Fermi problem

We can analyze the Fermi problem, i.e., the question of how the excitation probability of detector $\mathcal{B}$, which starts out in the ground state at $t = 0$, is affected by the presence of the other detector starting out in its excited state. From (3.33) we see that the detector $\mathcal{B}$ ends up in the state

$$\xi\left(|e_{\mathcal{A}}\rangle\langle e_{\mathcal{A}}|\right) = \begin{pmatrix} P + A & 0 \\ 0 & 1 - P - A \end{pmatrix}. \tag{4.3}$$

So the factor A describes the probability for the detector $\mathcal{B}$ to become excited due to the presence of the initially excited detector $\mathcal{A}$. If we compare this output to the case where the detector $\mathcal{A}$ is initially prepared in its ground state,

$$\xi\left(|g_{\mathcal{A}}\rangle\langle g_{\mathcal{A}}|\right) = \begin{pmatrix} P + B & 0 \\ 0 & 1 - P - B \end{pmatrix}, \tag{4.4}$$

we see that B describes the contribution to the probability of finding detector $\mathcal{B}$ excited after the interaction due to the presence of the other detector starting out in the ground state.

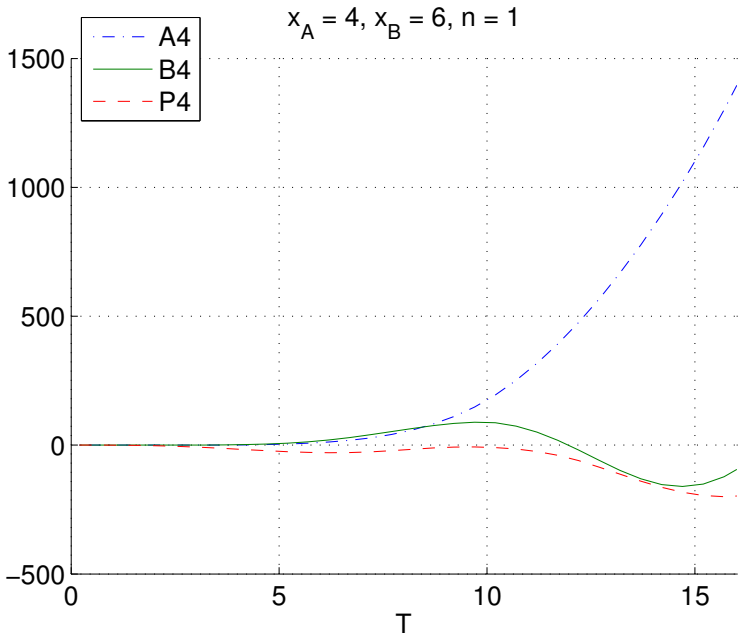

Figure 4.2: [39] Numerical values of the $\mathcal{O}(\lambda^4)$ coefficients defined in (3.35),(3.36) and (3.34) for the quantum channel in the Fermi problem. The length of the cavity is $L = 10$ and the distance between the two detectors is $|x_{\mathcal{A}} - x_{\mathcal{B}}| = 2$. (All plotted quantities are dimensionless.)

As we have seen in (3.35) and (3.36), the factors A and B are of order $\mathcal{O}(\lambda^4)$. I.e., if Alice wants to send a message to Bob, or just a single bit, and tries to encode it by either preparing her detector in the ground or excited state initially, she only influences Bob's final measurement result at fourth order $\mathcal{O}(\lambda^4)$ in the coupling constant.

In Figure 4.2, one example of the lowest order contributions to A and B is plotted. The general behaviour is that A_4 is non-negative and grows faster with the switching length T than the other contributions of order $\mathcal{O}(\lambda^4)$, whereas B_4 is oscillating.

We also see that A_4 and B_4 vanish outside the lightcone, i.e., for switching times $T < |x_{\mathcal{A}} - x_{\mathcal{B}}|$ smaller than the distance between the two detectors. Of course this is necessary to prevent superluminal signalling: If A or B were not to vanish for $T < |x_{\mathcal{A}} - x_{\mathcal{B}}|$ then the state of detector $\mathcal{B}$ at time $t = T$ would be influenced by the the state of detector $\mathcal{A}$ at $t = 0$, and thus retrieve information about the initial state of $\mathcal{A}$, although no light signal could have reached $\mathcal{B}$ within this time.

It was shown in [19] that the quantum channel ξ is causal in the continuum scenario

at leading order in perturbation theory. All the factors A, B, C and D in (3.33) vanish outside the lightcone, which relies on the property of the field commutator to vanish for spacelike separations.

This also holds in the cavity if all (infinite) field modes are taken into account. However, when a UV-cutoff is introduced such that only a finite number of modes N_C are taken into account, the commutator does not vanish outside the lightcone any longer. Hence a model with only a finite number of field mode also predicts that superluminal signalling between two detectors is possible for certain settings. In the following we want to investigate how these acausalities depend on the number of modes N_C and how the model of light-matter interaction behaves more and more causally with increasing cutoffs to a point where the predicted acausal behaviour would be undetectable in practice.

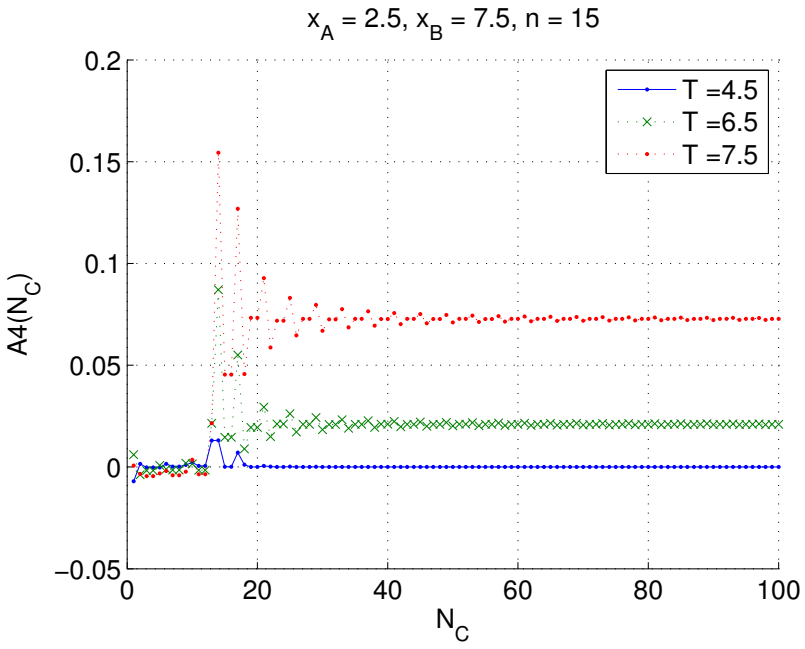

Figure 4.3: [39] Numerical values of the lowest order contribution A_4 from (3.35) to the signalling term in the Fermi problem for two detectors separated by $|x_A - x_B| = 5$ for different switching times T, depending on the number of modes below the cutoff N_C. The biggest contribution are acquired around the resonance mode number $n = 15$. For $N_C > n$ the results oscillate around a limiting value which is approached for higher cutoffs. For the lowest switching time the detectors are spacelike separated during the interaciton with the field, hence no signalling is possible. (All plotted quantities are dimensionless.)

Figure 4.3 illustrates how the result obtained for the coefficient in the channel, in this case of A, improves with the number of modes N_C taken into account. As expected the main contribution to the coefficient originates from the mode to which the detectors are resonant. For cutoffs $N_C > n$ larger than the resonance mode the results begin to converge toward a limit in an oscillating manner. This limit is positive when T is chosen to be larger than the distance between the operators so that signalling is possible. If we have $T \leq |x_{\mathcal{A}} - x_{\mathcal{B}}|$ then the results for A_4 converge to zero.

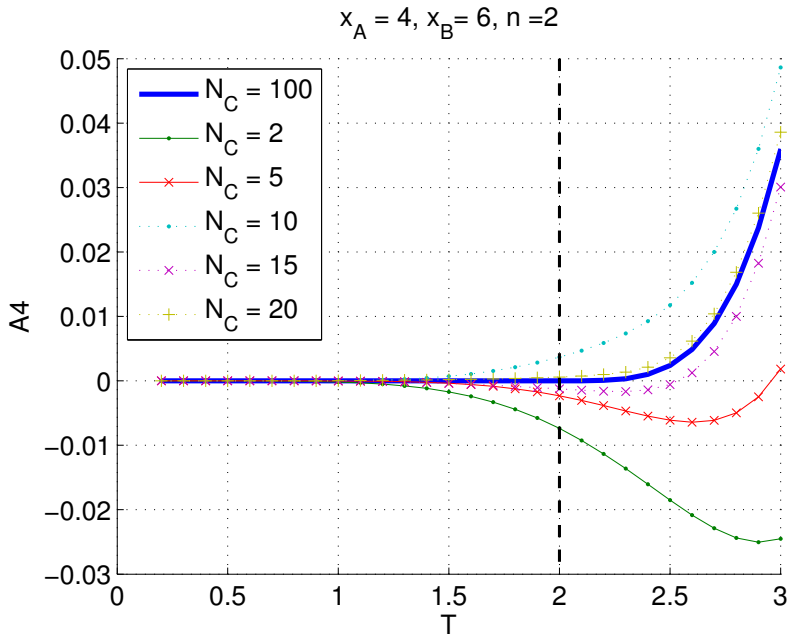

Figure 4.4: [39] The signalling term A_4 from (3.35) in the Fermi problem for two detectors at a distance of $|x_{\mathcal{A}} - x_{\mathcal{B}}| = 2$ for different switching times T for increasing cutoffs at N_C. The dashed line indicates the lightcone. In general the values of A_4 inside the lightcone grow towards the lightcone. Hence to check the level of causality violation for a specific cutoff the value on the lightcone, i.e., for a switching time $T = |x_{\mathcal{A}} - x_{\mathcal{B}}|$ is relevant. (All plotted quantities are dimensionless.)

The most relevant figures are Fig. 4.4 and 4.5. There we study the behaviour of $A_4(T)$ in the proximity of the light cone as the UV cutoff N_C is increased.

In Figure 4.4, we see that for low values of N_C the contribution A_4 is not vanishing for switching times $T < |x_{\mathcal{A}} - x_{\mathcal{B}}|$ shorter than the distance between the detectors. This would allow for superluminal signalling. Only with increasing N_C the graph approaches

the exact limit and causal behaviour is restored. We also observe in Figure 4.4 that the values outside of the lightcone, i.e., for switching times $T < |x_{\mathcal{A}} - x_{\mathcal{B}}|$, grow with increasing switching times T. Hence, the lightcone where the switching time $T = |x_{\mathcal{A}} - x_{\mathcal{B}}|$ equals the distance between the detectors marks a critical case which we can use to quantify the violation of causality in a model with UV-cutoff: To avoid superluminal signalling the coefficients of the channel in (3.33), like A, have to vanish on the lightcone. As the value of $|A_4(T)|$ for a fixed cutoff N_C is larger on the lightcone than further outside the lightcone, we can take $|A_4(T = |x_{\mathcal{A}} - x_{\mathcal{B}}|)|$ as a measure for the violation of causality.

In other words, given that the coefficients A, B, C, D are smooth functions of time, their being zero outside the light cone implies that their value is also zero right on the light cone. If we are looking for an estimation of how big the acausal error in signalling is for a finite number of modes N_C, we can analyze the value of the contributions of Alice's detector initial state to Bob's detector right on the light cone, since this is the most conservative scenario.

Because of the oscillating behaviour that we observed in Figure 4.3 for large cutoffs, it is not convenient to directly compare values of $|A_4(T = |x_{\mathcal{A}} - x_{\mathcal{B}}|)|$ obtained for different values of N_C to each other directly. Instead, in Figure 4.5, for a given cutoff N_C, we plot the maximum value obtained for $|A_4(T = |x_{\mathcal{A}} - x_{\mathcal{B}}|)|$ for any cutoff N larger than or equal to N_C.

Notice that for all switching times T the value of $A_4(T)$ depends also on the mode n with which the detectors are resonant. In general, all contributions to the channel coefficients A, B, C, D and P in (3.33) tend to be smaller for higher mode numbers n. Therefore, in order to be able to compare the values for detectors being resonant with different modes n on equal footing, in Figure 4.5, we show the value of the A_4 term on the light cone divided by the respective value of A_4 for each n at a time inside the lightcone. Hence we are computing the relative magnitude of the faster-than-light signalling signature as compared to the causal signal. In particular, the values in Figure 4.5 have been normalized by the respective value of $|A_4(T = \frac{3}{2}|x_A - x_B|, N_C = 100)|$.

Interestingly, we observe that this value decays following a power law for cutoffs N_C well above the resonance mode n.

The asymptotic power of this decay is the same for different choices of the mode the detectors are tuned to be in resonance with. Similarly, the distance between the two detectors and their positioning inside the cavity do not change the slope of the decay, but only shift the asymptotic behaviour along the y-axis in a double-logarithmic plot as in Figure 4.5. This shift in the double-logaritmic plot corresponds to a multiplying factor in front of the functional relation between N_C and A_4.

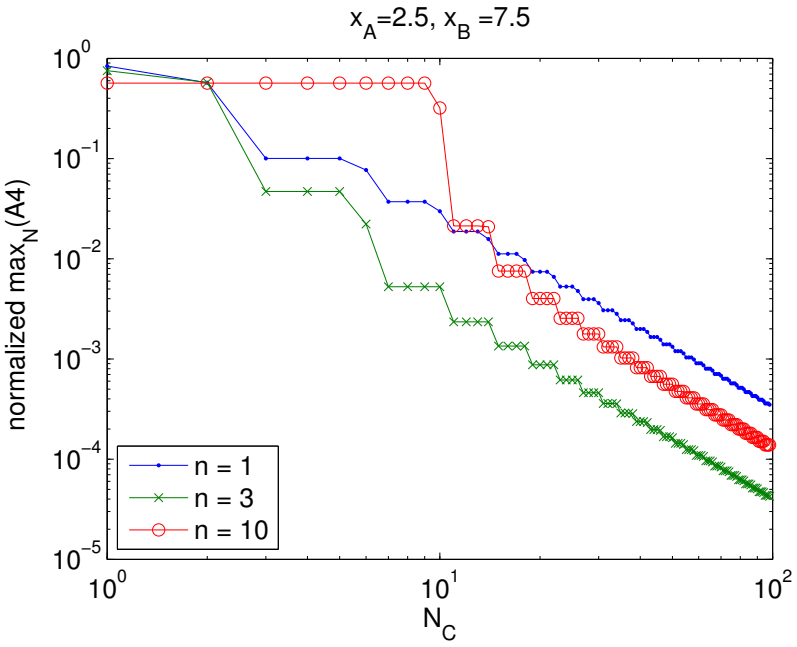

Figure 4.5: [39] The plot shows $\max_{N \geq N_C} |A_4(N)|$, the maximum value of the signalling term A_4 from (3.35) on the light cone $|A_4(T = |x_{\mathcal{A}} - x_{\mathcal{B}}|)|$ obtained for any higher cutoff, i.e., for any number of modes $N \geq N_C$ larger than or equal to N_C. For different n the modes have been normalized as explained in the text. The values of $|A_4|$ on the lightcone, i.e., for $T = |x_{\mathcal{A}} - x_{\mathcal{B}}|$ approach zero following a power law for large numbers of modes N_C. (All plotted quantities are dimensionless.)

The power law decay can be traced back to the structure of A_4 as it is given in equation (A.2) of the appendix. Inside the cavity the two-point function of the field is given by a sum with a single contribution from each field mode. Hence the four-point function which occurs in A_4 is given by a twofold sum with two summation variables running over all the field modes, because the four-point function can be expressed in terms of two-point functions in the usual way. For each term in this sum the time integrations of equation (A.2) lead to a polynomial in the summation variables (with the physical parameters and trigonometric functions as coefficients) which is divided by a common denominator. This denominator is itself a polynomial in the summation variables. Hence for higher cutoffs the asymptotic power law behaviour should emerge from the leading behaviour of the polynomial fraction for high values of the summation variables.

4.3 Signalling using $|+\rangle$ and $|-\rangle$ states

In this section we extend the analysis above to the error terms that appear in leading order $\mathcal{O}(\lambda^2)$ signalling terms. The previous section was only concerned with the subdominant $\mathcal{O}(\lambda^4)$ terms that arise in the Fermi problem where the sending detector $\mathcal{A}$ is prepared in an energy eigenstate. In order to obtain leading order signalling contributions we will, in a slight modification of the Fermi problem, consider the case where detector $\mathcal{A}$ starts out in a superposition of energy eigenstates instead.

In (3.33) we see that the off-diagonal elements of $\rho_{\mathcal{B},T}$ are given by products of the factors C and D (and their complex conjugates) with the off-diagonal elements γ and γ^* of $\rho_{\mathcal{A},0}$. So in general (i.e., unless $\rho_{\mathcal{A},0}$ is diagonal) the initial state of detector $\mathcal{A}$ has an influence on the final state of detector $\mathcal{B}$ at second order in the coupling strength, because $C, D \sim \mathcal{O}(\lambda^2)$. However to make use of this effect, e.g., for signalling, the off-diagonal element of the input state γ has to be large and, on the recipients side, the off-diagonal elements of $\rho_{\mathcal{B},T}$ have to be measured.

As a simple example for this we look at the following protocol: The system is assumed to start out in the same state as before, i.e., the field is prepared in the vacuum, detector $\mathcal{B}$ in its ground state and detector $\mathcal{A}$ in an arbitrary state

$$\rho_{\mathcal{A},0} = \begin{pmatrix} \theta & \gamma \\ \gamma^* & \beta \end{pmatrix}. \tag{4.5}$$

Now, however, after the interaction has taken place between $t = 0$ and $T = 0$ a measurement on detector $\mathcal{B}$ is performed in the $\{|+\rangle, |-\rangle\}$ basis, where

$$|\pm\rangle = \frac{1}{\sqrt{2}} \left(|g\rangle \pm |e\rangle \right). \tag{4.6}$$

We find that the projectors onto these two states are given by

$$P_\pm(t=0) = |\pm\rangle\langle\pm| = \frac{1}{2} \begin{pmatrix} 1 & \pm 1 \\ \pm 1 & 1 \end{pmatrix}. \tag{4.7}$$

Because we work in the interaction picture $P_\pm$ needs to be evolved with the corresponding free Hamiltonian $H_\mathcal{B} = \Omega_\mathcal{B} |e\rangle\langle e|$.

$$P_\pm(t) = \exp(\mathrm{i}H_\mathcal{B} t)\, P_\pm(t=0)\, \exp(-\mathrm{i}H_\mathcal{B} t) = \frac{1}{2} \begin{pmatrix} 1 & \pm e^{\mathrm{i}\Omega_\mathcal{B} t} \\ \pm e^{-\mathrm{i}\Omega_\mathcal{B} t} & 1 \end{pmatrix} \tag{4.8}$$

So for $t > T$ the probability to find detector $\mathcal{B}$, e.g., in the $|+\rangle$-state is given by:

$$\mathrm{Tr}\left(P_+(t)\rho_{T,B}\right) = \frac{1}{2} + \mathrm{Re}\left(\left(\gamma C + \gamma^* D^*\right) e^{-\mathrm{i}\Omega_{\mathcal{B}} t}\right) \tag{4.9}$$

As expected from the Bloch picture analysis of the channel in Section 3.3.4, this detection probability is completely independent of all other terms occuring in the general form of the channel. It is independent of A and B and hence from the diagonal elements of $\rho_{\mathcal{A},0}$ and the single detector excitation probability P does not have any influence either.

By choosing the time of Bob's measurement the signalling strenght can be optimized: Say the detector $\mathcal{A}$ was intially prepared in the $|+\rangle$-state, for which $\gamma = \frac{1}{2}$ or the $|-\rangle$-state, for which $\gamma = -\frac{1}{2}$. Then for a given set of parameters, i.e., if C and D are known, the time point of the measurement on detector $\mathcal{B}$ can be chosen such, that the probability to find detector $\mathcal{B}$ in the $|+\rangle$-state is given by

$$p\left(\mathcal{B} = |+\rangle \,|\mathcal{A} = |\pm\rangle\right) = \frac{1}{2} \pm |C + D^*| \,. \tag{4.10}$$

Figure 4.6 plots one example of the lowest order contributions to this probability. As known from the analysis of the channel's capacity for the transmission of one single bit in Section 3.4.1 the effect could be further optimized up to $\frac{1}{2} \pm |C| + |D|$ by optimizing Alice's input state (or the time of onset of the coupling).

Figures 4.6 and 4.7 show that the dependence of $|C_2 + D_2^*|$ on the size of the cutoff N_C is similar to the behaviour obtained for the signalling term in the Fermi problem in the previous section. Figure 4.6 illustrates the behaviour of $|C_2 + D_2^*|$ close to the lightcone. If a too small number of modes are taken into account, the model is clearly inconsistent with causality but for higher and higher cutoffs the curve approaches the limit of full causality. In Figure 4.7 we see that the errors again decay according to a power law, as already observed in the previous section.

4.4 Conclusion

This chapter showed that light-matter interactions in cavities can be reliably modelled for short interaction times and relativistic scenarios, even with only finitely many field modes.

As a measure for the accuracy that is achievable with a given cutoff on the number of field modes, we studied the size of unwanted non-causal error terms in the signalling between two Unruh-DeWitt detectors. These errors decay following a power law when the

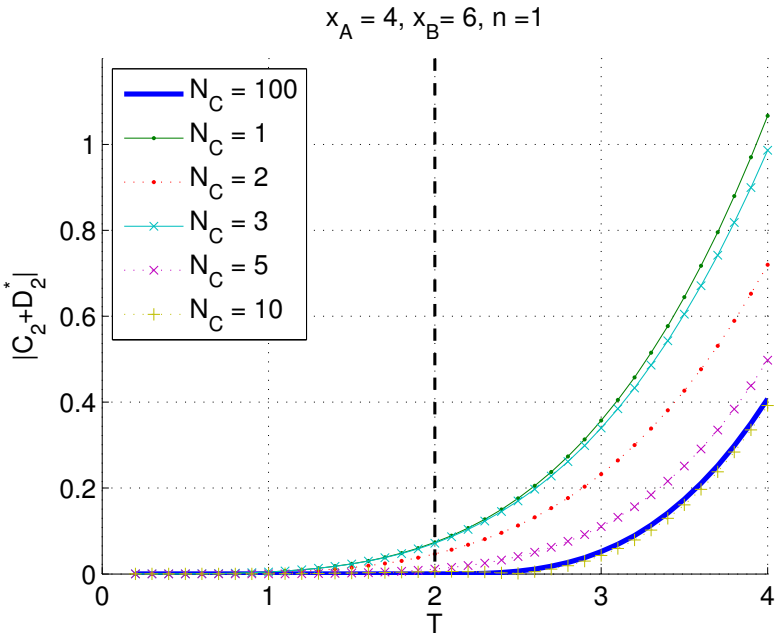

Figure 4.6: [39] Plot of $|C_2 + D_2^*|$ as defined in (3.37), (3.38), the lowest order contribution to the detection probability in (4.10), for different cutoffs N_C. The detectors are located at a distance of $|x_A - x_B| = 2$. The dashed line indicates the lightcone. The use of $|\pm\rangle$-states enhances signalling by two orders of magnitude in the coupling constant as compared to the use of energy eigenstates. (All plotted quantities are dimensionless.)

number of modes is increased. The power law decay arises from the convergence behaviour of the channel coefficients. Therefore, it is universal and does not depend on the particular initial states of the detectors. A study of the convergence behaviour of the signal strength estimator $|C_2| + |D_2|$ might demonstrate this more distinctly.

The result of this chapter is particularly relevant for numerical calculations, such as in Chapter 7, where necessarily only a finite number of field modes can be taken into account.

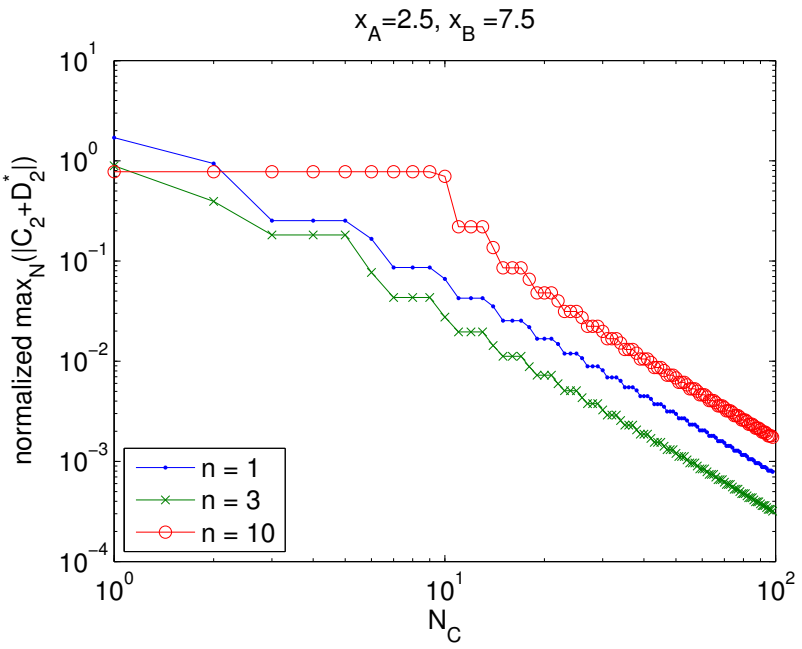

Figure 4.7: [39] The plot shows $\max_{N \geq N_C} |C_2(N) + D_2^*(N)|$ on the light cone, i.e., for $T = |x_A - x_B| = 5$. Analogous to Figure 4.5, also here the values for different n have been normalized in order to be able to compare them better. Again we observe a power law decay for high cutoffs N_C. (All plotted quantities are dimensionless.)

Chapter 5

Characteristics of timelike and lightlike signals

In this chapter, we explore how signalling between two detectors is affected by the distance and separation between the detectors, by their motion, and by their parameters such as switching times and energy gap. To this end, we study the leading order signalling term $|C_2| + |D_2|$, which we introduced as an estimate for the signalling strength in Chapter 3, in various scenarios.

Most interestingly, we observe that signalling is not only possibly between lightlike separated detectors, but in 1+1D and 2+1D Minkowski spacetime also appears between timelike separated detectors. We anticipated this in our discussion of the Klein-Gordon field propagator in Chapter 2.

When sender and receiver are in lightlike contact while they couple to the field, the signalling strength is maximized when sender and receiver are tuned into resonance. For detectors at resonance this means having identical detector gaps. However, when the detectors move relative to each other, then they need to account for the relativistic Doppler effect.

Resonance plays no role for signalling between timelike separated detectors. Instead, sender and receiver just need to optimize their energy gap according to their own switching parameters.

Another scenario where resonance cannot be achieved is signalling between a detector at rest and a uniformly accelerated detector. Although they are in lightlike contact, the Doppler shift ranges from infinitely blue-shifted to infinitely red-shifted which leads to final signalling strengths even for infinite interaction times.

The number of different signalling scenarios we need to consider is conveniently reduced by a time-inversion symmetry of the leading order signalling terms. We find that "running the movie backwards", such that the detectors move backwards in time and the receiver turns into the sender, results in the same signalling strength.

5.1 Lightlike versus timelike signalling

In Chapter 3 we showed that the quantity $|C_2| + |D_2|$ determines the signalling strength between two Unruh-DeWitt detectors to leading order. For example, it improves the probability for the correct transmission of a one bit, in a single use of the channel, from the mere guessing probability of $\frac{1}{2}$ up to (see (3.92))

$$P_{\text{bit}} = \frac{1}{2} + \lambda_{\mathcal{A}}\lambda_{\mathcal{B}}\left(|C_2| + |D_2|\right) + \mathcal{O}(\lambda^4). \tag{5.1}$$

The integrals represented by C_2 and D_2, derived and defined in Section 3.2, are

$$C_2 = \int_0^T \mathrm{d}t_1 \int_0^{t_1} \mathrm{d}t_2 \; \chi_{\mathcal{A}}(t_2)\chi_{\mathcal{B}}(t_1)\mathrm{e}^{\mathrm{i}(\Omega_{\mathcal{B}}\tau_{\mathcal{B}}(t_1)-\Omega_{\mathcal{A}}\tau_{\mathcal{A}}(t_2))}\left[\phi(t_2,\vec{x}_{\mathcal{A}}(t_2)),\phi(t_1,\vec{x}_{\mathcal{B}}(t_1))\right] \tag{5.2}$$

$$D_2 = \int_0^T \mathrm{d}t_1 \int_0^{t_1} \mathrm{d}t_2 \; \chi_{\mathcal{A}}(t_2)\chi_{\mathcal{B}}(t_1)\mathrm{e}^{-\mathrm{i}(\Omega_{\mathcal{B}}\tau_{\mathcal{B}}(t_1)+\Omega_{\mathcal{A}}\tau_{\mathcal{A}}(t_2))}\left[\phi(t_1,\vec{x}_{\mathcal{B}}(t_1)),\phi(t_2,\vec{x}_{\mathcal{A}}(t_2))\right]. \tag{5.3}$$

Here t denotes the coordinate time. And $\chi(t) = \frac{\mathrm{d}\tau}{\mathrm{d}t}\eta(\tau)$ is the product of the detector's switching function and the derivative of the detector's proper time with respect to coordinate time. Also, we assumed that the interaction between field and detectors takes place within the coordinate time interval $t \in [0, T]$. We note that the second integral $D_2(\Omega_{\mathcal{A}}.\Omega_{\mathcal{B}}) = -C_2(\Omega_{\mathcal{A}}, -\Omega_{\mathcal{B}})$ arises from the first one by an overall change of sign, and by changing the sign of $\Omega_{\mathcal{B}}$. Therefore, we focus on C_2 in the following discussion.

The nesting of the time integrations above originates from the Dyson expansion of the time evolution operator, which imposes $t_1 > t_2$. We can tighten the upper boundary of the the integral over t_2 further, by using that signals propagate at most at the speed of light, and assuming that the sender only couples to the field within some time interval $t \in [0, T_A] \subset [0, T]$. (Compare Figure 5.1.)

The final propagation velocity of the signal is encoded in the commutator, because the commutator vanishes at spacelike separations. Therefore, for a fixed value of t_1, the

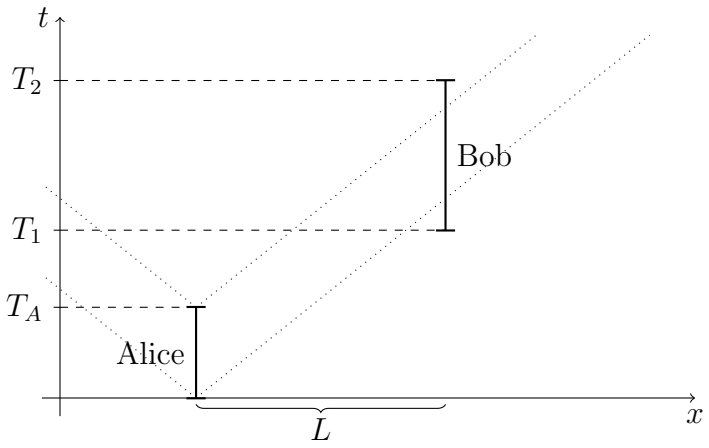

Figure 5.1: Spacetime diagram of signalling scenario between two detectors at rest. Alice couples within the coordinate time interval $t \in [0, T_A]$ to the field. Depending on the timing of Bob's coupling for $t \in [T_1, T_2]$ the detectors are lightlike or timelike separated. [40]

integrand vanishes when t_2 is so large that the lightray which emanates from the sender at t_2 reaches the receiver only at a time later than t_1. We denote the coordinate time at which the lightray, emanating at t_1 from the sender, reaches the receiver by $\tilde{t}(t_1)$. The time window of the sender's coupling to the field is given by the switching function's support $\operatorname{supp} \chi_{\mathcal{A}} \subset [0, T_A]$. Therefore, the integrand also vanishes if $t_2 > T_A$. Thus, altogether we can express the nested integration boundary as

$$C_2 = \int_{T_1}^{T_2} \mathrm{d}t_1 \int_{0}^{\min(T_A, \tilde{t}(t_1), t_1)} \mathrm{d}t_2 \; \chi_{\mathcal{A}}(t_2)\chi_{\mathcal{B}}(t_1) \mathrm{e}^{\mathrm{i}(\Omega_{\mathcal{B}}\tau_{\mathcal{B}}(t_1) - \Omega_{\mathcal{A}}\tau_{\mathcal{A}}(t_2))} \left[\phi(t_2, \vec{x}_{\mathcal{A}}(t_2)), \phi(t_1, \vec{x}_{\mathcal{B}}(t_1))\right], \tag{5.4}$$

where we added the assumption that the receiver couples to the field within the time window $[T_1, T_2]$.

The integration boundaries are independent if and only if the receiver is strictly timelike separated from the sender, i.e, if no lightray that emanates from the sender while the sender is coupling to the field reaches the receiver while the receiver is coupling to the field. In this case the inner integral is independent of t_1 and always runs over the interval $0 \leq t_2 \leq T_A$. We will see that this has the consequence that timelike signals do not depend on sender and receiver being resonant with each other.

In contrast, lightlike signals can grow much larger when sender and receiver are resonant to each other, i.e., have identical detector gaps, or when their detector gaps are tuned such as to account for any Doppler-shift effects.

5.2 Lightlike signalling

5.2.1 Resting detectors

To study the properties of lightlike signals, we begin with the simple setting of two detectors, Alice and Bob, at rest in Minkowski space. A spacetime diagram of this general scenario is shown in Figure 5.1. In this setup we can explore the role that the detectors' energy gaps, and the distance between the detectors plays for the signalling strength. Interestingly, we find that the signalling strength decays slower than the energy density emitted by the sender has to decay when the distance between the sender and the receiver is increased. This is what we already expect from the discussion of the field commutator's behaviour in Chapter 2.3.

We assume that Bob couples to the field exactly during the time interval when he is lightlike separated from Alice. This means Bob's detector is switched on when the first lightray emanating from Alice reaches him, and Bob's detector is switched off when the last lightray from Alice reaches Bob. With the notation introduced above, where Alice couples to the field $0 \leq t \leq T_A$ and Bob for $T_1 \leq t \leq T_2$, this means

$$T_1 = L, \qquad T_2 = L + T_A, \tag{5.5}$$

where L is the distance between Alice and Bob.

Under these conditions the integrals of the leading order signalling contributions take the form

$$C_2 = \int_L^{L+T_A} \mathrm{d}t_1 \int_0^{t_1-L} \mathrm{d}t_2 \; \chi_{\mathcal{A}}(t_2)\chi_{\mathcal{B}}(t_1)\mathrm{e}^{\mathrm{i}(\Omega_{\mathcal{B}}t_1 - \Omega_{\mathcal{A}}t_2)} \left[\phi(t_2, \vec{x}_{\mathcal{A}}(t_2)), \phi(t_1, \vec{x}_{\mathcal{B}}(t_1))\right], \tag{5.6}$$

and accordingly for $D_2 = -C_2(\Omega_{\mathcal{A}}, -\Omega_{\mathcal{B}})$. For sharp switching functions, as defined in (3.11), this integral has a straightforward solution in 1+1D Minkowski spacetime and in 3+1D Minkowski spacetime.

In 3+1D the field commutator (see Section 2.3) is

$$[\phi(t_2,\vec{x}_2),\phi(t_1,\vec{x}_1)] = \frac{\mathrm{i}}{4\pi\,|\vec{x}_1-\vec{x}_2|}\left(\delta\left(t_2-t_1+|\vec{x}_2-\vec{x}_1|\right)-\delta\left(t_2-t_1-|\vec{x}_2-\vec{x}_1|\right)\right) \tag{5.7}$$

and we have

$$\begin{aligned} C_2 &= \int_L^{L+T_A}\mathrm{d}t_1\int_0^{t_1-L}\mathrm{d}t_2\;\chi_{\mathcal{A}}(t_2)\chi_{\mathcal{B}}(t_1)\mathrm{e}^{\mathrm{i}(\Omega_{\mathcal{B}}t_1-\Omega_{\mathcal{A}}t_2)}\frac{\mathrm{i}}{4\pi L}\delta(t_1-t_2-L) \\ &= \int_L^{L+T_A}\mathrm{d}t_1\,\mathrm{e}^{\mathrm{i}(\Omega_{\mathcal{B}}-\Omega_{\mathcal{A}})t_1}\frac{\mathrm{i}\mathrm{e}^{\mathrm{i}\Omega_{\mathcal{A}}L}}{4\pi L} = \frac{\mathrm{e}^{\mathrm{i}\Omega_{\mathcal{B}}L}\left(1-\mathrm{e}^{\mathrm{i}(\Omega_{\mathcal{B}}-\Omega_{\mathcal{A}})T_A}\right)}{4\pi L(\Omega_{\mathcal{A}}-\Omega_{\mathcal{B}})}. \end{aligned} \tag{5.8}$$

In 1+1D, where the commutator is

$$[\phi(t_2,x_2),\phi(t_1,x_1)] = \frac{\mathrm{i}}{2}\,\mathrm{sgn}(t_1-t_2)\Theta\left((t_1-t_2)^2-(x_1-x_2)^2\right), \tag{5.9}$$

we have

$$C_2 = \frac{\mathrm{i}\mathrm{e}^{\mathrm{i}\Omega_{\mathcal{B}}L}}{2\Omega_{\mathcal{A}}\Omega_{\mathcal{B}}(\Omega_{\mathcal{A}}-\Omega_{\mathcal{B}})}\left((\Omega_{\mathcal{B}}-\Omega_{\mathcal{A}})\left(1-\mathrm{e}^{\mathrm{i}\Omega_{\mathcal{B}}T_A}\right)+\Omega_{\mathcal{B}}\left(\mathrm{e}^{\mathrm{i}(\Omega_{\mathcal{B}}-\Omega_{\mathcal{A}})T_A}-1\right)\right). \tag{5.10}$$

In both dimensions the leading order signal strength $|C_2|+|D_2|$ is maximized for resonant detectors which have $\Omega_{\mathcal{A}}=\Omega_{\mathcal{B}}$. (See Figure 5.2.) The reason for this is the nested integral structure, where t_1-L is the upper integration bound for t_2. This leads to a resonant term in the C_2 integral: When the inner integral over t_2 is performed, the upper bound adds a term with a complex phase factor of $\mathrm{e}^{\mathrm{i}\Omega_{\mathcal{A}}t_1}$ to the leftover t_1 integral. (See, e.g., the first step of (5.8).) If the two detectors are resonant, i.e., if $\Omega_{\mathcal{A}}=\Omega_{\mathcal{B}}$, then this complex factor cancels the factor of $\mathrm{e}^{-\mathrm{i}\Omega_{\mathcal{B}}t_1}$ that is already present in the integrand. This term in the integrand is then non-oscillatory and increases the absolute value of the integral.

When the detectors are resonant, i.e., for $\Omega=\Omega_{\mathcal{A}}=\Omega_{\mathcal{B}}$ the integrals simplify further. In 1+1D they are

$$C_2 = -\frac{\mathrm{e}^{\mathrm{i}\Omega L}\left(\mathrm{i}\left(\mathrm{e}^{\mathrm{i}\Omega T_A}-1\right)+\Omega T_A\right)}{2\Omega^2} \qquad D_2 = \frac{\mathrm{i}\mathrm{e}^{-\mathrm{i}(\Omega L+2\Omega T_A)}\left(\mathrm{e}^{\mathrm{i}\Omega T_A}-1\right)^2}{4\Omega^2}, \tag{5.11}$$

and in 3+1D

$$C_2 = \frac{\mathrm{i}\mathrm{e}^{\mathrm{i}\Omega L}T_A}{4\pi L} \qquad D_2 = -\frac{\mathrm{e}^{-\mathrm{i}\Omega(L+2T_A)}\left(\mathrm{e}^{\mathrm{i}2\Omega T_A}-1\right)}{8\pi\Omega L}. \tag{5.12}$$

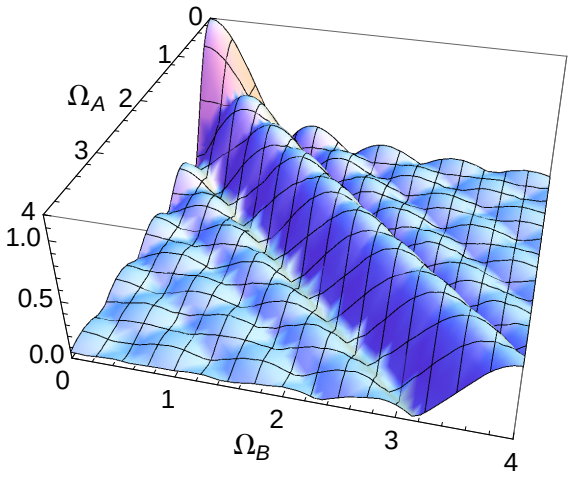

Figure 5.2: Dependence of the leading order signalling strength $|C_2| + |D_2|$ on the detector energy gaps, for two detectors at rest in 3+1D Minkowski space, as resulting from (5.8). The signalling strength is maximized for detectors with equal energy gap. The peak along the diagonal $\Omega_{\mathcal{A}} = \Omega_{\mathcal{B}}$ becomes more distinct when the interaction time T_A is increased. The distance between the detectors is set to $L = 1$, and the interaction time to $T_A = 7.5$. (The signalling strength is dimenionless in 3+1 dimensions.)

Note, that as discussed in Section 3.1, these terms are dimensionless in 3+1D, whereas they have mass dimension $C_2 = -2$ in 1+1D. As discussed earlier, this is because the coupling constant is dimensionless in 3+1D but has dimension $[\lambda] = 1$ in 1+1D, such that in all dimensions the perturbative contribution to the measurement probability $\sim \lambda^2 (|C_2| + |D_2|)$ is dimensionless, as it needs to be.

In 1+1D Minkowski spacetime for detectors at rest, the result for C_2 and D_2 suggest that the detector energy gap Ω is the natural scale to which the coupling constant λ should be compared: If we change the detector gap Ω, while leaving the number of detector periods for which the detectors are coupled to the field constant, $\Omega T_A = \text{const}$, then the term $|C_2| + |D_2|$ scales as $\sim \Omega^{-2}$. This could be corrected for by rescaling λ^2 such that $\lambda/\Omega = \text{const}$, which would keep the resulting contribution to the excitation probabilities constant.

Zero-gap detectors

The signalling strength is maximized for zero-gap detectors, i.e., in the limit $\Omega \to 0$. When applying this limit to the result for resonant detectors $\Omega = \Omega_{\mathcal{A}} = \Omega_{\mathcal{B}}$ above, D_2 differs from C_2 only by a sign, such that in 1+1D

$$|C_2| + |D_2| = 2 \left| \frac{\mathrm{i} {T_A}^2}{4} \right| = \frac{{T_A}^2}{2}, \tag{5.13}$$

and in 3+1D

$$|C_2| + |D_2| = 2 \left| \frac{\mathrm{i} T_A}{4\pi L} \right| = \frac{T_A}{2\pi L}. \tag{5.14}$$

For zero-gap detectors there is an analytic solution even for 2+1D Minkowski space. Here the commutator is given by

$$[\phi(t_2, \vec{x}_2), \phi(t_1, \vec{x}_1)] = \frac{\mathrm{i}}{2\pi} \frac{\mathrm{sgn}(t_1 - t_2)}{\sqrt{(t_2 - t_1)^2 - |\vec{x}_2 - \vec{x}_1|^2}}. \tag{5.15}$$

which, with $\Omega_{\mathcal{A}} = \Omega_{\mathcal{B}} = 0$, yields

$$\begin{aligned} |C_2| + |D_2| = \frac{T_A + L}{2\pi} \Bigg| & \frac{2\sqrt{{T_A}^2 + 2T_A L}}{T_A + L} \\ & + \ln\left(\frac{1}{L^2} \left(2{T_A}^2 + 4T_A L - 2{T_A}^{3/2} \sqrt{T_A + 2L} + L^2 - 2L\sqrt{T_A^2 + 2T_A L} \right) \right) \Bigg|. \end{aligned} \tag{5.16}$$

Zero gap detectors maximize the signalling strength, because the free detector time evolution is frozen out. This is different from the usual case of gapped detectors with $\Omega > 0$. There, in the Dirac interaction picture, the free detector Hamiltonian $H_{\mathcal{D}} = \Omega \, |e\rangle\langle e|$ causes all operators that act on the detector to spin around the Z-axis of the Bloch sphere. This also affects the monopole operator in the interaction Hamiltonian, which is, therefore, rotating in the equator $X - Y$-plane of the Bloch sphere. This leads to an averaging effect of the interaction over the time the detector is coupled to the field.

However, when the detector gap, and thus, the free detector Hamiltonian $H_{\mathcal{D}}$ vanish, operators that act on the detector do not evolve in time anymore, and the interaction Hamiltonian couples constantly through the monopole operator, which corresponds to the

Pauli σ_X-operator. In this case, Alice and Bob can choose their initial states such that they maximize the effect of the coupling at all times, without being averaged out. Therefore, the leading order signalling strength is maximal for zero gap detectors.

A particular feature of zero gap detectors is that in 1+1D and in 2+1D Minkowski space the signalling strength scales super-linearly with the total interaction time T_A. This is in contrast to gapped detectors where the scaling is linear as seen in the exact solutions for 1+1D and 3+1D above, and as numerical evaluations of the 2+1D case show. For zero-gap detectors in 1+1D, however, we see above that $|C_2| + |D_2|$ is proportional to ${T_A}^2$. The behaviour of the signalling term in 2+1D Minkowski space lies in between linear and quadratic, and is of order $\mathcal{O}(T_A \ln T_A)$ as $T_A \to \infty$.

Scaling of signalling strength with distance between detectors

In 1+1D Minkowski space the signalling strength is independent of the distance between sender and receiver. This is in agreement with the intuition that the surface of a wavefront propagating in one dimension does not increase, hence the signal should not dilute.

Accordinlgy, one might expect that in higher dimensions the signalling strength would dilute at the same rate as the surface of the spherical wavefront emitted by the sender increases. Such that in 2+1D Minkowski space $|C_2| + |D_2| \sim 1/L$, and in 3+1D Minkowski space $|C_2| + |D_2| \sim 1/L^2$.

However, the commutator, and accordingly the signalling strength decay slower than this. We see above that in 3+1D the signalling strength scales as

$$|C_2| + |D_2| \sim \frac{1}{L}, \tag{5.17}$$

and in 2+1D we find an asymptotic behaviour of

$$|C_2| + |D_2| \sim \frac{1}{\sqrt{L}} \tag{5.18}$$

of the analytic solution for zero-gap detectors, and on numerical evaluations for gapped detectors.

This scaling behaviour points towards the decoupling of the propagation of information from the propagation of energy, because it shows that the ratio between signal strength and resulting channel capacity, and the energy carried by the signal has no upper bound. The energy density emitted by the sender has to dilute at least at the rate at which the

emitted wavefront's surface grows, because the total energy is conserved. However, the signal strength decays slower.

This shows that signals imprinted in the amplitude of massless fields cannot be thought of as being supported by a flow of energy. This aspect will be most plainly highlighted by timelike signals in 1+1D, and discussed in depth in Chapter 6.

5.2.2 Time-mirror symmetry of signalling strength

Considering signalling between moving detectors, one of the first questions one might want to address is whether it is easier to signal between two detectors moving towards each other, and therefore perceiving each other blue-shifted, than between two detectors moving apart, and perceiving each other red-shifted? Or, whether it is easier to signal from an accelerated to an inertial detector, than the other way around?

Interestingly, the answer is that, under very general assumptions, the leading order signalling strength typically is the same in both directions. This is due to a time-mirror symmetry of the C_2 and D_2 terms: If time is inverted, such that the motion of the detectors runs backwards and also the role of sender and receiver are interchanged, then the C_2 and D_2 integrals of the new scenario are exactly the same as in the original scenario.

To show this we rewrite C_2 in its most general form that does not make any assumptions on the time intervals in which the detectors couple to the field:

$$C_2 = \int \mathrm{d}t_1 \int^{t_1} \mathrm{d}t_2 \, \chi_{\mathcal{A}}(t_2)\chi_{\mathcal{B}}(t_1) \mathrm{e}^{\mathrm{i}(\Omega_{\mathcal{B}}\tau_{\mathcal{B}}(t_1)-\Omega_{\mathcal{A}}\tau_{\mathcal{A}}(t_2))} \left[\phi(t_2, \vec{x}_{\mathcal{A}}(t_2)), \phi(t_1, \vec{x}_{\mathcal{B}}(t_1))\right] \tag{5.19}$$

Without loss of generality, we may assume that $\tau_{\mathcal{A}}(t=0) = \tau_{\mathcal{B}}(t=0) = 0$. The time-mirrored scenario is then given by the worldlines

$$\vec{x}'_{\mathcal{A}}(t) = \vec{x}_{\mathcal{A}}(-t) \qquad \vec{x}'_{\mathcal{B}}(t) = \vec{x}_{\mathcal{B}}(-t) \tag{5.20}$$

and hence

$$\tau'_{\mathcal{A}}(t) = -\tau_{\mathcal{A}}(-t) \qquad \tau'_{\mathcal{B}}(t) = -\tau_{\mathcal{B}}(-t). \tag{5.21}$$

The mirrored switching functions are given by $\chi'(t) = \chi(-t)$. In this scenario the signalling term for signalling from Bob to Alice is then given by

$$C'_2 = \int \mathrm{d}t_1 \int^{t_1} \mathrm{d}t_2 \, \chi'_{\mathcal{B}}(t_2)\chi'_{\mathcal{A}}(t_1) \mathrm{e}^{\mathrm{i}(\Omega_{\mathcal{A}}\tau'_{\mathcal{A}}(t_1)-\Omega_{\mathcal{B}}\tau'_{\mathcal{B}}(t_2))} \left[\phi(t_2, \vec{x}'_{\mathcal{B}}(t_2)), \phi(t_1, \vec{x}'_{\mathcal{A}}(t_1))\right] \tag{5.22}$$

by changing the integration variables to $s_1 = -t_1$ and $s_2 = -t_2$ we obtain

$$\begin{aligned} C_2' &= \int \mathrm{d}s_1 \int_{s_1} \mathrm{d}s_2\, \chi_{\mathcal{B}}'(-s_2)\chi_{\mathcal{A}}'(-s_1)\mathrm{e}^{\mathrm{i}(\Omega_{\mathcal{A}}\tau_{\mathcal{A}}'(-s_1)-\Omega_{\mathcal{B}}\tau_{\mathcal{B}}'(-s_2))} \\ &\qquad \times [\phi(-s_2,\vec{x}_{\mathcal{B}}'(-s_2)),\phi(-s_1,\vec{x}_{\mathcal{A}}'(-s_1))] \\ &= \int \mathrm{d}s_2 \int^{s_2} \mathrm{d}s_1\, \chi_{\mathcal{B}}(s_2)\chi_{\mathcal{A}}(s_1)\mathrm{e}^{\mathrm{i}(-\Omega_{\mathcal{A}}\tau_{\mathcal{A}}(s_1)+\Omega_{\mathcal{B}}\tau_{\mathcal{B}}(s_2))}\,[\phi(-s_2,\vec{x}_{\mathcal{B}}(s_2)),\phi(-s_1,\vec{x}_{\mathcal{A}}(s_1))] \\ &= \int \mathrm{d}s_2 \int^{s_2} \mathrm{d}s_1\, \chi_{\mathcal{B}}(s_2)\chi_{\mathcal{A}}(s_1)\mathrm{e}^{\mathrm{i}(-\Omega_{\mathcal{A}}\tau_{\mathcal{A}}(s_1)+\Omega_{\mathcal{B}}\tau_{\mathcal{B}}(s_2))}\,[\phi(s_1,\vec{x}_{\mathcal{A}}(s_1)),\phi(s_2,\vec{x}_{\mathcal{B}}(s_2))] = C_2. \end{aligned} \tag{5.23}$$

Whereas for the D_2 term, the mirrored term $D_2' = -D_2^*$ differs from the complex conjugate of the original coefficient by an overall sign. This shows that the leading order contribution to the signalling strength

$$|C_2'| + |D_2'| = |C_2| + |D_2| \tag{5.24}$$

is identical in the mirrored and the original scenario. Therefore, as far as the leading order signal strength is concerned, it suffices to, e.g., only analyze leading order signalling strength between detectors moving apart from each other since the signalling between two detectors moving towards each other is identical.

5.2.3 Doppler shift for inertial detectors

When the sender and the receiver are moving relative to each other, the signalling strength is in general not optimal if both detectors have identical energy gaps. The reason for this is that the motion causes the receiver to perceive the sender as red- or blue-shifted. In fact, between two inertially moving detectors exactly the Doppler effect appears in the leading order signalling strength terms.

The relative motion between sender and receiver enters the integral terms by the same mechanism that favored resonance between detectors at rest. Due to the nested integral structure, the inner integral produces a term that depends on the outer integration variable, when sender and receiver are lightlike separated. This term contains an exponential phase factor. Thus, if the receiver's gap is tuned to match the shifted gap of the detector, the

two complex phase factors cancel each other such that the integral now contains a non-oscillatory contribution.

To illustrate this, we look at a scenario where Alice is moving inertially whereas Bob is at rest, with respect to the chosen coordinate system. Alice couples to the field for a proper time interval $0 \leq \tau_{\mathcal{A}} \leq T_A$. At the beginning of her interaction she is at a distance L away from Bob, and during the coupling she moves at constant velocity $v \geq 0$ away from Bob. Without loss of generality we may assume that $t(\tau_{\mathcal{A}} = 0) = 0$. Then, the lightrays that emanate from Alice while she is coupling to the field reach Bob at coordinate time $L \leq t \leq L + \zeta T_A$. Where

$$\zeta = \sqrt{\frac{1+v}{1-v}} \tag{5.25}$$

is the relativistic Doppler factor. The factor appears because the length of the coordinate time interval in which Bob receives lightrays from Alice is

$$\Delta t = \frac{T_A}{\sqrt{1-v^2}}(1+v) = T_A\sqrt{\frac{1+v}{1-v}}. \tag{5.26}$$

If Bob couples to the field for this time interval, then the C_2 term takes the following form,

$$C_2 = \int_L^{L+\zeta T_A} \mathrm{d}t_1 \int_0^{(t_1-L)/\zeta} \mathrm{d}\tau_{\mathcal{A}}\, \eta_{\mathcal{A}}(\tau_{\mathcal{A}})\chi_{\mathcal{B}}(t_1)\mathrm{e}^{\mathrm{i}(\Omega_{\mathcal{B}}t_1 - \Omega_{\mathcal{A}}\tau_{\mathcal{A}})}\left[\phi(t(\tau_{\mathcal{A}}), \vec{x}_{\mathcal{A}}(\tau_{\mathcal{A}})), \phi(t_1, \vec{x}_{\mathcal{B}}(t_1))\right] \tag{5.27}$$

where $t(\tau_{\mathcal{A}}) = \tau_{\mathcal{A}}/\sqrt{1-v^2}$. The appearance of the Doppler factor ζ in the integration boundary of the inner integral allows for the cancellation of the complex phase factors, only if Bob's detector is tuned such as to match the red-shifted energy gap of Alice's detector.

For example, in 3+1D Minkowski spacetime, for sharp switching functions, we find

$$\begin{aligned} C_2 &= \int_L^{L+\zeta T_A} \mathrm{d}t_1 \int_0^{(t_1-L)/\zeta} \mathrm{d}\tau_{\mathcal{A}}\, \mathrm{e}^{\mathrm{i}(\Omega_{\mathcal{B}}t_1 - \Omega_{\mathcal{A}}\tau_{\mathcal{A}})} \frac{\mathrm{i}}{4\pi\left|L + \frac{v\tau_{\mathcal{A}}}{\sqrt{1-v^2}}\right|}\delta\left(t_1 - L - \tau_{\mathcal{A}}\zeta\right) \\ &= \frac{\mathrm{i}\mathrm{e}^{\mathrm{i}\Omega_{\mathcal{B}}L}}{4\pi}\int_0^{T_A}\mathrm{d}\tau_{\mathcal{A}}\, \mathrm{e}^{\mathrm{i}(\Omega_{\mathcal{B}}\zeta - \Omega_{\mathcal{A}})\tau_{\mathcal{A}}}\frac{1}{L + \frac{v\tau_{\mathcal{A}}}{\sqrt{1-v^2}}} \end{aligned}$$

$$= \frac{\mathrm{i}\sqrt{1-v^2}}{4\pi v} \mathrm{e}^{\mathrm{i}L\left(\Omega_{\mathcal{B}}+\frac{\sqrt{1-v^2}}{v}(\Omega_{\mathcal{A}}-\zeta\Omega_{\mathcal{B}})\right)} \times \left(\Gamma\left(0, \frac{\mathrm{i}L\sqrt{1-v^2}}{v}(\Omega_{\mathcal{A}}-\zeta\Omega_{\mathcal{B}})\right) - \Gamma\left(0, \frac{\mathrm{i}(T_A v + L\sqrt{1-v^2})}{v}(\Omega_{\mathcal{A}}-\zeta\Omega_{\mathcal{B}})\right)\right) \tag{5.28}$$

with the incomplete Gamma function

$$\Gamma(a,x) = \int_x^\infty \mathrm{d}t\, t^{a-1} e^{-t}. \tag{5.29}$$

The plot in Figure 5.3 shows how the Doppler shift affects Bob's optimal choice of detector frequency. If Bob chooses his detector energy gap to optimally match Alice's red-shifted frequency, i.e., such that $\Omega_{\mathcal{B}} = \Omega_{\mathcal{A}}/\zeta$, the solution simplifies to

$$C_2 = \frac{\mathrm{i}\mathrm{e}^{\mathrm{i}\Omega_{\mathcal{B}}L}}{4\pi}\frac{\sqrt{1-v^2}}{v}\ln\left(1+\frac{vT_A}{L\sqrt{1-v^2}}\right). \tag{5.30}$$

Which also correctly reproduces our previous result for resting detectors,

$$\lim_{v\to 0} C_2 = \frac{\mathrm{i}\mathrm{e}^{\mathrm{i}\Omega_{\mathcal{B}}L}}{4\pi}\frac{T_A}{L}. \tag{5.31}$$

Also in 1+1D Minkowski spacetime, for sharp switching functions, the integral has an exact solution. Here we obtain

$$C_2 = -\frac{\mathrm{e}^{\mathrm{i}\Omega_{\mathcal{B}}L}}{2\Omega_{\mathcal{A}}}\left(R + \frac{\mathrm{i}}{\Omega_{\mathcal{B}}}\left(\mathrm{e}^{\mathrm{i}\Omega_{\mathcal{B}}\zeta T_A}-1\right)\right) \tag{5.32}$$

where

$$R = \begin{cases} \zeta T_A & \text{if } \Omega_{\mathcal{B}} = \Omega_{\mathcal{A}}/\zeta \\ \frac{2\mathrm{i}}{\Omega_{\mathcal{B}}-\Omega_{\mathcal{A}}/\zeta}\mathrm{e}^{\mathrm{i}(\Omega_{\mathcal{B}}\zeta-\Omega_{\mathcal{A}})\frac{T_A}{2}}\sin\left((\Omega_{\mathcal{B}}\zeta-\Omega_{\mathcal{A}})\frac{T_A}{2}\right) & \text{else} \end{cases}. \tag{5.33}$$

We assumed here that $v \geq 0$ such that the detectors are moving apart from each other. Therefore Bob perceives Alice as red-shifted and has to lower his detector frequency in order to match Alice's shifted frequency and to optimize the signalling strength.

It is interesting to note that this lowering of Bob's frequency also plays out to optimize the signalling strength in the time-inverted scenario. Although there, Bob and Alice

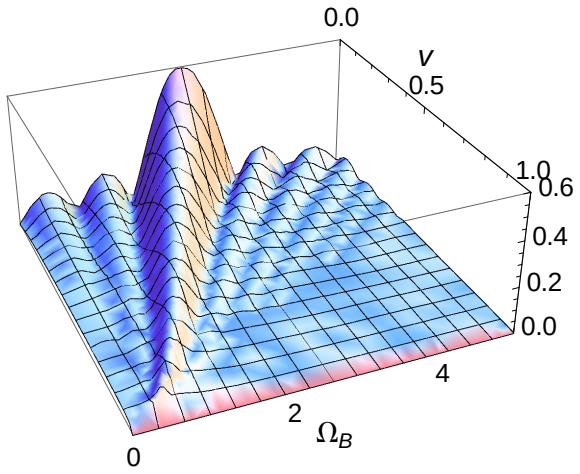

Figure 5.3: The Doppler effect between inertially moving detectors requires Bob to tune his detector gap $\Omega_{\mathcal{B}}$ to correct for the red-shifted signal from Alice, who is moving away from him at speed v. The initial distance between the detectors is $L = 1$, Alice's detector gap is set to $\Omega_{\mathcal{A}} = 2.5$ and Alice is coupled to the field for the duration of $T_A = 7.5$ according to her proper time. (The signalling strength is dimenionless in 3+1 dimensions.)

perceive each other as blue-shifted because they are moving towards each other. However, Bob is now the sender and hence needs to lower his detector gap in order to correct for the blue-shift. The amount by which Bob has to lower his gap is a sender, is exactly the same amount by which Bob has to lower his detector gap as a receiver in the original scenario, in order to correct for the red-shift when Alice moves away from him.

5.2.4 Signalling across acceleration horizon

In the context of quantum field theory, a canonical example of non-inertial motion is uniformly accelerated motion. Under this motion, a single detector experiences the Unruh effect when he is coupled to the Minkowski vacuum of the field. Earlier works that study communication under uniform acceleration include [13, 25].

The interesting feature of a uniformly accelerated wordline is that it is causally disconnected from one quarter of the Minkowski spacetime, also referred to as a Rindler wedge. This is the case, because the worldline of a uniformly accelerated observer takes the form

of a hyperbola in the spacetime diagram. We can choose inertial coordinates such that the worldline of an observer, accelerating uniformly with proper acceleration a is given by

$$t(\tau) = \frac{1}{a}\sinh(a\tau) \qquad x^1 = \frac{1}{a}\cosh(a\tau) \tag{5.34}$$

where τ is the observer's proper time, and the remaining spatial coordinates are set to vanish, $x^2 = ... = x^n = 0$. Since the motion of the accelerated observer is restricted to the so called right Rindler wedge where $0 < |t| < x$, the observer will never be reached by signals from spacetime points for which $t > x$. Also, the accelerated observer is unable to signal to any spacetime point with $t < -x$.

The Unruh effect [81] is a consequence of this causal divide as well. It shows that a uniformly accelerated observer perceives the field as being in a thermal state with a temperature proportional to his proper acceleration, while inertial observers would describe the same state as the vacuum state of the field.

Here, we want to study the signalling strength in a scenario where the sender is moving on the accelerated wordline above, while the receiver is at rest at $x^1 = 0$, just behind the acceleration horizon. We will see that the signalling strength is finite even for infinite coupling lengths, because of the infinite blue-shift and red-shift of the sender for early and late times. The leading order signalling strength in the mirrored scenario, with a resting sender and a uniformly accelerated receiver, is the same due to the time-mirror symmetry.

We will give analytic solutions to the C_2 and D_2 integrals in 1+1D an 3+1D Minkowski space, beginning with the latter case. Before this, we make a few geometric notes on the distance between Alice and Bob at different times. First, we note that the lightray that emanates from Alice at her proper time $\tau_\mathcal{A}$ reaches Bob at coordinate time

$$t_\mathcal{B}(\tau_\mathcal{A}) = x^1(\tau_\mathcal{A}) + t(\tau_\mathcal{A}) = \frac{1}{a}\left(\cosh(a\tau_\mathcal{A}) + \sinh(a\tau_\mathcal{A})\right) = \frac{1}{a}\mathrm{e}^{a\tau_\mathcal{A}}. \tag{5.35}$$

The inverse of this function will appear as the integration boundary in the nested integral,

$$\tau_\mathcal{A}(t_\mathcal{B}) = \frac{1}{a}\ln(at_\mathcal{B}). \tag{5.36}$$

Secondly, the spatial distance between Alice's spacetime point at her proper time $\tau_\mathcal{A}$ and Bob's location (at $x^1 = 0$) is

$$r = x^1(\tau_\mathcal{A}(t_\mathcal{B})) = \frac{1}{a}\cosh\left(\ln(at_\mathcal{B})\right) = \frac{1}{2a}\left(at_\mathcal{B} + \frac{1}{at_\mathcal{B}}\right) = \frac{a^2t_\mathcal{B}^2 + 1}{2a^2t_\mathcal{B}}. \tag{5.37}$$

3+1D Minkowski spacetime

In 3+1D Minkowski spacetime, the leading order signalling terms are finite even for constantly switched-on detectors. We can therefore set $\chi_{\mathcal{A}} \equiv \chi_{\mathcal{B}} \equiv 1$. The integral is then

$$\begin{aligned}
C_2 &= \int_0^\infty \mathrm{d}t_1 \int_{-\infty}^{\frac{\ln(at_1)}{a}} \mathrm{d}\tau_{\mathcal{A}}\, \mathrm{e}^{\mathrm{i}(\Omega_{\mathcal{B}} t_1 - \Omega_{\mathcal{A}}\tau_{\mathcal{A}})} \frac{\mathrm{i}}{4\pi r}\delta\left(\tau_{\mathcal{A}} - \frac{1}{a}\ln(at_{\mathcal{B}})\right) \\
&= \int_0^\infty \mathrm{d}t_1\, \mathrm{e}^{\mathrm{i}(\Omega_{\mathcal{B}} t_1 - \Omega_{\mathcal{A}}\frac{\ln(at_{\mathcal{B}})}{a})} \frac{\mathrm{i}a^2 t_{\mathcal{B}}}{2\pi(a^2 t_{\mathcal{B}}^2 + 1)} \\
&= \frac{a^{-\frac{\mathrm{i}\Omega_{\mathcal{A}}}{a}}}{4\pi}\left[2\mathrm{i}\Gamma\left(-\frac{\mathrm{i}\Omega_{\mathcal{A}}}{a}\right)|\Omega_{\mathcal{B}}|^{\frac{\mathrm{i}\Omega_{\mathcal{A}}}{a}}\right. \\
&\qquad \times\left(\mathrm{sgn}(\Omega_{\mathcal{B}})\sinh\left(\frac{\pi\Omega_{\mathcal{A}}}{2a}\right) + \cosh\left(\frac{\pi\Omega_{\mathcal{A}}}{2a}\right)\right)\, {}_1F_2\left(1; \frac{\mathrm{i}\Omega_{\mathcal{A}}}{2a}+\frac{1}{2}, \frac{\mathrm{i}\Omega_{\mathcal{A}}}{2a}+1; \frac{\Omega_{\mathcal{B}}^2}{4a^2}\right) \\
&\quad \left. + \pi a^{\frac{\mathrm{i}\Omega_{\mathcal{A}}}{a}}\left(\mathrm{sgn}(\Omega_{\mathcal{B}})\mathrm{sech}\left(\frac{\pi\Omega_{\mathcal{A}}}{2a}\right)\sinh\left(\frac{|\Omega_{\mathcal{B}}|}{a}\right) + \mathrm{csch}\left(\frac{\pi\Omega_{\mathcal{A}}}{2a}\right)\cosh\left(\frac{|\Omega_{\mathcal{B}}|}{a}\right)\right)\right] \quad (5.38)
\end{aligned}$$

with the generalized hypergeometric function[1]

$${}_1F_2(a_1; b_1, b_2; z) = \sum_{k=0}^{\infty} \frac{(a_1)_k z^k}{(b_1)_k (b_2)_k k!}. \quad (5.39)$$

From this we obtain a total leading order signal strength of

$$\begin{aligned}
|C_2| + |D_2| = \frac{1}{4\pi}\Bigg|&2\pi\cosh\left(\frac{\pi\Omega_{\mathcal{A}} - 2\Omega_{\mathcal{B}}}{2a}\right)\mathrm{csch}\left(\frac{\pi\Omega_{\mathcal{A}}}{a}\right)a^{\frac{\mathrm{i}\Omega_{\mathcal{A}}}{a}} \\
&+2\mathrm{i}e^{-\frac{\pi\Omega_{\mathcal{A}}}{2a}}\Omega_{\mathcal{B}}^{\frac{\mathrm{i}\Omega_{\mathcal{A}}}{a}}\Gamma\left(-\frac{\mathrm{i}\Omega_{\mathcal{A}}}{a}\right){}_1F_2\left(1; \frac{\mathrm{i}\Omega_{\mathcal{A}}}{2a}+\frac{1}{2}, \frac{\mathrm{i}\Omega_{\mathcal{A}}}{2a}+1; \frac{\Omega_{\mathcal{B}}^2}{4a^2}\right)\Bigg| \\
+\Bigg|&2\pi\cosh\left(\frac{\pi\Omega_{\mathcal{A}} + \Omega_{\mathcal{B}}}{2a}\right)\mathrm{csch}\left(\frac{\pi\Omega_{\mathcal{A}}}{a}\right)a^{\frac{\mathrm{i}\Omega_{\mathcal{A}}}{a}} \\
&+2\mathrm{i}e^{\frac{\pi\Omega_{\mathcal{A}}}{2a}}\Omega_{\mathcal{B}}^{\frac{\mathrm{i}\Omega_{\mathcal{A}}}{a}}\Gamma\left(-\frac{\mathrm{i}\Omega_{\mathcal{A}}}{a}\right){}_1F_2\left(1; \frac{\mathrm{i}\Omega_{\mathcal{A}}}{2a}+\frac{1}{2}, \frac{\mathrm{i}\Omega_{\mathcal{A}}}{2a}+1; \frac{\Omega_{\mathcal{B}}^2}{4a^2}\right)\Bigg|
\end{aligned}$$

[1] See also: http://functions.wolfram.com/HypergeometricFunctions/Hypergeometric1F2/02/

$$= \frac{1}{4\pi}\left|2\mathrm{i}e^{-\frac{\pi y}{2}}\Gamma(-\mathrm{i}y)\,{}_1F_2\left(1;\frac{\mathrm{i}y}{2}+\frac{1}{2},\frac{\mathrm{i}y}{2}+1;\frac{x^2}{4}\right)x^{\mathrm{i}y}\right.$$
$$\left.+2\pi\cosh\left(\frac{1}{2}(\pi y-2x)\right)\mathrm{csch}(\pi y)\right|$$
$$+\left|2\mathrm{i}e^{\frac{\pi y}{2}}\Gamma(-\mathrm{i}y)\,{}_1F_2\left(1;\frac{\mathrm{i}y}{2}+\frac{1}{2},\frac{\mathrm{i}y}{2}+1;\frac{x^2}{4}\right)x^{\mathrm{i}y}\right.$$
$$\left.+2\pi\cosh\left(\frac{1}{2}(2x+\pi y)\right)\mathrm{csch}(\pi y)\right| \tag{5.40}$$

where in the last step we measured the detectors' energy gaps in multiples of the proper acceleration by introducing $x = \Omega_{\mathcal{B}}/a$ and $y = \Omega_{\mathcal{A}}/a$. Interestingly, this shows that the leading order signalling strength in 3+1D is a function only of the ratio between the detector gaps and the acceleration.

A plot of the signalling strength as a function of x and y is given in Figure 5.4. The case where Alice uses a zero-gap detector, i.e., $\Omega_{\mathcal{A}} = 0$, or equivalently $y = 0$ for constant x, has an exact solution. It reads

$$|C_2| + |D_2| = \frac{1}{4}\left|\frac{G^{2,1}_{1,3}\left(\frac{x^2}{4}\middle|\begin{matrix}0\\0,0,\frac{1}{2}\end{matrix}\right)}{\sqrt{\pi}} - ie^{-x}\right| + \frac{1}{4}\left|\frac{G^{2,1}_{1,3}\left(\frac{x^2}{4}\middle|\begin{matrix}0\\0,0,\frac{1}{2}\end{matrix}\right)}{\sqrt{\pi}} + ie^{-x}\right| \tag{5.41}$$

where G is the Meijer G-function[2]

$$G^{m,n}_{p,q}\left(z\middle|\begin{matrix}a_1,\ldots,a_n,a_{n+1},\ldots,a_p\\b_1,\ldots,b_m,b_{m+1},\ldots,b_q\end{matrix}\right)$$
$$= \frac{1}{2\pi\mathrm{i}}\int_{\mathcal{L}}\mathrm{d}s\,\frac{\left(\prod_{k=1}^{m}\Gamma(s+b_k)\right)\prod_{k=1}^{n}\Gamma(1-a_k-s)}{\left(\prod_{k=n+1}^{p}\Gamma(s+a_k)\right)\prod_{k=m+1}^{q}\Gamma(1-b_k-s)}z^{-s}. \tag{5.42}$$

The limit $x \to 0$ appears not to exist. As x approaches zero, for fixed values of y, the signalling strength becomes highly oscillatory. However, it appears to remain bounded from above.

The particular case of equal detectors, i.e., $\Omega_{\mathcal{A}} = \Omega_{\mathcal{B}} = \Omega$ such that $x = y = \Omega/a$, diverges in the limit of $\Omega/a \to 0$. This is interesting, because this limit can arise in two ways, which appear to by physically very different.

[2]See also http://functions.wolfram.com/HypergeometricFunctions/MeijerG/02/

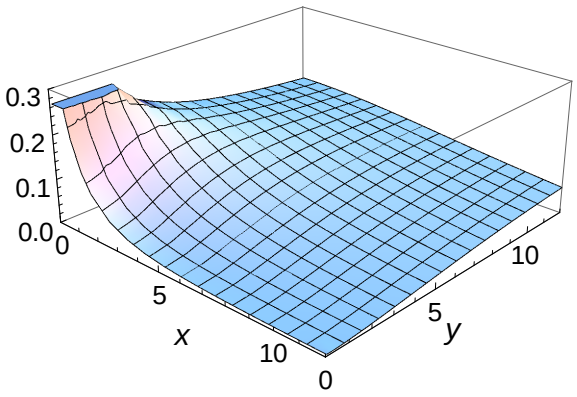

Figure 5.4: The leading order signalling strength, $|C_2| + |D_2|$, across the acceleration horizon in 3+1D Minkowski spacetime as found in (5.40). The sender is uniformly accelerated sender with proper acceleration a, the receiver is located just behind the sender's acceleration horizon. The signalling strength only depends on the ratios $x = \frac{\Omega_{\mathcal{B}}}{a}$ and $y = \frac{\Omega_{\mathcal{A}}}{a}$. It is highly oscillatory as $x \to 0$, which cannot be seen in this plot.

On the one hand, this limit could be achieved by lowering the detector frequency whereas keeping the acceleration and worldlines of the detectors fixed. Then the divergence of the signalling strength could be explained by the gradual freeze of the free time evolution of the detectors due to the lower energy gap of the detector. This would make the relativistic Doppler shift only be relevant at very early and very large times, thus, giving more and more time for the signalling terms to acquire growth.

Alternatively, one could achieve the limit by keeping the detector frequencies fixed while increasing the acceleration. Here, the increase in signalling strength seems to be explained by the decrease of distance between sender and receiver, which is $\frac{1}{a}$ for $t = 0$. However, vanishing distance leads to a divergence in 3+1D Minkowski spacetime, due to the divergence of the commutator at zero separation. (Remember, that we arranged the receiver to be located just behind the acceleration horizon of the sender.)

The impact of these two effects on the signalling strength is equivalent, not only for resonant detectors, but also in general, since the signalling strength only depends on the ratios of $x = \frac{\Omega_{\mathcal{B}}}{a}$ and $y = \frac{\Omega_{\mathcal{A}}}{a}$.

1+1D Minkowski spacetime

In 1+1D Minkowski spacetime, C_2 and D_2 are solvable for sharp switching functions with arbitrary finite interaction time intervals for Alice and Bob. However, the limit of infinite interaction times does not exist due to oscillatory boundary terms. The integrals appear to be bounded for arbitrary interaction interval lengths but a limit does not exist. The origin of this oscillatory behaviour lies in contributions from timelike signals, which we will discuss in detail in the subsequent section.

In order to suppress the oscillatory terms for the scenario that we are considering here, we introduce switching functions

$$\eta_{\mathcal{D}}(\tau) = \mathrm{e}^{-|\tau|/\sigma} = \Theta(\tau)\mathrm{e}^{-\tau/\sigma} + \Theta(-\tau)\mathrm{e}^{\tau/\sigma} \tag{5.43}$$

for both detectors, and take the limit of $\sigma_{\mathcal{D}} \to \infty$ after the integration. For the solution of the integral, it is helpful to split the integration up in two parts.

$$\begin{aligned} C_2(\sigma_{\mathcal{A}}, \sigma_{\mathcal{B}}) &= \int_0^\infty \mathrm{d}t_1 \int_{-\infty}^{\frac{\ln(at_1)}{a}} \mathrm{d}\tau_{\mathcal{A}}\, \mathrm{e}^{-t_{\mathcal{B}}/\sigma_{\mathcal{B}}} \mathrm{e}^{-|\tau_{\mathcal{A}}|/\sigma_{\mathcal{A}}} \mathrm{e}^{\mathrm{i}(\Omega_{\mathcal{B}} t_1 - \Omega_{\mathcal{A}}\tau_{\mathcal{A}})} \frac{\mathrm{i}}{2} \\ &= \int_0^\infty \mathrm{d}t_1 \int_{-\infty}^{\min(0, \frac{\ln(at_1)}{a})} \mathrm{d}\tau_{\mathcal{A}}\, \mathrm{e}^{-t_{\mathcal{B}}/\sigma_{\mathcal{B}}} \mathrm{e}^{\tau_{\mathcal{A}}/\sigma_{\mathcal{A}}} \mathrm{e}^{\mathrm{i}(\Omega_{\mathcal{B}} t_1 - \Omega_{\mathcal{A}}\tau_{\mathcal{A}})} \frac{\mathrm{i}}{2} \\ &\quad + \int_{\frac{1}{a}}^\infty \mathrm{d}t_1 \int_0^{\frac{\ln(at_1)}{a}} \mathrm{d}\tau_{\mathcal{A}}\, \mathrm{e}^{-t_{\mathcal{B}}/\sigma_{\mathcal{B}}} \mathrm{e}^{-\tau_{\mathcal{A}}/\sigma_{\mathcal{A}}} \mathrm{e}^{\mathrm{i}(\Omega_{\mathcal{B}} t_1 - \Omega_{\mathcal{A}}\tau_{\mathcal{A}})} \frac{\mathrm{i}}{2} \end{aligned} \tag{5.44}$$

These integrals are solvable, and yield

$$C_2 = \lim_{\sigma_{\mathcal{A}}\to\infty, \sigma_{\mathcal{B}}\to\infty} C_2(\sigma_{\mathcal{A}}, \sigma_{\mathcal{B}}) = -\frac{\left(-\frac{\mathrm{i}\Omega_{\mathcal{B}}}{a}\right)^{\frac{i\Omega_{\mathcal{A}}}{a}} \Gamma\left(-\frac{\mathrm{i}\Omega_{\mathcal{A}}}{a}\right)}{2a\Omega_{\mathcal{B}}}, \tag{5.45}$$

such that the signalling strength is

$$|C_2| + |D_2| = \frac{1}{a\Omega_{\mathcal{B}}} \cosh\left(\frac{\pi\Omega_{\mathcal{A}}}{2a}\right) \sqrt{\frac{\pi}{\frac{\Omega_{\mathcal{A}}}{a}\sinh\left(\frac{\pi\Omega_{\mathcal{A}}}{a}\right)}}. \tag{5.46}$$

Here, the signalling strength is not directly dependent on Alice's detector gap but only on its ratio to her proper acceleration $\Omega_{\mathcal{A}}/a$. However, the signalling strength is directly dependent, and inverse proportional, to both the absolute value of the proper acceleration and Bob's detector gap. Their appearance in front of the perturbative term suggests that $\Omega_{\mathcal{B}}$ sets the scale for the receiver's coupling constant, whereas the acceleration a sets the scale for the sender's coupling constant $\lambda_{\mathcal{A}}$.

The signalling strength is divergent when either of the detector energy gaps or the proper acceleration approach zero. However, in 1+1D Minkowski space the limit of infinite acceleration exists and is

$$\lim_{a\to\infty} |C_2| + |D_2| = \frac{1}{\Omega_{\mathcal{A}}\Omega_{\mathcal{B}}}. \tag{5.47}$$

We will see in the following that this is a quarter of the maximum leading order signalling strength that is achievable between strictly timelike separated detectors.

5.3 Timelike signalling

The appearance of timelike signals in massless fields, i.e., signals propagating slower than the speed of light, is the most counter-intuitive of the signalling phenomena that are discussed in this thesis. This impression probably derives from our intuition being based on 3+1D Minkowski spacetime, where the Klein-Gordon equation actually obeys the strong Huygens principle such that timelike signals do not appear.

However, as discussed in Chapter 2 this is an exception rather than the norm. In general curved spacetimes, and also in odd-dimensional Minkowski spacetime and 1+1D Minkowski spacetime, the strong Huygens principle is violated and the commutator has timelike support. In this case, it is possible to have leading order signalling effects between timelike separated observers, because the leading order signalling strength $|C_2| + |D_2|$ depends directly on the commutator.

In this section, by analyzing the leading order signalling strength, we will see that an important characteristics of timelike signals is that they do not depend on the sender and receiver being resonant with each other. This suggests that timelike signals can be interpreted as a static imprint from the sender on the field amplitude, which remains, or slowly decays, inside the future lightcone of the sender.

In 1+1D Minkowski space the C_2 and D_2 integrals take a particularly simple form when Alice and Bob are timelike separated, i.e., when Bob couples to the field only inside

the future lightcone of Alice's coupling to the field. Because the commutator takes the constant value $\frac{\mathrm{i}}{2}$ in the future lightcone, and also because the interdependence on the nested integrals drops out when Bob is timelike separated from Alice.

Even more conveniently, the integral can be performed in terms of the detectors' proper times without any explicit reference to their relative motion. Assuming that Alice couples within the coordinate time interval $0 \leq t_2 \leq T_A$ and Bob within the coordinate time interval $T_1 \leq t_1 \leq T_2$ we have

$$\begin{aligned} C_2 &= \int_{T_1}^{T_2} \mathrm{d}t_1 \int_0^{T_A} \mathrm{d}t_2 \; \chi_{\mathcal{A}}(t_2)\chi_{\mathcal{B}}(t_1)\mathrm{e}^{\mathrm{i}(\Omega_{\mathcal{B}}\tau_{\mathcal{B}}(t_1)-\Omega_{\mathcal{A}}\tau_{\mathcal{A}}(t_2))}\frac{\mathrm{i}}{2} \\ &= \frac{\mathrm{i}}{2}\left(\int_0^{T_A} \mathrm{d}t_2 \; \chi_{\mathcal{A}}(t_2)\mathrm{e}^{-\mathrm{i}\Omega_{\mathcal{A}}\tau_{\mathcal{A}}(t_2)}\right)\left(\int_{T_1}^{T_2} \mathrm{d}t_1 \, \chi_{\mathcal{B}}(t_1)\mathrm{e}^{\mathrm{i}\Omega_{\mathcal{B}}\tau_{\mathcal{B}}(t_1)}\right) \\ &= \frac{\mathrm{i}}{2}\left(\int \mathrm{d}\tau_{\mathcal{A}} \; \eta_{\mathcal{A}}(\tau_{\mathcal{A}})\mathrm{e}^{-\mathrm{i}\Omega_{\mathcal{A}}\tau_{\mathcal{A}}}\right)\left(\int \mathrm{d}\tau_{\mathcal{B}} \, \eta_{\mathcal{B}}(\tau_{\mathcal{B}})\mathrm{e}^{\mathrm{i}\Omega_{\mathcal{B}}\tau_{\mathcal{B}}}\right) \end{aligned} \tag{5.48}$$

where in the last step we dropped the integration boundaries, since they are implied by the support of the detectors switching function $\eta_{\mathcal{D}}(\tau_{\mathcal{D}})$ already.

We see that the signalling coefficients C_2 and D_2 between timelike separated detectors in 1+1D Minkowski space are nothing but the product of the Fourier transform of the detector switching functions evaluated at the detectors' energy gap frequency. This means that Alice and Bob do not have to cooperate in order to optimize the signalling strength of timelike signals. They only need to separately optimize their own switching function and detector gap. They do not need to tune their detectors into resonance as they have to optimize lightlike signals, which we discussed above.

Also, the signalling strength is completely independent of the relative motion of sender and receiver. The only relevant parameter is the profile of their switching function with respect to their proper time.

Intuitively speaking a receiver in the future lightcone of the sender only sees the final displacement of the field amplitude that the sender imprinted into the field. The sender then has to optimize his switching parameters such that the effect of any displacement of the field amplitude on his detector is maximized. This is in contrast to scenarios with lightlike separations between sender and receiver. Here the receiver sees the change of field amplitude that the sender created at her side during her coupling to the field. So if the

receiver adjusts his detector to the frequency of the oscillations in the field amplitude, this results in a resonant driving of his detector and thus a larger signalling strength.

A particular simple solution to the signalling coefficients is obtained by using instantaneous switching functions, i.e.,

$$\eta_{\mathcal{D}}(\tau) = \begin{cases} 1 & \text{if } \tau_0 \leq \tau \leq \tau_0 + \Delta\tau_{\mathcal{D}} \\ 0 & \text{else} \end{cases}. \tag{5.49}$$

Here the integrals evaluate to

$$C_2 = \frac{2\mathrm{i}}{\Omega_{\mathcal{A}}\Omega_{\mathcal{B}}} \mathrm{e}^{\mathrm{i}\frac{\Omega_{\mathcal{B}}}{2}(2\tau_{\mathcal{B},0}+\Delta\tau_{\mathcal{B}})} \mathrm{e}^{-\mathrm{i}\frac{\Omega_{\mathcal{A}}}{2}(2\tau_{\mathcal{A},0}+\Delta\tau_{\mathcal{A}})} \sin\left(\frac{\Omega_{\mathcal{A}}}{2}\Delta\tau_{\mathcal{A}}\right) \sin\left(\frac{\Omega_{\mathcal{B}}}{2}\Delta\tau_{\mathcal{B}}\right). \tag{5.50}$$

Accordingly, the leading order signalling strength between timelike separated detectors in 1+1D Minkowski space with instantaneous switching functions is

$$|C_2| + |D_2| = \frac{4}{\Omega_{\mathcal{A}}\Omega_{\mathcal{B}}} \left| \sin\left(\frac{\Omega_{\mathcal{A}}}{2}\Delta\tau_{\mathcal{A}}\right) \sin\left(\frac{\Omega_{\mathcal{B}}}{2}\Delta\tau_{\mathcal{B}}\right) \right|. \tag{5.51}$$

Here we see that both Alice and Bob should couple their detectors to the field for an integer multiple plus one half of their own detector period, i.e., for $\Delta\tau = (k + \frac{1}{2})\frac{2\pi}{\Omega}$ in order to maximize the signalling strength, which then is

$$|C_2| + |D_2| = \frac{4}{\Omega_{\mathcal{A}}\Omega_{\mathcal{B}}}. \tag{5.52}$$

Also, Alice can completely suppress the C_2 and D_2 coefficients for timelike observers by coupling to the field for an integer multiple of her detector frequency. In this way she leaves no remaining imprint on the field amplitude that is detectable in her future lightcone.

The sharp switching also maximizes the signalling strength in the sense that adding a smooth transitions to the switching function in which the switching function ramps up and down to its constant value of $\eta = 1$ for times $\tau_0 \leq \tau \leq \Delta\tau_0 + \tau_0$ generally decreases the absolute value of the integral

$$\int \mathrm{d}\tau\, \eta(\tau) \mathrm{e}^{\mathrm{i}\Omega\tau}. \tag{5.53}$$

The most significant property of timelike signals in 1+1D Minkowski space is that they are independent of the time delay between the sender and receiver. This is a consequence

of the factoring of the C_2 into two separate integrals, which occurs because the commutator is constant in the future lightcone. This means that Bob can detect timelike signals from Alice at any point in the future lightcone without any change in the leading order signalling strength. In principle, it makes no difference whether Bob decides to detect the timelike signal that Alice imprinted into the field a second after Alice coupled to the field, or a day later.

Also in 2+1D Minkowski spacetime, signalling between timelike separated detectors is possible, because the commutator has timelike support. As seen in Figure 5.5, also in 2+1D timelike separated detectors need not be tuned into resonance in order to maximize the strength of timelike signals, just as in 1+1D.

However, in 2+1D the signalling strength of timelike signals dilutes with increasing timelike separation between sender and receiver. This is a consequence of the commutator being proportional to $\propto 1/\sqrt{\Delta t^2 - \Delta x^2}$. (See equation (5.15).) This leads the signalling strength to decay at the same rate. Numerical evaluations confirm that when the coupling duration of sender and receiver is kept constant, but the time delay between their couplings $\Delta T = T_1 - T_A$ is kept constant, then the signalling strength decays as

$$|C_2| + |D_2| \sim \frac{1}{\Delta T} \tag{5.54}$$

for large time delays $\Delta T \to \infty$.

This decay of the signalling strength of timelike signals is still slower than the decay of the energy that is injected by the sender into their future lightcone, just as we argued at the end of Chapter 2, and will see in detail in Chapter 6. Therefore, in 2+1D Minkowski space, we find an asymptotic decoupling of the information flow from the flow of energy for large timelike separations between the sender and the receiver, in the sense that the ratio of transmitted energy to signalling strength goes to zero.

5.4 Conclusion

In the scenarios that we discussed, the leading order signalling strength between two particle detectors behaves much as one would expect, based on intuition on classical fields. This is not surprising, since the leading order signalling strength derives from the commutator which is given by the classical Greens function of the field.

We see that the signalling strength is optimized between resonant detectors, when sender and receiver are in lightlike contact. To achieve resonance between moving detectors, the classical, relativistic Doppler shift needs to be taken into account.

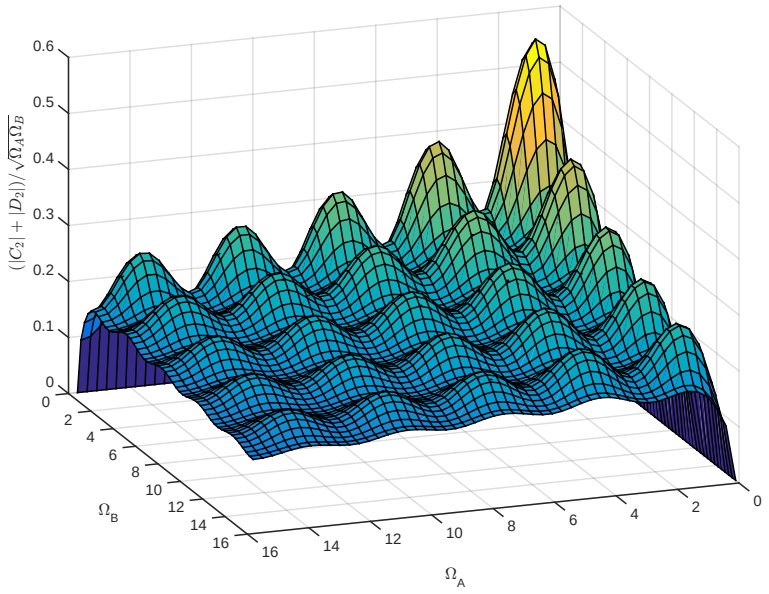

Figure 5.5: The leading order signalling strength for timelike signalling in 2+1D Minkowski space for different detector energy gaps of the sender $\Omega_{\mathcal{A}}$ and the receiver $\Omega_{\mathcal{B}}$. The sender and receiver are at rest at the same position, however, couple to the field after each other. The sender couples to the field for $t = 0...2$, the receiver for $t = 2.1...4.1$. The signalling strength does not depend on the sender and receiver being resonant. The plot shows $(|C_2|+|D_2|)/\sqrt{\Omega_{\mathcal{A}}\Omega_{\mathcal{B}}}$, i.e., the leading order signalling strength normalized by the geometric mean of the detector gaps.

In contrast, signals between timelike separated observers are not dependent on sender and receiver being resonant with each other. This suggests that timelike signals can be understood as a static remainder from the sender's interaction with the field, that is imprinted on the field's amplitude in the future lightcone. Accordingly, to optimize the signalling strength, Alice has to choose coupling parameters which maximize her imprint on the field. Whereas Bob, independently, has to choose parameters which are as sensitive as possible to any imprint Alice may have left behind.

We found that, interestingly, both for lightlike as well as for timelike signals the signalling strength between more distant detectors decays slower than the surface of the wave front emitted by the sender. This indicates that the ratio between the information flow encoded in the amplitude of the massless field, decouples from the energy flow. The subsequent chapter will analyze the energy transmission between sender and receiver in detail.

We will find that the energy cost associated with the coupling and decoupling of detectors and field plays an important role in the energy budget of signalling.

The characteristics of timelike signals in 2+1D Minkowski space can help to build intuition for timelike signals in curved spacetimes. Because even when the commutator is non-vanishing inside the future lightcone, it tends to decay with increasing distance. Following up on the results presented in this thesis, and published in [40], timelike signals have been considered for different examples of expanding spacetimes in [10, 11]. There it was found that timelike signals might serve as a channel to obtain information about the early universe. With methods as developed in [18, 87], it should be possible to extend the analysis of the leading order signalling strength to black hole spacetimes.

As shown in Chapter 3 the channel capacity between two detectors does not directly compete with the noise in the channel, to leading order. Nevertheless, it should be interesting to compare the leading order signalling strength with the local noise from the quantum fluctuations of the field, that the receiver experiences. For example, when signalling across an acceleration horizon the leading order signalling strength, due to the time inversion symmetry, is the same from an accelerated to a resting detector as vice versa. However, an accelerated observer would experience thermal noise through the Unruh effect, whereas a resting observer only experiences vacuum noise.

A conclusive analysis of how the interplay of signalling and noise effects impacts the channel capacity may require a non-perturbative analysis. Non-perturbative methods are also necessary for scenarios where many receivers try to obtain timelike signals from a single sender. Such scenarios are interesting both from the perspective of energy transmission, as well as for questions concerning the quantum capacity of the channel.

Chapter 7 will demonstrate timelike signals non-perturbatively between harmonic oscillators coupling to the field inside a Dirichlet cavity. Further prospects for non-perturbative methods are also discussed in the final conclusions of the thesis.

Chapter 6

Energy exchange between Unruh-DeWitt detectors

The appearance of timelike signals in massless fields may not only be surprising, on first sight, it may even appear to be in conflict with energy conservation: In previous chapters we have seen that in 1+1D Minkowski space Alice's timelike signals reach arbitrarily far into the future light cone, without being diluted. Therefore, it is possible to have an arbitrary large number of receivers in Alice's future lightcone which all detect Alice's signal in parallel. The receivers can even be arranged to be spacelike separated from each other such that they have no influence on each others measurement outcomes at all. Therefore, if they initialize their detectors as discussed in Chapter 3, they all receive the same positive leading order contribution to the expectation value of their detector energy due to Alice's signal.

This means that the total increase in the energy of the many receiver detectors, caused by Alice, is unbounded because the number of receivers can be arbitrary large. How could Alice possibly know, in advance, how much energy she needs to send into the future lightcone in order to excite all potential receivers?

The answer is that Alice sends no energy at all. In fact, she does not have the means to send any energy into the future lightcone in 1+1D Minkowski spacetime, since, as discussed in Chapter 2.4, the field energy density in 1+1D propagates strictly lightlike. Instead, much as in a collect call, the receivers have to pay the energy expense for exciting their detectors themselves by the work necessary to couple and decouple their detectors from the field.

In this chapter, we analyze the role of energy exchange in signalling between Unruh-DeWitt detectors. In Section 6.1, we calculate the total energy, and the distribution of

energy density that a single detector injects into the field when coupling to the vacuum, to first order in perturbation theory.

In Section 6.2 we analyze how, under the coupling of the field and detector, the different parts of the system exchange energy. Coupling and de-coupling the detector and the field, can introduce energy into the field. We discuss how this energy cost is balanced by the work necessary to switch the detector.

Based on this analysis, we discuss the exchange of energy in signalling between a pair of Unruh-DeWitt detectors in Section 6.3. We find that timelike signals, in particular, can modulate the energy cost of coupling a detector to the field inside the sender's future lightcone. On the one hand, this additional energy cost resolves the apparent energy conservation paradox we discussed above. On the other hand, it also means that the information content of timelike signals can be viewed as being encoded in the energy cost incurred by the receiver when switching their detector.

6.1 Energy injected into the field by a single detector

Note: Figures and certain passages of this section concerning 1+1D Minkowski spacetime are reproduced from [38].

In this section, we discuss how much energy an Unruh-DeWitt detector coupling to the vacuum injects into the field, and how this energy propagates in spacetime. We approach this question using perturbation theory and calculate the leading order contributions to the expectation value of the field energy density, and the expectation value of the total field energy.

For 1+1D and for 2+1D Minkowski spacetime we obtain closed expressions even for sharply switched, pointlike detectors. In 1+1D, these show that all energy that is injected by the detector in the field propagates strictly at the speed of light, confirming the decoupling of the flow of information from the flow of energy in 1+1D Minkowski spacetime.

We obtain general expressions for the leading order contributions in higher dimensions in terms of distributional momentum integrals. The support of these integrals encode where the field energy density propagates that is emitted by the detector.

In 2+1D Minkowksi spacetime we find that energy propagates into the future lightcone, as expected from the discussion in Chapter 2. Interestingly, the leading order contribution to this timelike propagating energy density is found to be independent of the detector's initial state.

Our discussion extends a large body of literature that addresses the radiation and energy flux originating from a Unruh-DeWitt detector. In particular, the question whether an accelerated detector emits radiation while the detector experiences the Unruh effect has found particular attention. This question has been considered for stationary, and non-stationary couplings both of two-level, and harmonic oscillator type detectors in (1+1)- and (1+3)-dimensional Minkowski space. Later works on this topic which give a review of previous work include [49, 45, 46, 61, 3].

6.1.1 Field energy density in Minkowski space

We begin with a brief derivation of the operators for the field's energy and energy density. The field energy density of the field is given by the T_{00} component of the field's energy-momentum tensor. For a massless Klein-Gordon field in n+1D Minkowski spacetime it reads [8]

$$T_{00} = \frac{1}{2}\left((\partial_t\phi)^2 + \sum_{i=1}^{n}(\partial_i\phi)^2\right). \tag{6.1}$$

It is also called Hamiltonian density, since, when normal ordered, its integral over a slice of constant coordinate time yields the field's Hamiltonian

$$H_f = \int \mathrm{d}^n\vec{x}\ :T_{00}: = \int \mathrm{d}^n\vec{k}\, k\, a^\dagger_{\vec{k}}\, a_{\vec{k}}. \tag{6.2}$$

Here, $k = \left|\vec{k}\right|$ denotes the norm of the momentum vector, and we have used the expansion of the field operator as introduced in Chapter 2. Using the notation

$$k^\mu x_\mu = k_0 x_0 - \vec{k}\cdot\vec{x} = k_0 x_0 - \sum_{i=1}^{n} k_i x_i \tag{6.3}$$

for the Minkowski product, the expansion of the field operator reads

$$\phi(t,\vec{x}) = \int \mathrm{d}^n\vec{k}\,\frac{1}{(2\pi)^{\frac{n}{2}}}\frac{1}{\sqrt{2k}}\left(\mathrm{e}^{-\mathrm{i}k^\mu x_\mu}a_{\vec{k}} + \mathrm{e}^{\mathrm{i}k^\mu x_\mu}a^\dagger_{\vec{k}}\right). \tag{6.4}$$

Accordingly, its derivatives are given by

$$\partial_t\phi(x) = \frac{-\mathrm{i}}{(2\pi)^{\frac{n}{2}}}\int \mathrm{d}^n\vec{k}\,\sqrt{\frac{k}{2}}\left(\mathrm{e}^{-\mathrm{i}k^\mu x_\mu}a_{\vec{k}} - \mathrm{e}^{\mathrm{i}k^\mu x_\mu}a^\dagger_{\vec{k}}\right) \tag{6.5}$$

$$\partial_i \phi(x) = \frac{\mathrm{i}}{(2\pi)^{\frac{n}{2}}} \int \mathrm{d}^n \vec{k}\, \frac{k_i}{\sqrt{2k}} \left(\mathrm{e}^{-\mathrm{i}k^\mu x_\mu} a_{\vec{k}} - \mathrm{e}^{\mathrm{i}k^\mu x_\mu} a^\dagger_{\vec{k}} \right). \tag{6.6}$$

To obtain the normal-ordered energy density operator of the field, $:T_{00}:$, we plug these expansions into the energy density, and apply normal-ordering to the creation and annihilation operators:

$$\begin{aligned} :T_{00}: = \frac{-1}{4(2\pi)^n} \int \mathrm{d}^n \vec{k} \int \mathrm{d}^n \vec{k'} \left(\sqrt{kk'} + \frac{\vec{k} \cdot \vec{k'}}{\sqrt{kk'}} \right) \\ \times \left(\mathrm{e}^{-\mathrm{i}(k+k')^\mu x_\mu} a_{\vec{k}} a_{\vec{k'}} + \mathrm{e}^{\mathrm{i}(k+k')^\mu x_\mu} a^\dagger_{\vec{k}} a^\dagger_{\vec{k'}} - 2\mathrm{e}^{\mathrm{i}(k-k')^\mu x_\mu} a^\dagger_{\vec{k}} a_{\vec{k'}} \right) \end{aligned} \tag{6.7}$$

We readily see that integrating the normal-ordered energy density up over a slice of constant time indeed yields the Hamiltonian of the field. Since $\int \mathrm{d}^n \vec{x}\, \mathrm{e}^{-\mathrm{i}(\vec{k}-\vec{k'})\cdot\vec{x}} = (2\pi)^n \delta\left(\vec{k} - \vec{k'}\right)$ and $kk - \vec{k} \cdot \vec{k} = 0$, the first two terms drop out of the integral, and the last one exactly gives back the Hamiltonian

$$\int \mathrm{d}^n \vec{x}\, :T_{00}: = \int \mathrm{d}^n \vec{k}\, k\, a^\dagger_{\vec{k}} a_{\vec{k}} = H_f. \tag{6.8}$$

Therefore, the first two terms in the energy density do not enter the Hamiltonian. This also is inevitable, because these terms consist of two creation or annihilation operators and are, therefore, non-diagonal in the Fock basis of the field, in contrast to the field Hamiltonian H_f. However, these two terms, despite having no influence on the total energy of the field, ensure that the field's energy density propagates causally. For example, in our following calculations, they cancel out contributions to the energy density from the last term in $:T_{00}:$ that have spacelike support.

6.1.2 Leading order contributions to the field energy density

This section derives the leading order contributions to the field energy density from an Unruh-DeWitt detector coupling to the field in general, n+1D Minkowski spacetime. For all of this chapter, we assume that the detector initially is in a pure state, denoted by

$$|\psi_0\rangle = \alpha\, |e\rangle + \beta\, |g\rangle\,, \tag{6.9}$$

whereas the field initially is in its vacuum state. Thus, the initial density matrix of field and detector is

$$\rho_0 = |\psi_0\rangle\langle\psi_0| \otimes |0\rangle\langle 0| = \left(|\alpha|^2\, |e\rangle\langle e| + \alpha\beta^*\, |e\rangle\langle g| + \alpha^*\beta\, |g\rangle\langle e| + |\beta|^2\, |g\rangle\langle g| \right) \otimes |0\rangle\langle 0|\,. \tag{6.10}$$

At this point we make no assumptions on the detector's wordline yet. Therefore, we denote the interaction Hamiltonian with respect to the detector's proper time τ by

$$H_{\text{int}} = \lambda\eta(\tau) \underbrace{\left(\mathrm{e}^{-\mathrm{i}\Omega\tau} \left|g\right\rangle\!\left\langle e\right| + \mathrm{e}^{\mathrm{i}\Omega\tau} \left|e\right\rangle\!\left\langle g\right|\right)}_{m(\tau)} \otimes \phi(a), \tag{6.11}$$

where $x_a = x_a(\tau) = (t_a(\tau), \vec{x}_a(\tau))$ is the detector's location in spacetime at proper time τ.

We calculate the time evolution of the system under the detector-field interaction in the interaction picture using the Dyson expansion for the time evolution operator, just as previously in Chapter 3. From this we obtain a perturbative expansion for the time-evolved density matrix of the total system.

$$\rho \sim \rho_0 + \underbrace{\left(U^{(1)}\rho_0 + \rho_0 U^{(1)\dagger}\right)}_{\rho^{(1)} \sim \mathcal{O}(\lambda)} + \underbrace{\left(U^{(1)}\rho_0 U^{(1)\dagger} + U^{(2)}\rho_0 + \rho_0 U^{(2)\dagger}\right)}_{\rho^{(2)} \sim \mathcal{O}(\lambda^2)} + \mathcal{O}(\lambda^3) \tag{6.12}$$

For the expectation value of the field energy density this results in

$$\operatorname{Tr}\left(:T_{tt}:\rho\right) \sim \underbrace{\operatorname{Tr}\left(:T_{tt}:\rho_0\right)}_{=0} + \operatorname{Tr}\left(:T_{tt}:\rho^{(1)}\right) + \operatorname{Tr}\left(:T_{tt}:\rho^{(2)}\right) + \mathcal{O}(\lambda^3). \tag{6.13}$$

Here the zeroth order contribution to the expectation value of the field energy density vanishes, since the field starts out in the vacuum state.

The first order contribution $\operatorname{Tr}\left(:T_{tt}:\rho^{(1)}\right) = \operatorname{Tr}\left(:T_{00}:\left(U^{(1)}\rho_0 + \rho_0 U^{(1)\dagger}\right)\right)$ vanishes as well, because

$$\begin{aligned} U^{(1)}\rho_0 = -\mathrm{i}\int_{-\infty}^{\infty} \mathrm{d}\tau\, \eta(\tau) \int \mathrm{d}^n\vec{k}\, \frac{\mathrm{e}^{\mathrm{i}k^\mu a_\mu}}{(2\pi)^{\frac{n}{2}}\sqrt{2k}} \\ \left(|\alpha|^2\mathrm{e}^{-\mathrm{i}\Omega\tau} \left|g\right\rangle\!\left\langle e\right| + |\beta|^2\mathrm{e}^{\mathrm{i}\Omega\tau} \left|e\right\rangle\!\left\langle g\right| + \alpha\beta^*\mathrm{e}^{-\mathrm{i}\Omega\tau} \left|g\right\rangle\!\left\langle g\right| + \alpha^*\beta\mathrm{e}^{\mathrm{i}\Omega\tau} \left|e\right\rangle\!\left\langle e\right|\right) \otimes \left|1_{\vec{k}}\right\rangle\!\left\langle 0\right|. \end{aligned} \tag{6.14}$$

contains matrix elements that are off-diagonal between the one-particle sector and the vacuum state of the field, but the energy desnity $:T_{00}:$ is quadratic in creation and annihilation operators.

The leading order contribution from an Unruh-DeWitt detector to the field energy density of the vacuum is, therefore, of order $\mathcal{O}(\lambda^2)$, and consists of the terms

$$\operatorname{Tr}\left(:T_{00}:U^{(1)}\rho_0 U^{(1)\dagger}\right) + \operatorname{Tr}\left(:T_{00}:U^{(2)}\rho_0\right) + \operatorname{Tr}\left(:T_{00}:\rho_0 U^{(2)\dagger}\right). \tag{6.15}$$

The first term can be written as

$$\begin{aligned}&\mathrm{Tr}\left(:T_{00}:U^{(1)}\rho_0 U^{(1)\dagger}\right)\\&\quad=\lambda^2\int_{-\infty}^{\infty}\mathrm{d}\tau\int_{-\infty}^{\infty}\mathrm{d}\tau'\,\frac{\eta(\tau)\eta(\tau')}{4(2\pi)^{2n}}\left(|\alpha|^2\mathrm{e}^{\mathrm{i}\Omega(\tau-\tau')}+|\beta|^2\mathrm{e}^{-\mathrm{i}\Omega(\tau-\tau')}\right)D^{(n)}(x-x_a,x'_a-x)\end{aligned}\tag{6.16}$$

and the second terms, which are complex conjugates of each other, can be written as

$$\begin{aligned}&\mathrm{Tr}\left(:T_{00}:U^{(2)}\rho_0\right)=\mathrm{Tr}\left(:T_{00}:\rho_0 U^{(2)\dagger}\right)^*\\&\quad=\lambda^2\int_{-\infty}^{\infty}\mathrm{d}\tau\int_{-\infty}^{\tau}\mathrm{d}\tau'\,\frac{\eta(\tau)\eta(\tau')}{4(2\pi)^{2n}}\left(|\alpha|^2\mathrm{e}^{\mathrm{i}\Omega(\tau-\tau')}+|\beta|^2\mathrm{e}^{-\mathrm{i}\Omega(\tau-\tau')}\right)D^{(n)}(x_a-x,x'_a-x)\end{aligned}\tag{6.17}$$

Here, by $D^{(n)}(y,z)$, we denoted the momentum space integral

$$D^{(n)}(y,z):=\int\mathrm{d}^n\vec{k}\int\mathrm{d}^n\vec{k'}\left(1+\frac{\sum_i k_i k'_i}{kk'}\right)\mathrm{e}^{\mathrm{i}k'^{\mu}y_{\mu}}\mathrm{e}^{\mathrm{i}k^{\mu}z_{\mu}}.\tag{6.18}$$

This integral represents a distribution in spacetime. Hence, in general, it has to be integrated against test functions in order to guarantee well-defined results, i.e., one would have to use smeared rather than pointlike detectors.

The distributional integral $D^{(n)}(y,z)$ determines how the energy that the detector injects into the field propagates, and spreads out in spacetime. The integral can be split into its imaginary and real part, $D^{(n)}(y,z)=D^{(n)}_{\Re}(y,z)+\mathrm{i}D^{(n)}_{\Im}(y,z)$, with

$$D^{(n)}(y,z)=D^{(n)}(z,y),\qquad D^{(n)}(y,z)^*=D^{(n)}(-y,-z).\tag{6.19}$$

This can be used to rewrite the leading order contribution to the expectation value of the field energy density as

$$\begin{aligned}&\mathrm{Tr}\left(:T_{00}:(x)\rho^{(2)}\right)\\&\quad=\lambda^2\int_{-\infty}^{\infty}\mathrm{d}\tau\int_{-\infty}^{\infty}\mathrm{d}\tau'\,\frac{\eta(\tau)\eta(\tau')}{4(2\pi)^{2n}}\left(|\alpha|^2\mathrm{e}^{\mathrm{i}\Omega(\tau-\tau')}+|\beta|^2\mathrm{e}^{-\mathrm{i}\Omega(\tau-\tau')}\right)D^{(n)}(x-x_a,x'_a-x)\\&\qquad+\lambda^2\int_{-\infty}^{\infty}\mathrm{d}\tau\int_{-\infty}^{\infty}\mathrm{d}\tau'\,\frac{\eta(\tau)\eta(\tau')}{4(2\pi)^{2n}}\left(|\alpha|^2\mathrm{e}^{\mathrm{i}\Omega(\tau-\tau')}+|\beta|^2\mathrm{e}^{-\mathrm{i}\Omega(\tau-\tau')}\right)D^{(n)}_{\Re}((x-x'_a),(x-x_a))\\&\qquad+\lambda^2 2\int_{-\infty}^{\infty}\mathrm{d}\tau\int_{-\infty}^{\tau}\mathrm{d}\tau'\,\frac{\eta(\tau)\eta(\tau')}{4(2\pi)^{2n}}\sin(\Omega(\tau-\tau'))\left(|\alpha|^2-|\beta|^2\right)D^{(n)}_{\Im}((x-x'_a),(x-x_a)).\end{aligned}\tag{6.20}$$

In this form it is evident that the expression is real-valued, since the first two terms do not change under complex conjugation, and the last integrand is real-valued.

We note that $D^{(n)}(y,z)$ has support even for spacelike separated points y and z. However, we will see below that the spacelike contributions from the different terms in $\mathrm{Tr}\left(:T_{00}:(x)\rho^{(2)}\right)$ in 1+1D Minkowski spacetime cancel against each other, such that the result propagates causally. This could suggest that one might be able to rewrite the above expression in a form where the causal propagation is more evident, also in general spacetime dimensions.

6.1.3 Leading order contributions to the field energy

To obtain the leading order contribution to the expectation value of the total field energy, we integrate the expectation value of the energy density over a slice of constant time. Before equation (6.8) we discussed that the field Hamiltonian arises from the term which is diagonal in the Fock basis of the field. The same kind of argument shows that the expectation value of the field Hamiltonian is given by

$$\langle H_f \rangle \sim \int \mathrm{d}^n\vec{x}\ \mathrm{Tr}\left(:T_{00}: U^{(1)}\rho_0 U^{(1)\dagger}\right) + \mathcal{O}(\lambda^3). \tag{6.21}$$

The integral expression for this leading order contribution is given by

$$\begin{aligned}
&\int \mathrm{d}^n\vec{x}\ \mathrm{Tr}\left(:T_{00}: U^{(1)}\rho_0 U^{(1)\dagger}\right) \\
&\quad = \lambda^2 \int_{-\infty}^{\infty}\mathrm{d}\tau \int_{-\infty}^{\infty}\mathrm{d}\tau'\, \frac{\chi(\tau)\chi(\tau')}{2(2\pi)^n}\left(|\alpha|^2\mathrm{e}^{-\mathrm{i}\Omega(\tau-\tau')} + |\beta|^2\mathrm{e}^{\mathrm{i}\Omega(\tau-\tau')}\right)\int \mathrm{d}^n\vec{k}\,\mathrm{e}^{\mathrm{i}k(t_a-t'_a)_0}\mathrm{e}^{-\mathrm{i}\vec{k}\cdot(\vec{x}_a-\vec{x}'_a)}.
\end{aligned} \tag{6.22}$$

For a detector at rest it simplifies to

$$\begin{aligned}
&\int \mathrm{d}^n\vec{x}\ \mathrm{Tr}\left(:T_{00}: U^{(1)}\rho_0 U^{(1)\dagger}\right) \\
&\quad = \lambda^2 \int_{-\infty}^{\infty}\mathrm{d}\tau \int_{-\infty}^{\infty}\mathrm{d}\tau'\, \frac{\chi(\tau)\chi(\tau')}{2(2\pi)^n}\left(|\alpha|^2\mathrm{e}^{-\mathrm{i}\Omega(\tau-\tau')} + |\beta|^2\mathrm{e}^{\mathrm{i}\Omega(\tau-\tau')}\right)\int \mathrm{d}^n\vec{k}\,\mathrm{e}^{\mathrm{i}k(\tau-\tau')} \\
&\quad = \lambda^2 \int_{-\infty}^{\infty}\mathrm{d}\tau \int_{-\infty}^{\infty}\mathrm{d}\tau'\, \frac{\chi(\tau)\chi(\tau')}{2^n(\pi)^{n/2}\Gamma(\frac{n}{2})}\left(|\alpha|^2\mathrm{e}^{-\mathrm{i}\Omega(\tau-\tau')} + |\beta|^2\mathrm{e}^{\mathrm{i}\Omega(\tau-\tau')}\right)\int_0^{\infty}\mathrm{d}k\, k^{n-1}\mathrm{e}^{ik(\tau-\tau')},
\end{aligned} \tag{6.23}$$

since $\vec{x}_a(\tau) = \vec{x}_a(\tau')$ is constant, and the proper time $\tau = t_a$ coincides with coordinate time. The distributional momentum integral can be represented alternatively by

$$\int_0^\infty \mathrm{d}k\, k^{n-1} e^{\mathrm{i}ks} = \mathrm{i}^n (n-1)! \mathcal{P}\frac{1}{s^n} + \mathrm{i}^{3n+1}\pi\delta(n-1)(s). \tag{6.24}$$

We obtain this representation by applying the iϵ-prescription discussed in Section 2.3.1 to the integral, and then applying the Sokhotskii formulae (2.35).

Except for 1+1D, this expression is UV-divergent for sharp switching functions. If we insert $\chi(\tau) = \chi_{[0,T]}(\tau)$ above, and perform the time integration first, we obtain

$$\begin{aligned}
&\int \mathrm{d}^n\vec{x}\ \mathrm{Tr}\left(:T_{00}: U^{(1)}\rho_0 U^{(1)\dagger}\right) \\
&= \lambda^2 \int_{-\infty}^{\infty}\mathrm{d}\tau \int_{-\infty}^{\infty}\mathrm{d}\tau' \frac{\chi_{[0,T]}(\tau)\chi_{[0,T]}(\tau')}{2^n(\pi)^{n/2}\Gamma(\frac{n}{2})}\left(|\alpha|^2\mathrm{e}^{-\mathrm{i}\Omega(\tau-\tau')} + |\beta|^2\mathrm{e}^{\mathrm{i}\Omega(\tau-\tau')}\right)\int_0^\infty \mathrm{d}k\, k^{n-1}\mathrm{e}^{ik(\tau-\tau')} \\
&= \frac{\lambda^2}{2^{n-2}(\pi)^{n/2}\Gamma(\frac{n}{2})}\int_0^\infty \mathrm{d}k\, k^{n-1}\left(\frac{|\alpha|^2}{(\Omega-k)^2}\sin^2\left((\Omega-k)\frac{T}{2}\right) + \frac{|\beta|^2}{(\Omega+k)^2}\sin^2\left((\Omega+k)\frac{T}{2}\right)\right).
\end{aligned} \tag{6.25}$$

This integral diverges for $n \geq 2$ as $k \to \infty$. Therefore, in Minkowski spacetime of 2+1D and higher dimensions smooth switching functions are necessary to obtain well-defined, finite leading order contributions to the expectation value of the field energy.

6.1.4 Lightlike energy propagation in 1+1D Minkowski spacetime

In 1+1D Minkowski spacetime, the momentum integrals appearing in the leading order contributions to the field energy, and to the field energy density, have finite closed form solutions even for pointlike and sharply switched detectors.

These solutions agree with our discussion in Section 2.4, where we showed that the energy density of a massless field in 1+1D propagates lightlike. We will see that all energy that a sender injects into the field propagates away strictly at the speed of light. The information carried by lightlike signals into the future lightcone of the sender is, therefore, completely decoupled from the flow of energy emanating from the sender.

We note that the infrared ambiguity of the massless field in (1+1)-dimensional Minowski space does not affect the expectation values of the energy-momentum tensor. This explains why the results for the detector's effect on the field energy, and field energy density, are finite, whereas the excitation probability for a pointlike detector in 1+1 dimensions is infrared-divergent and has to be regularized [80, 41].

The distributional integral which appears in the contributions to the energy density can be readily expressed in terms of Dirac, and principal value distributions, in 1+1D Minkowski spacetime. Using formula (2.35), which yields

$$\int_0^\infty \mathrm{d}k\, \mathrm{e}^{\mathrm{i}kr} = \pi\delta(r) + \mathrm{i}\mathcal{P}\frac{1}{r}, \tag{6.26}$$

we find

$$\begin{aligned} D^{(1)}(y,z) = 2\left(\pi\delta(y_-) + \mathcal{P}\frac{\mathrm{i}}{y_-}\right)\left(\pi\delta(z_-) + \mathcal{P}\frac{\mathrm{i}}{z_-}\right) \\ + 2\left(\pi\delta(y_+) + \mathcal{P}\frac{\mathrm{i}}{y_+}\right)\left(\pi\delta(z_+) + \mathcal{P}\frac{\mathrm{i}}{z_+}\right) \end{aligned} \tag{6.27}$$

where for $y = (y_0, y_1)$ and $z = (z_0, z_1)$ we introduced the lightcone coordinates $y_\pm = y_0 \pm y_1$ and $z_\pm = z_0 \pm z_1$. These lightcone coordinates are zero for points that are lightlike separated from the origin. Splitting the distribution up into its real and imaginary part

$$\begin{aligned} D^{(1)}_{\Re}(y,z) &= 2\pi^2\delta(y_-)\delta(z_-) - 2\mathcal{P}\frac{1}{y_-}\mathcal{P}\frac{1}{z_-} + 2\pi^2\delta(y_+)\delta(z_+) - 2\mathcal{P}\frac{1}{y_+}\mathcal{P}\frac{1}{z_+} \\ D^{(1)}_{\Im} &= 2\pi\delta(y_-)\mathcal{P}\frac{1}{z_-} + 2\pi\delta(z_-)\mathcal{P}\frac{1}{y_-} + 2\pi\delta(y_+)\mathcal{P}\frac{1}{z_+} + 2\pi\delta(z_+)\mathcal{P}\frac{1}{y_+}. \end{aligned} \tag{6.28}$$

we see that the double principal value term in the real part means that the distribution has support even at spacelike separations. However, this term cancels out in the expression for the energy density, which we find to be

$$\begin{aligned} &\mathrm{Tr}\left(:T_{tt}(t,x):\rho^{(2)}\right) \\ &\quad = \lambda^2 \int \mathrm{d}\tau \int \mathrm{d}\tau' \, \frac{\chi(\tau)\chi(\tau')}{4}\left(|\alpha|^2 \mathrm{e}^{\mathrm{i}\Omega(\tau-\tau')} + |\beta|^2 \mathrm{e}^{-\mathrm{i}\Omega(\tau-\tau')}\right) \\ &\qquad \times \left(\delta(x_+ - a_+)\delta(x_+ - a'_+) + \delta(x_- - a_-)\delta(x_- - a'_-)\right) \end{aligned}$$

$$+\left(|\alpha|^2-|\beta|^2\right)\int \mathrm{d}\tau \int^{\tau}\mathrm{d}\tau' \,\frac{\chi(\tau)\chi(\tau')}{2\pi}\sin(\Omega(\tau-\tau'))$$
$$\times\left(\delta(x_+-a_+)\mathcal{P}\frac{1}{x_+-a'_+}+\delta(x_--a_-)\mathcal{P}\frac{1}{x_--a'_-}\right) \tag{6.29}$$

where $x_\pm = t \pm x$, $a'_\pm = t_a(\tau') \pm x_a(\tau')$ and $a_\pm$ is defined accordingly.

At this point we have not yet introduced any assumptions on the detector's wordline, or the switching function. However, due to the $\delta(x_\pm - a_\pm)$-distributions, a non-zero contribution to the energy density of the field can only be found at spacetime points (t, x) that have one lightcone coordinate, $t \pm x$, in common with a spacetime point at which the detector interacted with the field. This means that the detector only affects the expectation value of the energy density of the field at spacetime points which are lightlike connected to the detector's worldline: Any energy that the detector injects into the field propagates strictly at the speed of light.

For a detector at rest, say at $x_a = 0$, the detector's proper time coincides with coordinate time. If we couple the detector to the field for a time T using a sharp switching function

$$\chi(\tau) = \begin{cases} 1 & \text{if } 0 < \tau < T \\ 0 & \text{else} \end{cases} \tag{6.30}$$

the leading order contribution to the energy density evaluates to

$$\mathrm{Tr}\left(:T_{tt}(t,x):\rho^{(2)}\right) = \lambda^2\left(\frac{\chi(x_+)}{4}+\left(|\alpha|^2-|\beta|^2\right)\frac{\chi(x_+)}{2\pi}\mathrm{Si}(\Omega x_+)\right.$$
$$\left.+\left(\frac{\chi(x_-)}{4}+\left(|\alpha|^2-|\beta|^2\right)\frac{\chi(x_-)}{2\pi}\mathrm{Si}(\Omega x_-)\right)\right). \tag{6.31}$$

A plot of the spatial profile of this contribution to the energy density is given in Fig. 6.1 for the case of a detector starting out in its excited state, $|\alpha|^2 = 1$, and for the case of a detector starting out in its ground state, $|\beta|^2 = 1$. For other input states the energy density can take any value in between, depending on the value of $|\alpha|^2 - |\beta|^2$. In particular, if the detector starts out in an equal superposition of energy eigenstates, i.e., $|\alpha|^2 = |\beta^2|$, then the oscillatory contributions to the energy density vanish.

The energy density injected into the field by the detector oscillates with a larger amplitude at times right after the onset of the interaction. In the plot these are the points most distant from the origin, where the detector is located. Towards later times, the oscillations

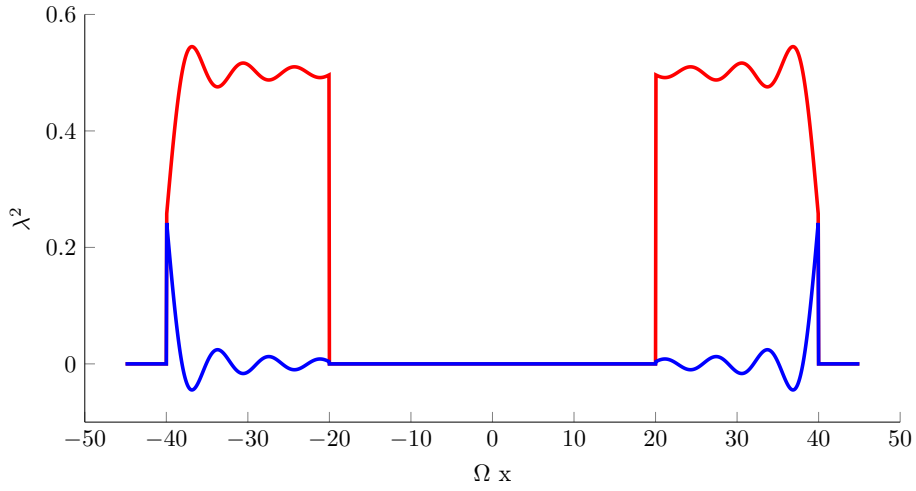

Figure 6.1: [38] Leading order contribution to the normal ordered energy density $\langle{:}T_{tt}(t\Omega, x){:}\rangle$ from equation (6.31) injected into the field by an Unruh-DeWitt detector at rest, starting out in its excited state (upper, red line), or its ground state (lower, blue line). The detector frequency Ω is used to obtain dimensionless distances and times. The detector is coupled to the field at $x_a = 0$ for the time interval $t = 0...20/\Omega$. The graph shows the energy density on the spatial slice of 1+1D Minkowski space with $t = 40/\Omega$, i.e., the graph plots $\langle{:}T_{tt}(t = 30/\Omega, x){:}\rangle$. The energy density is only non-vanishing at points which are ligthlike connected to the interacting detector.

diminish and the energy density approaches a constant limit of $\frac{\lambda^2}{2}$ for the excited detector, and zero for the detector in the ground state. Interestingly, the detector in the ground state causes negative energy densities to occur.

The abrupt switching through step functions used above can be problematic, e.g., for the calculation of detector excitation probabilities, because it does not comply with the mathematically rigorous requirement of being a smooth test function [54, 74]. The change of energy expectation values for smooth switching functions converges to the results obtained for abrupt switching, as the smooth switching functions approach step functions [40]. The oscillating fringes in the energy density of Fig. 6.1 are a consequence of steep switching, and are smoothened out for switching functions with lower slopes.

The total energy injected into the field by the interaction with the sharply switched detector is

$$\mathrm{Tr}\left(H_f \rho^{(2)}\right) = \lambda^2 T\left(\frac{1}{2} + \frac{(|\alpha|^2 - |\beta|^2)}{\pi}\left(\mathrm{Si}(\Omega T) + \frac{\cos(\Omega T) - 1}{T\Omega}\right)\right). \tag{6.32}$$

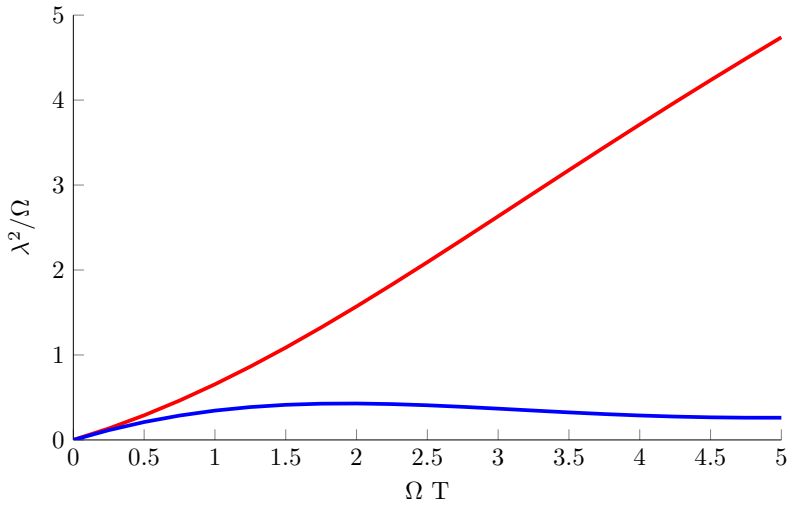

Figure 6.2: [38] Leading order perturbative contribution to the total energy injected into the field by an Unruh-DeWitt detector, with energy gap Ω, coupling to the field for the time interval $t = 0...T$ while at rest, see (6.32). The upper line shows a detector starting out in its excited state. Here the contribution to the energy scales linearly with the total interaction time ΩT. The lower line shows a detector starting out in its ground state. Here the total energy approaches the limit of $\langle H_f \rangle \to \lambda^2/(\pi\Omega)$ as $T \to \infty$, see (6.33).

A plot of the total energy injected into the vacuum state of the field by a detector in its ground, or in its excited state is given in Fig. 6.2.

When the detector starts out in its excited state, this contribution scales linearly with the total interaction time, so that $\langle H_f \rangle \sim \lambda^2\ T$ as $T \to \infty$. For long interaction times this divergence might be overcome by higher order perturbative contributions, otherwise, it indicates the limits of the perturbative regime.

For a detector starting in its ground state the limit of long interaction times yields

$$\lambda^2 T\left(\frac{1}{2} - \frac{1}{\pi}\left(\mathrm{Si}(\Omega T) + \frac{\cos(\Omega T) - 1}{T\Omega}\right)\right) \overset{T\to\infty}{\longrightarrow} \lambda^2 \frac{1}{\pi\Omega}. \tag{6.33}$$

as $T \to \infty$. This means that even in the limit of an infinitely long interaction time window, a detector starting out in its ground state injects energy into the field. This energy originates from the energy density injected early, after the abrupt switch-on of the interaction. Any energy that is injected into the field propagates away at the speed of light. Hence, there are no means to retain it later at the detector's location.

This indicates that there has to be an energetic cost for decoupling the detector from the field: After the interaction is switched off the field will be in a state of higher energy, because it is not in the vacuum anymore. Also the energy of the detector can only increase under the interaction, since the detector started out in the ground state. The only mechanism by which this overall energy gain can be introduced to the system is through the time-dependent switching of the interaction Hamiltonian.

Therefore, in a sense, the energy which is injected into the field by a detector in its ground state can be viewed as a binding energy between the detector and the field. We will analzye the exact energy budget of switching a detector, and the role the different parts of the systems's Hamiltonian play in Section 6.2.

6.1.5 Timelike energy propagation in 2+1D Minkowski spacetime

In 2+1D Minkowski spacetime, a part of the energy density that the detector injects into the field can propagate into the detector's future lightcone. The leading order contribution to this timelike propagating energy density behaves in a way which appears to support the interpretation of timelike signals as a static imprint on the amplitude of the field, that we arrived at in Chapter 5, because we find this contribution to be independent of the detector's initial state.

In higher dimensions the evaluation of the distributional integral $D^{(n)}(y,z)$, from equation (6.18), that appears in the leading order contribution to the expectation value of the field energy density, is more involved than in 1+1D Minkowski spacetime. In 2+1D, we can obtain an iϵ-representation for the distribution (see Section 2.3) which reads

$$D^{(2)}(y,z) = 4\pi^2 \frac{(-\mathrm{i}y_0+\epsilon)(-\mathrm{i}z_0+\epsilon) - \cos\theta|\vec{y}||\vec{z}|}{((-\mathrm{i}y_0+\epsilon)^2+|\vec{y}|^2)^{3/2}\,((-\mathrm{i}z_0+\epsilon)^2+|\vec{z}|^2)^{3/2}}, \tag{6.34}$$

where $\theta = \sphericalangle(\vec{y},\vec{z})$ is the angle enclosed by the spatial part of y and z. In general, this distribution needs to be integrated against smooth test functions in order to obtain a finite result for the leading order contribution to the expectation value of the field energy density. A pointlike, sharply switched detector will necessarily yield a divergent contribution to the energy density, because we know that its leading order contribution to the total field energy is already divergent.

Nevertheless, an interesting observation about the energy density propagating into the future lightcone of a detector can be made from the iϵ-representation above. This observation suggests that the divergent contributions to the energy density, that would arise from

a sharply switched and pointlike detector, do not propagate into the future lightcone of such a detector.

Let us consider the field energy density at a resting detector's own position in space, after the interaction has been switched off. In the corresponding integral we encounter the distribution $D^{(2)}(y,z)$ only with arguments that have vanishing spacelike parts, i.e., $\vec{y}=\vec{z}=0$. In this case, the expression for $D^{(2)}$ simplifies.

$$D^{(2)}(y_0,\vec{0},z_0\vec{0}) = \frac{4\pi^2}{(y_0+\mathrm{i}\epsilon)^2(z_0+\mathrm{i}\epsilon)^2} = 4\pi^2\left(\mathcal{P}\frac{1}{y_0^2}+\mathrm{i}\pi\delta'(y_0)\right)\left(\mathcal{P}\frac{1}{z_0^2}+\mathrm{i}\delta'(z_0)\right) \tag{6.35}$$

As we are evaluating the energy density in the future lightcone of the interaction of the detector with the field, we will have $y_0, z_0 > 0$. Therefore the δ' terms do not contribute, and also the principal value prescription is irrelevant, since the integral expression does not involve the singularity. Thus, the leading order contribution to the expectation value of the field energy density, which we derived in equation (6.20), from a detector at rest at $\vec{x}_d$, after the interaction has been switched off, takes the simple form

$$\mathrm{Tr}\left(:T_{00}:(t,\vec{x}_a)\rho^{(2)}\right) = \frac{\lambda^2}{8\pi^2}\int_{-\infty}^{\infty}\mathrm{d}\tau\int_{-\infty}^{\infty}\mathrm{d}\tau'\,\eta(\tau)\eta(\tau')\frac{\left(|\alpha|^2\mathrm{e}^{\mathrm{i}\Omega(\tau-\tau')}+|\beta|^2\mathrm{e}^{-\mathrm{i}\Omega(\tau-\tau')}\right)}{(t-\tau)^2(t-\tau')^2} \tag{6.36}$$

at the detector's own position. This integral has a well-defined solution even for a sharp switching function $\chi(\tau)=\chi_{[0,T]}(\tau)$. It reads

$$\begin{aligned}
&\mathrm{Tr}\left(:T_{00}:(t,\vec{x}_a)\rho^{(2)}\right)\\
&\quad=\lambda^2\frac{\mathrm{e}^{-\mathrm{i}t\Omega}}{8\pi^2t^2(t-T)^2}\left(t\Omega(t-T)\mathrm{e}^{\mathrm{i}t\Omega}(\mathrm{Ei}(-\mathrm{i}t\Omega)-\mathrm{Ei}(-\mathrm{i}(t-T)\Omega))+\mathrm{i}\left(T+t\left(-1+\mathrm{e}^{\mathrm{i}T\Omega}\right)\right)\right)\\
&\qquad\times\left((t-T)\left(t\Omega(\mathrm{Ei}(\mathrm{i}t\Omega)-\mathrm{Ei}(\mathrm{i}(t-T)\Omega))+\mathrm{i}\mathrm{e}^{\mathrm{i}t\Omega}\right)-\mathrm{i}t\mathrm{e}^{\mathrm{i}\Omega(t-T)}\right)
\end{aligned} \tag{6.37}$$

where $\mathrm{Ei}(z)=-\int_{-z}^{\infty}\mathrm{d}t\,\mathrm{e}^{-t}/t$ is the exponential integral function.

The most remarkable property of this solution is, that it is independent of the detector's initial state. Instead, the energy density inside the future lightcone only depends on the mere presence of the interacting detector, irrespective of its state.

The energy density in the lightcone is mainly determined by the time that has passed since the detector was decoupled, i.e., on the time interval $t-T$. The asymptotic dependence of the energy density on the time delay since the detector has been switched off is

independent of the detector gap. For vanishing delays, as $t \to T$, we have

$$\mathrm{Tr}\left(:T_{00}:(t,\vec{x}_a)\rho^{(2)}\right) \sim \frac{1}{8\pi^2(t-T)^2}, \tag{6.38}$$

and for large time delays, $t \to \infty$, the energy density falls off as

$$\mathrm{Tr}\left(:T_{00}:(t,\vec{x}_a)\rho^{(2)}\right) \sim \frac{1-\cos(T\Omega)}{4\pi^2\Omega^2 t^4} + \frac{T\sin^2(T\Omega/2)}{\pi^2\Omega^2 t^5}. \tag{6.39}$$

Increasing the duration of the coupling T only increases the energy density that is observed a certain time after the detector is switched off up to some maximum that is soon attained, as seen in Figure 6.3. Only in the limiting case of a zero-gap detector, $\Omega \to 0$, where

$$\mathrm{Tr}\left(:T_{00}:(t,\vec{x}_a)\rho^{(2)}\right) = \frac{T^2}{8\pi^2 t^2(t-T)^2} \tag{6.40}$$

can the energy density grow unbounded for longer interaction durations T.

6.2 Energy budget of switching a single detector

We have seen that coupling a detector to the field injects energy into the field. Also, we know that such a coupling can excite a detector that was initially in its ground state into its excited state. In general, such effects are stronger the shorter the interaction, and the sharper the switching is.

In fact, after the coupling is switched off again, both the energy of the detector, as well as the field energy can be elevated from their initial ground state, which means that, overall, energy has been added to the combined detector-field system by the coupling. What is the source of this energy, or, more precisely, what is the source of this rise in the energy expectation value of the system?

The change of the energy expectation value can only be caused by the time-dependence of the Hamiltonian, introduced by the time-dependent switching of the detector, because the entire time evolution of the combined field-detector system is unitary.

In this section we discuss how much energy an observer needs to locally couple a detector to the field, and how this energy expense accounts for the excitation of the field and the detector. In the following section, this analysis reassures us that timelike signalling do not violate energy conservation, and, most interestingly, it shows that the information carried by timelike signals can be viewed as being encoded in the energy expense their detection requires from the receiver.

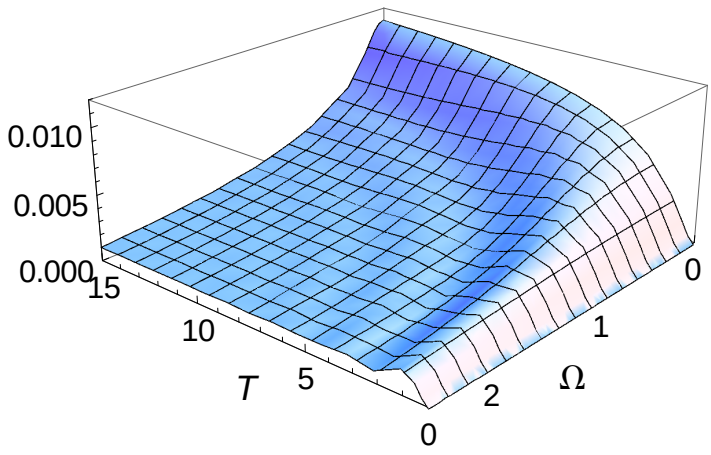

Figure 6.3: Leading order contribution to the energy density $\mathrm{Tr}\left(:T_{00}:(t,\vec{x}_a)\rho^{(2)}\right)/\lambda^2$, from equation (6.37), from a detector with energy gap Ω, at rest at $\vec{x}_a$ in 2+1D Minkowski spacetime, coupling to the vacuum for a duration T, at time $t = T$. The energy density soon attains a maximum for increasing coupling durations T. Only for zero-gap detectors can the energy density grow unbounded, see (6.40)

6.2.1 Energy change from time-dependent Hamiltonian

To begin with let us review and formalize the assertion made in the previous paragraph that the time-dependent switching changes the energy of the system. For a time-dependent Hamiltonian we have that its expectation value evolves as

$$\frac{\mathrm{d}}{\mathrm{d}t}\langle H(t)\rangle = \left\langle \frac{\partial H}{\partial t}\right\rangle, \tag{6.41}$$

i.e., the time derivative of the energy expectation value of a non-autonomous system is given by the expectation value of the time derivative of the Hamiltonian. Being a statement about expectation values, this is independent of the particular (Schrödinger, Heisenberg, Dirac) picture we use for our calculations.

The formula is most easily derived, and applied to our case, in the Schrödinger picture. So we will use the Schrödinger picture for the purpose of this section. There we find that

$$\frac{\mathrm{d}\langle H(t)\rangle}{\mathrm{d}t} = \frac{\mathrm{d}}{\mathrm{d}t}\langle\psi_0| U^\dagger(t)H(t)U(t)|\psi_0\rangle \tag{6.42}$$

$$= \langle\psi_0| \left(U^\dagger(t)\, \mathrm{i}H(t)H(t)\, U(t) + U^\dagger(t) \left(\frac{\partial}{\partial t} H(t) \right) U(t) \right.$$
$$\left. + U^\dagger(t)\, H(t)(-\mathrm{i})H(t)\, U(t) \right) |\psi_0\rangle \tag{6.43}$$
$$= \langle\psi_0|\, U^\dagger(t) \frac{\partial H(t)}{\partial t} U(t)\, |\psi_0\rangle = \left\langle \frac{\partial H(t)}{\partial t} \right\rangle . \tag{6.44}$$

In our case the Hamiltonian consists of the sum of the free Hamiltonians of the field and the detector, and of the interaction Hamiltonian $H_{\mathrm{int}}(t)$.

$$H(t) = H_f + H_d + H_{\mathrm{int}}(t) \tag{6.45}$$

The interaction Hamiltonian is the only part of the Hamiltonian that is time-dependent, whereas the free Hamiltonians, of the field $H_f = \int \mathrm{d}^n \vec{k}\, k\, a^\dagger_{\vec{k}} a_{\vec{k}}$ and the detector $H_d = \Omega\, |e\rangle\langle e|$, are constant. Therefore, the change of the total energy expectation value of the system is given by the expectation value of the interaction Hamiltonian's time derivative.

$$\left\langle \frac{\partial H(t)}{\partial t} \right\rangle = \left\langle \frac{\partial H_{\mathrm{int}}(t)}{\partial t} \right\rangle \tag{6.46}$$

The interaction Hamiltonian is, in general, time-dependent both through the switching of the detector, as well as through the detector's motion, because in the Schrödinger picture the interaction Hamiltonian reads

$$H_{\mathrm{int}}(t) = \lambda\, \eta(t)\, \hat{m}\, \phi(x_d(t)). \tag{6.47}$$

Here, if the detector is moving, the field operator is changing in time such that, even when the switching function is constant, the motion of the detector can introduce energy into the detector-field system.

In the following we restrict our attention to detectors at rest, i.e., $\vec{x}_d(t) = \vec{x}_d = \mathrm{const}$. In this case the field operator is constant in the Schrödinger picture. So the time derivative of the interaction Hamiltonian and, thus, the time derivative of the total energy expectation value of the field-detector system is given by

$$\frac{\mathrm{d}}{\mathrm{d}t} \langle H(t) \rangle = \left\langle \frac{\partial H_{\mathrm{int}}(t)}{\partial t} \right\rangle = \left\langle \lambda \left(\frac{\partial \eta(t)}{\partial t} \right) \hat{m}\, \phi(\vec{x}_d) \right\rangle = \frac{\partial \eta(t)}{\partial t} \langle \lambda\, \hat{m}\, \phi(\vec{x}_d) \rangle$$
$$= \frac{\partial \eta(t)}{\partial t} \langle h_I \rangle , \tag{6.48}$$

where we defined the 'stripped' interaction Hamiltonian as

$$h_I = \lambda \, \hat{m} \, \phi(\vec{x}_d). \tag{6.49}$$

The advantage of this notation is that its expectation value $\langle h_I \rangle$ does not depend on which picture we are applying. So for all calculations in the following we can switch back to the interaction picture and use perturbation theory to calculate $\langle h_I \rangle$.

6.2.2 Exchange of energy under constant coupling

Before we analyze how the switching of the detector changes the total energy, we review briefly how the different parts of the Hamiltonian exchange energy when the switching function $\eta(t)$ is constant, i.e., the interaction is constantly switched on or off.

When the interaction is switched off, i.e., $\eta(t) = 0$, no exchange of energy takes place since the free detector and the free field evolve in time independently from each other. So the expectation value of each of the Hamiltonians is constant, and therefore of course also their sum which is the total Hamiltonian.

$$\langle H \rangle = \underbrace{\langle H_f \rangle}_{=\text{const}} + \underbrace{\langle H_D \rangle}_{=\text{const}} = \text{const} \tag{6.50}$$

During time intervals, where the interaction is switched on and constant, $\eta(t) = \text{const}$, the total energy expectation value is conserved because the interaction Hamiltonian is constant

$$\eta = \text{const} \Rightarrow \left\langle \frac{\partial H_{\text{int}}}{\partial t} \right\rangle = 0 \Rightarrow \langle H \rangle = \langle H_f \rangle + \langle H_D \rangle + \langle H_{\text{int}} \rangle = \text{const}. \tag{6.51}$$

However, the individual expectation values of the field, the detector and the interaction Hamiltonians can now change. With the interaction term present, the Hamiltonian is now acting non-trivially on the product Hilbert space of field and detector spaces, $\mathcal{H} = \mathcal{H}_f \otimes \mathcal{H}_D$. So $\langle H_f \rangle$, $\langle H_D \rangle$ and $\langle H_{\text{int}} \rangle$ change over time, and only their sum is kept constant: Energy is exchanged between the different terms in the Hamiltonian and can flow from one subsystem to the other. This is a consequence of the coupled system having different energy eigenstates than the free uncoupled system.

The exchange of energy can lead to non-trivial energy distributions between the field and the detector, mainly because the interaction Hamiltonian is not positive. This is easily

seen from the monopole operator's eigenvalues being ± 1. Therefore, even when the total energy expectation value vanishes, $\langle H \rangle = 0$, the energies of the field and the detector can both be positive, $\langle H_f \rangle, \langle H_d \rangle > 0$ at the expense of having a negative expectation value of the interaction Hamiltonian, $\langle H_{\text{int}} \rangle < 0$.

The next section shows, that this is how both the field and the detector can gain energy when they are coupled to each other. The negative expectation value of the interaction Hamiltonian corresponds to the energy which is on average necessary to decouple the detector and the field when switching off the detector.

6.2.3 Energy cost of switching a detector

The only time when the total energy expectation value of the field and a detector at rest can be raised or lowered is when the switching function is changing. If we assume that the switching function is changing within the interval $a \leq t \leq b$, then, as shown above, the total energy introduced during this process into the system is given by

$$\Delta \langle H \rangle = \int_a^b \mathrm{d}t \, \frac{\partial \langle H \rangle}{\partial t} = \int_a^b \mathrm{d}t \, \left(\frac{\partial \eta(t)}{\partial t} \langle h_I \rangle \right). \tag{6.52}$$

If we use a sharp switching function $\eta(t) = \chi_{[0,T]}(t)$, which as defined earlier is 1 if $0 \leq t \leq T$ and vanishes elsewhere, then its time derivative consists of two Dirac δ-distributions.

$$\eta'(t) = \chi'_{[0,T]}(t) = \delta(t) - \delta(t - T). \tag{6.53}$$

This means that when the detector is switched on, the energy introduced to system is

$$\Delta \langle H \rangle = \int_{-\epsilon}^{\epsilon} \mathrm{d}t \, \left(\frac{\partial \chi_{[0,T]}(t)}{\partial t} \langle h_I \rangle \right) = \int_{-\epsilon}^{\epsilon} \mathrm{d}t \, \left((\delta(t) - \delta(t - T)) \, \langle h_I \rangle \right) = \langle h_I \rangle (t = 0) \tag{6.54}$$

which is the expectation value of the stripped interaction Hamiltonian $\langle h_I \rangle = \langle \lambda \hat{m} \phi(\vec{x}_d) \rangle$ at the time of switching. Analogously, the change in energy at the switch-off is given by the negative of the expectation value of the stripped interaction Hamiltonian

$$\Delta \langle H \rangle = - \langle h_I \rangle (t = T). \tag{6.55}$$

The expectation value of the interaction Hamiltonian can be either positive or negative such that, depending on the state of the field and detector, switching a detector can cost or yield energy.

When detector and field are in a product state, as we typically assume them to be initially, then the expectation value of the stripped interaction Hamiltonian is just the product of the expectation values of the monopole operator and the field operator.

$$\langle h_I \rangle = \lambda \langle \hat{m} \rangle \langle \phi(\vec{x}_d) \rangle \tag{6.56}$$

If either of these expectation values vanishes, switching a detector sharply does not change the energy expectation value of the combined system. This is the case, for example, if the detector is in an energy eigenstate, or when the field is in a Fock state.

In particular, coupling a detector to the field's vacuum state does not require any energy. When the detector is switched on sharply, the total energy of the system just remains unchanged. Instead all changes to the expectation values of the field Hamiltonian and the detector Hamiltonian that arise from the coupling, are balanced by opposite contributions to the interaction Hamiltonian. This balance has to be accounted for when switching the detector off. Here, as much energy as has been introduced into the system, is required to switch the detector off and decouple the field and the detector.

The expectation value of the interaction Hamiltonian therefore corresponds to a binding energy between field and detector, which can be positive or negative.

The energy change that is introduced by the switch-off depends on the state that field and detector have evolved into. It can be evaluated order by order in perturbation theory, following the same approach that we used before. In fact, we can already deduce the expectation value of the interaction Hamiltonian from previous results, since it is exactly the opposite of the expectation value of the detector Hamiltonian and the field Hamiltonian. The former is just given by the probability to find the detector in its excited state, which has been widely studied in the literature, and the latter we calculated in the previous section.

This also shows that when the perturbative corrections to the expectation values of the detector and the field energy diverge, so does the expectation value of the interaction Hamiltonian. Therefore, in 1+1D we encounter the same IR-divergence as for the single detector excitation probability. In higher dimensions, sharp switching of pointlike detectors yields the same UV-divergence in the expecation value of the interaction Hamiltonian, that we encountered in the field energy in the previous section.

However, in signalling scenarios the leading order perturbative terms that depend on the interaction of both detectors with the field, i.e., terms of order $\mathcal{O}(\lambda_{\mathcal{A}}\lambda_{\mathcal{B}})$ do not suffer from

these divergences. Therefore we will consider pointlike and sharply switched detectors in our analysis. It is straightforward to show that the results we obtain for the perturbative contributions, using a sharp switching functions as above, are exactly recovered when considering a smooth switching function that changes from $\eta(t) = 0$ to $\eta(t) = 1$ in an interval $-\epsilon \leq t \leq \epsilon$, and taking the limit of $\epsilon \to 0$.

6.3 Energy exchange in signalling

Above, we have discussed the energy flows involved in coupling a single detector to the field. Now, we apply the approach to analyze the role of energy transport and exchange in signalling between two detectors. In a perturbative analysis we will see to which part excitations of the receiver's detector are fuelled by the energy that Bob has to provide in order to couple his detector and the field, and to which part the excitation can be fuelled by energy that Alice injected into the field.

We assume that both Alice and Bob each have a pointlike detector, which start out in pure states that we denote by

$$|\psi_{\mathcal{A}}\rangle = \alpha_{\mathcal{A}} |e_{\mathcal{A}}\rangle + \beta_{\mathcal{A}} |g_{\mathcal{A}}\rangle , \qquad |\psi_{\mathcal{B}}\rangle = \alpha_{\mathcal{B}} |e_{\mathcal{B}}\rangle + \beta_{\mathcal{B}} |g_{\mathcal{B}}\rangle , \tag{6.57}$$

whereas the field is assumed to start out in the vacuum. The geometrical setup is the same as in Figure 5.1: The detectors are assumed to be at rest, at a fixed distance L from each other. Alice couples her detector first for the interval $t \in [0, T_A]$, and Bob for $t \in [T_1, T_2]$. We assume that Bob couples to the field after Alice has decoupled her detector $T_1 > T_A$. Depending on the distance L between them, Alice and Bob can still be spacelike, lightlike or timelike separated.

As above, we calculate the resulting time evolution of the expectation values of the different parts of the Hamiltonian perturbatively. The balance between the different parts of the Hamiltonian, that we discussed in Section 6.2.2, will then hold order by order in perturbation theory: The terms of a particular order contributing to one side of the equation balance the terms of the same order on the other side of the equation.

The leading order contributions to the energy contain three different kinds of terms. They are either of order $\mathcal{O}(\lambda_{\mathcal{A}}^2)$ or $\mathcal{O}(\lambda_{\mathcal{B}}^2)$, or of order $\mathcal{O}(\lambda_{\mathcal{A}}\lambda_{\mathcal{B}})$. The terms of order $\mathcal{O}(\lambda_{\mathcal{A}}^2)$ arise from Alice's interaction with the field. They contribute to the field Hamiltonian $\langle H_f \rangle$ and to her detector's Hamiltonian $\langle H_{\mathcal{A}} \rangle$. These contributions are balanced by opposite contributions to her part of the interaction Hamiltonian $\langle H_{\text{int},\mathcal{A}} \rangle$, which determine the energy that Alice needs to provide in order to decouple her detector. Similarly, the terms

of order $\mathcal{O}(\lambda_{\mathcal{B}}^2)$ arise from Bob's interaction with the field. These leading order terms are not influenced by Alice's presence at all, i.e., they are no different from a scenario where Bob would be coupling to the field alone.

The terms of order $\mathcal{O}(\lambda_{\mathcal{A}}\lambda_{\mathcal{B}})$ arise due to the interaction of both Alice and Bob with the field. We therefore refer to them as signalling terms. They describe the leading order effects of how Alice's past action on the field modulates the switching costs, and the energy exchange between Bob's detector and the field. They contribute to $\langle H_f \rangle$, $\langle H_{\mathcal{B}} \rangle$ and $\langle H_{\text{int},\mathcal{B}} \rangle$. The signalling contributions to Alice's Hamiltonian vanish, which is to be expected since they would constitute means for Bob to signal into his past.

The signalling effects can be very different depending on the detector states and the spacetime dimension. For example, in 3+1D Minkowski space, Alice can modulate the energy exchange between Bob and the field without affecting Bob's interaction Hamiltonian, i.e., without changing the energy Bob requires to switch his detector. Contrary to that, in 1+1D, timelike signalling does not lead to any energy exchange between Bob and the field, but instead only affects the energy cost of Bob's switching.

6.3.1 Leading order signalling contributions to the Hamiltonians

The general form of the leading order signalling contributions to the different Hamiltonians' expectation values indicate already their different propagation behaviour. The signalling contribution to Bob's detector Hamiltonian is nothing but the product of Bob's detector energy gap and the probability of finding Bob's detector excited after the coupling. In terms of the notation for the initial states that we introduced above it reads

$$\langle H_{\mathcal{B}} \rangle \sim |\alpha_{\mathcal{B}}|^2 + 4\lambda_{\mathcal{A}}\lambda_{\mathcal{B}}\Omega_{\mathcal{B}} \int_{T_1}^{T_2} \mathrm{d}t_2\, \eta_B(t_2) \int_0^{T_A} \mathrm{d}t_1\, \eta_A(t_1) \\ \times \Re\left(\alpha_{\mathcal{A}}\beta_{\mathcal{A}}^* \mathrm{e}^{-\mathrm{i}\Omega_{\mathcal{A}}t_1}\right) \Re\left\{\alpha_{\mathcal{B}}^*\beta_{\mathcal{B}} \mathrm{e}^{\mathrm{i}\Omega_{\mathcal{B}}t_2} \left[\phi(t_1, \vec{x}_{\mathcal{A}}), \phi(t_2, \vec{x}_{\mathcal{B}})\right]\right\} + \mathcal{O}(\lambda_{\mathcal{B}}^2). \quad (6.58)$$

It is closely related to the C_2 and D_2 terms from Chapter 3, and depends on the commutator of the field. From the results there, we know that the leading order signalling contributions require Alice to be in a superposition of energy eigenstates, i.e., $\alpha_{\mathcal{A}} \neq 0, \beta_{\mathcal{A}} \neq 0$, and in order to have leading order contributions to the detector Hamiltonian, also Bob needs to be in a superposition of energy eigenstates initially, i.e., $\alpha_{\mathcal{B}} \neq 0, \beta_{\mathcal{B}} \neq 0$.

The signalling contribution to the field energy expectation value, after all the interac-

tions have taken place, is

$$\langle H_f\rangle \sim 4\lambda_{\mathcal{A}}\lambda_{\mathcal{B}}\int_{T_1}^{T_2}\mathrm{d}t_2\,\eta_B(t_2)\int_0^{T_A}\mathrm{d}t_1\,\eta_A(t_1)\Re\left(\alpha_A\beta_A^*\mathrm{e}^{-\mathrm{i}\Omega_{\mathcal{A}}t_1}\right)\Re\left(\alpha_B\beta_B^*\mathrm{e}^{-\mathrm{i}\Omega_{\mathcal{B}}t_2}\right)$$
$$\times\,\Re\left(\frac{1}{(2\pi)^n}\int\mathrm{d}^n\vec{k}\,\mathrm{e}^{-\mathrm{i}\left(k(t_1-t_2)-\vec{k}\cdot(\vec{x}_{\mathcal{A}}-\vec{x}_{\mathcal{B}})\right)}\right)+\mathcal{O}(\lambda_{\mathcal{A}}^2)+\mathcal{O}(\lambda_{\mathcal{B}}^2). \tag{6.59}$$

Here, a distributional integral different from the commutator determines for which spacetime separations between Alice and Bob the field energy is changed by signalling contributions. It can be readily evaluated in different dimensions. In 1+1D we have

$$\Re\left(\frac{1}{2\pi}\int_{-\infty}^{\infty}\mathrm{d}k\,\mathrm{e}^{-\mathrm{i}|k|(t_1-t_2)-k(x_{\mathcal{A}}-x_{\mathcal{B}})}\right)$$
$$=\frac{1}{2}\left(\delta(|x_{\mathcal{A}}-x_{\mathcal{B}}|-(t_1-t_2))+\delta(|x_{\mathcal{A}}-x_{\mathcal{B}}|+(t_1-t_2))\right). \tag{6.60}$$

Here the energy of the field is only affected by signalling between lightlike separated detectors. In contrast to this, signalling is possible between timelike separated observers, and signalling contributions to the detector Hamiltonian and the interaction Hamiltonian do arise from such signals.

In 2+1D Minkowski space, if $|t_2-t_1|>|\vec{x}_{\mathcal{A}}-\vec{x}_{\mathcal{B}}|$

$$\Re\left(\frac{1}{4\pi^2}\int_0^{\infty}\mathrm{d}k\,k\int_0^{2\pi}\mathrm{d}\varphi\,e^{-\mathrm{i}k(t_1-t_2)}e^{\mathrm{i}k|\vec{x}_{\mathcal{A}}-\vec{x}_{\mathcal{B}}|\cos\varphi}\right)=\frac{-|t_2-t_1|}{((t_1-t_2)^2-|\vec{x}_{\mathcal{A}}-\vec{x}_{\mathcal{B}}|^2)^{3/2}}, \tag{6.61}$$

such that even signalling between timelike separated detectors can have an effect on the field energy. This integral vanishes for spacelike separations, i.e., if $|t_2-t_1|<|\vec{x}_{\mathcal{A}}-\vec{x}_{\mathcal{B}}|$ [37].

In 3+1D Minkowski space

$$\Re\left\{\frac{1}{8\pi^3}\int_0^{\infty}\mathrm{d}k\,k^2\int_{-1}^{1}\mathrm{d}\cos\theta\int_0^{2\pi}\mathrm{d}\varphi\,e^{-\mathrm{i}k(t_1-t_2)}e^{\mathrm{i}k|\vec{x}_{\mathcal{A}}-\vec{x}_{\mathcal{B}}|\cos\theta}\right\}$$
$$=\frac{-1}{4\pi|\vec{x}_{\mathcal{A}}-\vec{x}_{\mathcal{B}}|}\left(\delta'\left(|\vec{x}_{\mathcal{A}}-\vec{x}_{\mathcal{B}}|+(t_1-t_2)\right)+\delta'\left(|\vec{x}_{\mathcal{A}}-\vec{x}_{\mathcal{B}}|-(t_1-t_2)\right)\right), \tag{6.62}$$

again, signalling contributions to the field energy only arise from signalling between lightlike separted observers.

The signalling contribution to Bob's interaction Hamiltonian expectation value, $\langle h_{I,\mathcal{B}}\rangle$ is different from the previous two in that it only involves one time integration. This is because the interaction Hamiltonian already contains a factor of $\lambda_{\mathcal{B}}$ itself. Therefore the leading order contribution, at order $\mathcal{O}(\lambda_{\mathcal{A}}\lambda_{\mathcal{B}})$ only depends on the change of the field state caused by Alice but does not take into account the action of Bob's own detector on the field. This means that Alice determines the signalling contribution to Bob's interaction Hamiltonian, and thus modulates when it is energetically favourable for Bob to switch his detector. Therefore, at any given time t after Alice has coupled to the field, the leading order signalling contribution to Bob's interaction Hamiltonian is

$$\langle h_{I,\mathcal{B}}\rangle \sim 4\mathrm{i}\lambda_{\mathcal{A}}\lambda_{\mathcal{B}}\Re\left(\alpha_B\beta_B^*\mathrm{e}^{-\mathrm{i}\Omega_{\mathcal{B}}t}\right)\int_0^{T_A}\mathrm{d}t_1\,\eta_A(t_1)\Re\left(\alpha_A\beta_A^*\mathrm{e}^{-\mathrm{i}\Omega_{\mathcal{A}}t_1}\right)\left[\phi(\vec{x}_{\mathcal{A}},t_1),\phi(\vec{x}_{\mathcal{B}},t)\right]+\mathcal{O}(\lambda_{\mathcal{B}}^2). \tag{6.63}$$

Here, as for the expectation value of Bob's detector energy, the commutator decides at which spacetime separations signalling effects occur.

As mentioned above, the interplay between the different parts of the Hamiltonian depends very much on the dimension of the spacetime. In the following we will compare 1+1D, 2+1D and 3+1D Minkowski space.

6.3.2 3+1D Minkowski spacetime

The probably most intuitive scenario is 3+1D Minkowski spacetime, since here all signalling effects propagate strictly at the speed of light. In particular, this means that if Bob switches his detector on before the first lightray emanating from Alice reaches him, and switches his detector off after the last lightray from Alice has passed by him, then the energy required to switch his detector is, to leading order, the same as if Bob was coupling to the vacuum. This is due to the appearance of the commutator in the signalling contribution to $\langle h_{I,\mathcal{B}}\rangle$. It means that Alice's signal does not influence the energy cost for Bob to switch his detector.

The signalling contributions to $\langle H_f\rangle$ and $\langle H_{\mathcal{B}}\rangle$ will in general not vanish. While their integrand has only lightlike support, the terms are integrated over both Alice's and Bob's worldline, in contrast to the expression for $\langle h_{I,\mathcal{B}}\rangle$. In fact, this implies that the signalling contributions at order $\mathcal{O}(\lambda_{\mathcal{A}}\lambda_{\mathcal{B}})$ to $\langle H_f\rangle$ and $\langle H_{\mathcal{B}}\rangle$ exactly balance each other, because at this order no energy is injected into the system through the switching.

Thus, the signalling effect Alice has onto Bob's detector corresponds to a modulation of the energy exchange between Bob's detector and the field. Any amount by which Bob's energy expectation value is raised or lowered due to the signal, is taken or injected into the field. This leads us towards an interesting observation about the relation between the signalling contributions and the other single detector contributions at order $\mathcal{O}(\lambda_{\mathcal{A}}^2)$ and $\mathcal{O}(\lambda_{\mathcal{B}}^2)$ to the field energy.

In equation (5.14) we saw that the signalling strength between two detectors at rest, which is proportional to the signalling contribution to $\langle H_{\mathcal{B}} \rangle$, scales as the inverse $\sim \frac{1}{L}$ of the distance L between the detectors. Now, if one receiver at distance L is able to extract some amount of energy from the field at order $\mathcal{O}(\lambda_{\mathcal{A}}\lambda_{\mathcal{B}})$, then it is possible to spherically arrange a certain number of pairwise spacelike separated receivers at the same distance from the sender which, accordingly, all can extract the same amount of energy from the field into their detectors. However, the maximum number of spacelike separated receivers scales as $\sim L^2$ whereas the the amount of energy extracted from the field into the detectors only decays as $\frac{1}{L}$. Could we extract an arbitrary amount of energy from the field by increasing the distance between sender and receivers, and drive $\langle H_f \rangle$ to arbitrary negative values?

The answer is, of course, that this cannot happen since the Hamiltonian of the field is a non-negative operator, i.e., $\langle H_f \rangle \geq 0$ is never negative. The negative signalling contributions are outweighed by positive single detector contributions to the field Hamiltonian.

$$\langle H_f \rangle \sim \mathcal{O}(\lambda_{\mathcal{A}}\lambda_{\mathcal{B}}) + \mathcal{O}(\lambda_{\mathcal{A}}^2) + \mathcal{O}(\lambda_{\mathcal{B}}^2) \geq 0 \tag{6.64}$$

This is not obvious at first sight, because the single detector contributions do not depend on the distance to other detectors, or even their presence. Also, the coupling constants of the sender and the receivers could be changed independently. Decreasing the receivers' coupling constants by a certain factor while increasing the sender's coupling constant by the same factor would leave the signalling contributions unchanged. However, it could significantly lower the single detector contributions from the many receivers while only raising the one contribution from the sender.

This apparent paradox can be resolved by using the positiveness of the Hamiltonian and the Cauchy-Schwartz inequality. Let us denote the perturbative expansion of the systems state by

$$|\psi\rangle = |\psi^0\rangle + |\psi^1\rangle + |\psi^2\rangle + \mathcal{O}(\lambda^3), \tag{6.65}$$

where $|\psi^0\rangle = |\psi_{\mathcal{A}}\rangle \otimes |\psi_{\mathcal{B}}\rangle \otimes |0\rangle$ is the initial state. Then leading order of the perturbative expansion of the field Hamiltonian is

$$\langle H_f \rangle = \underbrace{\langle \psi^0 | H_f}_{=0} \left(|\psi^0\rangle + |\psi^1\rangle + |\psi^2\rangle \right) + \left(\langle \psi^0 | + \langle \psi^1 | + \langle \psi^2 | \right) \underbrace{H_f |\psi^0\rangle}_{=0}$$

$$+ \left\langle \psi^1 \right| H_f \left| \psi^1 \right\rangle + \mathcal{O}(\lambda^4). \tag{6.66}$$

The first order contribution to the state is the sum of the first order correction through Alice's coupling and the first order correction through Bob's coupling.

$$\left| \psi^1 \right\rangle = \underbrace{\left| \psi^1_{\mathcal{A}} \right\rangle}_{\mathcal{O}(\lambda_{\mathcal{A}})} + \underbrace{\left| \psi^1_{\mathcal{B}} \right\rangle}_{\mathcal{O}(\lambda_{\mathcal{B}})} \tag{6.67}$$

This yields an easy expression for the different leading order perturbative contributions to the energy expectation of the field,

$$\langle H_f \rangle \sim \left\langle \psi^1 \right| H_f \left| \psi^1 \right\rangle = \underbrace{\left\langle \psi^1_{\mathcal{A}} \right| H_f \left| \psi^1_{\mathcal{A}} \right\rangle}_{\mathcal{O}(\lambda^2_{\mathcal{A}})} + \underbrace{\left\langle \psi^1_{\mathcal{B}} \right| H_f \left| \psi^1_{\mathcal{B}} \right\rangle}_{\mathcal{O}(\lambda^2_{\mathcal{B}})} + \underbrace{2\Re\left(\left\langle \psi^1_{\mathcal{A}} \right| H_f \left| \psi^1_{\mathcal{B}} \right\rangle \right)}_{\mathcal{O}(\lambda_{\mathcal{A}}\lambda_{\mathcal{B}})}. \tag{6.68}$$

Since H_f is a positive operator on the orthogonal complement of the vacuum state of the field, we can view a term $\langle \psi | H_f | \phi \rangle$ as a modified scalar product between states that are orthogonal to the vacuum state. In particular, we have a Cauchy-Schwartz inequality (CSI) for the expression which yields

$$\left| \langle \psi | H_f | \phi \rangle \right|^2 \leq \langle \psi | H_f | \psi \rangle \langle \phi | H_f | \phi \rangle . \tag{6.69}$$

The first order contribution $|\psi^1\rangle$ lies in the one-particle sector of the field's Fock space, hence it lies in the orthogonal complement of the vacuum state. Applying this CSI we get

$$\begin{aligned}
\langle \psi_1 | H_f | \psi_1 \rangle &= \left\langle \psi^1_{\mathcal{A}} \right| H_f \left| \psi^1_{\mathcal{A}} \right\rangle + \left\langle \psi^1_{\mathcal{B}} \right| H_f \left| \psi^1_{\mathcal{B}} \right\rangle + 2\Re\left(\left\langle \psi^1_{\mathcal{A}} \right| H_f \left| \psi^1_{\mathcal{B}} \right\rangle \right) \\
&\geq \left\langle \psi^1_{\mathcal{A}} \right| H_f \left| \psi^1_{\mathcal{A}} \right\rangle + \left\langle \psi^1_{\mathcal{B}} \right| H_f \left| \psi^1_{\mathcal{B}} \right\rangle - 2\left| \left\langle \psi^1_{\mathcal{A}} \right| H_f \left| \psi^1_{\mathcal{B}} \right\rangle \right| \\
&\geq \left\langle \psi^1_{\mathcal{A}} \right| H_f \left| \psi^1_{\mathcal{A}} \right\rangle + \left\langle \psi^1_{\mathcal{B}} \right| H_f \left| \psi^1_{\mathcal{B}} \right\rangle - 2\sqrt{\left\langle \psi^1_{\mathcal{A}} \right| H_f \left| \psi^1_{\mathcal{A}} \right\rangle} \sqrt{\left\langle \psi^1_{\mathcal{B}} \right| H_f \left| \psi^1_{\mathcal{B}} \right\rangle} \\
&= \left(\sqrt{\left\langle \psi^1_{\mathcal{A}} \right| H_f \left| \psi^1_{\mathcal{A}} \right\rangle} - \sqrt{\left\langle \psi^1_{\mathcal{B}} \right| H_f \left| \psi^1_{\mathcal{B}} \right\rangle} \right)^2 \geq 0.
\end{aligned} \tag{6.70}$$

Thus, indeed, the leading order single detector contributions are, in absolute value, at least as large as the signalling contributions to the field Hamiltonian's expectation value. This ensures that their sum, the total leading order contribution at order $\mathcal{O}(\lambda^2)$, cannot be negative.

6.3.3 1+1D Minkowski spacetime

The energy budget for signalling between timelike separated detectors in 1+1D Minkowski space is diametrically opposite to what we just observed for signalling in 3+1D.

In both dimensions, the field energy only obtains signalling contributions if sender and receiver are in lightlike contact. However, the particular property of the commutator in 1+1D of being constant in the future lightcone, leads to signalling contributions to the detector energy, even when sender and receiver are strictly timelike separated. Therefore, if Alice and Bob are timelike separated, any signalling contributions to Bob's detector Hamiltonian are balanced by opposite contributions to the energy cost of Bob switching his detector on and off, because the signalling contributions to the field Hamiltonian vanish.

In fact, for sharp switching functions $\eta_{\mathcal{A}}(t) = \chi_{[0,T_A]}(t)$ and $\eta_{\mathcal{B}}(t) = \chi_{[T_1,T_2]}(t)$, we find that the final signalling contribution to Bob's detector Hamiltonian are

$$\begin{aligned}\left\langle \psi^1_{\mathcal{A}} \right| H_{\mathcal{B}} \left| \psi^1_{\mathcal{B}} \right\rangle + \left\langle \psi^1_{\mathcal{B}} \right| H_{\mathcal{B}} \left| \psi^1_{\mathcal{A}} \right\rangle \\ = \frac{2\lambda_{\mathcal{A}}\lambda_{\mathcal{B}}}{\Omega_{\mathcal{A}}} \Re\left(\alpha^*_B \beta_B \left(\mathrm{e}^{\mathrm{i}\Omega_{\mathcal{B}} T_2} - \mathrm{e}^{\mathrm{i}\Omega_{\mathcal{B}} T_1}\right)\right) \Im\left(\alpha_A \beta^*_A \left(1 - \mathrm{e}^{-\mathrm{i}\Omega_{\mathcal{A}} T_A}\right)\right). \end{aligned} \tag{6.71}$$

This is exactly the difference between the energy that Bob has to provide when he switches his detector on, and when he switches it off, because the signalling contribution to the expectation value of his interaction Hamiltonian at any time t in the future lightcone of Alice is

$$\left\langle \psi^0 \right| h_{I,\mathcal{B}} \left| \psi^1_{\mathcal{A}} \right\rangle + \left\langle \psi^1_{\mathcal{A}} \right| h_{I,\mathcal{B}} \left| \psi^0 \right\rangle = \frac{2\lambda_{\mathcal{A}}\lambda_{\mathcal{B}}}{\Omega_{\mathcal{A}}} \Re\left(\alpha_B \beta^*_B \mathrm{e}^{-\mathrm{i}\Omega_{\mathcal{B}} t}\right) \Im\left(\alpha_A \beta^*_A \left(\mathrm{e}^{-\mathrm{i}\Omega_{\mathcal{A}} T_A} - 1\right)\right). \tag{6.72}$$

This means that any change of Bob's detector energy that results from a timelike signal from Alice, is provided for by Bob himself through the net energy he needs to switch his detector on and off. This difference can be positive or negative. In fact all signalling contributions that we are discussing in this section change their sign whenever either Alice or Bob changes their initial detector state into its orthogonal, because this changes the sign of the product $\alpha_D \beta^*_D$.

This observation is the answer to the apparent violation of energy conservation through timelike signalling to many receivers in the future lightcone of Alice in 1+1D Minkowski space. Just as in a collect call, the receivers have to provide the energy themselves by which Alice's signal may have increased their detector energy.

6.3.4 2+1D Minkowski space

The energy budget of timelike signals in 2+1D Minkowski space shows a mixture of energy exchange between all the parts of the Hamiltonian. There are signalling contributions that

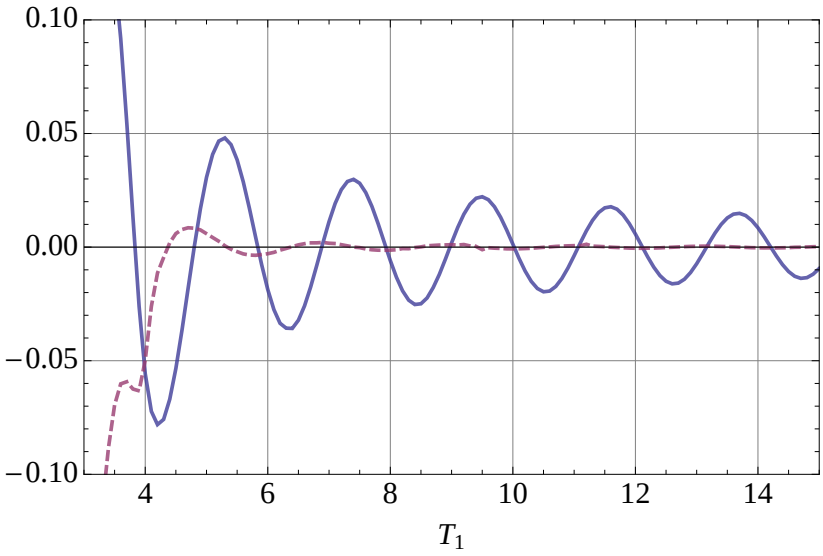

Figure 6.4: [40] Signalling contributions to $\langle H_{\mathcal{B}} \rangle$ from (6.58) (solid) and to $\langle H_f \rangle$ from (6.59) (dashed) divided by $\lambda_A \lambda_B$ for two detectors of frequency $\Omega_A = \Omega_B = 3$ at a distance $L = 1$ in 2+1D Minkowski space. Alice starts out in the state $(|e_A\rangle - \mathrm{i}\,|g_A\rangle)/\sqrt{2}$ and is switched on for $t = 0...3$. Bob starts in the state $(|e_B\rangle + |g_B\rangle)/\sqrt{2}$ and is switched on for $t = T_1...T_1 + 3$. For $T_1 > 4$ the detectors are timelike separated.

cause an energy exchange between the detector and the field, but also, there are signalling dependent switching costs for a receiver in the future lightcone. These switching costs can contribute both to the detector energy and the field.

There are signalling contributions to the field energy expectation value even for timelike separated detectors, since the momentum integral, which we evaluated in (6.61), has non-vanishing timelike support. However, with increasing timelike distance between the receiver and the sender, the signalling contribution to the field energy density decays at a higher power than the contribution to the detector energy. Figure 6.4 plots an example of this.

For large timelike separations between Alice and Bob, the energy exchange with the field becomes subdominant. Instead, it is the net energy that Bob requires to switch his detector on and off, which balances the timelike signalling contributions to Bob's detector Hamiltonian.

For smaller separations between Alice and Bob, the field Hamiltonian contributes to the signalling contributions and, thus, also affects the switching costs. However, as we see in Figure 6.4, the signalling contributions to the field and the detector energies are

not in phase. Therefore, the signalling contributions from the field Hamiltonian can be thought of as superimposed modulation on Bob's switching costs, which are dominated by the contributions from the detector Hamiltonian. There are timing parameters where Bob only adds energy to the field through his switching, there are parameters where he only adds to the detector energy, and seldom there are parameters such that the net switching cost is zero and there is only energy exchange between the field and the detector.

In general scenarios, such as in the figure, the signalling contributions can be evaluated numerically. Or, the simple scenario of a timelike separated sender and receiver that couple to the field after each other at the same location has analytic solutions that can be obtained with a computer algebra system.

We can use these, to find the scalings of the signalling contributions to the different Hamiltonians for large timelike separations between sender and receiver. For sharp switching functions that couple Alice to the field for $0 \leq t \leq T_A$, and Bob for $T_1 \leq t \leq T_1 + \Delta T$, the signalling contributions to the energy expectation values scale as

$$\langle H_{\mathcal{B}} \rangle \sim \frac{\lambda_{\mathcal{A}} \lambda_{\mathcal{B}}}{T_1 - T_A}, \quad \langle H_f \rangle \sim \frac{\lambda_{\mathcal{A}} \lambda_{\mathcal{B}}}{(T_1 - T_A)^2}, \tag{6.73}$$

as $T_1 \to \infty$. Thus $\langle H_{\mathcal{B}} \rangle$ decays with the same power as the commutator, and $\langle H_f \rangle$ with the same power as the momentum space integral in (6.61).

6.4 Conclusion

The motivation for this chapter was the surprising scaling and range of the leading order signalling strength that we had observed previously in Chapter 5. There, we concluded that both timelike and lightlike signals between two detectors cannot be viewed as being tied to an energy flow, which would be carrying them. This was obvious for timelike signals from our analysis of 1+1D Minkowski spacetime in Section 2.4. However, even for the lightlike signals in 3+1D Minkowski spacetime we saw that their leading order decayed much slower for increasing distance between sender and receiver, than the energy radiated spherically symmetric from the sender.

Both types of signals yield leading order contributions to the energy expectation value of appropriately prepared receivers. However, by the perturbative analysis of this chapter we were able to show that there are different mechanisms underlying the energy transfer.

Energy increases from timelike signals in 1+1D Minkowski spacetime are accounted for by changes to the energy required from the receiver to couple and decouple their detector.

Therefore, the receiver could equally obtain the sender's message just from a measurement of the switching costs, without performing a measurement on the detector itself.

In contrast, in 3+1D Minkowski spacetime the energy cost of switching the receiver's detector contain no information about any leading order signals from the sender. The joint switching costs of the sender and receiver were shown to be at least as high as the amount by which the receiver's energy is elevated. However, the switching costs contain no information about the signal, and are, to leading order, the same as if receiver and sender were just individually coupling to the vacuum.

In 2+1D Minkowski spacetime we observed both types energy transmission superimposed. Due to the support of the commutator in the future lightcone, the switching costs of receivers can be modulated by timelike signals. And, due to the decay of the commutator inside the lightcone, timelike signals can transfer energy from the field to the receiver's detector.

Consequently, on general curved spacetimes, we also should expect both types of energy transmission, because the commutator generally decays into the future lightcone. Expanding FLRW spacetimes, where the signalling strength of timelike signals has already been studied [10, 11], could yield a first scenario to test whether the intuition, that we developed in this chapter in flat spacetime, carries over to spacetimes with curvature.

Chapter 7

Signalling with Harmonic Oscillators

Note: This chapter mainly consists of adapted and extended parts of [38].

At this point we have achieved an understanding of the communication channel between two localized relativistic observers. We know that the commutator dominantly determines whether classical information can be transmitted through the quantum field. And, we were able to explain how exactly information transmission can decouple from energy transmission through timelike signalling, based on a perturbative analysis of the time evolution.

The next important question is to investigate the transmission of quantum information through relativistic quantum fields between localized observers. To address this question requires us to go beyond perturbation theory for several reasons.

First of all, the transmission of a qubit from the sender's detector into the field, let alone subsequently from the field to the receiver's detector, is more than a perturbative correction to the system's state. Also, in this context, since quantum information may get dispersed in the field and cannot be amplified or multiplied, it may also become relevant to consider scenarios with many receivers trying to cooperatively recover the sent quantum information from the field. However, having more receivers means having a larger interaction Hamiltonian, thus, the limits of the perturbative regime are reached earlier. Moreover, the influence of the quantum properties of the field state, encoded in the real part of the Wightmann function, only become visible in higher order terms.

One setup in which the exact time evolution of detectors and the field can be calculated is obtained by just a small modification to our earlier setups: Upgrading the detectors from two-level systems to being harmonic oscillators makes it possible to treat the combined time evolution of the detector and the field using symplectic methods [15, 16]. (See also [82, 49, 50].)

In this chapter we will consider signalling between harmonic oscillators that couple to the field inside a one-dimensional Dirichlet cavity, just as in Chapter 4. Except now, because we are using harmonic oscillator detectors, the exact time evolution of the detectors and the field modes can be calculated numerically following the approach of [15].

This chapter's sections introduce the general setup (Section 7.1), review some basics of symplectic methods (Section 7.2), and characterize timelike signalling between harmonic oscillators (Section 7.3). Finally, we discuss the influence of the lack of translation invariance in the Dirichlet cavity (Section 7.4), and the possibility of (timelike) signalling with harmonic oscillators that are resonant with the fundamental mode of the cavity (Section 7.5).

7.1 Harmonic oscillators inside a Dirichlet cavity

The interaction Hamiltonian between the field and a harmonic oscillator detector located at rest at x_d inside the cavity reads

$$H_{\text{int}} = \lambda\Omega \left(\mathrm{e}^{-\mathrm{i}\Omega t} a_d + \mathrm{e}^{\mathrm{i}\Omega t} a_d^\dagger \right) \phi(t, x_d) \tag{7.1}$$

in the interaction picture. Here now the operators a_d and $a_d^\dagger$ are the ladder operators acting on the harmonic oscillator detector. Since for the purpose of this chapter we are only concerned with the field in one-dimensional cavities, we multiplied the Hamiltonian by the harmonic oscillator's energy level spacing Ω, so as to make the coupling constant λ dimensionless. We also dropped the switching function, since we will only consider sharp switchings of the interaction between the detectors and the field.

The advantage of a Dirichlet cavity is that the full unitary time evolution of the detectors and the field can be calculated numerically with the methods developed in [15]. In contrast, in a periodic cavity the zero mode of the field would require separate analysis.

However, this advantage comes at the price of loosing spatial translational invariance: Inside a Dirichlet cavity the field modes have varying intensity at different locations, because they exhibit maxima and node points due to the boundary conditions. These maxima and nodes lie at different points for the individual modes depending on their wave length. Therefore also the behaviour of a detector coupling to the field inside a Dirichlet cavity depends on the detector's location.

As far as signalling between two detectors is concerned, these effects are negligible when sender and receiver are strictly timelike separated, in the sense that not even lightrays

reflected by the cavity walls can connect the sender to the receiver. We will discuss this aspect in detail in Section 7.4.

In a numerical calculation, of course, only a finite number of N field modes can be taken into account. This means introducing a UV cutoff in the field expansion (2.44)

$$\phi(t,x) = \sum_{j=1}^{N} \frac{1}{\sqrt{j\pi}} \sin(j\pi x/L) \left(a_j \mathrm{e}^{-\mathrm{i}\frac{j\pi}{L}t} + a_j^\dagger \mathrm{e}^{\mathrm{i}\frac{j\pi}{L}t} \right) \tag{7.2}$$

exactly of the kind that was studied in Chapter 4. There we saw that the cutoff needs to be chosen large enough in order to capture the relativistic properties of the field with accuracy, which is satisfyingly achievable on a standard desktop computer. (This aspect is also discussed in [15] for harmonic oscillator detectors.)

The interaction Hamiltonian (7.1) between field and detectors is strictly quadratic in the creation and annihilation operators, without any linear terms. Under the time evolution of such a Hamiltonian, Gaussian states remain Gaussian states. And the time evolution of Gaussian states can be very efficiently described in the symplectic formalism.

To exploit this we restrict ourselves to Gaussian initial states. As far as the field is concerned, this is what we have been doing before. The vacuum state, consisting of the ground state for each individual mode, of course already is a Gaussian state. For the detectors we will mostly use the ground state, squeezed states or thermal states as signalling input states.

7.2 Miniature review of Gaussian methods

Continuous variable, and Gaussian quantum information methods provide a widely developed and powerful framework, e.g., for optical quantum information. There are various reviews, such as [14, 85], and different introductions to the topic, such as [1, 65]. These methods were first applied to the context of particle detectors in [15] which gives a detailed explanation of the relevant Gaussian methods. Here, we will restrict ourselves here to a very basic review.

Gaussian states are fully characterized by the first two moments of all quadrature operators. These can be conveniently combined into a vector. To this end, we organize the quadrature operators of the two detectors (whose annihilation operators we denote as a_A

and a_B) and the N field modes into one $(2N+4)$-dimensional vector

$$\mathbf{x} = \frac{1}{\sqrt{2}}\Big(\Big(a_A + a_A^\dagger\Big), \Big(a_B + a_B^\dagger\Big), ..., \Big(a_N + a_N^\dagger\Big), \\ -\mathrm{i}\Big(a_A - a_A^\dagger\Big), -\mathrm{i}\Big(a_B - a_B^\dagger\Big), ..., -\mathrm{i}\Big(a_N - a_N^\dagger\Big)\Big), \tag{7.3}$$

such that the first $(N+2)$ entries correspond to the detectors' and field modes' canonical position operators

$$q_i = \frac{1}{\sqrt{2}}\Big(a_i + a_i^\dagger\Big), \tag{7.4}$$

and the second $(N+2)$ entries correspond to the canonical momentum operators

$$p_i = \frac{-\mathrm{i}}{\sqrt{2}}\Big(a_i - a_i^\dagger\Big). \tag{7.5}$$

The first two moments which fully characterize a Gaussian state are then given by the expectation value of the quadrature operator vector $\langle\mathbf{x}\rangle$, and by its covariance matrix σ. For the latter we use the convention

$$\sigma_{ij} \equiv \frac{1}{2}\langle\{\Delta\mathbf{x}_i, \Delta\mathbf{x}_j\}\rangle = \frac{1}{2}\left(\langle\mathbf{x}_i\mathbf{x}_j + \mathbf{x}_j\mathbf{x}_i\rangle - 2\langle\mathbf{x}_i\rangle\langle\mathbf{x}_j\rangle\right), \tag{7.6}$$

such that the ground state of a harmonic oscillator has the covariance matrix $\sigma_{ij} = \frac{1}{2}\delta_{ij}$. (It is important to note that there is an alternative convention without the factor $\frac{1}{2}$ in front, which is used in [15, 1].) To obtain the covariance matrix of a subsystem one only needs to delete the rows and columns belonging to the other part of the system from the covariance matrix. This is analogous to taking the partial trace of a state's density operator.

An important class of Gaussian states are squeezed state. These states have one of their covariances enlarged at the expense of the other. For a single mode it therefore can be written as

$$\sigma = \frac{1}{2}\begin{pmatrix} \mathrm{e}^{-2r} & 0 \\ 0 & \mathrm{e}^{2r} \end{pmatrix} \tag{7.7}$$

with r being called the squeezing parameter. Squeezed states are pure states, and they optimize the Heisenberg uncertainty principle.

Another important class are thermal states. A thermal state of temperature τ has the covariance matrix

$$\sigma_{th} = \frac{1}{2}\coth\left(\frac{\Omega}{2\tau}\right)\mathbb{I} \tag{7.8}$$

where Ω is the energy level spacing of the mode. It is interesting to note that any zero-mean Gaussian state can be viewed as a squeezed thermal state. This is possible since covariance matrices are positive and symmetric such that any covariance matrix can be diagonalized by a rotation matrix.

The overlap of a zero-mean Gaussian state of M modes with the vacuum, i.e., the probability to measure the system in its overall ground state, is given by

$$P_0 = \frac{2^M}{\sqrt{\det \sigma \det \left(\sigma^{-1} + 2\mathbb{I}_{2M}\right)}} \tag{7.9}$$

which for a single mode simplifies to

$$P_0 = \frac{2}{\sqrt{4 \det \sigma + 2 \operatorname{Tr} \sigma + 1}}. \tag{7.10}$$

The time evolution of the system is captured by the so called symplectic matrix $\mathbf{S}(t)$ which takes the role of the unitary time evolution operator. In the Heisenberg picture, it evolves the quadrature operators simply by mutliplication

$$\mathbf{x}(t) = \mathbf{S}(t)\mathbf{x}(0). \tag{7.11}$$

The moments of a Gaussian state, which are picture independent since they are expectiaton values, accordingly evolve as

$$\langle \mathbf{x}(t) \rangle = \mathbf{S} \langle \mathbf{x}_0 \rangle \tag{7.12}$$

$$\sigma(t) = \mathbf{S}\sigma_0 \left(\mathbf{S}\right)^T \tag{7.13}$$

where $\mathbf{S}^T$ denotes the transpose of the symplectic matrix. We see that the first and second moments evolve independent of each other. In particular this means, that a state with vanishing first moments, called a zero-mean state, always remains a zero-main state.

The symplectic matrix $\mathbf{S}(t)$ is determined by an analogue of the Schrödinger equation, which for time-dependent Hamiltonians can be solved by numerical methods. However, since we use sharp switchings only, we have a Hamiltonian which is piecewise constant in time. For constant Hamiltonians the symplectic matrix is solved for by a matrix exponential

$$\mathbf{S}(t) = \exp\left(\mathbf{\Omega}\mathbf{F}^{\mathrm{sym}} t\right) \tag{7.14}$$

with the symplectic form

$$\mathbf{\Omega} = \begin{pmatrix} 0 & \mathbb{I} \\ -\mathbb{I} & 0 \end{pmatrix}. \tag{7.15}$$

And the matrix $\mathbf{F}^{\text{sym}} = \mathbf{F} + \mathbf{F}^T$ is the symmetrized part of the matrix which is obtained be rewriting the Hamiltonian of the system as

$$H = \mathbf{x}^T \mathbf{F}\, \mathbf{x}. \tag{7.16}$$

This is possible since the Hamiltonian is strictly quadratic in the creation and annihilation operators, and thus also quadratic in the quadrature operators. Formulae for the construction of $\mathbf{F}$ are found in [15].

The definition of $\mathbf{F}$ refers to the full Hamiltonian of the field, i.e., to the sum of the free Hamiltonians of the field and the detectors, and the interaction Hamiltonian. Therefore, depending on which detectors couple to the field during which intervals of time, different symplectic matrices need to be constructed for the different time intervals, during which the Hamiltonian is constant.

Finally, we note that by treating the time evolution of quantum harmonic oscillators to the quantum field in this formalism we *en passant* also solve the behaviour of the corresponding classical system. Because by the Ehrenfest theorem the first moment, the mean $\langle \mathbf{x} \rangle$, evolves according to the classical equations of motion. All signalling effects that we observe for the mean of the detectors would thus also be osbervable between classical harmonic oscillator coupling to a string with fixed boundary conditions.

7.3 Timelike signals between harmonic oscillators

The signalling scenario that we will study with the harmonic oscillator detectors is the same as the scenarios previoulsy considered for timelike signalling between detectors at rest: Initially the field is in its vacuum state, i.e, all the field modes are in their ground state. The sender's detector is initialized in some pure Gaussian state, and coupled to the field for time $t = 0...T_A$. Then, with some delay, the receiver, being initialized in its ground state, is coupled to the field for time $t = T_1...T_2$. The time delay between the couplings $T_1 - T_A$ determines whether the two detectors are timelike or lightlike separated.

After the receiver is decoupled from the field, the mean displacement of the sender's harmonic oscillator depends linearly on the initial mean displacement of the sender. From equation (7.12) follows

$$\langle \mathbf{x_B}(T_2) \rangle = \begin{pmatrix} S_{2\,1} & S_{2\,N+3} \\ S_{N+4\,1} & S_{N+4\,N+3} \end{pmatrix} \langle \mathbf{x_A}(0) \rangle \tag{7.17}$$

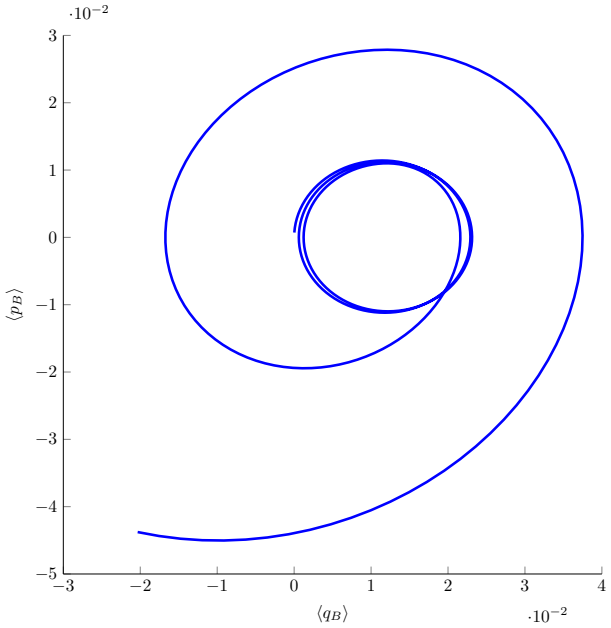

Figure 7.1: [38] Phase space plot of receiver's final mean $\langle \mathbf{x_B}(T_2) \rangle = (\langle q_B \rangle, \langle p_B \rangle) = \frac{1}{\sqrt{2}} \left(a_B + a_B^\dagger, -\mathrm{i}(a_B - a_B^\dagger) \right)$. The inner circles correspond to timelike separation between the sender and the receiver (see Figure 7.2). The sender is located at $a = 0.5L$, and the receiver at $b = 0.6L$. The sender couples to the field for $t = 0...0.3L$. The receiver couples to the field for $t = 0.46L...T_2$. The points in this plot correspond to $T_2 = 0.46...1.2L$. The detectors' energy gap is $\Omega = 10\pi/L$ and the coupling constant $\lambda = 0.075$. For the computation $N = 200$ field modes were taken into account.

with $\mathbf{x_d} = (q_d, p_d) = \frac{1}{\sqrt{2}} \left(a_d + a_d^\dagger,\ -\mathrm{i}(a_d - a_d^\dagger) \right)$ for $d = A, B$.

Figures 7.1 and 7.2 show that even for strictly timelike separation between sender and receiver, i.e., when not even lightrays reflecting of the cavity walls can connect the sender to the receiver, the sender can induce a displacement of the receiver's final state. For this the sender needs to prepare an initial state with non-vanishing displacement in canonical momentum $\langle p_A \rangle$, such as $\langle \mathbf{x_A}(0) \rangle = (0, 1)$.

An initial displacement in canonical position $\langle q_A \rangle$, hardly affects a timelike separated receiver, when the sender interacts with the field for times on the order of a few detector periods $\Omega/(2\pi)$, and is resonant with higher modes of the cavity. An initial displacement in $\langle q_A \rangle$ only affects receivers reached by (reflected) light rays, as seen in Section 7.4. This is different for detectors resonant with the base mode of the cavity ($\Omega = \pi/L$) where also

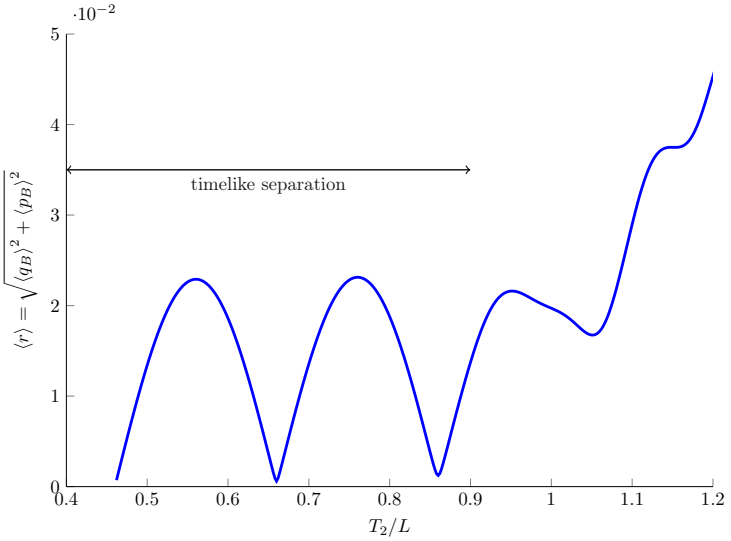

Figure 7.2: [38] Displacement $\langle r \rangle = \sqrt{\langle q_B \rangle^2 + \langle p_B \rangle^2}$ of the receiver's final state over different coupling times for the receiver in the same setting as Figure 7.1. The receiver and sender are strictly timelike separated for $T_2 < 0.9L$. For lightlike separations between sender and receiver see Section 7.4.

$\langle \mathbf{x_A} \rangle = (1, 0)$ leads to timelike signalling, as seen in Section 7.5.

To maximize timelike signalling effects, the sender needs to couple to the field for a multiple plus a half of a detector period, i.e., for $T_A = (2n + 1)\,\Omega/(4\pi)$ with $n \in \mathbb{N}$. The timelike effects vanish when the sender is coupled for an integer multiple of its detector period, i.e., for $T_A = n\Omega/(2\pi)$.

In the example of Figure 7.1 and 7.2 (coupling constant $\lambda = 0.075$) we observe a displacement of the receiver's final state which is in the percentile range of the sender's initial displacement. (Higher values of the coupling constant increase the effect.) This displacement decreases the overlap between the sender's final state and its initial ground state and could thus be used for classical information transmission [40], both via the quantum field as well as in its classical analogue.

When the sender is initialized in a zero-mean Gaussian state (just as the receiver and the field modes always are as they are initialized in their ground state), then no displacement of the receiver's final state occurs. Because, as mentioned earlier, zero-mean Gaussian states remain zero-mean Gaussian states under Hamiltonians that are only quadratic in creation and annihilation operators .

However, timelike signals can also be evoked by zero-mean Gaussian states, by the second moments of the state. Denoting the covariance matrix elements of the sender's and receiver's detector into three-vectors

$$\vec{\sigma_{\mathbf{A}}} = \begin{pmatrix} \sigma_{1\,1} \\ \sigma_{N+3\,N+3} \\ \sigma_{1\,N+3} \end{pmatrix} \qquad \vec{\sigma_{\mathbf{B}}} = \begin{pmatrix} \sigma_{2\,2} \\ \sigma_{N+4\,N+4} \\ \sigma_{2\,N+4} \end{pmatrix}, \tag{7.18}$$

it follows from equation (7.13) that the receiver's final covariance elements are given by

$$\begin{aligned} \vec{\sigma_{\mathbf{B}}}(t) = &\begin{pmatrix} (S_{2\,1})^2 & (S_{2\,N+3})^2 & 2S_{2\,1}S_{2\,N+3} \\ (S_{N+4\,1})^2 & (S_{N+4\,N+3})^2 & 2S_{N+4\,1}S_{N+4\,N+3} \\ S_{2\,1}S_{N+4\,1} & S_{2\,N+3}S_{N+4\,N+3} & S_{2\,1}S_{N+4\,N+3} + S_{2\,N+3}S_{N+4\,1} \end{pmatrix} \vec{\sigma_{\mathbf{A}}}(0) \\ &+ \sum_{i\neq 1,N+3} \frac{1}{2} \begin{pmatrix} (S_{2\,i})^2 \\ (S_{N+4\,i})^2 \\ S_{2\,i}S_{N+4\,i} \end{pmatrix} \end{aligned} \tag{7.19}$$

where we used that all field modes and the receiver's detector are initially in their ground state. The covariance matrix elements of the receiver's final state consist of an affine part, which can be viewed as background noise, on top of which a contribution is added which is linear in the sender's initial covariance matrix elements.

Due to these contributions there is a certain excitation probability $P_e = 1 - P_0$ to measure the receiver in a state other than the ground state after its interaction with the field. If this probability is affected by the sender's action, this influence can be used to transmit classical information, since it constitutes a binary asymmetric channel as in Section 3.4.1.

Figure 7.3 shows an example where initializing the sender in a thermal state, as an example of a zero-mean state, can be used for signalling to a timelike separated receiver. Just as for the effects on the mean displacement, the sender needs to couple for a time $T_A = (2n+1)\Omega/(4\pi)$ to maximize the effect on a strictly timelike separated receiver's covariance matrix. These effects vanish when the sender is coupled for $T_A = n\Omega/(2\pi)$, i.e., for a multiple of a detector period.

Similarly to the signalling via the state's mean, the variance of the sender's initial canonical momentum $\sigma_{N+3\,N+3} = \Delta p_A = \langle p_A^2 \rangle - \langle p_A \rangle^2$ evokes stronger timelike signalling effects than the sender's initial variance in canonical position $\sigma_{1\,1} = \Delta x_A = \langle x_A^2 \rangle - \langle x_A \rangle^2$, as one would expect comparing equations (7.17) and (7.19). This can be demonstrated by initializing the sender in differently rotated squeezed states. There we find that timelike signalling is stronger for states squeezed in position (with large Δp_A) than for timelike

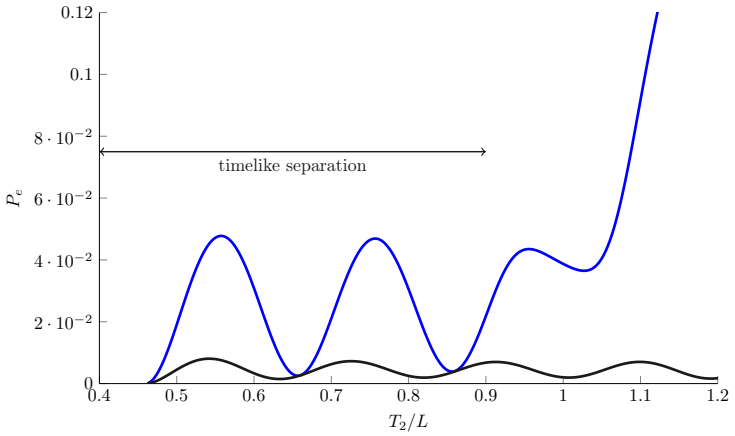

Figure 7.3: [38] Timelike signalling via thermal states. P_e is the excitation probability for the receiver. The lower line shows P_e when the receiver is coupling to the vacuum state of the field, in the absence of a sender. The upper line shows the elevation of P_e by the sender in the signalling scenario. The sender is initialized in a thermal state with $\Omega/\tau = 6 \cdot 10^{-3}$, located at $a = 0.5L$, and coupled to the field for $t = 0...0.3L$. The receiver is located at $b = 0.6L$, and coupled to the field for $t = 0.46L...T_2$. Hence sender and receiver are strictly timelike separated for $T_2 < 0.9L$. The detectors' energy spacing is $\Omega = 10\pi/L$, the coupling constant $\lambda = 0.075$. For the numerical calculations $N = 200$ modes were used.

signalling effects are tiny for momentum squeezed states (with large Δx_A). However, when sender and receiver are connected by (reflected) lightrays the signals from momentum squeezed states are comparable in size to the signals from position squeezed states, as we will see in the next section.

7.4 Influence of position inside Dirichlet cavity

The field inside a Dirichlet cavity is not translationally invariant since the individual field modes exhibit nodes and maxima at different points in the cavity. This also affects the coupling between a detector and the field. For example, the probability to excite a single detector by coupling it to the vacuum of the field depends on the position of the detector inside the cavity, as shown in Figure 7.4, and as we observed for the excitation probability of a two-level detector in Figure 4.1.

The signalling between detectors is also affected by the sender's and the receiver's position inside the cavity. Figure 7.5 and Figure 7.6 show how the receiver's final mean

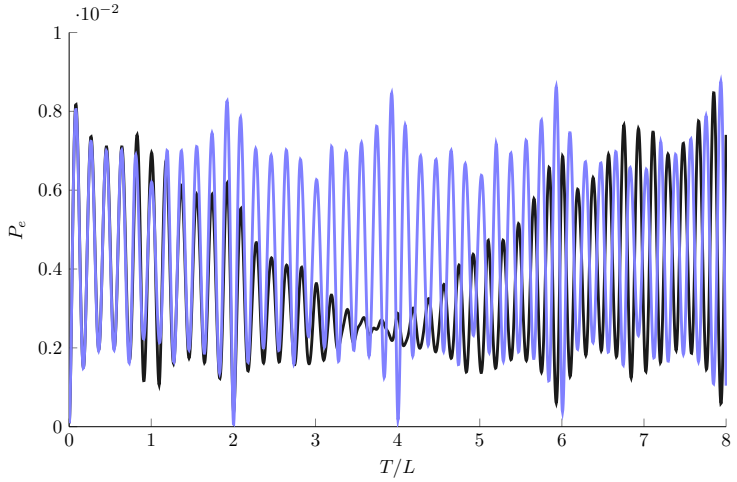

Figure 7.4: [38] Position dependence of vacuum excitation probability in a Dirichlet cavity for a single detector. A harmonic oscillator detector, resonant with the 10th field mode ($\Omega = 10\pi/L$) is initialized in its ground state and then coupled to the field for a time $t = 0...T$. The plot shows the probability P_e to find the detector in a state other than its ground state after the interaction with the field. For the black curve, whose oscillation amplitude diminishes towards 0.03 around $T = 3.75$, the detector is located at $x = 0.55L$ which is a maximum of the resonant 10th field mode. The light blue curve shows the detector located at $x = 0.6L$ which is a node of the resonant field mode. The coupling constant is $\lambda = 0.075$ For the numerical calculations $N = 200$ field modes were used.

displacement is affected, depending on whether sender and receiver are located at maxima or at node points of the cavity mode with which their detector is resonant. Figure 7.5 is hereby extending the setup of Figure 7.2 to longer coupling times of the receiver's detector.

We see that the strongest displacement arises when both sender and receiver are located at maxima of the resonant mode. When the sender and receiver both are at node points the signals are weaker, but still stronger than when when only the sender is located at a node point and the receiver is located at a maximum. (In the latter setup, even when reflected lightrays connect the sender to the receiver, the effects are not larger than for strictly timelike separation between sender and receiver.)

However, for strictly timelike separation between sender and receiver, the location of sender and receiver has no influence, and there is no difference in the final displacement of the sender.

When signalling with zero-mean Gaussian states the effect of the detectors' position

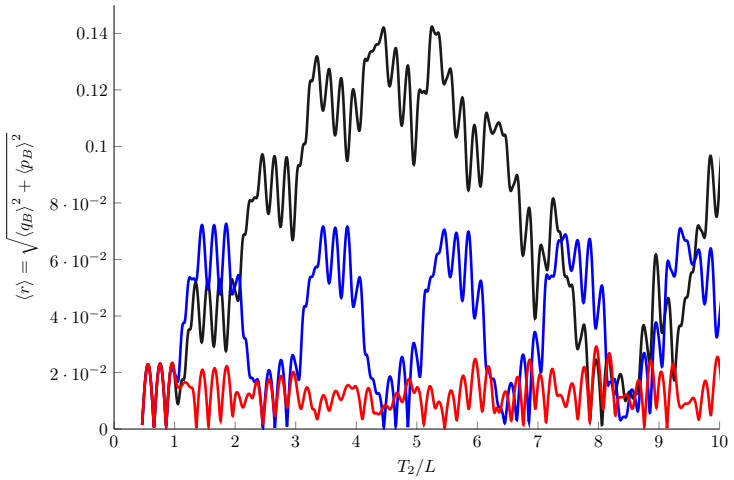

Figure 7.5: [38] Mean displacement $\langle r \rangle$ of final receiver state when the sender is initialized in a state with $\langle q_a \rangle = 0$ and $\langle p_A \rangle = 1$, i.e., with a non-zero displacement in canonical position. The plot shows different combinations of sender and receiver being located at maxima or node points of the field mode they are resonant with. The detectors' energy spacing is $\Omega = 10\pi/L$, i.e., they are resonant with the 10th cavity mode. The upper (black) curve corresponds to the sender being located at $a = 0.45L$ and the receiver at $b = 0.55L$ both of which are maxima of the 10th cavity mode. The middle (blue) curve correspond to both sender ($a = 0.5L$) and receiver ($b = 0.6L$) being located at node points. The lower (red) curve shows the sender at a node point ($a = 0.5L$) and the receiver at a maximum ($b = 0.55L$). The sender couples to the field for $t = 0...0.3L$, the receiver for $t = 0.46L...T_2$. The coupling constant is $\lambda = 0.075$. For the numerical calculations $N = 200$ field modes were used.

on the excitation probability of the receiver is very similar to the effect on the mean displacement. Figure 7.7 shows $\Delta P_e = P_e^{\text{sig}} - P_e^{\text{vac}}$, which is the difference between the receiver's excitation probability P_e^{sig} in the signalling scenario and the receiver's excitation probability P_e^{vac} when coupled only to the vacuum at the same location as in Figure 7.4.

In contrast to the mean displacement $\langle r \rangle$, the difference in excitation probability ΔP_e shows some dependence on the exact location of sender and receiver in the cavity even for strictly timelike separations. The size of this effect is however negligible. For example, in the setup of Figure 7.7 the differences in the value of ΔP_e for different locations of sender and receiver are $< 2 \cdot 10^{-5}$ whereas ΔP_e ranges up to $4 \cdot 10^{-2}$.

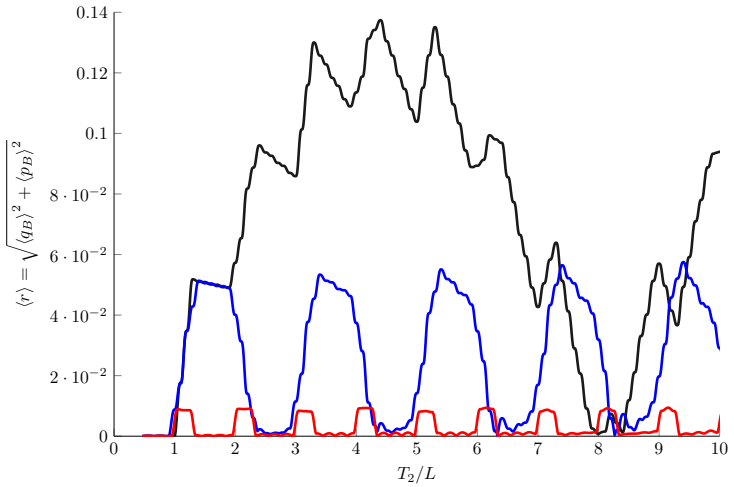

Figure 7.6: [38] Mean displacement $\langle r \rangle$ of final receiver state when the sender is initialized in a state with $\langle q_a \rangle = 1$ and $\langle p_A \rangle = 0$, i.e., with a non-zero displacement in canonical position. Otherwise setup identical to Figure 7.5.

7.5 Signalling with detectors resonant with the fundamental mode

In order to study timelike signalling via fields inside a cavity it appears natural to choose the cavity to be large, such that the receiver and sender can each couple to the field for some time, before lightrays that emanate from the sender and reflect off the cavity walls connect sender and receiver. If the interaction time of sender and receiver is to be on the order of a few detector periods $\Omega/(2\pi)$, then the detectors need to be resonant with higher modes of the cavity. For this reason we choose the detectors to be resonant with the 10th field mode in the numerical examples above.

It is still interesting to ask if timelike signalling also occurs between detectors that are resonant with the base mode of the cavity, i.e., have an energy level spacing of $\Omega = \pi/L$. Figure 7.8 and Figure 7.9 answer this question in the affirmative. They show the senders effect on the receivers final mean displacement, and on the receivers excitation probability for a zero-mean initial state of the sender. In this setup, in order to allow for timelike separation between sender and receiver, the sender is coupled to the field for less than half a detector period.

Figure 7.8 shows that, unlike detectors being resonant to higher field modes (Figure 7.2),

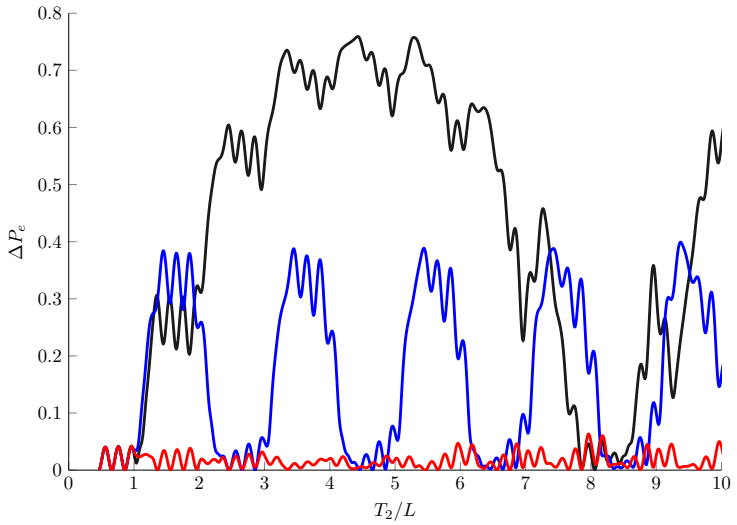

Figure 7.7: [38] Signalling with zero-mean Gaussian states. The plot shows $\Delta P_e = P_e^{\text{sig}} - P_e^{\text{vac}}$, which is the difference between the receiver's excitation probability P_e^{sig} in the signalling scenario and the receiver's vacuum excitation probability (see Figure 7.4). The sender was initialized in a thermal state with $\Omega/T = 6 \cdot 10^{-3}$. All other parameters and the detector locations are identical to Figure 7.5.

a displacement of the receiver's mean arises both from displacement in the sender's initial canonical momentum $\langle p_A \rangle$, as well as in position $\langle q_A \rangle$. Whereas the mean displacement continues to grow for longer coupling times of the receiver, it already reaches the percentile range while sender and receiver are still strictly timelike separated.

The long time behaviour of the mean displacement is again similar to the behaviour of the excitation probability for zero-mean states which is given in Figure 7.9. In Figure 7.9 we see the influence of a sender using a thermal, zero-mean Gaussian state on the excitation probability of the sender, analogous to Figure 7.7. Whereas ΔP_e grows up to values of about $\Delta P_e \approx 0.55$ for long coupling times, an influence on the order of $\Delta P_e \approx 0.04$ is already visible for timelike separations between sender and receiver at the chosen parameter values.

7.6 Conclusion

The results of this chapter show that signalling is possible between strictly timelike separated harmonic oscillators coupling to the field inside a cavity. These signals can be

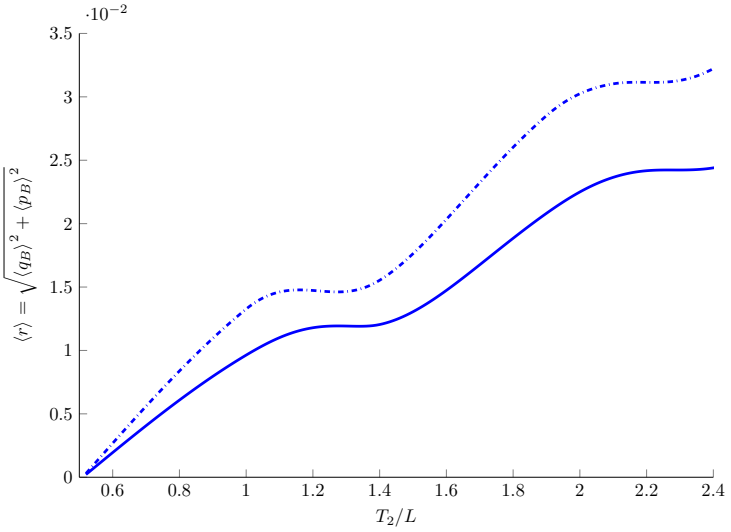

Figure 7.8: [38] Mean displacement $\langle r \rangle$ of the receiver's final state, for detectors resonant with the fundamental cavity mode. The dotted line shows the displacement resulting from a initial sender state with $\langle q_A \rangle = 1$ and $\langle p_A \rangle = 0$, i.e., non-vanishing mean in canonical position. The other line shows an sender initial state with $\langle q_A \rangle = 0$ and $\langle p_A \rangle = 1$. The sender is located at $a = 0.45L$, and coupled to the field for $t = 0...0.4L$. The receiver is located at $b = 0.55L$ and coupled to the field for $t = 0.51L...T_2$. Sender and receiver are timelike separated if $T_2 < L$. Both detectors have $\Omega = \pi/L$ and $\lambda = 0.01$. And $N = 200$ cavity modes were used for the numerical calculations.

transmitted both via the first as well as via the second moments of Gaussian states. Most importantly, these signals were treated non-perturbatively using symplectic methods. This makes the model an interesting tool for future research into the classical and quantum information capacity of timelike and energyless signals.

For example, it is possible to analyze scenarios with multiple receivers in Alice's future lightcone. We were able to clarify the budget of energy flows in such scenarios in the previous chapter. The next question would be to ask whether spacelike separated receivers in the future lightcone can perform independent measurements of Alice's signal, or to what extent their outcomes are correlated. First results show that the probabilities are highly correlated for a group of receivers to get excited out of their groundstates in the future lightcone of Alice.

Another higher-order effect that is accessible using the non-perturbative methods of this chapter, are signatures of the real part of the Wightmann function, which encodes the

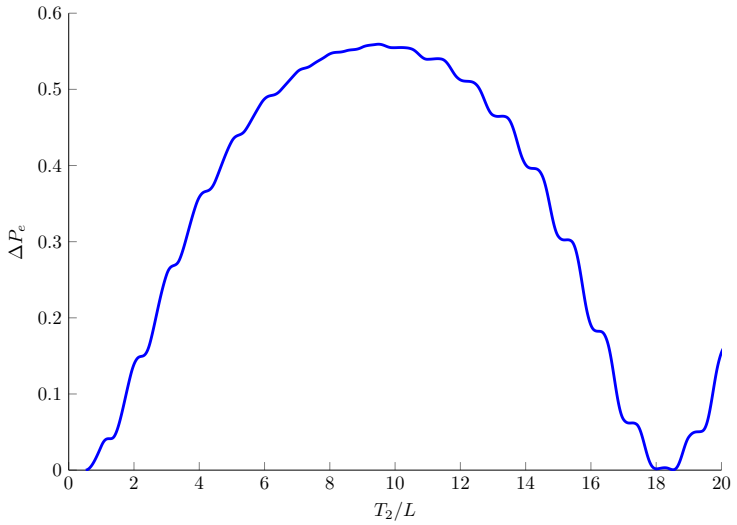

Figure 7.9: [38] Signalling via zero-mean Gaussian states between detectors resonant with the fundamental cavity mode. The plot shows $\Delta P_e = P_e^{\text{sig}} - P_e^{\text{vac}}$ the difference of excitation probability between the signalling scenario and coupling to the vacuum. (Compare Figure 7.7). The sender is initialized in a thermal state with $\Omega/T = 4 \cdot 10^{-3}$. All other parameters are identical to Figure 7.8. signalling arises already at timelike separations for $T_2 < L$.

quantum properties of the field state. In the perturbative treatment these only enter at next-to-leading order through already quite intricate integral terms. (See coefficient A_4 in (A.2).)

First results show, that they seem to occur as a modulation of timelike signals, via the second moments of the Gaussian detector states, that depends on the receiver's position in the lightcone. Signals via the mean of Gaussian states are not affected if the receiver is moved within the future lightcone of the sender. This is to be expected, since the mean of a Gaussian state evolves according to the classical equations of motion, i.e., it depends on the classical Greens function of the field which is, as we know, constant everywhere in the future lightcone.

Chapter 8

Conclusions and Outlook

The observation that information can be transmitted through massless fields without the transmission of energy contributes to the exploration of exciting frontiers in current research. Today, deep links between information theory, quantum field theory and general relativity continue to be discovered, and following rapid technological progress experiments in quantum information begin to enter relativistic regimes.

On the one hand, this thesis adds an interesting perspective to the question if the information encoded in a field is fundamentally related to its energy content, and the spacetime curvature which results from it. On the other hand, it may unveil both challenges, as well as novel prospects for the processing of quantum information using relativistic quantum fields. With respect to both aspects the operational approach, focused on the quantum channel between localized particle detectors, can be helpful. It can model the transmission of information between different regions of spacetime in theoretical considerations, as well as it can closely resemble experimental setups.

This closing chapter discusses directions for future research aimed at these goals, and reviews how they arise from the central results of the various thesis chapters. A very important objective of future research is to extend the study of this thesis to the transmission of *quantum* information. The present results consider the transmission of classical information via the quantum field. However quantum information as very distinct properties. Most crucially, it cannot be copied. As we discuss below this will impose very special limitations to the transmission of quantum information via quantum fields.

This and other future research questions also require the development of new theoretical methods for the analysis of signalling. In particular, as begun in the previous chapter, it

is necessary to go beyond the perturbative treatment of the interaction between observers and the field.

Relativistic Quantum Communication with Particle Detectors

Describing the transmission of information between localized observers strictly within quantum field theory is difficult because the construction of localized field states is highly non-trivial in relativistic quantum fields. The problem was resolved in this thesis by modelling sender and receiver as Unruh-DeWitt detectors.

Here, the interaction of a localized observer with a relativistic quantum field is described as a unitary interaction between quantum systems. Moreover, the quantum channel between two detectors provides an operational approach to the study of relativistic quantum communication via quantum fields to which the methods of quantum information theory can be directly applied.

Following up on the works of [19, 21], where this framework was first introduced, Chapter 3 completed the perturbative analysis of the structure and classical capacity of the quantum channel between two Unruh-DeWitt detectors.

The key result is that, within the perturbative regime, the optimal choice of signalling states for the sender are equal-weighted superpositions of energy eigenstates. The signalling strength and channel capacity of these optimal signals is determined by a relatively simple Fourier-type integral over the field commutator, see (3.107).

Interestingly, the optimal signalling states are different from the usual choice of energy eigenstates as initial states, when detectors are used to measure properties of the field. When measuring the field, the interaction Hamiltonian should have the strongest effect possible on the detector's state. This is achieved by energy eigenstates of the detector, which acquire a relative phase most quickly because they are superpositions of eigenstates of the monopole operator of the detector. On the contrary, when a detector is used for signalling, the impact of the detector onto the quantum field needs to be maximal. Therefore, eigenstates of the monopole operator are the optimal choice of signalling states.

The commutator of the field is given by the classical Green functions of the field. Therefore, to leading order, the characteristics of the signalling strength is independent from the quantum state of the field, and corresponds to the behaviour of the classical field. Chapter 5 evaluated the leading order signalling estimate in various settings of resting and moving detectors in Minkowski spacetime.

The leading order signalling effects make it possible to study the impact spacetime curvature has on signalling by deforming the Green functions of the field. Recent works that follow up on the results presented in this thesis study signalling in certain expanding universe cosmologies [10, 11]. Future research could study the impact of spacetime curvature onto communication in the vicinity of black holes, using methods such as [18, 87] for the representation of the classical Green functions of the field.

Beyond the impact of spacetime curvature that is encoded in the classical Green function of the field, spacetime curvature also impacts the quantum fluctuations of the field [73]. These fluctuations constitute a noise source in the quantum channel between detectors. Therefore, a comparison of noise and signalling strength in different scenarios could be used to explore the combined impact of spacetime curvature on classical and quantum properties of the field.

As shown in Chapter 3 the Holevo capacity of the channel combines both signalling strength and noise terms already at leading order. Other measures of channel capacity would require higher order terms, or non-perturbative treatments of the detector-field interactions.

Timelike Signals in Massless Fields

The appearance of timelike signals, i.e., signals propagating slower than the speed of light, in massless fields is a phenomenon that derives directly from the properties of the classical field. As such this phenomenon has long been known. Nevertheless, it may appear particularly counterintuitive in the context of quantum fields, because they break with assumptions that appear very natural within the particle picture often used to discuss quantum fields. Timelike signals, as discussed in Chapter 3, travel slower than the speed of light which massless particles are unable to do. Furthermore, they cannot be understood as the emission and absorption of on-shell field quanta, because they appear at leading order in perturbation theory.

The most surprising property of timelike signals, which this thesis demonstrates, is that they lead to a partial, or even complete, decoupling of the propagation of information from the propagation of energy in the field.

Chapter 6 showed that timelike signals, instead of transporting energy from the sender to the receiver, modulate the energy required by the receiver to couple his detector to the field. This relates to the observation of Chapter 5 that, whereas lightlike signals appear to have a dynamic characteristics to them which favours resonant detectors, timelike signals appear to behave as more of a static imprint in the future lightcone of the field which can

remain constant, as in 1+1D Minkowski space, or gradually decays, as in 2+1D Minkowski spacetime. As a consequence the leading order signalling strength of lightlike signals can grow unbounded, see (5.52), whereas for timelike signals it is bounded. This raises the question whether this behaviour persists when higher-order terms, or non-perturbative solutions are considered.

Furthermore, it is an interesting direction for further research to explore timelike signals, and their associated phenomena, in realistic fields such as the electro-magentic field. Also the prospect of proposing an implementation of these effects in experimental quantum information systems, e.g., in superconducting circuits, appears promising.

Non-perturbative Methods

Several interesting future research questions require us to go beyond the perturbative analysis of signalling between detectors. As mentioned above, non-perturbative approaches to signalling scenarios are key to the study of the quantum noise properties of the channel, as well as for the further study of timelike signals. In particular, they are instrumental to the study of quantum information transmission via relativistic quantum fields as will be discussed below.

A first non-perturbative approach was discussed in Chapter 7. Here signalling between harmonic oscillator detectors coupling to the field inside a cavity is studied using the Gaussian formalism. Gaussian quantum information has been widely developed over recent years such that there is a range of methods available. These could be applied to both numerical and analytical, non-perturbative studies of channel capacities and signalling effects between two, and multiple detectors.

Another possibility are non-perturbative solutions to the channel between two-level detectors. Very recently the channel between two zero-energy gap detectors was shown to be analytically solvable [48], and its channel capacities were calculated. This approach and its results carry over to the case of instantaneous couplings between field and detector, where the switching function consists of a Dirac δ-distribution $\eta(t) = \delta(t)$. Such models could be valuable in exploring the interplay between classical information transmission and the quantum noise of the field.

However, zero-energy gap detectors and instantaneously coupled detectors do not allow for the transmission of qubits between them. As shown in [48] the channel between two zero-gap detectors is entanglement-breaking, i.e., it has zero quantum capacity. The same can be shown to apply to instantaneously coupled detectors.

In both cases, the underlying reason is that the free detector evolution is frozen out, or, respectively, is irrelevant under the instantaneous coupling. Therefore, Bob's final state only depends on the expectation value of Alice's monopole operator, and no quantum information can be coherently transmitted through the channel. In fact, the entanglement breaking already happens at the first stage when Alice couples to the field.

It is conceivable that a sequence of, e.g., instantaneous couplings would allow for the coherent transmission of quantum information from Alice to the field and on to Bob, while still being analytical solvable. However, even if so there are further restrictions on the transmission of quantum information in relativistic scenarios arising from the fact that quantum information cannot be copied.

Quantum Information Transmission

A very basic argument can be made that shows that couplings between matter and fields that possess spatial symmetries, as they appear in nature and also in the standard Unruh-DeWitt model, can not be used for the coherent transmission of quantum information in relativistic scenarios. The reason is that a symmetric coupling leads to signals that propagate symmetrically in the quantum field.

For example, if in 1+1D a sender couples equally to the left-moving and the right-moving modes of a field, the signal will propagate equally to the left and to the right. In a relativistic scenario the duration for which sender, and later the receiver, couple to the field could be shorter than the propagation time from the sender to the receiver. This means that a mirror-receiver could exist on the left of the sender which is identical to the original receiver on the right. If the distance between the two receivers is large enough, they have no influence on each other, and accordingly the quantum channel from the sender to the mirror-receiver is identical to the quantum channel from the sender to the receiver. However, this means that the quantum channel is anti-degradable and, therefore, as no quantum capacity.

This shows that a symmetric coupling between signalling device and field leads to a delocalization of any transmitted quantum information. In order to be able to transmit quantum information coherently it is necessary to direct and focus the signal. It may very well be that Unruh-DeWitt model cannot reasonably be modified to allow for the directional signalling necessary for the transmission of quantum information, and that the development of other models such as [25] is required.

On the other hand, the famous Jaynes-Cunnings model can be derived from the Unruh-DeWitt coupling by non-relativistic approximations. In the Jaynes-Cunnings model the

transfer of qubits is possible. This raises the question as to where in the middle range between the non-relativistic Jaynes-Cunnings model and relativistic instantaneously switched detectors the transmission of quantum information becomes possible.

This question could unveil speed limitations in the processing of quantum information with quantum fields, which might be an obstacle to certain tasks like quantum state transfer. On the other hand, they may be useful for the implementation of information processing tasks such as relativistic bit commitment [44, 32, 2].

In view of the decoupling of classical information propagation from the propagation of energy, it is an interesting question to ask whether quantum information can be transmitted without the transmission of energy at all? After all, one could speculate whether the conservation of quantum information and the conservation of energy are two sides of the same coin, tied together by the unitary time evolution generated by the Hamiltonian of the system. In this context, it is interesting to note that it was shown recently that energy transport between two quantum sytems requires discord [52].

Information, Energy and Spacetime Geometry

A long term goal of future research is to put the findings of this thesis into the context of works that study the fundamental relation between the geometry of spacetime, which is formed by its energy and matter content, and the information that is encoded into it.

This refers to long-standing results such as Landauer's principle on the minimum energy cost of information processing, or Bekenstein's results on the information content of spacetime volumes and the energy cost of information transfer [4]. Moreover, it also refers to very recent results: For example, it has recently been suggested that a mechanism of energy storage at zero energy cost could contribute to a possible resolution of the black hole information paradox [31]. Interesting connections may also exist to [51], which derives Einstein's equation from quantum measurement limits in spacetime.

The approach of this thesis could add to this research the perspective of an operational framework which both models the measurement of the quantum field by a localized observer fully quantum-theoretical, as well as it considers the energy costs for the transmission and detection of signals in spacetime.

In this way studying signalling scenarios may contribute to understanding the interplay of quantum fields, as signal carriers and fundamental constituents of all matter, and the spacetime geometry traversed by the signals, which is determined by matter and energy according to the laws of general relativity.

References

[1] Gerardo Adesso, Sammy Ragy, and Antony R. Lee. Continuous variable quantum information: Gaussian states and beyond. *arXiv:1401.4679 [cond-mat, physics:math-ph, physics:physics, physics:quant-ph]*, January 2014.

[2] Emily Adlam and Adrian Kent. A Quantum Paradox of Choice: More Freedom Makes Summoning a Quantum State Harder. *arXiv:1509.04226 [quant-ph]*, September 2015.

[3] Jürgen Audretsch and Rainer Müller. Radiation from a uniformly accelerated particle detector: Energy, particles, and the quantum measurement process. *Physical Review D*, 49(12):6566–6575, June 1994.

[4] Jacob D. Bekenstein and Marcelo Schiffer. Quantum Limitations on the Storage and Transmission of Information. *arXiv:quant-ph/0311050*, November 2003. arXiv: quant-ph/0311050.

[5] Dionigi M. T. Benincasa, Leron Borsten, Michel Buck, and Fay Dowker. Quantum information processing and relativistic quantum fields. *Classical and Quantum Gravity*, 31(7):075007, 2014.

[6] Dominic W. Berry. Qubit channels that achieve capacity with two states. *Physical Review A*, 71(3), March 2005.

[7] Mary Beth Ruskai, Stanislaw Szarek, and Elisabeth Werner. An analysis of completely-positive trace-preserving maps on M2. *Linear Algebra and its Applications*, 347(1–3):159–187, May 2002.

[8] N. D. Birrell. *Quantum fields in curved space*. Cambridge monographs on mathematical physics ; [7]. Cambridge University Press, Cambridge Cambridgeshire, 1982.

[9] James D. Bjorken and Sidney David Drell. *Relativistic quantum fields*. McGraw-Hill, 1965.

[10] Ana Blasco, Luis J. Garay, Mercedes Martin-Benito, and Eduardo Martin-Martinez. Violation of the strong Huygen's principle and timelike signals from the early Universe. *Physical Review Letters*, 114(14), April 2015.

[11] Ana Blasco, Luis J. Garay, Mercedes Martín-Benito, and Eduardo Martín-Martínez. Timelike information broadcasting in cosmology. *Physical Review D*, 93(2):024055, January 2016.

[12] N. N. Bogolubov, Anatoly A. Logunov, A. I. Oksak, and I. Todorov. *General Principles of Quantum Field Theory*. Springer Science & Business Media, December 1989.

[13] Kamil Bradler, Patrick Hayden, and Prakash Panangaden. Quantum Communication in Rindler Spacetime. *Communications in Mathematical Physics*, 312(2):361–398, June 2012.

[14] Samuel L. Braunstein and Peter van Loock. Quantum information with continuous variables. *Reviews of Modern Physics*, 77(2):513–577, June 2005.

[15] Eric G. Brown, Eduardo Martín-Martínez, Nicolas C. Menicucci, and Robert B. Mann. Detectors for probing relativistic quantum physics beyond perturbation theory. *Physical Review D*, 87(8):084062, April 2013.

[16] David Edward Bruschi, Antony R. Lee, and Ivette Fuentes. Time evolution techniques for detectors in relativistic quantum information. *Journal of Physics A: Mathematical and Theoretical*, 46(16):165303, 2013.

[17] Lior M. Burko, Abraham I. Harte, and Eric Poisson. Mass loss by a scalar charge in an expanding universe. *Physical Review D*, 65(12), May 2002.

[18] Marc Casals, Sam Dolan, Adrian C. Ottewill, and Barry Wardell. Self-force and Green function in Schwarzschild spacetime via quasinormal modes and branch cut. *Physical Review D*, 88(4):044022, 2013.

[19] M. Cliche and A. Kempf. Relativistic quantum channel of communication through field quanta. *Physical Review A*, 81(1):012330, January 2010.

[20] M. Cliche and A. Kempf. Vacuum entanglement enhancement by a weak gravitational field. *Physical Review D*, 83(4):045019, February 2011.

[21] Mathieu Cliche. *Information propagation and entanglement generation between two Unruh-DeWitt detectors*. PhD thesis, University of Waterloo, Waterloo, Ontario, July 2010.

[22] S. R. Czapor and R. G. McLenaghan. Hadamard's Problem of Diffusion of Waves. *ACTA PHYSICA POLONICA SERIES B*, 1(1):55, 2007.

[23] B. S. DeWitt. Quantum gravity: the new synthesis. In Stephen Hawking and W. Israel, editors, *General relativity : an Einstein centenary survey*, page 680. Cambridge University Press, Cambridge Eng; New York, 1979.

[24] Robert Dickinson, Jeff Forshaw, and Peter Millington. Probabilities and signalling in quantum field theory. *Physical Review D*, 93(6):065054, March 2016.

[25] T. G. Downes, T. C. Ralph, and N. Walk. Quantum Communication with an Accelerated Partner. *arXiv:1203.2716 [quant-ph]*, March 2012.

[26] Phillippe H. Eberhard and Ronald R. Ross. Quantum field theory cannot provide faster-than-light communication. *Foundations of Physics Letters*, 2(2):127–149, March 1989.

[27] Enrico Fermi. Quantum Theory of Radiation. *Reviews of Modern Physics*, 4(1):87–132, January 1932.

[28] Stephen A. Fulling. *Aspects of Quantum Field Theory in Curved Spacetime*. Cambridge University Press, August 1989.

[29] G. W. Gibbons and S. W. Hawking. Cosmological event horizons, thermodynamics, and particle creation. *Physical Review D*, 15(10):2738–2751, May 1977.

[30] J. B. Hartle and S. W. Hawking. Path-integral derivation of black-hole radiance. *Physical Review D*, 13(8):2188–2203, April 1976.

[31] Stephen W. Hawking, Malcolm J. Perry, and Andrew Strominger. Soft Hair on Black Holes. *arXiv:1601.00921 [hep-th]*, January 2016.

[32] Patrick Hayden and Alex May. Summoning Information in Spacetime, or Where and When Can a Qubit Be? *arXiv:1210.0913 [gr-qc, physics:hep-th, physics:quant-ph]*, October 2012.

[33] Lee Hodgkinson and Jorma Louko. How often does the Unruh-DeWitt detector click beyond four dimensions? *Journal of Mathematical Physics*, 53(8):082301, 2012.

[34] Masahiro Hotta. Quantum measurement information as a key to energy extraction from local vacuums. *Physical Review D*, 78(4):045006, August 2008.

[35] Masahiro Hotta. Controlled Hawking process by quantum energy teleportation. *Physical Review D*, 81(4):044025, February 2010.

[36] Masahiro Hotta, Jiro Matsumoto, and Go Yusa. Quantum energy teleportation without a limit of distance. *Physical Review A*, 89(1):012311, January 2014.

[37] Alan Jeffrey and Daniel Zwillinger. *Table of Integrals, Series, and Products*. Academic Press, February 2007.

[38] Robert H. Jonsson. Information travels in massless fields in 1+1 dimensions where energy cannot. *arXiv:1512.05065 [gr-qc, physics:hep-th, physics:quant-ph]*, December 2015.

[39] Robert H. Jonsson, Eduardo Martin-Martinez, and Achim Kempf. Quantum signalling in cavity QED. *Physical Review A*, 89(2), February 2014.

[40] Robert H. Jonsson, Eduardo Martín-Martínez, and Achim Kempf. Information Transmission Without Energy Exchange. *Physical Review Letters*, 114(11):110505, March 2015.

[41] Benito A. Juárez-Aubry and Jorma Louko. Onset and decay of the 1 + 1 Hawking–Unruh effect: what the derivative-coupling detector saw. *Classical and Quantum Gravity*, 31(24):245007, 2014.

[42] W. Junker and E. Schrohe. Adiabatic Vacuum States on General Spacetime Manifolds: Definition, Construction, and Physical Properties. *Annales Henri Poincaré*, 3(6):1113–1181, December 2002.

[43] Bernard S. Kay and Robert M. Wald. Theorems on the uniqueness and thermal properties of stationary, nonsingular, quasifree states on spacetimes with a bifurcate Killing horizon. *Physics Reports*, 207(2):49–136, 1991.

[44] Adrian Kent. A no-summoning theorem in relativistic quantum theory. *Quantum Information Processing*, 12(2):1023–1032, July 2012.

[45] Hyeong-Chan Kim. Quantum field and uniformly accelerated oscillator. *Physical Review D*, 59(6):064024, February 1999.

[46] Hyeong-Chan Kim and Jae Kwan Kim. Radiation from a uniformly accelerated harmonic oscillator. *Physical Review D*, 56(6):3537–3547, September 1997.

[47] C. King and M. B. Ruskai. Minimal Entropy of States Emerging from Noisy Quantum Channels. *arXiv:quant-ph/9911079*, November 1999.

[48] Andre G. S. Landulfo. A non-perturbative approach to relativistic quantum communication channels. *arXiv:1603.06641 [gr-qc, physics:quant-ph]*, March 2016.

[49] Shih-Yuin Lin and B. L. Hu. Accelerated Detector - Quantum Field Correlations: From Vacuum Fluctuations to Radiation Flux. *Physical Review D*, 73(12), June 2006.

[50] Shih-Yuin Lin and B. L. Hu. Backreaction and Unruh effect: New insights from exact solutions of uniformly accelerated detectors. *Physical Review D*, 76(6), September 2007.

[51] Seth Lloyd. The quantum geometric limit. *arXiv:1206.6559 [gr-qc, physics:quant-ph]*, June 2012. arXiv: 1206.6559.

[52] Seth Lloyd, Vazrik Chiloyan, Yongjie Hu, Samuel Huberman, Zi-Wen Liu, and Gang Chen. No energy transport without discord. *arXiv:1510.05035 [quant-ph]*, October 2015.

[53] Jorma Louko and Alejandro Satz. How often does the Unruh-DeWitt detector click? Regularisation by a spatial profile. *Classical and Quantum Gravity*, 23(22):6321–6343, November 2006.

[54] Jorma Louko and Alejandro Satz. Transition rate of the Unruh-DeWitt detector in curved spacetime. *Classical and Quantum Gravity*, 25(5):055012, March 2008.

[55] R. B. Mann and T. C. Ralph. Relativistic quantum information. *Classical and Quantum Gravity*, 29(22):220301, 2012.

[56] Eduardo Martín-Martínez. Causality issues of particle detector models in QFT and quantum optics. *Physical Review D*, 92(10):104019, November 2015.

[57] Eduardo Martín-Martínez, David Aasen, and Achim Kempf. Processing Quantum Information with Relativistic Motion of Atoms. *Physical Review Letters*, 110(16):160501, April 2013.

[58] Eduardo Martin-Martinez, Eric G. Brown, William Donnelly, and Achim Kempf. Sustainable entanglement production from a quantum field. *arXiv:1309.1090 [gr-qc, physics:quant-ph]*, September 2013.

[59] Eduardo Martín-Martínez and Jorma Louko. Particle detectors and the zero mode of a quantum field. *Physical Review D*, 90(2):024015, July 2014.

[60] Eduardo Martín-Martínez and Nicolas C. Menicucci. Entanglement in curved spacetimes and cosmology. *Classical and Quantum Gravity*, 31(21):214001, November 2014.

[61] S. Massar and R. Parentani. From vacuum fluctuations to radiation. I. Accelerated detectors. *Physical Review D*, 54(12):7426–7443, December 1996.

[62] R. G. McLenaghan. An explicit determination of the empty space-times on which the wave equation satisfies Huygens' principle. *Mathematical Proceedings of the Cambridge Philosophical Society*, 65(01):139–155, January 1969.

[63] R. G. McLenaghan. On the validity of Huygens' principle for second order partial differential equations with four independent variables. Part I: Derivation of necessary conditions. In *Annales de l'IHP Physique théorique*, volume 20, pages 153–188, 1974.

[64] Michael A. Nielsen and Isaac L. Chuang. *Quantum Computation and Quantum Information: 10th Anniversary Edition*. Cambridge University Press, December 2010.

[65] Stefano Olivares. Quantum optics in the phase space - A tutorial on Gaussian states. *The European Physical Journal Special Topics*, 203(1):3–24, April 2012.

[66] Hirosi Ooguri. Spectrum of Hawking radiation and the Huygens principle. *Physical Review D*, 33(12):3573–3580, June 1986.

[67] Aron Pasieka, David W. Kribs, Raymond Laflamme, and Rajesh Pereira. On the Geometric Interpretation of Single Qubit Quantum Operations on the Bloch Sphere. *Acta Applicandae Mathematicae*, 108(3):697–707, January 2009.

[68] Eric Poisson, Adam Pound, and Ian Vega. The Motion of Point Particles in Curved Spacetime. *Living Reviews in Relativity*, 14, 2011.

[69] Benni Reznik, Alex Retzker, and Jonathan Silman. Violating Bell's inequalities in vacuum. *Physical Review A*, 71(4):042104, April 2005.

[70] Carlos Sabín, Marco del Rey, Juan José García-Ripoll, and Juan León. Fermi Problem with Artificial Atoms in Circuit QED. *Physical Review Letters*, 107(15):150402, October 2011.

[71] Carlos Sabín, Borja Peropadre, Marco del Rey, and Eduardo Martín-Martínez. Extracting Past-Future Vacuum Correlations Using Circuit QED. *Physical Review Letters*, 109(3):033602, July 2012.

[72] Grant Salton, Robert B. Mann, and Nicolas C. Menicucci. Acceleration-assisted entanglement harvesting and rangefinding. *New Journal of Physics*, 17(3):035001, 2015.

[73] Mehdi Saravani, Siavash Aslanbeigi, and Achim Kempf. Spacetime Curvature in terms of Scalar Field Propagators. *Physical Review D*, 93(4), February 2016.

[74] Alejandro Satz. Then again, how often does the Unruh-DeWitt detector click if we switch it carefully? *Classical and Quantum Gravity*, 24(7):1719–1731, April 2007.

[75] Benjamin Schumacher and Michael D. Westmoreland. Optimal signal ensembles. *Physical Review A*, 63(2):022308, January 2001.

[76] Claude E. Shannon and Warren Weaver. *The Mathematical Theory of Communication*. University of Illinois Press, April 2015.

[77] R. Silverman. On binary channels and their cascades. *IRE Transactions on Information Theory*, 1(3):19–27, December 1955.

[78] L. Sriramkumar and T. Padmanabhan. Finite-time response of inertial and uniformly accelerated Unruh - DeWitt detectors. *Classical and Quantum Gravity*, 13(8):2061, August 1996.

[79] Greg Ver Steeg and Nicolas C. Menicucci. Entangling power of an expanding universe. *Physical Review D*, 79(4):044027, February 2009.

[80] Shin Takagi. Vacuum Noise and Stress Induced by Uniform Acceleration Hawking-Unruh Effect in Rindler Manifold of Arbitrary Dimension. *Progress of Theoretical Physics Supplement*, 88:1–142, January 1986.

[81] W. G. Unruh. Notes on black-hole evaporation. *Physical Review D*, 14(4):870–892, August 1976.

[82] W. G. Unruh and W. H. Zurek. Reduction of a wave packet in quantum Brownian motion. *Physical Review D*, 40(4):1071–1094, August 1989.

[83] Guillaume Verdon-Akzam, Eduardo Martín-Martínez, and Achim Kempf. Asymptotically limitless quantum energy teleportation via qudit probes. *Physical Review A*, 93(2):022308, February 2016.

[84] Robert M. Wald. *Quantum field theory in curved spacetime and black hole thermodynamics*. Chicago lectures in physics. University of Chicago Press, Chicago, 1994.

[85] Christian Weedbrook, Stefano Pirandola, Raúl García-Patrón, Nicolas J. Cerf, Timothy C. Ralph, Jeffrey H. Shapiro, and Seth Lloyd. Gaussian quantum information. *Reviews of Modern Physics*, 84(2):621–669, May 2012.

[86] Mark M. Wilde. *Quantum Information Theory*. Cambridge University Press, April 2013.

[87] Huan Yang, Fan Zhang, Aaron Zimmerman, and Yanbei Chen. Scalar Green function of the Kerr spacetime. *Physical Review D*, 89(6):064014, March 2014.

[88] Erez Zohar and Benni Reznik. The Fermi Problem in Discrete Systems. *New Journal of Physics*, 13(7):075016, July 2011.

APPENDICES

Appendix A

Leading order contributions to channel coefficients

Note: This appendix is reproduced with minor adaptions from [39].

A.1 Integral form of the channel coefficients

In this section we present the integral form of the coefficients A, B and P defined in equations (3.34),(3.35) and (3.36). The lowest order integrals for the coefficients C and D are given in (3.47) and (3.48).

For the coefficient A we have

$$A = \lambda_{\mathcal{A}}^2 \lambda_{\mathcal{B}}^2 A_4 + \mathcal{O}(\lambda^6) \tag{A.1}$$

and

$$
\begin{aligned}
A_4 = &\int_0^T \mathrm{d}t_1 \int_0^{t_1} \mathrm{d}t_2 \int_0^T \mathrm{d}s_1 \int_0^{s_1} \mathrm{d}s_2 \\
&\times \big[\chi_{\mathcal{A}}(t_1)\chi_{\mathcal{A}}(s_2)\chi_{\mathcal{B}}(t_2)\chi_{\mathcal{B}}(s_1) \\
&\quad \Big(e^{\mathrm{i}\Omega_{\mathcal{B}}(\tau_{\mathcal{B}}(t_2)-\tau_{\mathcal{B}}(s_1))-\mathrm{i}\Omega_{\mathcal{A}}(\tau_{\mathcal{A}}(t_1)-\tau_{\mathcal{A}}(s_2))}\,\langle\phi(x_{\mathcal{A}}(s_2))\phi(x_{\mathcal{B}}(s_1))\phi(x_{\mathcal{A}}(t_1))\phi(x_{\mathcal{B}}(t_2))\rangle + \text{H.c.}\Big) \\
&\quad + \chi_{\mathcal{A}}(t_1)\chi_{\mathcal{A}}(s_1)\chi_{\mathcal{B}}(t_2)\chi_{\mathcal{B}}(s_2) \\
&\qquad \Big(e^{\mathrm{i}\Omega_{\mathcal{B}}(\tau_{\mathcal{B}}(t_2)-\tau-\mathcal{B}(s_2))-\mathrm{i}\Omega_{\mathcal{A}}(\tau_{\mathcal{A}}(t_1)-\tau_{\mathcal{A}}(s_1))}\,\langle\phi(x_{\mathcal{B}}(s_2))\phi(x_{\mathcal{A}}(s_1))\phi(x_{\mathcal{A}}(t_1))\phi(x_{\mathcal{B}}(t_2))\rangle\Big) \\
&\quad + \chi_{\mathcal{A}}(t_2)\chi_{\mathcal{A}}(s_2)\chi_{\mathcal{B}}(t_1)\chi_{\mathcal{B}}(s_1) \\
&\qquad \Big(e^{\mathrm{i}\Omega_{\mathcal{B}}(\tau_{\mathcal{B}}(t_1)-\tau_{\mathcal{B}}(s_1))-\mathrm{i}\Omega_{\mathcal{A}}(\tau_{\mathcal{A}}(t_2)-\tau_{\mathcal{A}}(s_2))}\,\langle\phi(x_{\mathcal{A}}(s_2))\phi(x_{\mathcal{B}}(s_1))\phi(x_{\mathcal{B}}(t_1))\phi(x_{\mathcal{A}}(t_2))\rangle\Big)\Big] \\
&- \int_0^T \mathrm{d}s \int_0^T \mathrm{d}t_1 \int_0^{t_1} \mathrm{d}t_2 \int_0^{t_2} \mathrm{d}t_3 \\
&\quad \times \big[\chi_{\mathcal{A}}(t_1)\chi_{\mathcal{A}}(t_2)\chi_{\mathcal{B}}(t_3)\chi_{\mathcal{B}}(s) \\
&\qquad \Big(e^{\mathrm{i}\Omega_{\mathcal{B}}(\tau_{\mathcal{B}}(t_3)-\tau_{\mathcal{B}}(s))+\mathrm{i}\Omega_{\mathcal{A}}(\tau_{\mathcal{A}}(t_1)-\tau_{\mathcal{A}}(t_2))}\,\langle\phi(x_{\mathcal{B}}(s))\phi(x_{\mathcal{A}}(t_1))\phi(x_{\mathcal{A}}(t_2))\phi(x_{\mathcal{B}}(t_3))\rangle + \text{H.c.}\Big) \\
&\qquad + \chi_{\mathcal{A}}(t_1)\chi_{\mathcal{A}}(t_3)\chi_{\mathcal{B}}(t_2)\chi_{\mathcal{B}}(s) \\
&\qquad \Big(e^{\mathrm{i}\Omega_{\mathcal{B}}(\tau_{\mathcal{B}}(t_2)-\tau_{\mathcal{B}}(s))+\mathrm{i}\Omega_{\mathcal{A}}(\tau_{\mathcal{A}}(t_1)-\tau_{\mathcal{A}}(t_3))}\,\langle\phi(x_{\mathcal{B}}(s))\phi(x_{\mathcal{A}}(t_1))\phi(x_{\mathcal{B}}(t_2))\phi(x_{\mathcal{A}}(t_3))\rangle + \text{H.c.}\Big) \\
&\qquad + \chi_{\mathcal{A}}(t_2)\chi_{\mathcal{A}}(t_3)\chi_{\mathcal{B}}(t_1)\chi_{\mathcal{B}}(s) \\
&\qquad \Big(e^{\mathrm{i}\Omega_{\mathcal{B}}(\tau_{\mathcal{B}}(t_1)-\tau_{\mathcal{B}}(s))+\mathrm{i}\Omega_{\mathcal{A}}(\tau_{\mathcal{A}}(t_2)-\tau_{\mathcal{A}}(t_3))}\,\langle\phi(x_{\mathcal{B}}(s))\phi(x_{\mathcal{B}}(t_1))\phi(x_{\mathcal{A}}(t_2))\phi(x_{\mathcal{A}}(t_3))\rangle + \text{H.c.}\Big)\Big]
\end{aligned}
\tag{A.2}
$$

The coefficient B is obtained by simply changing the sign of $\Omega_{\mathcal{A}}$ in the above formula.

$$
B = \lambda_{\mathcal{A}}^2\lambda_{\mathcal{B}}^2 B_4 + \mathcal{O}(\lambda^6) = A(-\Omega_{\mathcal{A}}, \Omega_{\mathcal{B}}) \tag{A.3}
$$

The single detector excitation probability only involves the receiver's coupling constant $\lambda_{\mathcal{B}}$. Its expansion up to order $\mathcal{O}(\lambda^4)$ is

$$
P = \lambda_{\mathcal{B}}^2\, P_2 + \lambda_{\mathcal{B}}^4\, P_4 + \mathcal{O}(\lambda_{\mathcal{B}}^6) \tag{A.4}
$$

where

$$
P_2 = \int_0^T \mathrm{d}t_1 \int_0^T \mathrm{d}t_2\; \chi_{\mathcal{B}}(t_1)\chi_{\mathcal{B}}(t_2)\, e^{\,\mathrm{i}\,\Omega_{\mathcal{B}}(\tau_{\mathcal{B}}(t_1)-\tau_{\mathcal{B}}(t_2))}\,\langle\phi(x_{\mathcal{B}}(t_2))\phi(x_{\mathcal{B}}(t_1))\rangle \tag{A.5}
$$

and

$$P_4 = -\int_0^T \mathrm{d}s \int_0^T \mathrm{d}t_1 \int_0^{t_1} \mathrm{d}t_2 \int_0^{t_2} \mathrm{d}t_3 \, [\chi_{\mathcal{B}}(t_1)\chi_{\mathcal{B}}(t_2)\chi_{\mathcal{B}}(t_3)\chi_{\mathcal{B}}(s) \\ \times \left(e^{\mathrm{i}\Omega_{\mathcal{B}}(\tau_{\mathcal{B}}(t_1)-\tau_{\mathcal{B}}(t_2)+\tau_{\mathcal{B}}(t_3)-\tau_{\mathcal{B}}(s))} \langle \phi(x_{\mathcal{B}}(s))\phi(x_{\mathcal{B}}(t_1))\phi(x_{\mathcal{B}}(t_2))\phi(x_{\mathcal{B}}(t_3))\rangle + \text{H.c.} \right) \Big] + \mathcal{O}(\lambda_{\mathcal{B}}^6). \tag{A.6}$$

Notice that in comparison to [19] the terms for A and B have a different integral structure, because we derived them using the Dyson expansion as in (3.30). In this form not all the integral boundaries are dependent on each other, which should be an advantage for numerical evaluations. Also, we can obtain two different expressions for the contributions to P, A and B from (3.30), one of which comes as the coefficient of $|e_{\mathcal{B}}\rangle\langle e_{\mathcal{B}}|$ whereas the other the comes with $|g_{\mathcal{B}}\rangle\langle g_{\mathcal{B}}|$. These two forms have different integral structures but are, of course, equivalent.

A.2 Integral form of the leading order channel coefficients

In this section we give a detailed calculation of the $\mathcal{O}(\lambda^2)$ contributions to (3.41). These are the leading order contributions to Bob's final density matrix in the most general case where Alice and Bob are allowed to start out in arbitrary initial states while the field still starts out in the vacuum state.

The interaction Hamiltonian in the interaction picture for two Unruh-DeWitt detectors coupled to the Klein-Gordon field is the sum of two single detector interaction Hamiltonians $H_{\text{int},\mathcal{A}}$ and $H_{\text{int},\mathcal{B}}$:

$$H_I(t) = H_{\text{int},\mathcal{A}} + H_{\text{int},\mathcal{B}} = \sum_{d=\mathcal{A},\mathcal{B}} \lambda_{\mathcal{D}} \, \chi_{\mathcal{D}}(t) \, m_{\mathcal{D}}(t) \, \phi(x_{\mathcal{D}}(t)) = \sum_{\mathcal{D}=\mathcal{A},\mathcal{B}} M_{\mathcal{D}}(t) \, \phi(x_{\mathcal{D}}(t)). \tag{A.7}$$

Here we introduced the shorthand notation $M_{\mathcal{D}}(t) = \lambda_{\mathcal{D}}\chi_{\mathcal{D}}(t)m_{\mathcal{D}}(t)$. As in section 3.2.2 we denote the initial state of the system by

$$\rho_0 = \underbrace{\rho_{\mathcal{A},0} \otimes \rho_{\mathcal{B},0}}_{\rho_{\mathcal{A}\mathcal{B}}} \otimes |0\rangle\langle 0| = \begin{pmatrix} \theta & \gamma \\ \gamma^* & \beta \end{pmatrix} \otimes \begin{pmatrix} \varphi & \delta \\ \delta^* & \kappa \end{pmatrix} \otimes |0\rangle\langle 0| \, . \tag{A.8}$$

From equation (3.24) the second order perturbative corrections $\rho_T^{(2)}$ to the total system's final state ρ_T are given by

$$\begin{aligned}
\rho_T^{(2)} &= U^{(2)}\rho_0 + \rho_0 U^{(2)\,\dagger} + U^{(1)}\rho_0 U^{(1)\,\dagger} \\
&= -\left(\int_0^T \mathrm{d}t_1 \int_0^{t_1} \mathrm{d}t_2 \; H_I(t_1)\, H_I(t_2)\right)\rho_0 - \rho_0 \left(\int_0^T \mathrm{d}t_1 \int_0^{t_1} \mathrm{d}t_2 \; H_I(t_2)\, H_I(t_1)\right) \\
&\quad + \left(\int_0^T \mathrm{d}t_1 \, H_I(t_1)\right)\rho_0 \left(\int_0^T \mathrm{d}t_2 \, H_I(t_2)\right) \\
&= -\int_0^T \mathrm{d}t_1 \int_0^{t_1} \mathrm{d}t_2 \; \Big[\left(H_{\mathrm{int}}A(t_1)H_{\mathrm{int}}A(t_2) + H_{\mathrm{int}}A(t_1)H_{\mathrm{int}}B(t_2) + H_{\mathrm{int}}B(t_1)H_{\mathrm{int}}A(t_2) + H_{\mathrm{int}}B(t_1)H_{\mathrm{int}}B(t_2)\right)\rho_0 \\
&\qquad\qquad + \rho_0 \left(H_{\mathrm{int}}A(t_2)H_{\mathrm{int}}A(t_1) + H_{\mathrm{int}}A(t_2)H_{\mathrm{int}}B(t_1) + H_{\mathrm{int}}B(t_2)H_{\mathrm{int}}A(t_1) + H_{\mathrm{int}}B(t_2)H_{\mathrm{int}}B(t_1)\right)\Big] \\
&\quad + \int_0^T \mathrm{d}t_1 \int_0^T \mathrm{d}t_2 \; \left[H_{\mathrm{int}}A(t_1)\rho_0 H_{\mathrm{int}}A(t_2) + H_{\mathrm{int}}A(t_1)\rho_0 H_{\mathrm{int}}B(t_2) + H_{\mathrm{int}}B(t_1)\rho_0 H_{\mathrm{int}}A(t_2) + H_{\mathrm{int}}B(t_1)\rho_0 H_{\mathrm{int}}B(t_2)\right] .
\end{aligned} \tag{A.9}$$

Bob's final density matrix $\rho_{\mathcal{B},T}$ is obtained by taking the partial trace over the field's and Alice's subspace (see (3.20)). Taking the partial trace of (A.9) over the field first leaves us with a two-point function in each term:

$$\begin{aligned}
\mathrm{Tr}_{\mathcal{F}}\,\rho^{(2)} = -\int_0^T \mathrm{d}t_1 \int_0^{t_1} \mathrm{d}t_2 \; \Big[&\left(M_{\mathcal{A}}(t_1)M_{\mathcal{A}}(t_2)\,\langle\phi(x_{\mathcal{A}}(t_1))\phi(x_{\mathcal{A}}(t_2))\rangle + M_{\mathcal{A}}(t_1)M_{\mathcal{B}}(t_2)\,\langle\phi(x_{\mathcal{A}}(t_1))\phi(x_{\mathcal{B}}(t_2))\rangle\right. \\
&\left. + M_{\mathcal{B}}(t_1)M_{\mathcal{A}}(t_2)\,\langle\phi(x_{\mathcal{B}}(t_1))\phi(x_{\mathcal{A}}(t_2))\rangle + M_{\mathcal{B}}(t_1)M_{\mathcal{B}}(t_2)\,\langle\phi(x_{\mathcal{B}}(t_1))\phi(x_{\mathcal{B}}(t_2))\rangle\right)\rho_{\mathcal{AB}} \\
&+ \rho_{\mathcal{AB}}\left(M_{\mathcal{A}}(t_2)M_{\mathcal{A}}(t_1)\,\langle\phi(x_{\mathcal{A}}(t_2))\phi(x_{\mathcal{A}}(t_1))\rangle + M_{\mathcal{A}}(t_2)M_{\mathcal{B}}(t_1)\,\langle\phi(x_{\mathcal{A}}(t_2))\phi(x_{\mathcal{B}}(t_1))\rangle\right. \\
&\left. + M_{\mathcal{B}}(t_2)M_{\mathcal{A}}(t_1)\,\langle\phi(x_{\mathcal{B}}(t_2))\phi(x_{\mathcal{A}}(t_1))\rangle + M_{\mathcal{B}}(t_2)M_{\mathcal{B}}(t_1)\,\langle\phi(x_{\mathcal{B}}(t_2))\phi(x_{\mathcal{B}}(t_1))\rangle\right)\Big] \\
&+ \int_0^T \mathrm{d}t_1 \int_0^T \mathrm{d}t_2 \; \left[M_{\mathcal{A}}(t_1)\rho_{\mathcal{AB}}M_{\mathcal{B}}(t_2)\,\langle\phi(x_{\mathcal{A}}(t_2))\phi(x_{\mathcal{A}}(t_1))\rangle + M_{\mathcal{A}}(t_1)\rho_{\mathcal{AB}}M_{\mathcal{B}}(t_2)\,\langle\phi(x_{\mathcal{B}}(t_2))\phi(x_{\mathcal{A}}(t_1))\rangle\right. \\
&\left. + M_{\mathcal{B}}(t_1)\rho_{\mathcal{AB}}M_{\mathcal{A}}(t_2)\,\langle\phi(x_{\mathcal{A}}(t_2))\phi(x_{\mathcal{B}}(t_1))\rangle + M_{\mathcal{B}}(t_1)\rho_{\mathcal{AB}}M_{\mathcal{B}}(t_2)\,\langle\phi(x_{\mathcal{B}}(t_2))\phi(x_{\mathcal{B}}(t_1))\rangle\right] .
\end{aligned} \tag{A.10}$$

Next we take the partial trace over Alice's detector. At this point the terms that describe interactions only between Alice and the field, but leave Bob's detector unaffected, drop out. This is because taken together the second order contributions to the system consisting only of Alice's detector and the field have vanishing trace, as we discussed in Section 3.2.1. For the terms that contain one factor of $M_{\mathcal{A}}(t)$ the partial trace gives a scalar factor which reads

$$\Gamma_{\mathcal{A}}(t) := \mathrm{Tr}\, M_{\mathcal{A}}(t)\rho_{\mathcal{A}} = \mathrm{Tr}\,\rho_{\mathcal{A}}M_{\mathcal{A}}(t) = \lambda_{\mathcal{A}}\chi_{\mathcal{A}}(t)\left(\gamma e^{-i\Omega_{\mathcal{A}}\tau_{\mathcal{A}}(t)} + \gamma^* e^{i\Omega_{\mathcal{A}}\tau_{\mathcal{A}}(t)}\right) . \tag{A.11}$$

With this definition we obtain

$$\begin{aligned}
\rho^{(2)}_{\mathcal{B},T} &= \mathrm{Tr}_{\mathcal{A}}\,\mathrm{Tr}_{\mathcal{F}}\,\rho^{(2)} \\
&= -\int_0^T \mathrm{d}t_1 \int_0^{t_1} \mathrm{d}t_2 \;\Big[\Gamma_{\mathcal{A}}(t_1)\,\langle\phi(x_{\mathcal{A}}(t_1))\phi(x_{\mathcal{B}}(t_2))\rangle\, M_{\mathcal{B}}(t_2)\rho_{\mathcal{B},0} + \Gamma_{\mathcal{A}}(t_2)\,\langle\phi(x_{\mathcal{B}}(t_1))\phi(x_{\mathcal{A}}(t_2))\rangle\, M_{\mathcal{B}}(t_1)\rho_{\mathcal{B},0} \\
&\qquad + \Gamma_{\mathcal{A}}(t_2)\,\langle\phi(x_{\mathcal{A}}(t_2))\phi(x_{\mathcal{B}}(t_1))\rangle\, \rho_{\mathcal{B},0}M_{\mathcal{B}}(t_1) + \Gamma_{\mathcal{A}}(t_1)\,\langle\phi(x_{\mathcal{B}}(t_2))\phi(x_{\mathcal{A}}(t_1))\rangle\, \rho_{\mathcal{B},0}M_{\mathcal{B}}(t_2) \\
&\qquad + \langle\phi(x_{\mathcal{B}}(t_1))\phi(x_{\mathcal{B}}(t_2))\rangle\, M_{\mathcal{B}}(t_1)M_{\mathcal{B}}(t_2)\rho_{\mathcal{B},0} + \langle\phi(x_{\mathcal{B}}(t_2))\phi(x_{\mathcal{B}}(t_1))\rangle\, \rho_{\mathcal{B},0}M_{\mathcal{B}}(t_2)M_{\mathcal{B}}(t_1)\Big] \\
&\quad + \int_0^T \mathrm{d}t_1 \int_0^{T} \mathrm{d}t_2 \;\Big[\Gamma_{\mathcal{A}}(t_1)\,\langle\phi(x_{\mathcal{B}}(t_2))\phi(x_{\mathcal{A}}(t_1))\rangle\, \rho_{\mathcal{B},0}M_{\mathcal{B}}(t_2) + \Gamma_{\mathcal{A}}(t_2)\,\langle\phi(x_{\mathcal{A}}(t_2))\phi(x_{\mathcal{B}}(t_1))\rangle\, M_{\mathcal{B}}(t_1)\rho_{\mathcal{B},0} \\
&\qquad + \langle\phi(x_{\mathcal{B}}(t_2))\phi(x_{\mathcal{B}}(t_1))\rangle\, M_{\mathcal{B}}(t_1)\rho_{\mathcal{B},0}M_{\mathcal{B}}(t_2)\Big]\,.
\end{aligned} \tag{A.12}$$

Inserting the definitions of $\Gamma_{\mathcal{A}}$ and $M_{\mathcal{B}}$ and switching to matrix notation for Bob's density matrix gives

$$\begin{aligned}
\rho^{(2)}_{\mathcal{B},T} = -\int_0^T \mathrm{d}t_1 \int_0^{t_1} \mathrm{d}t_2 \;\Big[&\lambda_{\mathcal{A}}\lambda_{\mathcal{B}}\Big(\chi_{\mathcal{A}}(t_1)\chi_{\mathcal{B}}(t_2)\left(\gamma e^{-i\Omega_{\mathcal{A}}t_1} + \gamma^* e^{i\Omega_{\mathcal{A}}t_1}\right)\langle\phi(x_{\mathcal{A}}(t_1))\phi(x_{\mathcal{B}}(t_2))\rangle \begin{pmatrix} \delta^* e^{i\Omega_{\mathcal{B}}t_2} & \kappa e^{i\Omega_{\mathcal{B}}t_2} \\ \varphi e^{-i\Omega_{\mathcal{B}}t_2} & \delta e^{-i\Omega_{\mathcal{B}}t_2}\end{pmatrix} \\
&\quad +\chi_{\mathcal{A}}(t_2)\chi_{\mathcal{B}}(t_1)\left(\gamma e^{-i\Omega_{\mathcal{A}}t_2} + \gamma^* e^{i\Omega_{\mathcal{A}}t_2}\right)\langle\phi(x_{\mathcal{B}}(t_1))\phi(x_{\mathcal{A}}(t_2))\rangle \begin{pmatrix} \delta^* e^{i\Omega_{\mathcal{B}}t_1} & \kappa e^{i\Omega_{\mathcal{B}}t_1} \\ \varphi e^{-i\Omega_{\mathcal{B}}t_1} & \delta e^{-i\Omega_{\mathcal{B}}t_1}\end{pmatrix} \\
&\quad +\chi_{\mathcal{A}}(t_2)\chi_{\mathcal{B}}(t_1)\left(\gamma e^{-i\Omega_{\mathcal{A}}t_2} + \gamma^* e^{i\Omega_{\mathcal{A}}t_2}\right)\langle\phi(x_{\mathcal{A}}(t_2))\phi(x_{\mathcal{B}}(t_1))\rangle \begin{pmatrix} \delta e^{-i\Omega_{\mathcal{B}}t_1} & \varphi e^{i\Omega_{\mathcal{B}}t_1} \\ \kappa e^{-i\Omega_{\mathcal{B}}t_1} & \delta^* e^{i\Omega_{\mathcal{B}}t_1}\end{pmatrix} \\
&\quad +\chi_{\mathcal{A}}(t_1)\chi_{\mathcal{B}}(t_2)\left(\gamma e^{-i\Omega_{\mathcal{A}}t_1} + \gamma^* e^{i\Omega_{\mathcal{A}}t_1}\right)\langle\phi(x_{\mathcal{B}}(t_2))\phi(x_{\mathcal{A}}(t_1))\rangle \begin{pmatrix} \delta e^{-i\Omega_{\mathcal{B}}t_2} & \varphi e^{i\Omega_{\mathcal{B}}t_2} \\ \kappa e^{-i\Omega_{\mathcal{B}}t_2} & \delta^* e^{i\Omega_{\mathcal{B}}t_2}\end{pmatrix}\Big) \\
&\quad +\lambda_{\mathcal{B}}^2\,\chi_{\mathcal{B}}(t_1)\chi_{\mathcal{B}}(t_2)\Big(\langle\phi(x_{\mathcal{B}}(t_1))\phi(x_{\mathcal{B}}(t_2))\rangle \begin{pmatrix} \varphi e^{i\Omega_{\mathcal{B}}(t_1-t_2)} & \delta e^{i\Omega_{\mathcal{B}}(t_1-t_2)} \\ \delta^* e^{-i\Omega_{\mathcal{B}}(t_1-t_2)} & \kappa e^{-i\Omega_{\mathcal{B}}(t_1-t_2)}\end{pmatrix} \\
&\qquad + \langle\phi(x_{\mathcal{B}}(t_2))\phi(x_{\mathcal{B}}(t_1))\rangle \begin{pmatrix} \varphi e^{-i\Omega_{\mathcal{B}}(t_1-t_2)} & \delta e^{i\Omega_{\mathcal{B}}(t_1-t_2)} \\ \delta^* e^{-i\Omega_{\mathcal{B}}(t_1-t_2)} & \kappa e^{i\Omega_{\mathcal{B}}(t_1-t_2)}\end{pmatrix}\Big)\Big] \\
+\int_0^T \mathrm{d}t_1 \int_0^{T} \mathrm{d}t_2 \;\Big[&\lambda_{\mathcal{A}}\lambda_{\mathcal{B}}\Big(\chi_{\mathcal{A}}(t_1)\chi_{\mathcal{B}}(t_2)\left(\gamma e^{-i\Omega_{\mathcal{A}}t_1} + \gamma^* e^{i\Omega_{\mathcal{A}}t_1}\right)\langle\phi(x_{\mathcal{B}}(t_2))\phi(x_{\mathcal{A}}(t_1))\rangle \begin{pmatrix} \delta e^{-i\Omega_{\mathcal{B}}t_2} & \varphi e^{i\Omega_{\mathcal{B}}t_2} \\ \kappa e^{-i\Omega_{\mathcal{B}}t_2} & \delta^* e^{i\Omega_{\mathcal{B}}t_2}\end{pmatrix} \\
&\quad +\chi_{\mathcal{A}}(t_2)\chi_{\mathcal{B}}(t_1)\left(\gamma e^{-i\Omega_{\mathcal{A}}t_2} + \gamma^* e^{i\Omega_{\mathcal{A}}t_2}\right)\langle\phi(x_{\mathcal{A}}(t_2))\phi(x_{\mathcal{B}}(t_1))\rangle \begin{pmatrix} \delta^* e^{i\Omega_{\mathcal{B}}t_1} & \kappa e^{i\Omega_{\mathcal{B}}t_1} \\ \varphi e^{-i\Omega_{\mathcal{B}}t_1} & \delta e^{-i\Omega_{\mathcal{B}}t_1}\end{pmatrix}\Big) \\
&\quad +\lambda_{\mathcal{B}}^2\,\chi_{\mathcal{B}}(t_1)\chi_{\mathcal{B}}(t_2)\,\langle\phi(x_{\mathcal{B}}(t_2))\phi(x_{\mathcal{B}}(t_1))\rangle \begin{pmatrix} \kappa e^{i\Omega_{\mathcal{B}}(t_1-t_2)} & \delta^* e^{i\Omega_{\mathcal{B}}(t_1+t_2)} \\ \delta e^{-i\Omega_{\mathcal{B}}(t_1+t_2)} & \varphi e^{-i\Omega_{\mathcal{B}}(t_1-t_2)}\end{pmatrix}\Big]\,,
\end{aligned} \tag{A.13}$$

where, to allow for a more compact notation, we wrote $\mathrm{e}^{\mathrm{i}\Omega t}$ instead of $\mathrm{e}^{\mathrm{i}\Omega\tau(t)}$ in all exponentials.

From this expression we can read off the second order contributions to the channel coefficients by comparison to (3.41). For the noise terms P, Q, R, S from (3.44) the lowest

order contributions are found to be:

$$P_2 = \int_0^T \mathrm{d}t_1 \int_0^T \mathrm{d}t_2 \; \chi_{\mathcal{B}}(t_1)\chi_{\mathcal{B}}(t_2) e^{i\Omega_{\mathcal{B}}(\tau_{\mathcal{B}}(t_1)-\tau_{\mathcal{B}}(t_2))} \langle \phi(x_{\mathcal{B}}(t_2))\phi(x_{\mathcal{B}}(t_1))\rangle \tag{A.14}$$

$$Q_2 = -\int_0^T \mathrm{d}t_1 \int_0^T \mathrm{d}t_2 \; \chi_{\mathcal{B}}(t_1)\chi_{\mathcal{B}}(t_2) e^{-i\Omega_{\mathcal{B}}(\tau_{\mathcal{B}}(t_1)-\tau_{\mathcal{B}}(t_2))} \langle \phi(x_{\mathcal{B}}(t_2))\phi(x_{\mathcal{B}}(t_1))\rangle \tag{A.15}$$

$$\begin{aligned} R_2 = -\int_0^T \mathrm{d}t_1 \int_0^{t_1} \mathrm{d}t_2 \; & \chi_{\mathcal{B}}(t_1)\chi_{\mathcal{B}}(t_2) e^{i\Omega_{\mathcal{B}}(\tau_{\mathcal{B}}(t_1)-\tau_{\mathcal{B}}(t_2))} \\ & \times \left(\langle \phi(x_{\mathcal{B}}(t_1))\phi(x_{\mathcal{B}}(t_2))\rangle + \langle \phi(x_{\mathcal{B}}(t_2))\phi(x_{\mathcal{B}}(t_1))\rangle\right) \end{aligned} \tag{A.16}$$

$$S_2 = \int_0^T \mathrm{d}t_1 \int_0^T \mathrm{d}t_2 \; \chi_{\mathcal{B}}(t_1)\chi_{\mathcal{B}}(t_2) e^{-i\Omega_{\mathcal{B}}(\tau_{\mathcal{B}}(t_1)+\tau_{\mathcal{B}}(t_2))} \langle \phi(x_{\mathcal{B}}(t_2))\phi(x_{\mathcal{B}}(t_1))\rangle \,. \tag{A.17}$$

The lowest order signalling terms from (3.42) contain a sum of different integral terms from (A.13). These integrals can be combined, e.g., for C we have

$$\begin{aligned} C_2 = -\int_0^T \mathrm{d}t_1 \int_0^{t_1} \mathrm{d}t_2 \; & \big(\chi_{\mathcal{A}}(t_1)\chi_{\mathcal{B}}(t_2) e^{i(\Omega_{\mathcal{B}}\tau_{\mathcal{B}}(t_2)-\Omega_{\mathcal{A}}\tau_{\mathcal{A}}(t_1))} \langle \phi(x_{\mathcal{A}}(t_1))\phi(x_{\mathcal{B}}(t_2))\rangle \\ & + \chi_{\mathcal{A}}(t_2)\chi_{\mathcal{B}}(t_1) e^{i(\Omega_{\mathcal{B}}\tau_{\mathcal{B}}(t_1)-\Omega_{\mathcal{A}}\tau_{\mathcal{A}}(t_2))} \langle \phi(x_{\mathcal{B}}(t_1))\phi(x_{\mathcal{A}}(t_2))\rangle\big) \\ + \int_0^T \mathrm{d}t_1 \int_0^T \mathrm{d}t_2 \; & \chi_{\mathcal{A}}(t_2)\chi_{\mathcal{B}}(t_1) e^{i(\Omega_{\mathcal{B}}\tau_{\mathcal{B}}(t_1)-\Omega_{\mathcal{A}}\tau_{\mathcal{A}}(t_2))} \langle \phi(x_{\mathcal{A}}(t_2))\phi(x_{\mathcal{B}}(t_1))\rangle \\ = \int_0^T \mathrm{d}t_1 \int_0^{t_1} \mathrm{d}t_2 \; & \chi_{\mathcal{A}}(t_2)\chi_{\mathcal{B}}(t_1) e^{i(\Omega_{\mathcal{B}}\tau_{\mathcal{B}}(t_1)-\Omega_{\mathcal{A}}\tau_{\mathcal{A}}(t_2))} \left[\phi(x_{\mathcal{A}}(t_2)), \phi(x_{\mathcal{B}}(t_1))\right] \end{aligned} \tag{A.18}$$

and for D we find

$$D_2 = \int_0^T \mathrm{d}t_1 \int_0^{t_1} \mathrm{d}t_2 \; \chi_{\mathcal{A}}(t_2)\chi_{\mathcal{B}}(t_1) e^{-i(\Omega_{\mathcal{B}}\tau_{\mathcal{B}}(t_1)+\Omega_{\mathcal{A}}\tau_{\mathcal{A}}(t_2))} \left[\phi(x_{\mathcal{B}}(t_1)), \phi(x_{\mathcal{A}}(t_2))\right] . \tag{A.19}$$

Here, a sign error in [19] in the exponent of (3.48) has been corrected. The remaining lowest order contributions can be expressed in terms of C_2 and D_2:

$$G_2 = -C_2, \quad H_2 = -D_2, \quad I_2 = D_2, \quad J_2 = C_2. \tag{A.20}$$